

# CENTRIFUGAL SEPARATIONS IN BIOTECHNOLOGY

WALLACE WOON-FONG LEUNG



# Centrifugal Separations in Biotechnology

*In God, I Trust*

# Centrifugal Separations in Biotechnology

*Wallace Leung*



ELSEVIER



AMSTERDAM • BOSTON • HEIDELBERG • LONDON • NEW YORK • OXFORD  
PARIS • SAN DIEGO • SAN FRANCISCO • SINGAPORE • SYDNEY • TOKYO

Academic Press is an imprint of Elsevier  
Linacre House, Jordan Hill, Oxford OX2 8DP

First published 2007

Copyright © 2007, Wallace Leung. Published by Elsevier Limited.  
All rights reserved

The right of Wallace Leung to be identified as the author of this work has been asserted in accordance with the Copyright, Designs and Patents Act 1988

No part of this publication may be reproduced, stored in a retrieval system or transmitted in any form or by any means electronic, mechanical, photocopying, recording or otherwise without the prior written permission of the publisher

Permission may be sought directly from Elsevier's Science & Technology Rights Department in Oxford, UK: phone (+44) (0) 1865 843830; fax (+44) (0) 1865 853333; email: [permissions@elsevier.com](mailto:permissions@elsevier.com). Alternatively you can submit your request online by visiting the Elsevier web site at <http://elsevier.com/locate/permissions>, and selecting *Obtaining permission to use Elsevier material*

#### Notice

No responsibility is assumed by the publisher for any injury and/or damage to persons or property as a matter of products liability, negligence or otherwise, or from any use or operation of any methods, products, instructions or ideas contained in the material herein. Because of rapid advances in the medical sciences, in particular, independent verification of diagnoses and drug dosages should be made

#### British Library Cataloguing in Publication Data

A catalogue record for this book is available from the British Library

#### Library of Congress Cataloguing in Publication Data

A catalogue record for this book is available from the Library of Congress

ISBN 13: 978-1-85-617477-0

For information on all Elsevier publications visit our website  
at [www.books.elsevier.com](http://www.books.elsevier.com)

07 08 09 10 11 11 10 9 8 7 6 5 4 3 2 1

Typeset by Charon Tec Ltd (A Macmillan Company), Chennai, India  
[www.charontec.com](http://www.charontec.com)

Printed and bound in United Kingdom

Working together to grow  
libraries in developing countries

[www.elsevier.com](http://www.elsevier.com) | [www.bookaid.org](http://www.bookaid.org) | [www.sabre.org](http://www.sabre.org)

ELSEVIER

BOOK AID  
International

Sabre Foundation

# Contents

<i>Preface</i>	<i>xiii</i>
<b>1 Introduction</b>	<b>1</b>
1.1 Introduction	1
1.2 Centrifugal Separation and Filtration	6
1.2.1 Sedimenting Centrifuge	7
1.2.2 Filtering Centrifuges	9
1.3 Pros and Cons of Filtration versus Centrifugation	10
1.4 Generic Flow Sheet for Biopharmaceutical Process	11
1.5 Other Centrifugal Separations	12
1.6 Inputs and Outputs of Centrifuge	13
1.7 Separation Metrics	13
1.7.1 Protein Yield	14
1.7.2 Centrate Suspended Solids	14
1.7.3 Throughput Rate	15
1.7.4 Cell Viability	15
1.8 Summary	15
References	16
Problems	17
<b>2 Principles of Centrifugal Sedimentation</b>	<b>19</b>
2.1 Introduction	19
2.2 Non-intuitive Phenomena	19
2.2.1 Pressure Distribution	19
2.2.2 Coriolis Effect	20
2.3 Intuitive Phenomena	23
2.3.1 Centrifugal Acceleration	24
2.3.2 Fluid in a Centrifuge Bowl not at Solid-Body Motion	26
2.3.3 Regimes of Sedimentation	28

2.3.4	Stokes' Law	30
2.3.5	Settling with Concentrated Solids	31
2.4	Process Functions	32
2.5	Summary	34
	References	34
	Problems	34
<b>3</b>	<b>Batch and Semi-Batch Centrifuges</b>	<b>37</b>
3.1	Spintube	37
3.2	Centrifugal Filter	40
3.3	Ultracentrifuges	42
3.3.1	Analytical Ultracentrifuge	42
3.3.2	Preparative Ultracentrifuge	44
3.3.3	Centrifugal Elutriation	44
3.4	Tubular Centrifuge	47
3.4.1	General Tubular Bowl Geometry	47
3.4.2	Ribs and Solids Scraper	51
3.4.3	Plunger Cake Discharge	54
3.4.4	Submerged Hub	54
3.5	Summary	57
	References	57
	Problems	57
<b>4</b>	<b>Disk Centrifuge</b>	<b>59</b>
4.1	Lamella/Inclined Plate Settler	59
4.1.1	Inclined Plate Settler Principle	59
4.1.2	Complications in Inclined Plate Settler	60
4.2	Disk-Stack Centrifuge	61
4.2.1	General Disk Geometry	61
4.2.2	Disk Angle	62
4.2.3	Disk Spacing	64
4.2.4	Process Functions of Disk Centrifuge	64
4.2.5	Feed Solids	65
4.2.6	Manual Disk Centrifuge	65
4.2.7	Intermittent Discharge	67
4.2.8	Chamber Bowl	71
4.2.9	Nozzle Discharge	71
4.2.10	Liquid Discharge	75
4.3	Feed Inlet and Accelerator	78
4.3.1	Introduction to Low Shear	78
4.3.2	Hydro-Hermetic Feed Design	78
4.3.3	Power Loss	80

4.3.4	Feed Acceleration Visual and Quantitative Testing	81
4.3.5	Improved Feed Accelerator	85
4.4	Other Considerations	87
4.4.1	Materials of Construction	87
4.4.2	Clean-in-Place	88
4.4.3	Steam Sterilization	88
4.4.4	Containment	88
4.4.5	Surface Finish	88
4.4.6	Temperature Control	89
4.4.7	Water Requirements	89
4.4.8	Noise Level	89
4.4.9	Explosion-Proof Design	89
4.5	Examples of Commercial Disk-Stack Centrifuge	89
4.6	Summary	92
	References	93
	Problems	93
<b>5</b>	<b>Decanter Centrifuge</b>	<b>95</b>
5.1	Solid Bowl or Decanter Centrifuge	95
5.2	Feed Rate	96
5.3	Pool Depth	96
5.4	Rotation Speed and <i>G</i> -force	97
5.5	Differential Speed	97
5.6	Sedimentation Enhancement using Chemicals	100
5.7	Three-Phase Separation	101
5.8	Cake Conveyance	103
5.8.1	Dry Beach	103
5.8.2	Hydraulic Assist	104
5.9	Summary	105
	References	106
	Problems	106
<b>6</b>	<b>Commercial Applications of Centrifugation in Biotechnology</b>	<b>109</b>
6.1	Generic Flow Sheet of Biopharmaceutical Processing	110
6.2	Mammalian Cell	112
6.3	Yeast Processing	115
6.4	Hormones Processing	117
6.5	Insulin Production	119
6.6	Biotech Separation of Inclusion Bodies	119
6.7	Vaccines Processing	120
6.7.1	Concentrated Cell-Based Product	121
6.7.2	Serum Product	121

6.8	Enzymes Processing	122
6.8.1	Extracellular Enzymes	122
6.8.2	Intracellular Enzymes	123
6.9	Ethanol Production	124
6.10	Other Biotech Processing	125
6.10.1	Recovery of Coagulation Factors from Blood Plasma	125
6.10.2	Tissue from Animal Cells	126
6.10.3	Laboratory Concentration and Buffer Exchange using Centrifugal Filter	126
6.11	Summary	127
	References	127
	Problems	128
<b>7</b>	<b>Concentrating Solids by Centrifugation</b>	<b>129</b>
7.1	Introduction	129
7.2	Concentrating Underflow	130
7.3	Compaction	131
7.4	Expression or Percolation	131
7.5	Compaction Testing	134
7.6	Compaction Pressure	135
7.7	Recommendations for Increasing Solids Concentration in Underflow	137
7.8	Summary	138
	References	139
	Problems	139
<b>8</b>	<b>Laboratory and Pilot Testing</b>	<b>141</b>
8.1	Process Objectives	141
8.2	Solid, Liquid and Suspension Properties	142
8.2.1	Solids Properties	142
8.2.2	Mother Liquid Properties	142
8.2.3	Feed Slurry Properties	142
8.3	Bench-Scale Testing	143
8.3.1	Separability	143
8.3.2	Flocculant and Coagulant in Bench Tests	143
8.3.3	Test Variables	144
8.3.4	Material Balance	145
8.3.5	Acceleration and Deceleration Time Duration	147
8.3.6	Settling Velocity	148
8.4	Pilot Testing	152
8.4.1	Material Balance Consideration for Pilot/ Production Scale	152

---

8.4.2	Product (Protein) Yield	154
8.4.3	Pilot Test Factors	157
8.5	Summary	163
	Reference	163
	Problems	163
<b>9</b>	<b>Selection and Sizing of Centrifuges</b>	<b>165</b>
9.1	Selection	165
9.1.1	Introduction	165
9.1.2	Tubular Centrifuge Selection	166
9.1.3	Disk Centrifuge Selection	166
9.1.4	Centrifuge Comparison	166
9.2	Centrifuge Sizing	169
9.2.1	Sizes and Rates	169
9.2.2	Dimensionless Le Number	170
9.2.3	Spintube (bottle) Centrifuge	171
9.2.4	Sizing for Disk Centrifuge	175
9.2.5	Sizing for Tubular, Chamber, and Decanter Centrifuge	181
9.3	Feed Particle Size Distribution	183
9.4	Summary	186
	References	186
	Problems	187
<b>10</b>	<b>Troubleshooting and Optimization</b>	<b>189</b>
10.1	Troubleshooting	189
10.1.1	Timescale of Occurrence	189
10.1.2	Mechanical or Process Problem	189
10.1.3	Process Problems	190
10.1.4	Mechanical Problems	193
10.2	Optimization	195
10.2.1	Separation Metrics	195
10.2.2	Monitored Variables	196
10.2.3	Controlled Variables	196
10.2.4	A Simple Optimization Scheme	197
10.3	Summary	199
	Problems	199
<b>11</b>	<b>Flow Visualization and Separation Modeling of Tubular Centrifuge</b>	<b>201</b>
11.1	Flow Visualization	202
11.2	Improved Moving Layer Flow Model	206

11.3	Effect of Velocity Profile	208
11.4	Effect of Friction within the Flow Layer	209
11.5	Dimensionless Le Parameter	210
11.6	Quantitative Prediction	210
11.6.1	Total Solids Recovery in Cake	210
11.6.2	Total Solids Recovery in the Centrate	211
11.6.3	Particle Size Distribution of Supernatant/ Overflow	211
11.6.4	Cumulative Size Recovery	211
11.7	Sedimentation Tests	212
11.7.1	Experiments on Sedimentation in Rotating Bowl Centrifuge	212
11.8	Summary	215
	References	215
	Problems	216
<b>12</b>	<b>Disk Stack Modeling</b>	<b>217</b>
12.1	Disk Model	218
12.1.1	Continuous Phase	219
12.1.2	Dispersed Phase	220
12.2	Model Validation	224
12.3	Complications	225
12.4	Summary	226
	References	227
	Problems	227
<b>13</b>	<b>Performance Projection of Centrifuges in Bioseparation</b>	<b>229</b>
13.1	Disk Centrifuge	229
13.1.1	Baseline Case (400-mm Disk)	230
13.1.2	Effect of Fine Size Distribution (400-mm Disk)	232
13.1.3	Effect of $G$ -Force (580-mm Disk)	233
13.1.4	Effect of Efficiency $\eta$ (580-mm Disk)	236
13.1.5	Disk Centrifuge for Yeast Processing (500-mm Disk)	238
13.1.6	Disk Centrifuge for Inclusion Body Separation (260-mm Disk)	239
13.1.7	Enzymes (580-mm Disk)	242
13.2	Tubular Centrifuge	244
13.2.1	High- $G$ Tubular (150-mm and 300-mm)	244
13.2.2	Lower- $G$ Tubular (150-mm and 300-mm)	245
13.3	Decanter	248
13.4	Spintube	250

---

13.5 Strategy of Developing Drug using Numerical Simulations	251
13.6 Summary	253
References	253
Problems	253
<b>14 Rotating Membrane in Bioseparation</b>	<b>255</b>
14.1 Membrane	255
14.1.1 Osmotic Pressure Resistance	256
14.1.2 Gel Resistance	257
14.1.3 Membrane Fouling and Cake Formation	258
14.1.4 Two Scenarios of Rotational Effect on Membrane Filtration	258
14.2 Rotating Disk Membrane with Surface Parallel to the $G$ -Force	258
14.2.1 Dimensionless Numbers	260
14.2.2 Governing Equations and Solutions	261
14.2.3 Gel Concentration	266
14.2.4 Determining Diffusivity	266
14.2.5 Parametric Effects	268
14.3 Rotating Membrane with Membrane Perpendicular to the $G$ -Force	271
14.3.1 Spintube Equipped with Membrane Module – Centrifugal Filter	272
14.3.2 Model on Swinging Bucket Equipped with UF Membrane	275
14.3.3 Comparing Test Results with Predictions	278
14.4 Summary	283
References	283
Problems	284
<i>Appendix A: Nomenclature</i>	285
<i>Appendix B: Answers to Problems in the Chapters</i>	289
<i>Index</i>	293



# Preface

Processing biological materials to produce high value-added intermediates or finished products, no matter whether it is liquid or solid, often involves a separation step, especially after the fermenter or bioreactor. In one instance, the high-value solid products in a dilute concentration have to be separated from the waste liquid with spent cells and debris; therefore it is essential to prevent loss of valuable solids in the liquid stream. A further requirement is that contaminants have to be washed from the solids. Alternatively, the high-value liquid containing dissolved protein needs to be separated from the biomass and the liquid product should be free of solid particulates to avoid downstream separation and contamination of purification equipment, such as a chromatography column. The difficulty in carrying out separation is that biosolids do not filter well and often foul and blind the filter, such as microfiltration and ultrafiltration membranes. Instead of filtration, separation by sedimentation utilizing the density difference between the solid and the suspending liquid can be employed. However, the density difference between biosolids and liquid (typically water-based) is very small, rendering the separation very slow and ineffective, especially under the Earth's gravity. In addition, if RNA and other protein materials are dissolved in the liquid, the liquid phase can be very viscous, which further slows down sedimentation. Another difficulty is that the solids concentration in suspension for processing is relatively dilute and requires equipment which has large volumetric capacity for handling the flow and process.

Centrifugation has proven to be a rather robust process for enhancing settling by using thousands to almost millions of times the Earth's gravitational acceleration. In biopharmaceutical processing for producing a recombinant therapeutic protein for antibiotics and drug substances from yeast, microbial, and mammalian cells such as the Chinese Hamster Ovary (CHO) cell, centrifuges have been widely used to perform separation, classification of cell debris, concentration of suspension, and separation and washing of solids such as inclusion body or crystalline protein. No doubt, given the escalating research activities in biotechnology, many new sources of therapeutic proteins and other valuable biological materials will be discovered and developed, and more stringent requirements will be demanded from separation/recovery and purification. There will be more growing needs of centrifugation in

combination with other separations and filtrations to perform the often overlooked, yet important, duty.

While there are many texts and reference books on bioseparation, there is very little coverage on centrifugation. This book is the first reference book of its kind devoted to centrifugal separation in biotechnology. It is an outgrowth of a series of seminars, short courses and presentations that the author has delivered to biopharmaceutical companies all over the world. This new and challenging topic has received excellent global reception, which is quite comforting and rewarding. The contents of this book are also based on the author's research and extensive experiences respectively in practice, mentoring and lecturing on the subject for over twenty years.

The book starts out with an introduction on the topic (Chapter 1) followed by Chapter 2 on sedimentation, which is the key step of separation. Subsequently, various batch (spintube centrifuge, ultracentrifuge) and semi-batch (tubular centrifuge) centrifuges are discussed in Chapter 3. The workhorse of the industrial separation process, disk-stack centrifuge, is presented and discussed at length in Chapter 4. Also, decanter centrifuge, which is more applicable to high-solids feed and relatively lower centrifugal acceleration, has been included in Chapter 5. However, the discussion will be brief in favor of giving room to various other topics. Commercial applications of centrifuges in biotechnology are discussed in Chapter 6. This is perhaps one of the most interesting topics for practitioners who are more concerned about where proven processes are, and how their new processes may build on what is already known and practiced. Despite there being lots of applications discussed in this chapter, unfortunately there might be applications that have been inadvertently omitted, given that the biotech applications are very diverse. Subsequently, we discuss in Chapter 7 the importance and practice of increasing, or at least maintaining, high solids concentration in the underflow stream of the centrifuge. Laboratory and pilot testing and selection and sizing are essential functions for establishing and implementing the biotech process and they are discussed, respectively, in Chapters 8 and 9. A new unified approach in scale-up and prediction with use of a dimensionless Leung ( $Le$ ) number is introduced. The  $Le$  number works for all types of centrifuges, including spintube, tubular, chamber, disk-stack, and decanter centrifuges. This provides a solid foundation for practitioners to scale-up equipment and analyze test results. Troubleshooting and optimization are two important topics of general interest, especially for installed machines, and they are discussed in Chapter 10. Subsequently, modeling of tubular and disk-stack centrifuges are covered in Chapters 11 and 12, respectively, for researchers who are interested. Readers who are not interested in modeling can go directly to Chapter 13. The  $Le$  number provides a basis for the scale-up and performance prediction covered in Chapter 13. Here, numerous examples are used to demonstrate the versatility of the numerical simulator built on the  $Le$ -approach to forecast performance in parallel with concurrent testing, which is often limited for various reasons. Numerical simulation can also be used to analyze laboratory, pilot and production test results

to validate machine and process performance. Therefore, numerical simulation can be used for lab screening, pilot testing, clinical manufacturing testing, full-scale production, and for small-scale testing in the laboratory to investigate alternatives and improvements to the existing process under production. Membranes process, such as microfiltration, ultrafiltration and diafiltration, are frequently used in bioseparation. Lastly, Chapter 14 is devoted to combining two separation processes: centrifugation and membrane separation. Two examples, respectively, on centrifugal filter in spintube and large rotating membrane systems are discussed. The general approach can be extended readily to other rotating membrane geometry.

Centrifugation has been treated as a black box in the past, as the subject is quite complex and non-intuitive. The subject involves multiple disciplines such as fluid dynamics, mechanics and vibration, design, material science, rheology, chemical and process engineering, chemistry, biology, and physics. I hope this text will fulfill the quest of knowledge by rendering centrifuge a lot more 'transparent' to biologists, biotechnologists, chemists, physicists, scientists, researchers and practicing engineers. The more they know the better they can deploy, comfortably and without reservation, centrifuge as handy process equipment.

Problems are listed at the end of each chapter in the text, and they complement and supplement the contents in the chapter. They are also meant to reinforce the concepts for the readers through practices, challenging their thoughts and understanding on the topic. Apart from practitioners and researchers, this book is written primarily for senior and first-year university undergraduates taking bioseparation, bioprocessing, unit-operation/process engineering, or similar courses.

I am grateful to Stella, Jessica, Jeffrey, my mother and my late father for putting up with me while I was devoted to preparing this book. My late father and my dear friend and mentor, the late Professor Ascher H. Shapiro, both demonstrated dedication and perseverance in their lives, which inspired me all along, especially during the trying times when I was working on the manuscript among other responsibilities that also demanded my undivided attention. I also thank Alice Tang for skillfully helping out with the manuscript work and meeting the publisher's deadline.

Wallace Woon-Fong Leung  
The Hong Kong Polytechnic University  
2007

Readers may refer to our website where the figures throughout this book are reproduced in colour.  
To access the figures visit:  
<http://books.elsevier.com/companions/9781856174770>

# Introduction

## 1.1 Introduction

Biotechnology has revolutionized our life in the twentieth century [1]. Its impact is only now being felt from engineering food [2,3], engineering and delivering drugs [4,5,6], to engineering consumable products. Without doubt it will continue to influence our daily lives for years to come. One of the many successful examples is that drugs, such as monoclonal antibodies and some basic drug substances (i.e. the building block for various drugs), can now be manufactured and formulated from bioreaction. One of the commonly used methods in biotechnology is the recombinant DNA technique [7,8]. A desired gene is isolated from one organism and this is inserted into a small piece of carrier DNA called a vector. It is highly desirable that the recombined DNA (vector plus gene) can propagate in a similar or unrelated host/recipient cell.

The mammalian cell, such as the Chinese Hamster Ovary (CHO) cell, is a popular host cell. Figure 1.1 shows a schematic of an animal cell which is very similar to that of a mammalian cell. A characteristic size of the mammalian cell is about 10–20 microns. Unlike a plant cell, there is no cell wall for animal and mammalian cells, so they rely on a plasma membrane to keep the intracellular contents intact. High shear stress acting on the cell can rupture the fragile membrane, releasing the intracellular material. Also yeast (see schematic in Figure 1.2) has been commonly used as a host cell in the recombinant DNA process, the knowledge and experience of which we have gained from the brewing industry. Unlike a mammalian cell, the yeast cell has a strong cell wall. Yeast cells are smaller than mammalian cells and are typically between 7 and 10 microns. In addition, bacteria, such as *Escherichia coli* (hereafter abbreviated as *E. coli*) and *Bacillus subtilis*, have been used as host cells for the recombinant DNA technique. A schematic of an *E. coli* bacteria cell is shown in Figure 1.3. Again, *E. coli* has a sturdy cell wall with both an outer and an inner membrane. *E. coli* is typically elongated with a dimension of 3–5 microns long by 1 micron width. Therapeutic protein can be ‘expressed’

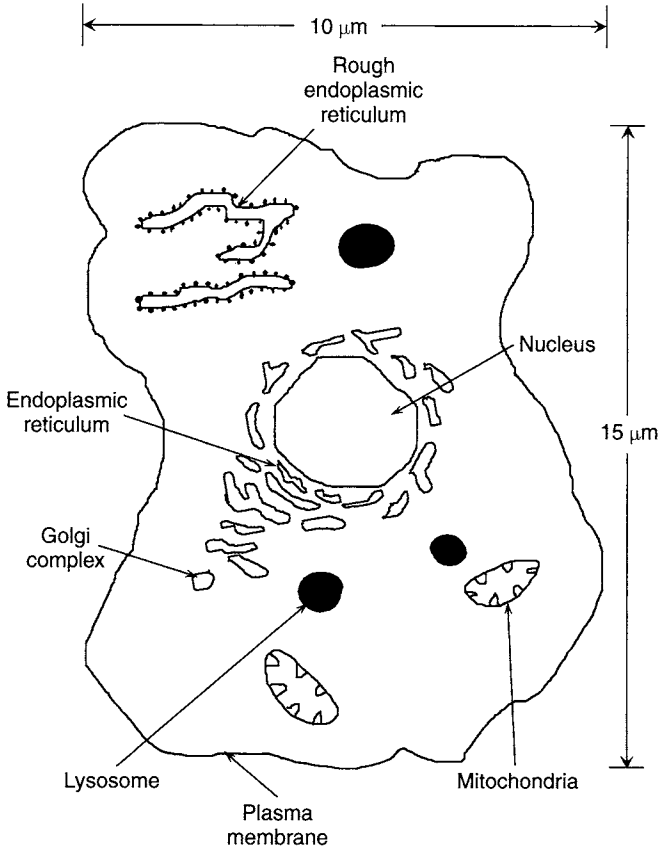


**Figure 1.1** Animal cell schematic showing plasma membrane

by these host cells or organisms with the recombinant DNA. The protein of interest may remain in the cell (intracellular) or be secreted to the exterior of the cell (extracellular). The aforementioned biosynthesis provides more engineering flexibility, specificity, versatility, reliability, and cost-effectiveness.

Therapeutic proteins are quite diverse in the application treatments, such as human insulin for diabetes, erythropoietin for anemia and chronic renal failure, interferon-beta and gamma for cancer, DNase for pulmonary treatment, vaccines for Hepatitis B, Interleukin-2 for AIDS, Prourokinase for heart attacks, tissue plasminogen activator (enzyme) for strokes, and in many different kinds of monoclonal antibodies for diagnosis and possible treatment of breast and lung cancers, and in a variety of diagnostics, to name just a few. The fast-growing biopharmaceutical business in producing therapeutic proteins is getting so popular that all major drug manufacturers also carry a parallel line of this business.

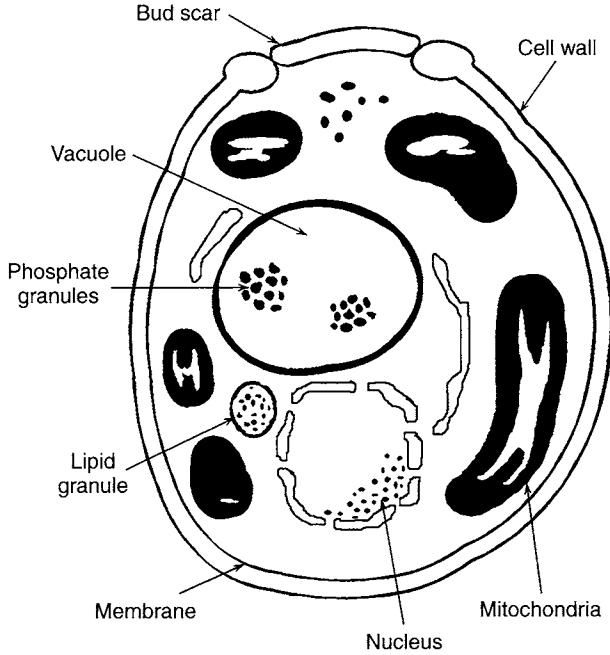


**Figure 1.2** Yeast cell schematic showing both cell wall and membrane

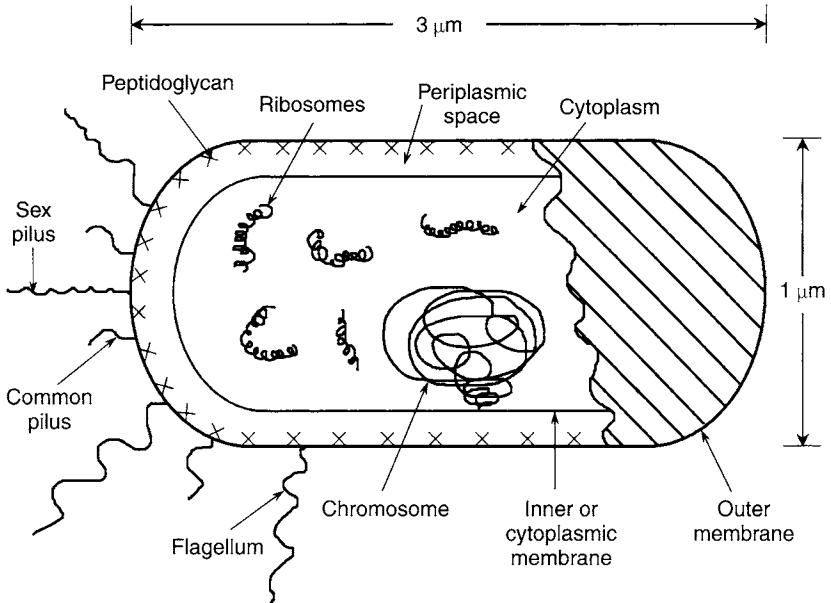


**Figure 1.3** *E. coli* cell schematic

Unfortunately the protein expressed from the bioprocess is in very small amounts in a large volume of suspension, i.e. low concentration. The two key hurdles in recombinant DNA techniques to produce therapeutic protein [9] are (a) to recover this small concentration of protein after fermentation by separation and (b) to provide high purity of the protein product through purification. It is prudent that both separation and purification processes should be robust and cost-effective for the biopharmaceutical technology to be viable and competitive. Although this book is focused on separation, one should bear in mind that given these two steps are sequential, poor separation can adversely affect purification downstream. Therefore, it is prudent to have an integrated approach for downstream processing. To say the least, if there is an upset from the fermenter upstream producing, say, off-spec finer feed, the centrifuge should take on the upset feed and try to produce a consistent output downstream to the filter, membrane and chromatography column downstream in the interim while the upset condition is being fixed. Otherwise the entire chain of downstream processes can be seriously affected.

Other biotechnology involves synthesis and/or modification of intermediates or final products. Frequently, this is in a suspension form so that mechanical mixing, separation, spray or thermal drying and other allied processes are required.

Given that separation is an important task [10–14] in biotechnology in lieu of the above, it can be a very difficult task due to the low concentration of the protein present and the large volume of liquid to handle, the fragility of the cells, the presence of cell debris, fine particulates and colloids, and the high viscosity due to dissolution of intracellular substances such as RNA. Typically, separation can be achieved by filtration and sedimentation. There are some specific problems relating to each as discussed in the following.

Filtering a suspension containing biomass is quite tricky as the material can foul the filter surface, reducing permeate or filtrate flow regardless whether the media is a microfiltration or an ultrafiltration membrane. It is equally challenging to settle biomass as the density of the biomass material is just slightly greater than that of the liquid phase, which often is aqueous based. Given that settling is proportional to the difference in the two densities, it takes a very long time to separate, translating – in simple terms – to an impractically low capacity operation and high cost. On the other hand, separation by sedimentation can be much enhanced under centrifugal acceleration. This is possible by introducing the suspension with biomass in a centrifuge rotating at high speed where

centrifugal acceleration can be hundreds to millions of times that of the Earth's gravitational acceleration.

Figure 1.4 shows the use of centrifugation in biopharmaceutical production of therapeutic protein using the commonly employed mammalian cells, bacteria, and yeasts. Centrifugation can be used for separation, clarification/polishing, thickening, classification, and washing-and-separation.

With reference to the left bioprocess in Figure 1.4, after harvesting from the bioreactor the cell culture suspension containing mammalian cells is sent to a centrifuge wherein the cells are separated from the liquid product which contains the extracellular protein secreted from the mammalian cells. The separated liquid is then sent to a depth filter for further polishing, removing any solid particulates before sending it downstream for processing.

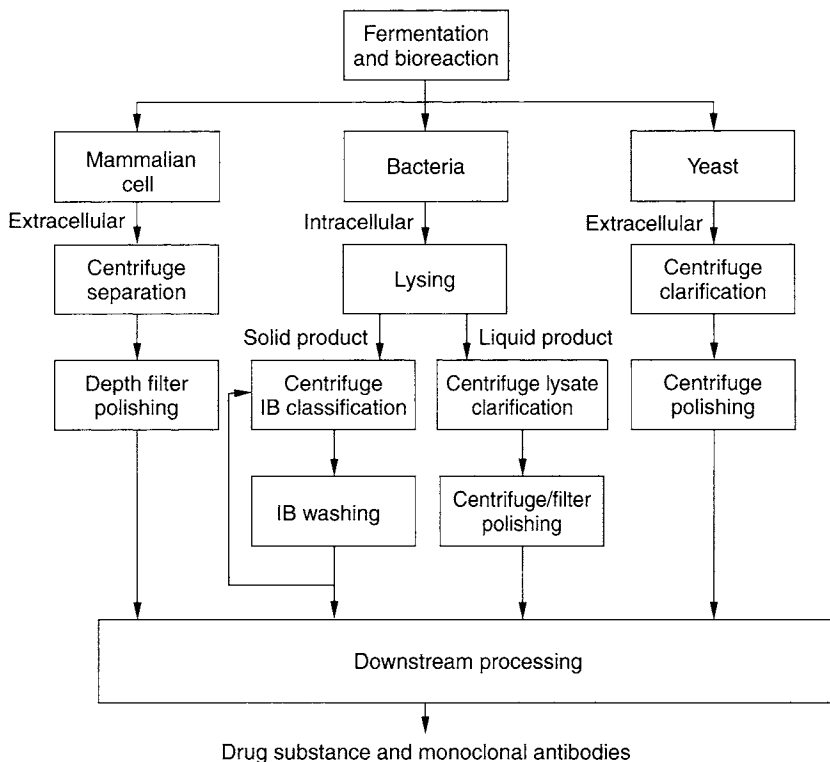


**Figure 1.4** Drug substances produced from fermentation and downstream processes where centrifugation has been widely employed for various duties

With reference to the middle bioprocess in Figure 1.4, the protein is expressed intracellular in the bacteria. After harvesting and homogenizing, the protein is released from the lysed bacteria in the inclusion bodies that need to be isolated before additional downstream processing. Centrifugation is used to sediment the inclusion bodies while the cellular contents, cell debris and finer materials leave with the liquid phase to wasting. The inclusion body is further washed and separated several times until it reaches the desired purity for downstream processing. Alternatively, the protein from the bacteria may be expressed in the intracellular liquid and upon homogenizing this protein is released in the liquid. The task is to remove all solid materials and to recover the liquid bearing the soluble protein. The biomass may have to be washed to ensure protein does not get adhered to the biomass surface, otherwise this represents a loss or lower yield for the process.

With reference to the right bioprocess in Figure 1.4, after harvesting from the fermenter the yeast suspension is sent to centrifugation where the liquid containing extracellular protein is separated from the yeast solids. The liquid leaving the centrifuge may have to be centrifuged again (i.e. clarification or polishing) to remove any particulates and turbidity before downstream processing.

The above three paths are central to biopharmaceutical production of therapeutic proteins using host cells. These will be discussed in much greater details throughout the text.

## 1.2 Centrifugal Separation and Filtration

Industrial centrifugal separation [15,16] can be divided generally into two classes: sedimenting and filtering. It should be noted that conventional centrifugation can only separate suspended solids and not dissolved solids with the exception of a centrifugal filter, to be discussed later, which can separate soluble solids. Heavier solids settle to the solid wall of a sedimenting centrifuge under centrifugal acceleration that is much greater than the Earth's gravity. A density difference between the solid and the liquid phase is required to effect separation. A schematic of a sedimenting solid-wall centrifuge is shown in Figure 1.5. Similarly, a lighter dispersed solid phase, like fat or solids with attached air bubbles, can also float (instead of sink) in a continuous liquid phase, and separation by flotation can be enhanced in a centrifugal field.

On the other hand, density difference between the two phases is not required to separate the solid from liquid phase in a filtering centrifuge. Both phases are driven under the centrifugal body force to the perforated

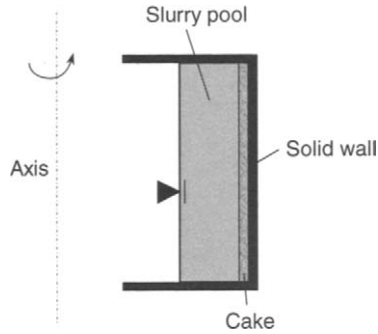


**Figure 1.5** Solid-wall sedimenting centrifuge

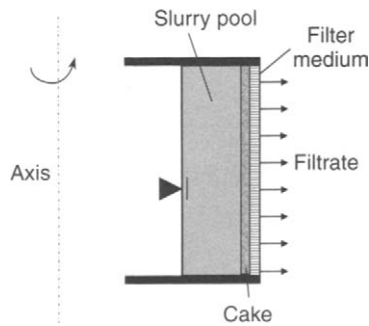


**Figure 1.6** Filtering perforate-wall centrifuge

wall lined with a filter medium. Liquid permeates (see Figure 1.6) through the filter medium while solids, comparable or larger in size than the openings of the filter medium, are retained. Sometimes even smaller solids can be retained as they ‘bridge across’ or ‘jam’ the medium openings precluding them from filtering through. As such, openings in the filter medium can be selected normally two to three times larger than the particle size to be retained. Once a ‘cake’ layer of particles form on the medium despite some smaller particles that may still percolate through during initial filtration, the cake layer further acts as another filter medium in series with the original medium to retain incoming particles. It can be seen that filtering centrifuges can separate particles and liquid regardless of their density difference; this is very much different from a sedimenting centrifuge that relies on density difference of the two phases to drive separation.

### 1.2.1 Sedimenting Centrifuge

Sedimenting centrifuge can be divided respectively into batch and continuous sediment discharge as represented by Figure 1.7. For batch discharge,

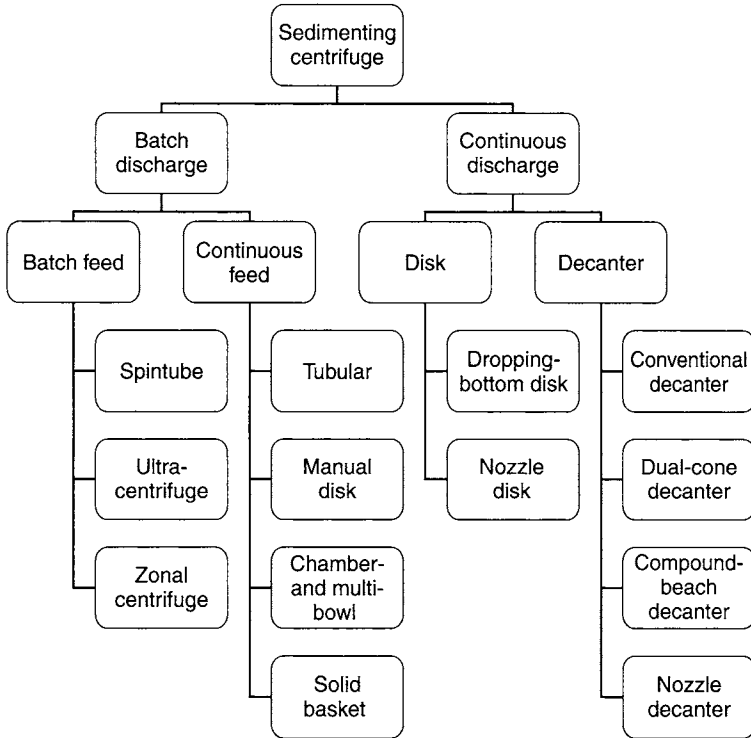


**Figure 1.7** Batch and continuous centrifuge classification

this can be further divided to batch and continuous feed. Spintube, ultracentrifuge and zonal centrifuge are all classified as batch-feed centrifuges, though some zonal centrifuges can have continuous feed and continuous removal features. In batch feed, a fixed amount of feed slurry is introduced to the centrifuge. Upon separation, heavier solids settle to the bowl wall or tube bottom at a large radius. Here they accumulate temporarily until separation stops.

Tubular, manual disk, chamber, multibowl and solid basket are considered as semi-continuous as they take continuous feed of suspension. Heavier and larger solids from suspension get settled under centrifugal acceleration and the sediment is stored temporarily in the bowl until the quality of the separated liquid becomes affected by the growing sediment in the bowl. At that point, feeding stops, the centrifuge is allowed to coast down, the liquid pool is drained, and the sediment is removed. The centrifuge needs to be cleaned before the next cycle.

For continuous or semi-continuous discharge of sediment, both disk and decanter centrifuge fall into this category. Under disk centrifuge, there are two types depending on how the concentrated solids are

discharged: dropping bottom with intermittent solid discharge and the nozzle disk with continuous solid discharge. On the other hand, there are four types under decanter: a conventional decanter, dual-cone decanter for classifying two solids and a liquid phase, compound-beach decanter for dewatering fine solids producing a paste-like cake [17], and nozzle decanter for classifying kaolin suspension with 1 to 2 micron particles.

## 1.2.2 Filtering Centrifuges

Filtering centrifuges are also divided into two types: batch and continuous fed (see Figure 1.8). Under batch discharge, there are two categories. First, a small-batch feed under which perforated spintube and basket, and centrifugal filter both fall. Second, a large-batch feed under which conventional basket, peelers, siphon, and inverting bag centrifuges all fall. Regardless of the large- or small-batch feed, they take a batch of

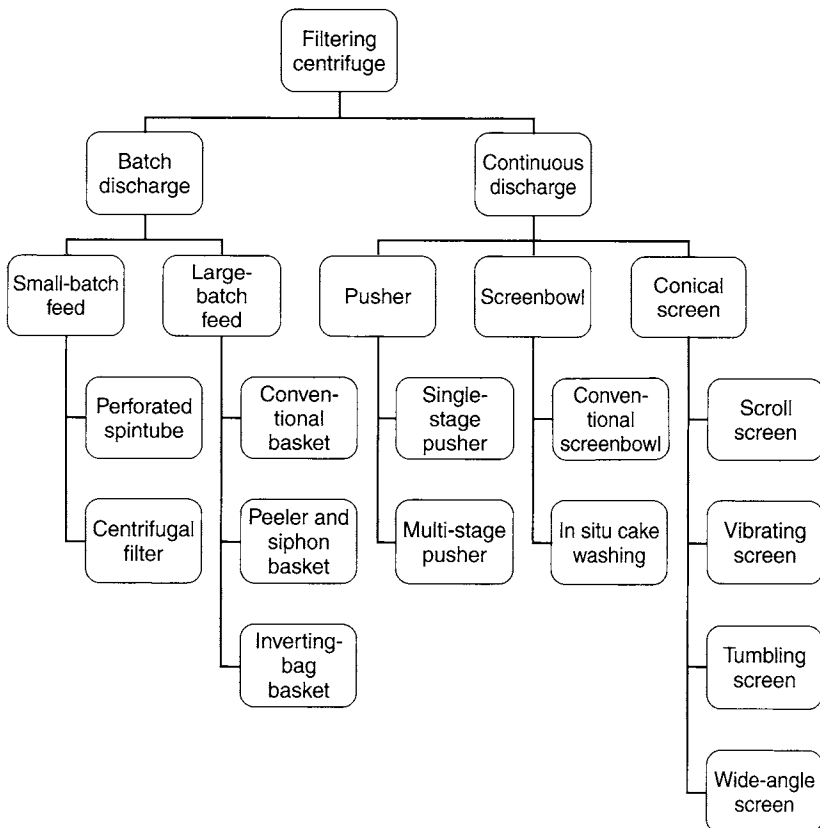


**Figure 1.8** Batch and continuous filtering centrifuge classification

feed suspension or 'charge' and perform various cycles to process the suspension, including filtering, washing, deliquoring/dewatering with or without drying, unloading and decelerating (for peeler) or decelerating and unloading (for regular baskets), and cleaning.

Pusher, conical screen, and screenbowl are continuous centrifuges. Feed is continuously introduced into these centrifuges and cake retained by the filter media is continuously being removed. Filtrate liquid, with minimal suspended solids, is also removed separately.

Suspension containing biological solids filter very slowly and they often clog up the filter media, forming an impermeable cake. As a consequence, filtration is often affected by a thin cake filtration in a controlled batch mode under moderate centrifugal gravity so that the cake does not compact to an impermeable 'skin' layer adjacent to the filter medium. In addition, solids should be at least greater than 10 microns, otherwise filtration is slow and impractical. If the valuable product is the liquid, it is possible to use a filter aid, such as diatomaceous earth, to enhance the filtration rate provided the filter aid does not interact with the product. In essence this increases the permeability of the filter cake. When the product protein is in the solids, such as in the biological cells, filter aid should not be used as it is almost impossible to separate the filter aid from the valuable biological material.

### **1.3 Pros and Cons of Filtration versus Centrifugation**

Centrifugation followed by depth filtration, two-stage depth filtration, or microfiltration-diafiltration, can all be used alone for solid-liquid separation when the valuable protein is in liquid phase. With reference to Figure 1.4, centrifugation is frequently used for lysed cells involving release of protein solids to be separated from the cell debris when bacteria are used as host cells. Table 1.1 compares the pros and cons of centrifugation and microfiltration. It is quite interesting that centrifugation actually generates less shear stress than tangential flow filtration contrary to conventional wisdom, provided a good feed acceleration is adopted in the centrifuge, see Chapter 4. Also, centrifugation does not suffer from the fouling of membrane that leads to costly membrane replacement and downtime. Also, it is a very robust system.

The solids in suspension for the process of interest are very small, in the domain of 10 microns and below, and sometimes even in the 1–2 micron range. While the small density difference affects sedimentation and not as much for filtration, as discussed, the fine biosolids affect depth

**Table 1.1** Comparing centrifugation and microfiltration (MF)

<b>Pros</b>	Less shear compared to that generated from TFF (tangential flow filtration/crossflow filtration) Cell debris does not foul or clog up pores leading to blinding; advantageous for higher feed solids (future trend) Remove solids down to 0.2 micron at high G Compact Less downtime (from fouling) Single pass or multiple passes Robust
<b>Cons</b>	Slightly higher capital costs

*Comparable operating costs (power and maintenance) as MF which requires periodic replacement of membranes from fouling.*

filtration, clogging the flow path of the filter, leading to rapid large pressure drop across the depth filter. For microfiltration, the membrane needs to stay ‘unclogged’ or ‘unfouled’ by the use of a crossflow membrane configuration using a high shear rate to scour the membrane surface, and to use a cleaning agent to wash the membrane during downtime. Also, diafiltration helps to maintain a lower solids concentration, to prevent fouling. Nevertheless, fouling leads to the replacement of the membrane and an associated downtime which are key drawbacks of microfiltration in this application. In addition, a much larger volume of liquid product (two to four times the original volume) results from washing or diafiltration to recover the protein. This implies a higher cost for the process as it involves more concentration by ultrafiltration and other processes downstream for treating the spent liquid.

A fourth possibility is to combine centrifugation with depth filtration as an integrated approach to separate mammalian cells. Centrifugation takes up the solids loading from the feed stream leaving the fermenter/bioreactor, while the depth filter works best in removing the submicron particles (separated liquid from the centrifuge) from a low-solids stream leaving the centrifuge. This will be discussed in more detail in Chapter 6.

## 1.4 Generic Flow Sheet for Biopharmaceutical Process

The recombinant protein process has become very popular for engineering a protein to have specific configurations and functions [6,7]. Various

recombinant proteins are commonly expressed through an engineering culture such as yeast, bacteria (e.g. *E. coli*), and living cells (e.g. mammalian and plant cells). The extracellular (exterior of cells) protein expressed by yeast and mammalian cells are in the liquid phase, while protein expressed by the engineered bacteria is inside the bacteria (i.e. intracellular), which subsequently needs to be lysed to release the protein. The process condition of a cell culture is carried out under a specific range of temperature, pressure and agitation/mixing, with fermentation usually subject to shorter time and more intensive conditions (higher process temperature, pressure and with more rigorous mixing) while bioreaction takes place under longer reaction time and milder conditions (lower process temperature, pressure and only moderate mixing).

Figure 1.9 shows a generic flow sheet for processing recombinant protein in which protein is expressed extracellularly wherein liquid is the product. The immediate first step – the separation step – is also referred to as primary recovery of protein. After solid-liquid separation, by any of the aforementioned four different possible separation methods, the protein buffer liquid may be replaced or diluted with a more appropriate buffer with a different pH and ionic strength followed by a concentration using an ultrafiltration and diafiltration combination. The end-product is a concentrated protein solution in a suitable buffer liquid. At this stage, the protein can be purified using ion-exchange or affinity chromatography to remove any impurities and contaminants. A final sterile filtration involves the use of a 0.2-micron size microfilter to remove bacteria that are incurred during processing. The final product is typically a drug substance or an antibiotic.

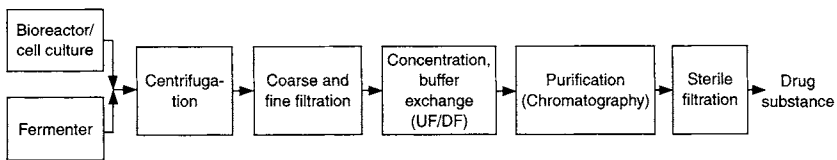


**Figure 1.9** Generic flow sheet of biopharmaceutical drug substance

## 1.5 Other Centrifugal Separations

Other than for primary recovery in the downstream process of recombinant protein, centrifugal separation is also used in many biotechnology solid-liquid separations in manufacturing of drugs/hormones such as insulin and many others. In the process of manufacturing, drugs (in solid form) frequently contain salt and other impurities. In such cases the drugs need to be washed by reslurrying followed by centrifugal

separation. Also crystallization and precipitation in the purification step require solid-liquid separation by centrifugation. The objective in these processes is to fully capture or recover the valuable suspended solids, unlike the recovery of soluble protein expressed extracellularly by yeast and mammalian cells wherein the product is the liquid. Another equally important objective is to reduce the impurity level of the crystals to an acceptable level for downstream formulation, such as washing followed by centrifugal separation.

## 1.6 Inputs and Outputs of Centrifuge

Centrifuge has often been considered as a black box, as the solid mechanics and fluid dynamics are quite complex. Here we will discuss the scientific basis and understanding of centrifugation and operation of various types of available centrifuges as commonly used in separation in biotechnology. In the simplest terms, for a centrifuge processing a wet feed suspension after centrifuging, a centrate, supernatant, or overflow containing a small amount of suspended solids leave the centrifuge together with a moist concentrate, wet cake, or underflow. This is depicted in Figure 1.10. There could be also another input such as chemicals (coagulants and flocculants) added to flocculate the feed suspension (not shown in Figure 1.10). Based on the previous discussion, the valuable protein product can be in the fine suspended solids, such as the inclusion bodies, crystals or precipitants containing protein, or in the centrate liquid phase, as in the extracellular protein expression (yeast and mammalian cells). The centrifuge needs to be tuned to separate the product from the rest (waste or recycle stream). Depending on the specific process, as discussed below, some metrics or measures are commonly used to assess the centrifugal separation.

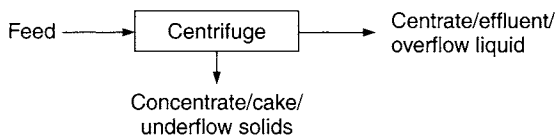


**Figure 1.10** Typical input and output streams of centrifugation

## 1.7 Separation Metrics

Several measures of centrifuge performance are common – protein yield, suspended solids in centrate or solid recovery, throughput or capacity, and cell viability.

### 1.7.1 Protein Yield

For a soluble protein expressed from extracellular process, one important measure of the separation performance of the centrifuge is the protein yield  $Y$ . Yield is defined as the ratio of the amount (e.g. kg/min or gm/min) of protein recovered in the liquid product to the amount (kg/min or g/min) of protein in the feed to the centrifuge. A complete recovery of protein without loss is 100%. Usually the yield should be very high before the separation process can be considered viable. A 90% or higher yield is not untypical. The specific yield depends on how difficult the separation is. An example on protein yield is given respectively in Chapters 7 and 8.

For continuous-feed centrifuge, the volumetric rate (L/m) and protein concentration of both feed and centrate need to be measured respectively for calculation of yield. For batch-feed centrifuge, the volume and protein concentration of both feed and supernatant (i.e. centrate) should be measured respectively for the yield calculation. It is evident that liquid loss in the concentrate or cake affects yield as the protein is dissolved in liquid, therefore the amount of liquid in the concentrate should be minimized (see Chapter 7).

### 1.7.2 Centrate Suspended Solids

The centrate suspended solids should be minimized unless this is for classification, wherein finer sized solids in the centrate are separated from larger solids in the concentrate as found for separating cell debris from inclusion bodies. A measure of clarity of the liquid centrate is the amount of suspended solids by weight, or by bulk volume after the centrate is spun in a spintube centrifuge for a prescribed time. For cell culture, only fine solids in the submicron range escape, with the centrate or supernatant to be ultimately captured by the downstream filter.

An indirect method of assessing centrate suspended solid is to measure the optical opacity (or turbidity) of the centrate liquid. The turbidity measurement should be calibrated against a standard on a frequent basis. A consequence of good clarification is that the solids recovered by sedimentation kg/h (dry basis) compared to the feed solids kg/h (dry basis) should be very high. The ratio is referred to the solid recovery  $R_s$ . When  $R_s$  is at 100%, this implies perfect separation and there is no solid in the product centrate or supernatant. For cell culture, we may achieve, say, 99.9% recovery of cells by centrifugation, leaving minimal cells escaped in centrate or supernatant.

### 1.7.3 Throughput Rate

The volumetric rate or capacity of centrifuge, in L/min, is an important measure of the volumetric liquid throughput capacity that a centrifuge can attain. Once the total capacity (size and number) of fermenter or bioreactor is fixed, the rate of the centrifuge(s) is determined and this in turn bears out the total capacity (size and number) of centrifuges. High-rate larger centrifuges require fewer centrifuges when compared to low-rate smaller centrifuges. On the other hand, a spare centrifuge needs to be furnished to cover the operating centrifuges when one of these centrifuges is rotated out for maintenance. Again, the operation planning requires the information on centrifuge throughput rate.

### 1.7.4 Cell Viability

Mammalian cells are gaining popularity in expressing protein as there is more flexibility in pursuing this route. However, unlike plant cells or yeast, mammalian cells are very shear sensitive as they do not have a cell wall. They are highly susceptible to shear such as during acceleration of the feed stream. Cells can be destroyed in the process, releasing an intracellular protein substance that can be harmful for downstream purification (cross-contamination of product protein) and finer debris which renders the separation problem more difficult, resulting in increased suspended solids loading up the depth filter. As a minimum, cell viability of mammalian cell lines should be maintained at a high level when making separation using production centrifuges. This will be discussed in detail in later chapters.

In subsequent chapters, the principle of centrifugation, types of centrifuges, application of centrifuges, selection, sizing, modeling and scale-up will be discussed.

## 1.8 Summary

In this chapter, some important applications in biotechnology, such as manufacturing of drug substances purely from biological derived products, have been presented. These processes are discussed generically so that they can be applicable for various situations. Also, it is important to understand that centrifugation should be partnered closely with other process equipment, both upstream and downstream, to make the entire process work following an integrated approach. Various separation metrics for centrifugation are discussed, including protein yield, centrate

suspended solids, throughput and cell viability. These subjects will be taken up in greater detail later in the text.

## References

- [1] C. Ratledge and B. Kristiansen, *Basic Biotechnology*, Cambridge University Press, 2001.
- [2] J. Sheppard, Spilling the genes: What we should know about genetically engineered foods, *The Genetic Forum*, 1996.
- [3] J.E. Smith, Safety, moral, social and ethical issues related to genetically modified foods, *Euro. J. Genet. Soc.* 2, pp. 15–24, 1996.
- [4] W.-S. Hu and M.V. Preshwa, Mammalian cells for pharmaceutical manufacturing, *ASM News*, 59(2), pp. 65–68, 1993.
- [5] R. Langer, Perspectives: Drug delivery – drugs on target, *Science*, 293: 58–59, 2001.
- [6] M. Prausnitz, S. Mitragotri, R. Langer, Current status and future potential of transdermal drug delivery, *Nature Reviews Drug Discovery*, 3: 115–124, 2004.
- [7] M. Singh, L.D. Silva, T.A. Holak, DNA-binding properties of the recombinant high-mobility-group-like AT-hook-containing region from human BRG1 protein, *Biological Chemistry*, vol. 387, issue 10–11, pp. 1469, 2006.
- [8] C. Budde, M.J. Schoenfish, M.E. Linder, R.J. Deschenes, Purification and characterization of recombinant protein acyltransferases, *Methods: A Companion to Methods in Enzymology*, vol. 40, issue 2, pp. 143–150, October 2006.
- [9] M. Desai (ed.), *Downstream Processing of Proteins*, Humana Press, Totowa, NJ, 2000.
- [10] M.S. Verrall and M.J. Hudson (eds), *Separations for Biotechnology*, Ellis Horwood Publishers, Chichester, and Society of Chemical Industry, London, 1987.
- [11] P.A. Belter, E.L. Cussler, W.-S. Hu, *Bioseparations: Downstream Processing for Biotechnology*, John Wiley, New York, 1988.
- [12] G. Subramanian (ed.), *Bioseparation and Bioprocessing*, John Wiley–VCH, Verlag GmbH, 1998.
- [13] R.G. Harrison, P. Todd, S.R. Rudge, D. Petrides, *Bioseparations Science and Engineering*, Oxford University Press, New York, 2003.
- [14] M.R. Ladisch, *Bioseparations Engineering: Principles, Practice, and Economics*, John Wiley, New York, 2001.
- [15] W.W.F. Leung, *Industrial Centrifugation Technology*, McGraw-Hill, New York, 1998.
- [16] W. Stahl, *Industrie-Zentrifugen, Maschinen-Verfahrenstechnik*, Dr. M Press, Maennedorf, Germany, 2004.
- [17] W.W.F. Leung and A.H. Shapiro, Dewatering of fine-particle slurries, *Minerals and Metallurgical Processing*, vol. 19, issue 1, pp. 1–8, February 2002.

---

## Problems

- (1.1) Can you engineer protein to be expressed reliably in intracellular contents of the cells in the form of soluble substance instead of in inclusion bodies (solid) using *E. coli* or *Bacillus subtilis*?
- (1.2) Assuming you can successfully express protein in intracellular form as in Problem (1.1), what are the downstream processes to extract, separate and purify the protein at the time of harvest?
- (1.3) If the protein from Problem (1.1) is in solid form, such as inclusion bodies which are 0.5 micron in equivalent diameter and specific gravity of 1.3, after homogenizing the bacteria cell how would you separate the inclusion bodies from other insolubles in the cells which are, say, 0.3 micron and smaller, together with other unlysed cells  $1 \times 3$  microns, assuming the insolubles and the unlysed bacteria have a specific gravity of 1.2?
- (1.4) Name a few more difficult bioseparation examples? What are the difficulties and how would you propose to overcome such difficulties?
- (1.5) In the process flow sheet shown in Figure 1.9, which is the most difficult step, and why? How would you address this most difficult step?
- (1.6) What are the pros and cons in using high centrifugal force to filter a biological solid, such as running equivalent to 10,000 times the Earth's gravity, through an ultrafiltration membrane?
- (1.7) Why can't you always resort to using high centrifugal acceleration, such as half a million times the Earth's gravity, to effect sedimentation as this apparently will overcome small density difference, viscous liquid, and small cell sizes of about one micron?



# Principles of Centrifugal Sedimentation

## 2.1 Introduction

Centrifugation makes use of high-speed rotation to generate centrifugal force acting on phases with different densities. Heavier phases tend to migrate to a location at a larger radius (toward the bowl periphery) while lighter phases are displaced to a location at smaller radius (toward the axis of the bowl). For continuous feed rate, dynamics is very important and some of the fluid dynamics in a rotating frame (such as a rotating bowl) is highly non-intuitive compared to the same occurring in a non-rotating reference frame. In this chapter, we will first present some non-intuitive phenomena such as Coriolis effect [1] and quadratic pressure behavior; this is followed by discussion of more intuitive key mechanisms such as centrifugal force and Stokes' law in sedimentation.

## 2.2 Non-intuitive Phenomena

### 2.2.1 Pressure Distribution

Under the Earth's gravitational acceleration,  $g$ , the hydrostatic pressure of a liquid varies linearly with increasing depth of the liquid, as shown in Equation 2.1.

$$p = p_a + \rho_L g h \quad (2.1)$$

In Equation 2.1,  $\rho_L$  is the liquid density,  $g$  is the Earth's gravity ( $9.81 \text{ m/s}^2$ ), and  $h$  is the liquid depth from the liquid surface at atmospheric pressure  $p_a$ . On the other hand, for a liquid rotating under a solid body in a container or bowl, the static pressure increases to the second power of increasing radius, as shown in Equation 2.2. Any change in radial distance produces larger change in pressure.

$$p = p_a + \frac{1}{2} \rho_L \Omega^2 (R^2 - R_p^2) \quad (2.2)$$

In Equation 2.2,  $\Omega$  is the angular rotational speed,  $R_p$  is the radius at the liquid pool surface and  $R (\geq R_p)$  is a radius in the liquid pool. The fluid pressure, which varies more than linearly proportional with radius, is another indication that a rotating fluid behaves non-intuitively compared to common experience encountered under non-rotating flow, in which fluid pressure varies linearly with fluid depth. Both the Earth's 'gravitational pressure distribution' and the 'centrifugal pressure distribution' are delineated, respectively, in Figure 2.1.

### 2.2.2 Coriolis Effect

Consider a ball rolling over a turntable rotating anticlockwise as shown in Figure 2.2. Once the ball enters the rotating turntable, it is subject to an additional Coriolis acceleration that orients perpendicular to the

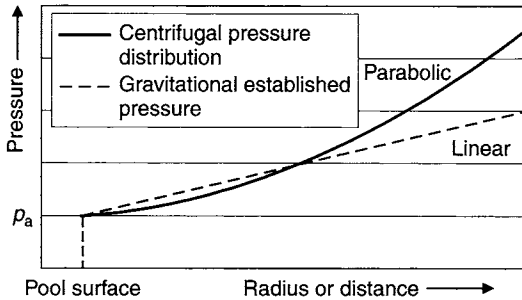


**Figure 2.1** Hydrostatic pressure distribution under the Earth's gravitational acceleration and centrifugal acceleration

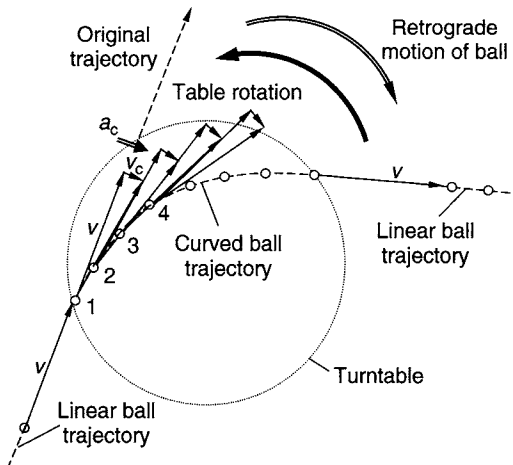


**Figure 2.2** Ball trajectory changing in a rotating turntable

velocity and specifically directs  $90^\circ$  clockwise away from the velocity vector. This Coriolis acceleration acts to skew the trajectory of the ball towards a direction opposite to that of rotation. The latter is referred to as *retrograde* motion [2]. As soon as the ball leaves the turntable, it again follows a straight path. The Coriolis acceleration is given by

$$\vec{a}_c = -2\vec{\Omega} \times \vec{v}_r \quad (2.3)$$

$\vec{\Omega}$  is the angular rotation vector (it is directed out of the paper when the sense of rotation is counterclockwise using the right-hand rule), and  $\vec{v}_r$  is the relative velocity vector in the rotating reference frame of the turntable. In Figure 2.2, take the relative velocity  $v_r = v$ ,  $v_c$  is the average Coriolis velocity as a result of the Coriolis acceleration  $a_c$  for an infinitesimal time  $\Delta t$ . The path that the ball takes is a curved trajectory toward the clockwise direction (retrograde motion) opposite to the rotation direction (anticlockwise) as a consequence of Coriolis velocity and acceleration directing the ball perpendicular rightward from the direction of the velocity  $v$ . (It is noted that given  $v_c = 1/2a_c\Delta t$ ,  $v_c$  is small as  $\Delta t$  is infinitesimally small, this does not change the magnitude but it does change the direction of the velocity vector  $v$  continuously until the ball leaves the turntable.)

A corn starch suspension was rotated by stirring using an external mixer (not shown), as depicted by the schematic in Figure 2.3a. At  $t = 0$ , stirring stops and the suspension is allowed to settle. Figures 2.3b–d shows, respectively, a sequence of pictures taken at different time intervals after the stirring had stopped. The end result after some time is that the suspended corn starch particles settled on the bottom of container at the center. Figure 2.3b shows that the suspended particles were still rotating with the flow at the periphery of the circular pan after a short time interval when stirring had ceased. Figure 2.3c shows that the corn starch particles settled as they were brought to the container center by secondary flow at a slightly longer time. Figure 2.3d shows that after 40 s the secondary flow had subsided, and particles concentrated and settled at the center of the container.

The diffusion coefficient  $D$  for corn starch as reported in the literature [3] is  $6.5\text{--}9.8 \times 10^{-6} \text{ cm}^2/\text{s}$  for temperature between  $7^\circ\text{C}$  and  $60^\circ\text{C}$ . Given the radius of the container is 20 cm, then the time for a corn starch particle to diffuse from the periphery to the center would have taken a long time, as shown by the following calculation.

$$t = \frac{L^2}{D} = \frac{20^2}{9.8(10^{-6})} \frac{1}{(3600)(24)(365)} = 1.29 \text{ years}$$

Some recent work [4] shows that the diffusion coefficient is even smaller than the values reported [3]. This translates to even longer time (at least

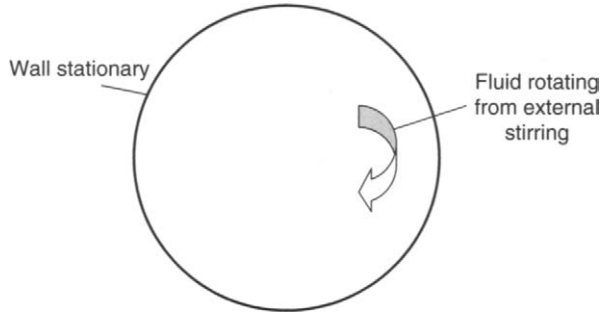


**Figure 2.3a** Fluid rotating from external stirring in a stationary container

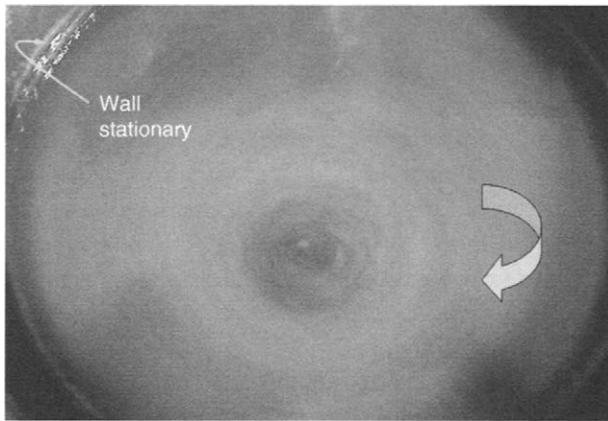


**Figure 2.3b** Liquid with suspended particulates forced to rotate by stirring; stirring stopped at  $t = 0$ , photo taken after stirring stopped at  $t = 5$  s, liquid still rotates



**Figure 2.3c** Photo taken at  $t = 25$  s after stirring stopped, liquid coming to standstill, particulates accumulate near center

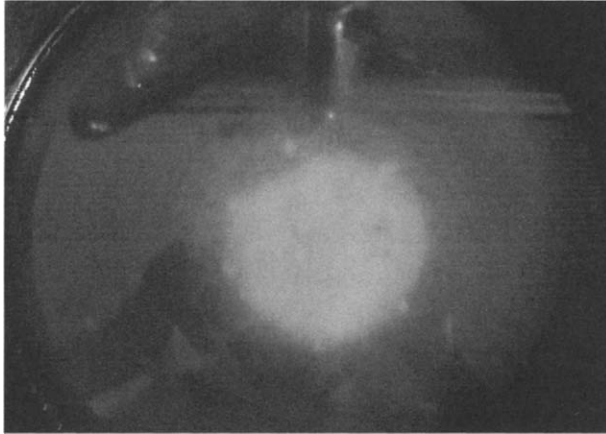


**Figure 2.3d** Photo taken at  $t = 40$  s, heavier solids (corn starch) sedimenting and accumulating at the center of the container

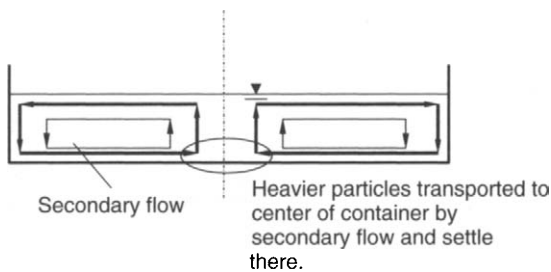


**Figure 2.3e** Cross-section of the diametric plane showing solids distribution being affected by both secondary flow from previous stirring and sedimentation of heavier solids

10 times) if diffusion is the mechanism behind the transport of particles. Irrespective of the actual value of diffusion coefficient for corn starch, slow mass diffusion could have never transported particles to the center of the container in 40 s if not for the fact that the secondary circulatory flow is doing the actual transport of the corn starch. Figure 2.3e sketches the secondary flow pattern responsible for transport during spindown of the liquid! It is equivalent to how tea leaves settle toward the center of the cup after stirring and flow have stopped.

## 2.3 Intuitive Phenomena

Besides the non-intuitive phenomena presented in the foregoing, there are other phenomena that occur in a centrifuge that are more intuitive than the ones mentioned, and they will be discussed in the following.

### 2.3.1 Centrifugal Acceleration

The magnitude of the centrifugal acceleration  $G$  is related to the tangential velocity  $v$  and the radius  $R$  from the axis of rotation via the kinematic relationship,

$$G = \frac{v^2}{R} \quad (2.4)$$

For the special case whereby the entire body rotates as a solid-body, the tangential velocity is linearly proportional to the radius  $R$  (see Figure 2.4), thus

$$v = \Omega R \quad (2.5a)$$

The proportional constant of the linear relationship is the angular speed,  $\Omega$ . Using Equations 2.4 and 2.5, the centrifugal acceleration  $G$  for a solid-body rotation becomes

$$G = \frac{v^2}{R} = \Omega^2 R \quad (2.5b)$$

The centrifugal acceleration is often expressed in terms of the Earth's gravitational acceleration  $g$  ( $= 9.81 \text{ m/s}^2$ ). The ratio between  $G$  and  $g$  is referred to as relative centrifugal force (RCF).

$$\text{RCF} = \frac{F_G}{F_g} = \frac{mG}{mg} = \frac{G}{g} = \begin{cases} \frac{v^2}{gR} \\ \frac{\Omega^2 R}{g} \end{cases} \quad (2.6a,b)$$

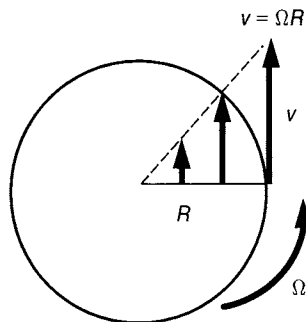


**Figure 2.4** Tangential velocity increases linearly with increasing radius from the axis of rotation for solid-body rotation

Equations 2.6a and 2.6b are for general cases (not attaining solid-body motion) and for solid-body rotation, respectively. With commonly used engineering units wherein  $v$  is expressed in m/s,  $\Omega$  in rpm, diameter  $D$  ( $= 2R$ ) in mm, thus

$$\frac{G}{g} = \begin{cases} 203.87 \frac{v^2}{D}, & v \neq \Omega R \\ 5.5893 \times 10^{-7} (\text{RPM})^2 D, & v = \Omega R \end{cases} \quad (2.6c,d)$$

For the case of a bowl with a diameter of 500 mm rotating at 6000 rpm, the  $G/g$  ratio becomes 10,061 or  $G = 10,061g$ . Figure 2.5 compiles a list of centrifuges with various speeds and diameters under solid-body rotation using Equation 2.6d. Small diameter centrifuges operate at lower capacity but at higher  $G$ , whereas large diameter centrifuges operate at higher capacity but at lower  $G$ . The upper limit for each type of centrifuge is only nominal. There are always exceptions depending on the specific design and material of construction as offered by the manufacturer.

The angular velocity, rpm, of the centrifuge may not be known if a strobe or a speed tachometer is not available for making measurement. However, if the centrifuge is belt-driven from a motor of known speed (from the name plate), then one can use an approximate kinematic relation to back out the centrifuge speed assuming little-to-negligible belt slip as follows (see Figure 2.6).

$$\text{rpm}_{\text{centrifuge}} = \text{rpm}_{\text{motor}} \frac{D_{\text{motor}}}{D_{\text{centrifuge}}} \quad (2.7a)$$

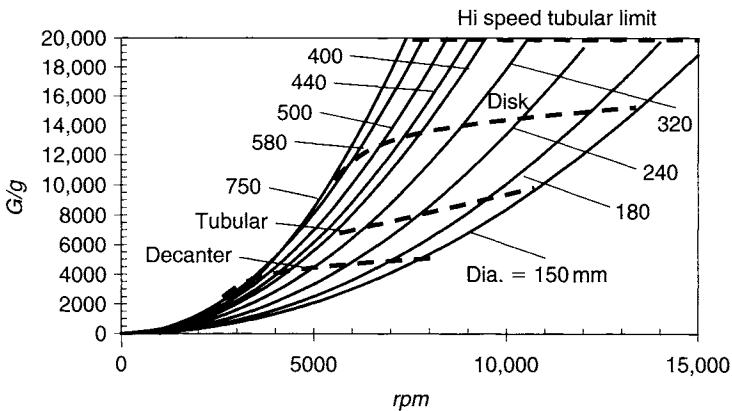


**Figure 2.5** Relative centrifugal acceleration versus rpm for various bowl sizes and nominal max  $G$  limits (dash curves) for various types of centrifuges

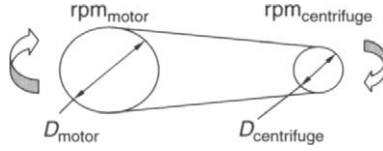


**Figure 2.6** Pulley ratio of driver and driven on rotation speed adjustment

or

$$\text{rpm}_{\text{centrifuge}} = \text{rpm}_{\text{motor}} \frac{N_{\text{motor}}}{N_{\text{centrifuge}}} \tag{2.7b}$$

$D$  is the diameter of the sheave or pulley, and  $N$  is the number of teeth on the gear. It is understood that the motor speed information can be spec out from the motor. The linear velocity of the pulley/sheave and gear are assumed to be the same or nearly the same in both Equations 2.7a and 2.7b.

**2.3.2 Fluid in a Centrifuge Bowl not at Solid-body Motion**

When a fluid is introduced to a rotating bowl, it takes time for the fluid in the bowl to accelerate to a solid-body rotation. In the interim, the tangential velocity fluid is less than that established for solid-body rotation, Equation 2.5. It is apparent that the higher the feed rate the less chance there is for the fluid to be accelerated to a solid-body motion. This will be discussed further in Chapter 4. Likewise, when fluid is suddenly directed from one radius to another radius significantly different from the initial radius, it takes some adjustment with slip and skidding before the fluid adjusts to the solid-body rotation speed at the new local radius. This scenario is commonly found for centrifuges with continuous feeding.

A fluid is accelerated or decelerated by viscous diffusion or by secondary flow. Viscous diffusion is used to transfer momentum from the solid wall of a rotating bowl to the adjacent fluid layer, which is rather slow and ineffective, as has been demonstrated earlier. A more effective way of accelerating and decelerating a fluid is by generating secondary flow.

One can define the acceleration efficiency  $\eta_a$  [5] to quantify the velocity of a fluid  $v$  in a container compared to that at solid-body rotation  $v = \Omega R$ .

$$\eta_a = \frac{v}{\Omega R} \tag{2.8}$$

In fact,  $\eta_a$  can change in as much as  $v$  can change in space and time. The tangential velocity and centrifugal acceleration for a fluid can be expressed, respectively, as

$$v = \eta_a \Omega R \quad (2.9)$$

$$G = \frac{v^2}{R} = \eta_a^2 \Omega^2 R \quad (2.10)$$

Comparing Equation 2.5b for a solid-body rotation to the case of a fluid which may not be under solid-body rotation Equation 2.9, it follows that the ratio of the two, which is defined as  $G$  efficiency  $\eta_G$ , is related to the acceleration efficiency  $\eta_a$  by

$$\eta_G = \frac{G}{G_{sb}} = \frac{(v^2/R)}{\Omega^2 R} = \eta_a^2 \quad (2.11)$$

In summary, the following conditions are applicable to Equations 2.8–2.11 wherein

- $\eta_a < 1$  for under-accelerated fluid
- $\eta_a = 1$  for fluid establishing solid-body motion
- $\eta_a > 1$  for over-accelerated fluid [5,6].

For example, given a fluid assuming three different possible scenarios, respectively,  $\eta_a = 70\%$ ,  $100\%$ , and  $140\%$  in a rotating bowl with  $R = 0.2$  m and  $\Omega = 500$ /s. Based on Equations 2.4–2.6,  $v$ ,  $G$ ,  $G/g$ , and  $\eta_G$  can be calculated; see the results in Table 2.1.

**Table 2.1** Speed,  $G$  and efficiencies for a fluid under various conditions in a rotating bowl for the example where  $R = 0.2$  m,  $\Omega = 500$ /s

	<i>Underspeeding</i>	<i>Solid-body rotation</i>	<i>Overspeeding</i>
$v$ (m/s)	70	100	140
$G$ (m/s <sup>2</sup> )	24,500	50,000	98,000
$G/g$	2497	5097	9990
Acceleration efficiency $\eta_a$	70%	100%	140%
$G$ efficiency $\eta_G$	49%	100%	196%

**Table 2.2** Speed,  $G$  and efficiencies for a fluid moved abruptly to a new radius either larger ( $R_2$ ) or smaller ( $R_3$ ) compared to initial radius  $R_1 = 0.2$  m and with  $\Omega = 500/s$

	$R_1$	$R_2$	$R_3$
$R$ , m	0.2	0.3	0.15
$v$ , m/s	100	67	133
$V_{sb}$ , m/s	100	150	75
$G/g$	5097	1510	12,081
$G_{sb}/g$	5097	7645	3823
Acceleration efficiency (%)	100	44	178
$G$ efficiency (%)	100	20	316

When a fluid at radius  $R_1$  and with tangential velocity  $v_1 = \eta_{a1}\Omega R_1$  is taken to a different radius  $R_2$ , the new tangential velocity can be determined by conservation of angular momentum as follows.

$$v_1 R_1 = v_2 R_2 \quad (2.12)$$

$$v_2 = \frac{v_1 R_1}{R_2} \quad (2.13)$$

$$\eta_{a2} = \frac{v_2}{\Omega R_2} = \frac{\left( \frac{\eta_{a1} \Omega R_1^2}{R_2} \right)}{\Omega R_2} = \eta_{a1} \left( \frac{R_1}{R_2} \right)^2 \quad (2.14)$$

$$\eta_{G2} = \frac{v_2^2}{R_2} \frac{1}{\Omega^2 R_2} = \eta_{a1}^2 \left( \frac{R_1}{R_2} \right)^4 = \eta_{G1} \left( \frac{R_1}{R_2} \right)^4 \quad (2.15)$$

The above implies that when the fluid is brought abruptly from a small radius to a new radius that doubles the original radius, the acceleration efficiency is reduced to 25% of the original efficiency. Likewise, when the new radius is half of that of the original, this overspeeds the fluid to 400% of the original efficiency. Table 2.2 shows an example calculation of speed,  $G$ , acceleration efficiency as well as the  $G$  efficiency for both increased and reduced radius respectively.

### 2.3.3 Regimes of Sedimentation

The sedimentation behavior of a suspension may be classified into four categories in accordance with the solids concentration in suspension

and the degree of aggregation of solids. This is illustrated in Figure 2.7, which in essence is a modified Fitch diagram. For dilute concentration and low degree of solids aggregation, solid particles settle independent of each other and they follow the Stokes' law of sedimentation, which was developed for spherical particles settling under the Earth's gravity,  $1\text{ g}$  ( $9.8\text{ m/s}^2$ ). As solids concentration increases the sedimentation rate of particles is affected hydrodynamically by neighboring particles despite there being no physical contact between them. Under this condition the settling rate may be less, or even higher, than the Stokes' settling velocity.

For a given solids concentration, as the particles tend to agglomerate due to weak or negligible electric repulsion they form an aggregate and settle as a large floc, which can be modeled by fractal analysis. This allows both small and large particles to settle at the same speed, also known as zone settling, without discriminating the size of individual particles. The addition of coagulant and flocculant (polymer) may further promote formation of agglomerates and flocs leading to zone settling; while introduction of dispersant extends the discrete particle settling condition well into the concentrated solids region in which hindered and zone settling normally prevail (see Figure 2.1). The former finds applications such as clarification of waste slurries, while the latter finds applications such as classification of valuable fine-particle slurries for the coating and pigment market.

Dense thick slurry forms networking as particle concentration and the degree of aggregation both increase in a suspension. Under gravitational body force the solid network or matrix compresses downward (compaction) while liquid expresses counter-currently upward (expression). This is delineated as the region to the upper right in Figure 2.7.

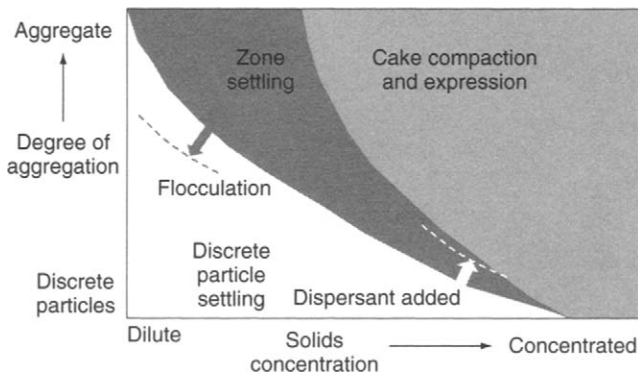


**Figure 2.7** Different regimes of sedimentation

### 2.3.4 Stokes' Law

Consider the separation velocity  $v_{so}$  of a spherical solid with diameter  $d$  and with density  $\rho_s$ , settling under gravitational acceleration  $g$  in a lighter fluid phase (liquid) with density  $\rho_L$  and fluid viscosity  $\mu$ . The settling velocity is determined under steady state by balancing all the relevant forces acting on the spherical solid. They are the viscous drag force, buoyancy force from the suspending fluid, and the body weight of the solid. The settling velocity thus becomes

$$v_{so} = \frac{1}{18} \frac{(\rho_s - \rho_L)gd^2}{\mu} \quad (2.16)$$

The subscript 'o' refers to settling of an individual particle with no influence from its neighboring particle in an ideal dilute suspension. Under high-speed rotation, the gravitational acceleration  $g$  is replaced by the centrifugal acceleration  $G$ , given by Equation 2.6a,b depending on whether the fluid has attained a solid-body rotation. Thus

$$v_{so} = \frac{1}{18} \frac{(\rho_s - \rho_L)Gd^2}{\mu} \quad (2.17)$$

Based on Equation 2.17, it is evident that high  $G$ , larger sized particle, viscosity reduction due to elevated temperature, all enhance separation or settling velocity. Figure 2.8 shows the viscosity of water with increasing temperature. Between 10°C and 60°C, the viscosity drops rapidly with increasing temperature. As such, it is advantageous to operate at the highest possible operating temperature for improving separation yet without affecting or destroying the product protein and functional biologics.

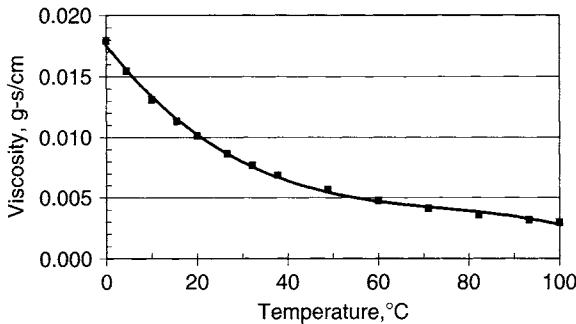


**Figure 2.8** Water viscosity as a function of process temperature

The cell density for biological cells in aqueous suspension is nominally about 1.0–1.1 g/mL, and liquid density of aqueous suspension is about 1 g/mL. Thus, the density difference between the two is about 0.0–0.1 g/mL, which is indeed very small. The viscosity of liquid can be anywhere from 1 cP (water at room temperature) to over 1000 cP depending on the protein and various biologics (such as RNA) dissolved in solution. Separation can be a very difficult task with cell sizes trending from 50 microns down to 1 micron and below as separation rate, in accordance to Equation 2.17, varies as the quadratic power of particle size.

Table 2.3 shows some common biological cell sizes. Some common cells used in protein expression are large mammalian cells, smaller yeast cells and much smaller bacteria cells. On the other hand, cell debris is much smaller and they are typically in the submicron range. They are removed by classification in the overflow after cell lysing.

**Table 2.3** Biological cells

<i>Cells</i>	<i>Size (microns)</i>
Plant	60–100
Mammalian	10–40
Chinese Hamster Ovary	10
Yeast	7–10
Bacteria	1–2
Cell debris	0.2–0.5

### 2.3.5 Settling with Concentrated Solids

As solids concentration increases, the settling rate  $v_s$  is reduced as each settling particle feels the effect from neighboring settling particles;  $v_s$  should be below that of the Stokes' free settling velocity  $v_{so}$ . The well-known Richardson and Zaki [7] correlation is frequently used to quantify the hindered settling effect.

$$\frac{v_s}{v_{so}} = (1 - \phi_f)^n \quad (2.18)$$

$\phi_f$  is the actual solid volume concentration of solids in suspension and  $n$  is an exponent;  $v_{so}$  is the Stokes' settling velocity of a single particle regardless of whether it is due to gravitational acceleration via Equation 2.16 or centrifugal acceleration via Equation 2.17. The hindered settling behavior of Richardson and Zaki (Equation 2.18) is plotted in Figure 2.9

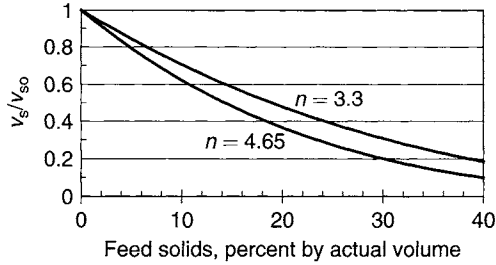


**Figure 2.9** Effect of hindered settling due to suspension solid concentration based on correlation of Richardson and Zaki for  $n = 4.65$  and  $3.3$ , respectively

for  $n = 4.65$  and  $3.3$  respectively. As can be seen for the case of  $n = 4.65$ , the separation velocity is reduced by 40% as the solids volume increases to 10%. The 40% solids on an actual volume basis for the abscissa scale in Figure 2.9 could have corresponded very well to 60–90% bulk volume (including both solids and liquid volume) depending on packing density. Solids concentration by bulk volume is a more readily available index as it is measured readily in practice using a rotating test tube centrifuge spinning for an arbitrary pre-fixed time duration. For the case with  $n = 3.3$ , the reduction in settling velocity due to hindered settling as compared with discrete Stokes' settling is less for a given solids concentration.

It should be noted that, depending on the solids and free ions in the aqueous phase, the solids may not act as individual discrete particles but may act as a blanket of solids settling all at one rate and speed independent of particle size once solids concentration increase beyond a certain level in which the particles start to form a network (i.e. moving right and up in Figure 2.7).

## 2.4 Process Functions

There are several process functions using centrifuges in biotech separation. These are listed below.

### 1 Separation (solid/liquid, solid/liquid/liquid and solid/solid/liquid separation)

Centrifuge can be used for solid-liquid separation provided the solids are heavier than the liquid. Centrifuge can also be used to separate a

heavy phase, and two lighter liquid phases, with one of the lighter phases being lighter than the other. As discussed, solids can be lighter than liquid and separation is by flotation of the dispersed solid phase.

## 2 **Clarification – minimal solids in liquid product**

Centrifuge can be used to clarify the discharged separated lighter liquid phase. The objective is to minimize the discrete suspended solids in the light continuous phase. Usually, only fine submicron biosolids are left uncaptured by centrifugation and they escape with the discharged light phase.

## 3 **Classification – sort by size and density**

Centrifuge is used to classify solids of different sizes. One of the several possible applications is to classify crystals of different size range, with the finer submicron sizes leaving with the light phase and retaining only the larger sizes in the separated heavy phase. Either of the separated solids can be the product. For example, the larger crystals can be the product crystals while the finer crystals are returned to the crystallizer to grow to larger crystals. Another similar application is to classify smaller size cell debris in the light liquid phase from the heavier products after homogenizing cells.

## 4 **Degritting – remove oversized and foreign particles**

Degritting is similar to classification where unwanted particles, larger or denser, are rejected in the sediment, with product (smaller or less dense) overflowing in the lighter liquid phase. Another situation is where smaller unwanted particles are rejected in the light liquid phase, and valuable heavier solids are settled with the heavier phase.

## 5 **Thickening or concentration – remove liquid, concentrate solids**

Centrifuge is frequently used to concentrate the solid phase by sedimentation and compaction, removing the excess liquid phase in the overflow or centrate. This reduces the volume of the product in downstream processing.

## 6 **Separation and repulping – remove impurities by washing or diluting**

With a concentrated suspension containing contaminants such as salts and ions, it is diluted and washed so that the contaminants are dissolved in the wash liquid. Subsequently, the suspension is sent for centrifugation to remove the spent wash liquid with dissolved contaminants or finely suspended solids. Subsequently, the product can be further concentrated by centrifugation.

The aforementioned processes can be combined to achieve several objectives concurrently or in series.

## 2.5 Summary

In this chapter, several non-intuitive phenomena, such as nonlinear increase in pressure with linear change in radial distance and Coriolis acceleration and associated force, have been discussed. Despite this they may not appear quite relevant, however they actually dictate some critical control on rotating flow and separation; as such their effects on flow and separation need to be understood as innovative centrifuge design can thus be developed. Other more intuitive phenomena, such as discrete particle settling versus aggregate of particles settling, are discussed. These cover the entire spectrum of real life possibilities. In particular, this chapter also presents Stokes' free settling of single particles and settling of a cluster of discrete particles at higher solids concentration at which particles settle under hydrodynamic influence of each other. Finally, various process functions of centrifugation, covering separation, clarification, classification, degritting, thickening, and impurities removal/valuable recovery by separation and repulping are discussed.

## References

- [1] H. Greenspan, *The Theory of Rotating Fluids*, Cambridge University Press, London, 1968.
- [2] H. Greenspan, Centrifugal separation of a mixture, *J. Fluid Mechanics*, 1983.
- [3] R.B. Leslie, P.J. Carillo, T.Y. Chung, S.G. Gilbert, K. Hayakawa, S. Marousis, G.D. Saravacos, M. Solberg, Water diffusivity in S-based systems, in H. Levin and L. Slade (eds), *Water Relationships in Food* (pp. 365–390), Plenum Press, New York, 1991.
- [4] A. Calzetta Resio, R.J. Aguerre, C. Suarez, The drying of amaranth grain: mathematical modeling and simulation, *Braz. J. Chem. Eng.* vol. 22, no. 2, Apr./June 2005.
- [5] W.W.F. Leung, *Industrial Centrifugation Technology*, McGraw-Hill, New York, 1998.
- [6] W.W.F. Leung and A. Shapiro, An accelerating vane apparatus for improved clarification and classification in decanter centrifuges, *Transactions of Filtration Society*, vol. 1 (3), April 2001.
- [7] J.F. Richardson and W.N. Zaki, The sedimentation of a suspension of uniform spheres under conditions of viscous flow, *Chem. Eng. Sci.*, 3 (1954), pp. 65–73.

## Problems

- (2.1) For a bioseparation process by sedimenting under the Earth's gravity of  $9.81 \text{ m/s}^2$ , a suspension has biological cells with density of  $1100 \text{ kg/m}^3$

- in a liquid with density of  $1000 \text{ kg/m}^3$  and viscosity of  $0.001 \text{ Pa}\cdot\text{s}$ , assuming particles have equivalent spherical diameter of 10 microns. How long does it take for the particle to settle in a graduated cylinder of height 10 cm?
- (2.2) If a small dose of coagulant can neutralize the charges so that the particles in Problem (2.1) agglomerate in size to 33 microns with all other conditions the same, how long does the agglomerated particle settle for 10 cm? How would you compare this result with that of Problem (2.1)?
  - (2.3) Repeat the same problem as in (2.1) but with a particle of 1 micron simulating a red blood cell. How long does the particle take to settle to the bottom of a 10-cm high graduated cylinder?
  - (2.4) For a bioseparation process by sedimenting under centrifugal gravity 1000 times that of the Earth's gravity, a suspension has biological cells with density of  $1100 \text{ kg/m}^3$  in a liquid with density of  $1000 \text{ kg/m}^3$  and viscosity of  $0.001 \text{ Pa}\cdot\text{s}$ , assuming particles have equivalent spherical diameter of respectively (a) 0.33 micron and (b) 1 micron. How long does it take for each of the particles to settle in a long spintube with a height of 10 cm?
  - (2.5) For the same conditions as in Problem (2.4) with the suspension viscosity increasing to  $1 \text{ Pa}\cdot\text{s}$  due to the presence of soluble matter and contaminants, how long does (a) 0.33 micron particle and (b) 1 micron particle take to settle in a 10 cm distance under RCF (relative centrifugal force,  $G/g$ ) of 10,000? Can centrifuge still make separation? Why or why not?
  - (2.6) What can one conclude from Problems (2.1)–(2.5) on the effect of particle size,  $G/g$ , and viscosity?
  - (2.7) A feed stream has accelerated to the tangential speed of  $30 \text{ m/s}$  at a radius of  $0.1 \text{ m}$ . If the feed is allowed to abruptly arrive at a larger radius of  $0.12 \text{ m}$ , what is the tangential speed of that feed stream?
  - (2.8) For the problem in (2.7), if a pool is already at a solid-body rotation, what would be the tangential speed of the pool at  $0.12 \text{ m}$  radius if the angular rotation of the centrifuge is  $300/\text{s}$ ? Is there any difference between the feed speed and that of the pool which is already at solid-body rotation?
  - (2.9) What is the centrifugal acceleration of the feed expressed as a ratio of  $g$ ? What is the supposedly  $G/g$  (i.e. RCF) for the solid-body pool at  $0.12 \text{ m}$  radius rotating at  $300/\text{s}$ ?
  - (2.10) Express the (a) acceleration efficiency of the feed and (b) the  $G$ -efficiency of the feed mathematically in terms of appropriate variables or parameters. What is the relationship between these two efficiencies?



# Batch and Semi-Batch Centrifuges

In this chapter, spintube, centrifugal filter, ultracentrifuge, and tubular centrifuge are discussed.

Spintube, ultracentrifuge, and centrifugal filter are bench centrifuges wherein they are batch-fed and involve the manual removal of sediment. For all three types of centrifuges, there are specific steps/cycles during operation, respectively, for feeding, rotor acceleration (or acceleration followed by feeding for ultracentrifuge), separation (for spintube and ultracentrifuge) or filtration (for centrifugal filter), rotor deceleration, clarified liquid decanting, sediment removal, and cleaning. Centrifugal filter has various insert modules that facilitate various duties to be performed, including sedimentation, filtration, and purification.

Tubular centrifuge operates on a semi-batch basis with continuous feed until sediment fills the bowl and the discharged clarified liquid turns turbid, at which point sediment has to be removed. Then it goes through a series of cycles on pool drainage, deceleration, sediment discharge, and cleaning. Some tubular centrifuge designs require manual removal of sediment while other designs have built-in automatic sediment removal.

## 3.1 Spintube

Measurements can be made using spintube under different  $G$  and  $t$  to determine the separation characteristics of a given sample. If there are sufficient solids in the feed that forms a decent size of sediment or pellet, a physical method can be used to determine qualitatively the integrity from which the handleability/flowability of the sediment can be inferred. For example, a glass rod can be inserted in the tube [1] at the end of the test to determine the amount of penetration that the rod makes in the sediment. It is a measurement of the yield stress of the sediment. Such a physical method is largely subjective. Also, chemicals can be added to neutralize the charges and agglomerate the fine particulates in suspension.

Spintube centrifuges are typically divided into two different configurations. The first type is a swinging bucket, or horizontal head, wherein the tube support rests at the small diameter on a bracket (or adaptor) that allows the tube to swing out with the tube axis being perpendicular to the axis of rotation of the centrifuge in full-swinging position, as illustrated by the right schematic diagram in Figure 3.1a. Numerous combinations of tubes are possible for this configuration. The centrifuge can accommodate a minimum of a pair of spintubes, or multiple tubes secured in a cup or holder. Table 3.1 shows some of the many configurations that are available commercially. One case shows two 50-mL tubes diametrically opposite and the other case shows as many as four cups spaced 90-degree apart with each cup holding four 10-mL tubes. For achieving flexibility in

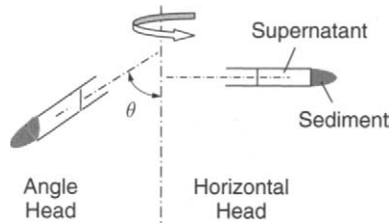


**Figure 3.1a** Angle head (left schematic) and horizontal head (right schematic) test-tube centrifuge

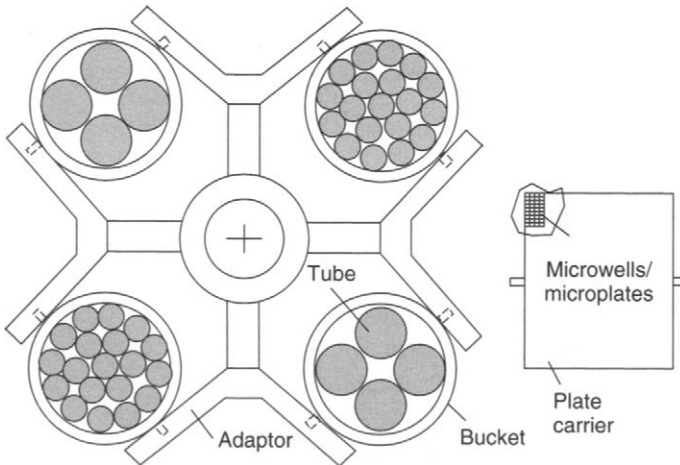


**Figure 3.1b** Left: Adaptor with swinging buckets with two diametrically opposing pairs with one pair each having 4 spintubes and the other pair each having 19 spintubes. Right: Plate carrier carrying microwells and microplates. The covers for the buckets and plate carrier are not shown

**Table 3.1** Some examples of horizontal head and angle head test-tube centrifuges

<i>Type</i>	<i>Number</i>	<i>Sample volume</i>
Horizontal head	2–16	10–50 mL
	To 296 microtubes	0.25 to 0.4 mL tube
Angle head ( $\theta = 40^\circ - 48^\circ$ )	2	600 mL bag
	6	250 mL bag
	60	15 mL bag
	4	50 mL tube
	48	0.5 mL tube

testing, the cups and support for multiple tubes can be interchanged with other bracket geometry that holds a small number of large-volume tubes or a large number of small-volume tubes. As an example of the latter, one can run  $60 \times 5/7$  mL,  $30 \times 15$  mL, and  $16 \times 50$  mL cell culture tubes or microplates without taking up additional space. Much smaller (0.25–0.4 mL) and large numbers (up to 296) of microtubes are also available. This can facilitate high-throughput screening.

As a demonstration on the different possible combinations, the left diagram of Figure 3.1b shows an adaptor for four swinging buckets, with one pair of diametrically opposing buckets each carrying four large tubes, and the other pair of diametrically opposing buckets each carrying 19 smaller tubes. The adaptor can also be used with microplates and microwells in a plate carrier (see right diagram of Figure 3.1b).

Microplates are small plastic reaction vessels. By design, they are trays or cassettes that are covered with wells or dimples arranged in orderly rows. These wells are used to conduct separate chemical reactions. The large number of wells, which typically number 96 or 384, depending upon the size of the microplate, allow for many different reactions to take place simultaneously. This can be useful if the goal is to determine a statistical basis for research results, to test for aberrations in an expected result, or to run a number of unrelated reactions at the same time. Microplates are ideal for high-throughput screening and research. They allow miniaturization of assays and are suitable for many applications, including drug testing, genetic study, and combinatorial chemistry. So far we have discussed centrifugation as being used to separate product from reactants based on density difference after chemical reaction; in

some cases it is used to enhance chemical reaction such as the use of microplates and microwells.

Angle head geometry or fixed-angle rotor can take higher centrifugal gravity  $G$  as the tubes are in a 'solid bowl' rotor with cut-outs that serve as tube holders or cups. The inclination between the tube centre axes and the vertical is typically between  $40^\circ$  and  $48^\circ$ . This is depicted in the left schematic of Figure 3.1a. Note that particles always settle along the direction of centrifugal gravity  $G$  which is perpendicular to the rotation axis. The trajectory of these particles follows the  $G$  field ( $90^\circ$  from vertical axis) and intercepts the wall of the angled tube ( $40\text{--}48^\circ$  from vertical axis), similar to an inclined plate settler [2]. This reduces the sedimentation path and settling time of particles and enhances particle capture. Various different sizes and numbers of tubes are available for the angle head centrifuges, some of which are listed in Table 3.1. For example, four 50-mL tubes can be used in one rotor, or as many as 48 0.5-mL tubes can be used in another rotor.

Most high-end bench centrifuge manufacturers provide precise micro-processor-based controls that ensure reproducible test runs in conformity with good laboratory practice (GLP) standards. To adjust protocols for spinning fragile samples, several acceleration and deceleration profiles are available with some designs. Some designs also provide refrigeration and cooling, maintaining a steady temperature from  $-10$  to  $40^\circ\text{C}$ , even at maximum speed.

For safety assurance, some designs have a double-lid locking system, armored chamber and other features to protect the operator. In case of excessive vibration, the rotor stops in seconds. Audible and visual messages alert operators to any anomalies. Some commercial vendors on spintube centrifuges are Beckman and Coulter, Eppendorf, Hermle Hettich, Kendro, Thermo/Forma and Thermo/IEC.

## 3.2 Centrifugal Filter

A centrifugal filter with a membrane filter or chromatography column can be inserted in a spintube for carrying out a variety of separation and purification functions on biosolids. The centrifugal filter can be a microspintube 15–20 mL with an insertion of a membrane module for separation or a chromatography column (also referred to as membrane absorber) for purification, as shown by the schematic in Figure 3.2. The centrifugal filter is inserted in a 50 mL spintube. Typically, the combo configuration can be used where centrifuges can attain 12,000 g. Smaller size microspintubes and containing tubes for addressing smaller samples are also available.

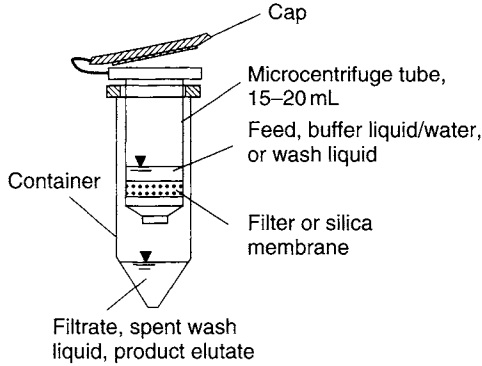


**Figure 3.2** Microcentrifuge tube 15–20 mL, housed in a larger containing tube, equipped with filter or membrane column

The following is an example of both separation and purification of RNA using a centrifugal filter. The objective is to separate RNA from a suspension containing RNA, DNA, salts, suspended particles, and other impurities. The centrifugal filter is first inserted with a microfiltration membrane, after which the mixture is added. Under centrifugation, micron-sized suspended contaminants and particles are removed by the microfiltration membrane. The microfilter is removed from the spintube, and the filtrate is decanted to a separate container. After cleaning, another microfilter with a chromatography column is inserted in the spintube. The liquid sample, now free from micron-sized suspended solids, is first chemically conditioned before pouring in the chromatography column. The liquid mixture runs through the column under  $G$ -force that further enhances the rate of the drainage process. Concurrent with liquid draining through the chromatography column, RNA is preferentially adhered to the column. Next, the column is washed under centrifugation with desalting liquid to remove salts and contaminants. Further, chemical/buffer liquid is added to the column subject to centrifugation to favor removal of DNA. Upon completion of removing DNA, purified RNA is released under centrifugal field from the column by elution using a conditioning agent. This example illustrates that the separation and purification process can be readily tailor-made for the specific process. Each step benefits from the enhanced centrifugal body force despite the liquid possibly being viscous, and normally takes a long time to flow through a column were this drainage process being carried out under the Earth's gravitational acceleration.

In general, sedimentation can be the first step followed by filtration and purification using the chromatography column. The centrifugal filter provides a comprehensive (all-in-one) package with interchangeable

modules for sedimentation, filtration and purification under the enhanced  $G$ -field.

### 3.3 Ultracentrifuges

An ultracentrifuge is also an angled spintube, and with a titanium rotor that provides mechanical integrity, i.e. for high shear and yield strengths. It can go up to 500,000–1,000,000  $g$  for separating very small particles, particles and liquid with a small density difference, and/or separation in a viscous liquid phase. A schematic of an ultracentrifuge is shown in Figure 3.3.

There are two kinds of ultracentrifuges: the analytical and the preparative. Both have important uses in molecular biology, biochemistry and polymer science. Theodor Svedberg invented the analytical ultracentrifuge in 1923, and won the Nobel Prize in Chemistry in 1926 for his research on colloids and proteins using the ultracentrifuge.

#### 3.3.1 Analytical Ultracentrifuge

In an analytical ultracentrifuge, a sample being spun can be monitored in real time through an optical detection system, using ultraviolet light absorption and/or an interference optical refractive index sensitive system. This allows the operator to observe the evolution of the sample concentration versus the axis of rotation profile as a result of the applied centrifugal field. With modern instrumentation, these observations are electronically digitized and stored for further mathematical analysis. Two kinds of experiments are commonly performed on these instruments: sedimentation velocity experiments and sedimentation equilibrium experiments.

Sedimentation velocity experiments aim to interpret the entire *transient sedimentation process*, and report on the shape and molar mass of the dissolved macromolecules, as well as their particle size-distribution. The size resolution of this method scales approximately with the square of the particle radii, and by adjusting the rotor speed of the experiment

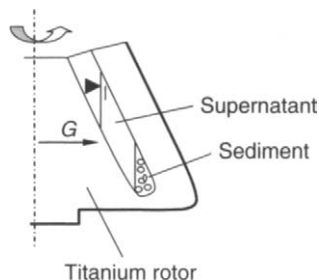


**Figure 3.3** Ultracentrifuge schematic

size ranges from 100 Da to 10 GDa can be covered. Sedimentation velocity experiments can also be used to study reversible chemical equilibria between macromolecular species, by either monitoring the number and molar mass of macromolecular complexes, by gaining information about the complex composition from multi-signal analysis exploiting differences in each component's spectroscopic signal, or by following the composition dependence of the sedimentation rates of the macromolecular system.

Sedimentation equilibrium experiments are concerned only with the *final steady state* of the experiment, where sedimentation is balanced by diffusion opposing the concentration gradients, resulting in a time-independent concentration profile. Sedimentation equilibrium distributions in the centrifugal field are characterized by Boltzmann distributions. This experiment is insensitive to the shape of the macromolecule, and directly reports on the molar mass of the macromolecules and, for chemically reacting mixtures, on chemical equilibrium constants.

The kinds of information that can be obtained from an analytical ultracentrifuge include the gross shape of macromolecules, the conformational changes in macromolecules, and size distributions of macromolecular samples. For macromolecules, such as proteins that exist in chemical equilibrium with different non-covalent complexes, the number and subunit stoichiometry of the complexes and equilibrium constants can be studied.

With interference and schlieren optics, the change in concentration can be measured as a dependence on time by the following equation:

$$\frac{S}{D} = \frac{1 - (\rho_L / \rho_p)}{RT} M \quad (3.1)$$

The above equation is known as the Svedberg equation.  $S$  is the sedimentation coefficient

$$S = \frac{v_{so}}{g} = \frac{(\rho_p - \rho_L)d^2}{18\mu} \quad (3.2)$$

$S$  is a ratio of the Stokes' settling velocity  $v_{so}$  to the Earth's gravitational acceleration  $g$ . It has a unit of time in seconds.  $R$  is the universal gas constant and  $T$  is temperature in Kelvin;  $\rho_p$  is the particle density and  $\rho_L$  is the liquid density;  $D$  is the diffusion coefficient. Molecular measurements typically give  $S$  in units of  $10^{-13}$  s is in honor of Svedberg; 1 svedberg is defined as  $10^{-13}$  s. From measurements, molecular weight  $M$ ,

sedimentation coefficient  $S$ , diffusion coefficient  $D$ , and partial specific volume  $1/\rho_p$  can be derived.

### 3.3.2 Preparative Ultracentrifuge

Preparative ultracentrifuges are available with a wide variety of rotors suitable for a great range of experiments. Most rotors are designed to hold tubes that contain the samples. Swinging bucket rotors or horizontal heads allow the tubes to hang on hinges so the tubes reorient to the horizontal as the rotor initially accelerates. Fixed-angle rotors are made of a single block of metal and hold the tubes in cavities bored at a predetermined angle. Zonal rotors are designed to contain a large volume of samples in a single central cavity rather than in tubes. Some zonal rotors are capable of dynamic loading and unloading of samples while the rotor is spinning at high speed. Figure 3.4a shows feed being introduced to the zonal centrifuge operating at, say, 2000 rpm after a sucrose solution with 10, 20, 30 and 40% with respective densities 1.0381, 1.0810, 1.127, and 1.1764 g/cm<sup>3</sup> is introduced to the zonal centrifuge. Figure 3.4b shows that after separation unloading can be effected by introducing water at the center while displacing product at the periphery. Figure 3.4c shows the opposite case, where water is introduced at the periphery displacing product at the center.

Preparative rotors are used in biology for pelleting of fine particulate fractions, such as cellular organelles (mitochondria, microsomes, and ribosomes) and viruses. They can also be used for gradient separations, in which the tubes are filled from top to bottom with an increasing concentration of a dense substance in solution. Sucrose gradients are typically used for separation of cellular organelles. Gradients of cesium salts with much wider density ranges are used for separation of nucleic acids. After the sample has spun at high speed for sufficient time to produce the separation, the rotor is allowed to coast to a smooth stop and the gradient is gently pumped out of each tube to isolate the separated components. This is also referred to as isopycnic separation. Great care is taken not to disturb the layers during intake and out-take.

### 3.3.3 Centrifugal Elutriation

The zonal centrifuge can be operated so that it can classify cells based on the sedimentation velocity. Assuming the cells are of the same density and shape, then classification is by size only. A special zonal rotor is operated such that fluid is introduced from the periphery of the rotor so that the fluid velocity just balances the particle settling velocity in the

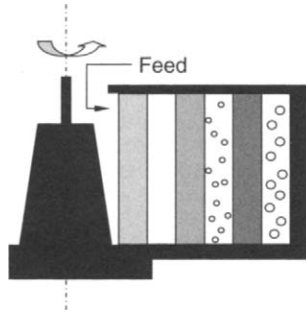


**Figure 3.4a** Feed is introduced to the zonal centrifuge after loading gradient solution, such as a sucrose or cesium chloride solution

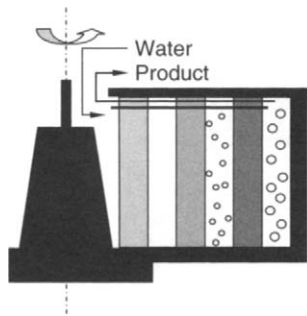


**Figure 3.4b** Product is unloaded by injecting water/buffer liquid at the center while product is removed at the periphery

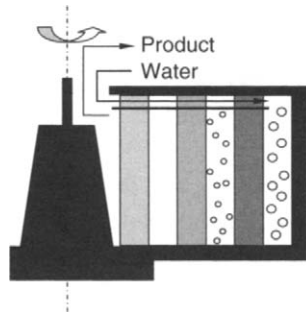


**Figure 3.4c** Product is unloaded by injecting water/buffer liquid at the periphery while product is removed at the center

separation zone, as illustrated in Figure 3.4d (for the purpose of illustration a linear geometry is shown instead of a radial geometry). If there are particles of smaller size, they will be carried by the fluid leaving the separation zone to exit at the small radius, while particles larger than the ones in the separation zone settle to the large radius and get collected at the exit.

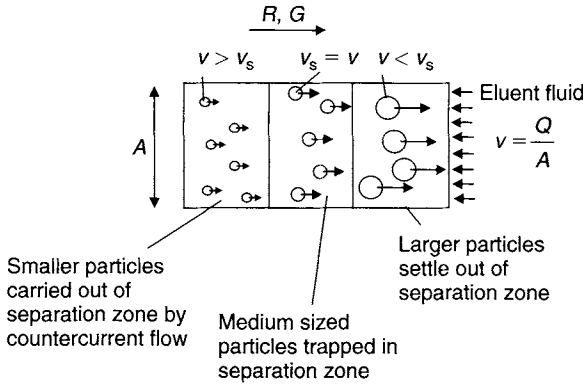


**Figure 3.4d** Centrifugal elutriation with undersized particles removed at small radius and oversized particles at large radius

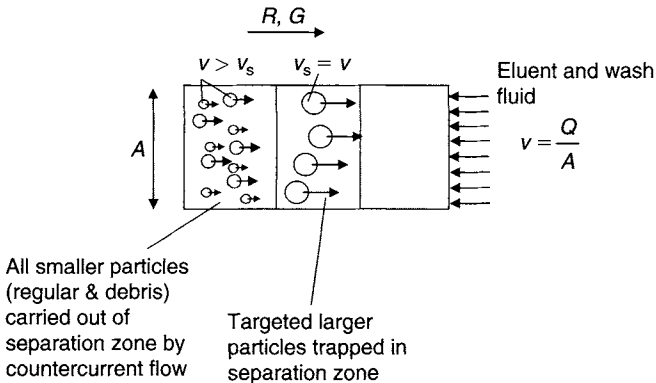


**Figure 3.4e** Increasing eluent flow rate to remove undersized particles. Wash liquid can be added to clean the targeted cells

For a mixture of cells, separation is possible if there are specific target cells in which modification can be made to their size, such as with addition of a reagent [3], and these target cells swell in size beyond that of normal cells. The mixture with the swollen target cells is introduced to the rotor and the eluent fluid is fed at the periphery at a rate so that the radial inflow velocity in the separation zone just balances the settling velocity of regular cells. Because the swollen target cells have a larger diameter they settle out of the separation zone, while cells of finer sizes are carried out of the separation zone by the eluent fluid to exit at the small radius. This is shown in Figure 3.4d.

Alternatively, reagents can be added to get the unwanted cells to swell and settle out of the separation zone while the target cells remain

in the separation zone, as shown in Figure 3.4d. After removal of cell debris and the unwanted cells, the target cells can be washed with other buffer liquid to elute any contaminants attached to the target cells.

A third possibility is illustrated in Figure 3.4e. The velocity of eluent can be increased so that the swollen cells can be held stationary in the separation zone while cell debris and normal cells are eluted. After the cell debris and normal cells are removed, wash liquid can be added to further wash the swollen cells (products).

A fourth possibility is to increase the  $G$ -force so that larger target particles (unwanted cells) settle quickly towards the large radius, leaving the separation zone that may have the normal cells, while the finer sub-micron debris leave with the carrier fluid exiting at the small diameter. This is somewhat similar to the second alternative (Figure 3.4d).

In summary, there are various possibilities in the cell classification process: (a) use of reagent to modify cell size (target cells or unwanted cells), (b) different values of  $G$ -force to control the particle sedimentation velocity and thus the particle size to be retained in the separation zone, and (c) the eluent flow rate/velocity for use in elutriation.

## 3.4 Tubular Centrifuge

### 3.4.1 General Tubular Bowl Geometry

Tubular bowl centrifuge or tubular centrifuge is typically vertically oriented. It has a rotating tubular bowl with length  $L$  and bowl diameter  $D$ . The aspect ratio  $L/D$  is large anywhere from 5 to 7.3 with the traditional tubular design, a listing of which is shown in Table 3.2. Feed slurry is brought in the centrifuge either from the top (top feed) or from the bottom (bottom feed). A schematic diagram of the bottom-feed tubular is shown in Figure 3.5a, with a more detailed layout shown in Figure 3.5b.

**Table 3.2** Large  $L/D$  tubular centrifuge

$D$ (mm)	Length (mm)	$L/D$	RPM	$G/g$ (RCF)	Vol. rate (L/min)	Motor (kW)
44*	229	5	50,000	62,400	0.2–0.4	/
105**	762	7.25	15,000	13,200	0.4–12	1.5
127**	762	6	15,000	15,900	0.8–25	2.2

\*Turbine drive for steam or compressed air.

\*\*Motor drive.

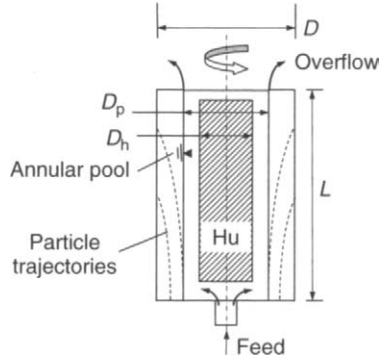


**Figure 3.5a** Schematic of tubular centrifuge

A thin annular pool is maintained between the bowl wall and the inner air core when the centrifuge is operating at full speed. The tubular centrifuge is top mounted (or top suspended) and top driven. When the rotor bowl is at operating speed, the center of gravity of the unit is below the mounting support to maintain dynamic stability with minimal whirling.

Industrial-scale tubular centrifuges have bowls 102 to 127 mm in diameter and 762 mm long. It is capable of delivering 18,000–20,000 g. The smallest tubular, 44 mm diameter by 229 mm long, is a laboratory model capable of developing up to 62,500 g (see Table 3.2). It is also used for separating difficult biological solids, cells, and viruses.

The bowl is suspended from an upper bearing and drive (electric or turbine motor) assembly through a flexible-drive spindle with a loose guide in a controlled damping assembly at the bottom. The unit finds its axis of rotation if it becomes slightly unbalanced due to process load.

In some designs, feed is accelerated to a solid-body rotation by a set of vanes or channels which start at the axis of rotation and terminate at a larger radius below the pool. This assures that the feed slurry is accelerated [3] to angular speed before being introduced to the annular pool for separation. In other designs, the feed is sent to a set of parallel plates where feed is accelerated from a small to a large radius inside the radial annular space formed between the plates. This type of acceleration is less effective due to viscosity of liquid not being an effective mechanism for momentum transfer, unless the viscosity is very large. Exceptions to the above are (a) when the viscosity of the slurry is very high [4] and the plates are closely spaced on the order of millimeters, and (b) where the plates are equipped with accelerating vanes and a smoothener at the large diameter to smoothen the discrete feed streams to a continuous sheet of accelerated feed liquid laying onto the pool [5].

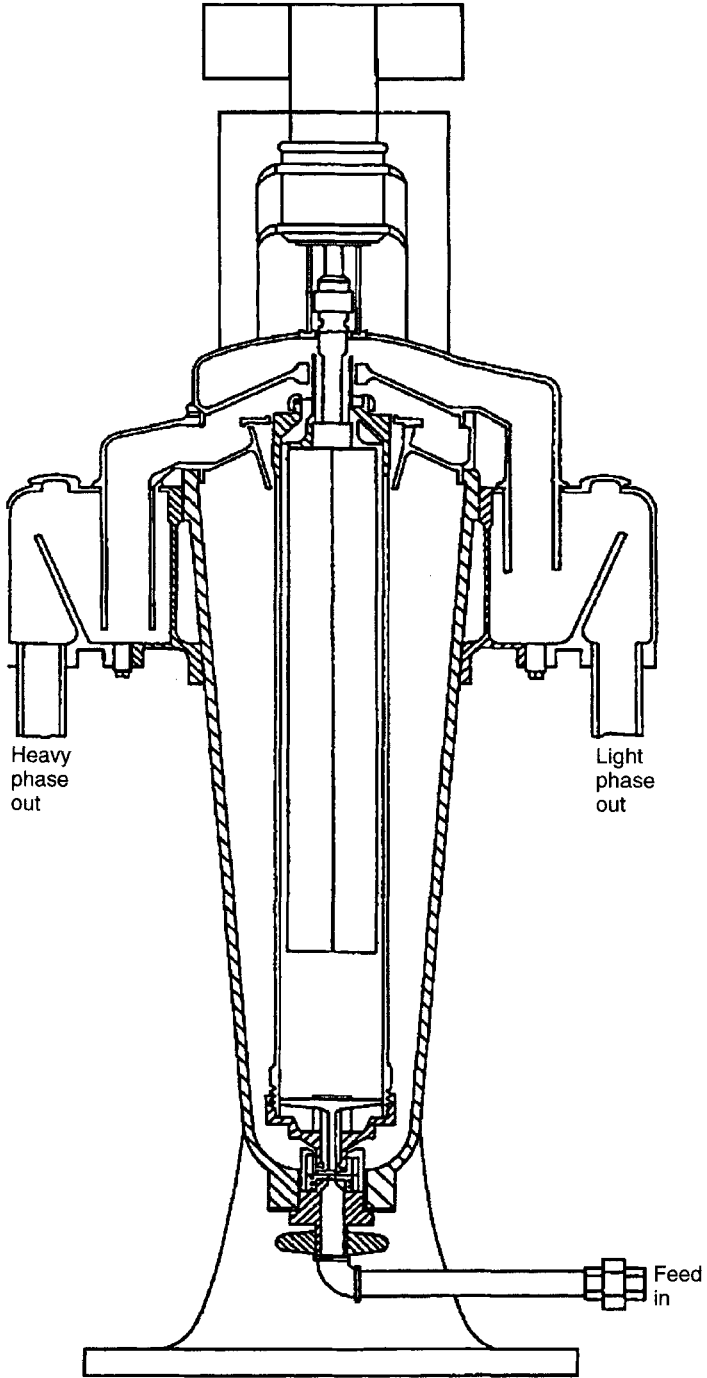


**Figure 3.5b** Layout of traditional tubular centrifuge, typically with high-speed ratio ( $L/D \gg 1$ )

Feed comes in from one end of the bowl and exits at the opposite end of the bowl. After feed slurry enters the annular pool, solids of various sizes, shape and densities settle while they are also transported along the bowl by the main flow. Recent studies [6] show that the flow takes place in a very thin boundary layer, or moving layer, along the surface of the liquid pool regardless of the geometry of the bowl. Particles that have not settled in the bowl are carried out in the overflow. The effluent discharge takes the form of flow over a weir at fixed discharge diameter under atmospheric pressure. Effluent can also be discharged under pressure through paring discs or centripetal pumps (to be discussed in Chapter 4). The pressured liquid flows downstream for processing without the need of additional pumping. This arrangement also reduces the foaming from destroying the kinetic energy of the high-velocity liquid centrate by impinging it on the stationary wall of the housing, if the liquid is discharged through an overflow weir. The destroyed energy creates an additional liquid-air interface, i.e. foam, especially when the liquid contains protein.

The suspended solids in the centrate of the centrifuge are closely monitored by sampling periodically, or continuously, through turbidity measurement. When the growing sediment in the bowl gets close to the surface of the annular pool it interferes with the fast-moving liquid. Sediment can be entrained by the liquid leading to resuspension and high turbidity if the sediment does not settle back in due course. The closer the sediment to the surface of the pool, the more likely the entrainment is and the less time for the resuspended solids to resettle leading to high turbidity. Once a pre-set limit on turbidity has been reached, the solids need to be removed from the bowl. The rotor goes through coast down, the pool liquid is drained, and the sediment removed by either plough, plunger, other automatic mechanisms, or manually when the bowl comes to a complete stop. Subsequently, the bowl is flushed during the clean-in-place (CIP) cycle with an appropriate cleaning liquid to remove any residual solids. The bowl may be momentarily rotated and stopped to allow wash liquid sloshing in the bowl to provide an effective rinsing. Some centrifuges also include steam-in-place (SIP) to further kill any biological materials to avoid cross-contamination between batches.

Recently, some specially designed versions of the tubular centrifuge have been developed that are hybrid versions between the traditional tubular with high  $L/D$  ratio and solid-basket centrifuge with small  $L/D \sim O(1)$ . These hybrid designs (still referred herein as tubular centrifuge) have  $L/D$  in the range of  $1.5 > (L/D) > 1$ . They take advantage of the solid-bowl basket design that has more bowl volume facilitating temporary storage of cake solids. There are three possible designs on cake discharge.

### 3.4.2 Ribs and Solids Scraper

One commonly used tubular design is the rib design, as shown in Figure 3.6a. A photo of the machine from a particular manufacturer is shown in Figure 3.6b. This machine can automatically discharge solids when the bowl is filled, eliminating the laborious manual cake removal process as in the case of the conventional tubular centrifuge. The bowl is equipped with a set of annular rings spaced axially along the bowl with the ring outer diameter reaching the bowl diameter and the ring inner diameter slightly below the surface of the annular pool. The functions of the set of

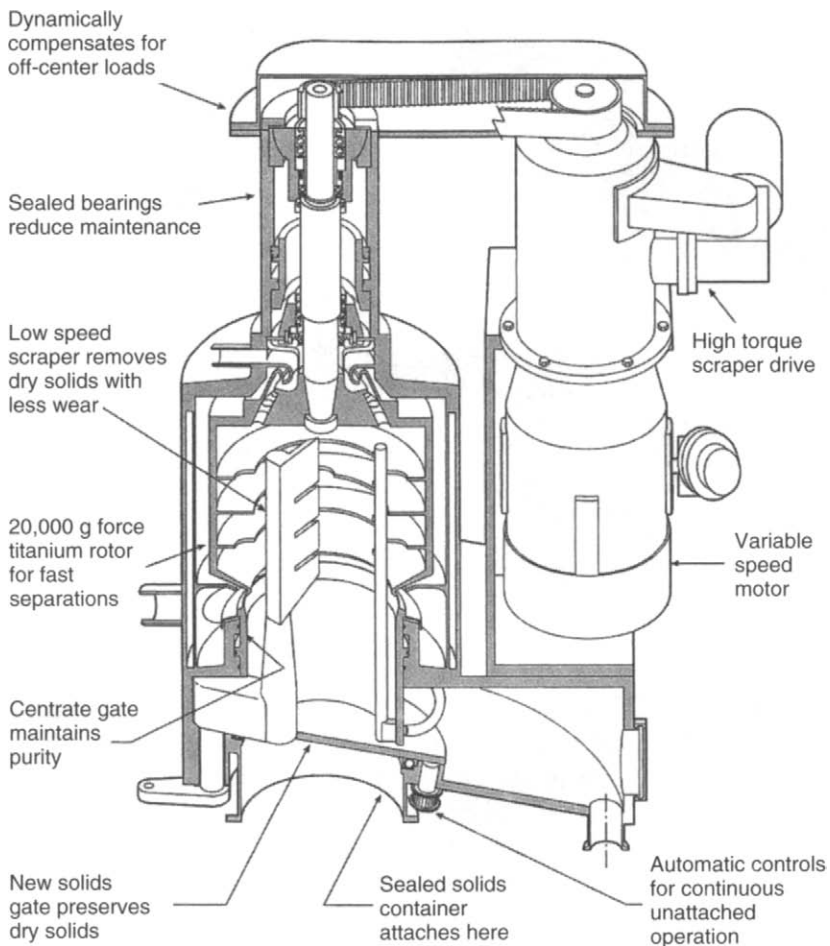


**Figure 3.6a** High-speed centrifuge up to 20,000 g with fully automatic cycle,  $LD < 1.5$  (Reproduced by permission of the CARR-CENTRITECH Separations Group of Pneumatic Scale)



**Figure 3.6b** A 457-mm diameter high-speed 20,000 g centrifuge with slurry  $SG < 1.5$  with fully automatic cycle (Reproduced by permission of the CARR-CENTRITECH Separations Group of Pneumatic Scale)

rings are twofold: to maintain rigidity of the bowl at rotational speed equivalent to 20,000 g, and to reduce, if not eliminate, traveling waves along the axial direction. The liquid slurry communicates between compartments through cut-outs, or orifices, adjacent to the inner diameter of these rings. These cut-outs are staggered (not in alignment between adjacent rings) to avoid traveling waves propagating axially along the bowl.

The bowl is first filled by feed slurry after the feed has been accelerated by contacting with a rotating accelerating cone which directs the feed to the larger bowl diameter, see Figure 3.7a. Once the feed suspension fills to the cut-outs, it overflows at the cut-outs and is uniformly spread into other compartments formed between the annular rings until

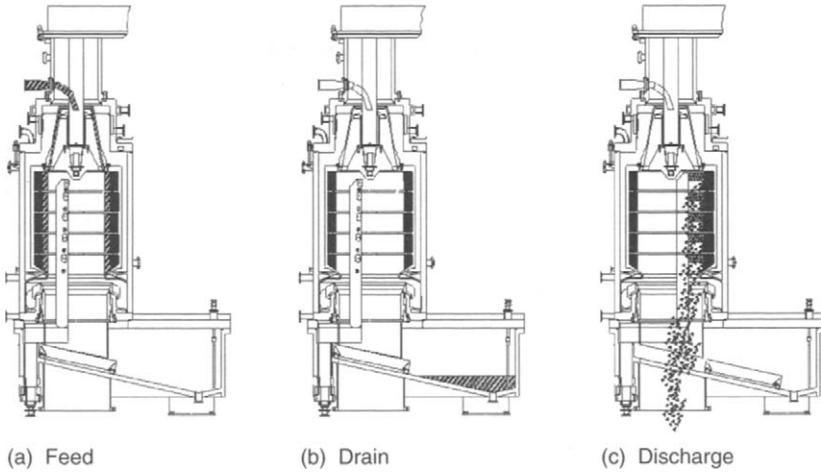


**Figure 3.7** (a) Feeding, centrate liquid diverted to centrate discharge, (b) feed stops and pool liquid drains to lower compartment, and (c) solids discharge to cake chute of high-speed centrifuge (Reproduced by permission of the CARR-CENTRITECH Separations Group of Pneumatic Scale)

a constant suspension pool depth is reached among all compartments. Subsequently, the liquid further fills up the bowl until it spills at the opposite end (from the feed accelerator cone) of the bowl at a smaller radius. During continuous feeding, the heavier solids settle toward the bowl forming a sediment layer which increases over time. For a 457-mm bowl with a maximum feed rate of 28 L/min, the bowl volume is 36 L while the solids holding space is 32 L, which is 89% of the bowl volume. There is quite a large percentage of bowl volume to inventory solids as liquid flows only in a thin moving layer near the pool surface and does not get interfered with until the sediment surface gets close to the pool surface, at which solid entrainment can take place. This contradicts disk-stack centrifuge, in which about 50% of the bowl volume is allocated for solid storage (as will be discussed in Chapter 4). Feeding stops when the centrate turbidity increases as a result of entrainment of the sediment by the moving layer. The centrate compartment gate is closed and the annular pool is allowed to drain to the lower compartment of the machine, see Figure 3.7b. Upon completing pool draining, an eccentrically located scraper or plough, in the form of a comb shape, rotates into position and ploughs the sediment deposited in the compartments of the bowl, diverting the sediment to a cake chute located at the lower part of the machine, as illustrated in Figure 3.7c. The residual sediments are

removed during the cleaning cycle and CIP. The equipment is equipped with CIP spray balls and CIP nozzles directing water wash, heated caustic and acid wash, water rinse, and WFI (water for injection) final rinse to all product contact areas.

Several sizes are available, including bowl diameter of 150, 300 and 457 mm. The spec of two sizes of this type of centrifuge is given in Table 3.3. The bowl diameter of the latter two is larger than the traditional large L/D tubular centrifuges with the maximum diameter of 127 mm (see Table 3.2). The centrifugal force is adjustable between 500–20,000 g with feed rates in the range from 0.1 to 28 L/min and solids capacity from 1 to 36 kg/cycle. A photo of the 457-mm diameter unit is shown in Figure 3.6b.

### 3.4.3 Plunger Cake Discharge

Another tubular design also allows separation at a  $G$ -force of 10,000 g. During cake/sediment discharge when the bowl has stopped, a plunger is used to push the sediment off the bowl wall after the liquid pool has been drained. This further reduces any residual heel cake solids left between the plough and the bowl wall. The cake consistency can be in the form of a paste. Depending on the centrifuge size, it can serve 10–10,000 L reactors.

### 3.4.4 Submerged Hub

Still another tubular design has a cylindrical hub that extends radially towards the pool surface. This design forces the separation pool to a thin annulus at a larger pool diameter, so that a higher separation force can

**Table 3.3** Hybrid tubular centrifuge with  $1 < (L/D) < 1.5$

<i>Hybrid tubular</i>	<i>D (mm)</i>	<i>rpm</i>	<i>G/g (RCF)</i>	<i>Vol. rate (L/min)</i>	<i>Bowl volume (L)</i>
Knife discharge	150	15,320	20,000	0.1–1*	1.1 (1)
	457	8846	20,000	0.1–28	36 (32*)
Cake reslurry, submerged hub design	150	10,832	10,000	0.1–4	1.3
	300	5417	5000	1–40	16.7

\*Three minute discharge typical.

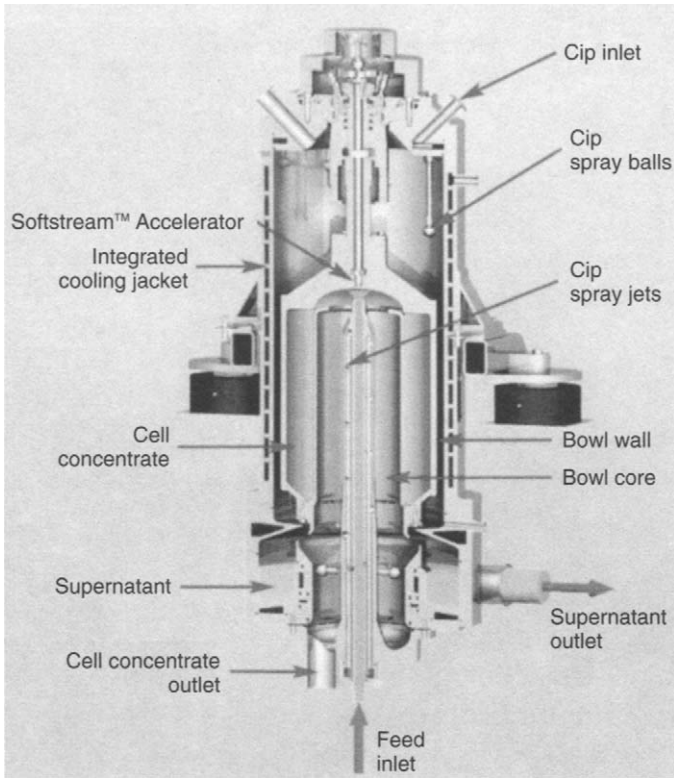


**Figure 3.8** Schematic of a 300-mm diameter tubular centrifuge with clean-in-place and steam-in-place features. Note that the hub diameter is large, touching the pool surface, i.e.  $D_h = D_p$  (Reproduced by permission of the CARR-CENTRITECH Separations Group of Pneumatic Scale)

be realized for separation. The design is illustrated in Figure 3.8. As can be seen, the incoming feed is distributed uniformly by a parabolic feed distributor [4] and is accelerated from the axis to the annular pool at a larger diameter.

The submerged hub design is tailored for cell harvest and supernatant recovery of cells of various sizes. Capable of separating a wide variety of mammalian and insect cells with little or no damage, the submerged hub design offers intact cell recovery efficiencies in excess of 99% with low cell concentrations in clarified supernatant. The model provides two sizes respectively: 150-mm and 300-mm bowl. The 300-mm diameter unit is depicted in Figure 3.9. Also, the spec for this type of centrifuge is included in Table 3.3.

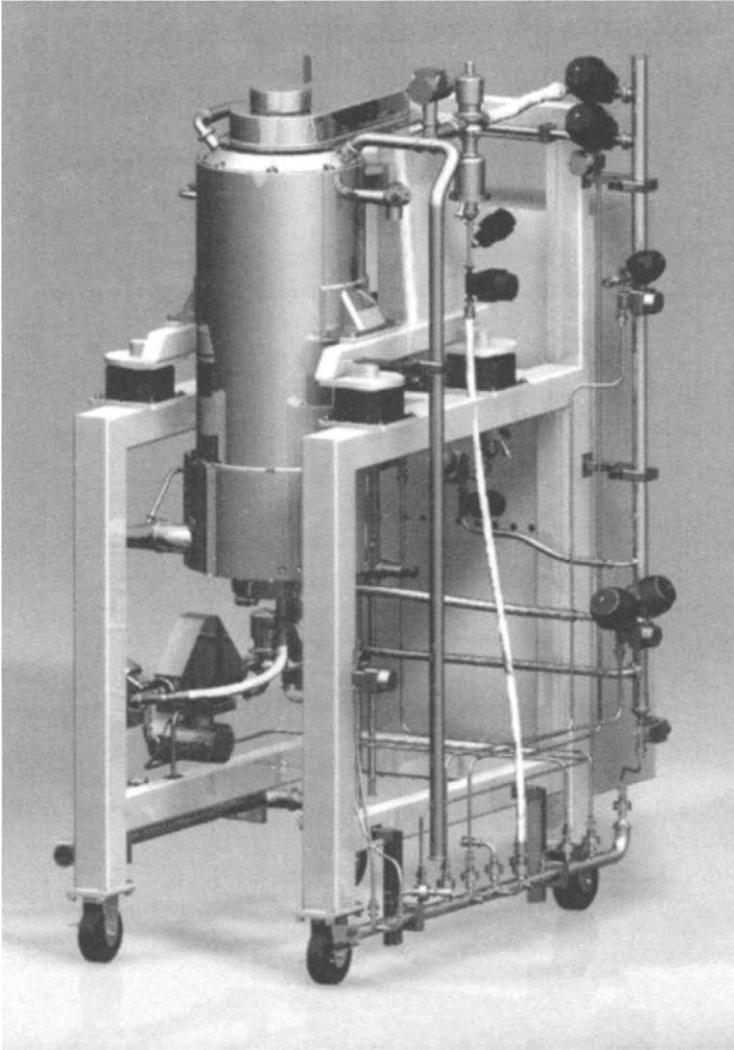


**Figure 3.9** Submerged hub design with hub touching pool surface and 300-mm bowl (Reproduced by permission of the CARR-CENTRITECH Separations Group of Pneumatic Scale)

During cake discharge, after the pool is drained, liquid is introduced to flush the solids left compacted against the bowl wall to re-suspend the sediment, and the suspension is subsequently drained. One merit of this centrifuge is that it operates at lower centrifugal acceleration and the sediment is not well compacted, hence it is ideal for resuspension when the cake needs to be removed. It is a closed system operation from feeding to cake discharge and cleaning, and there is no need to break the ‘containment’.

### 3.5 Summary

In this chapter, the batch spintube and ultracentrifuge have been presented. Also, the versatile centrifugal filter that combines sedimentation, filtration, and chromatography carried out with different functional modules has been presented. Each process can be enhanced by the centrifugal field, including the chromatography process which otherwise requires a pressurized system to send the process feed through a chromatography column. In this case, the centrifugal field provides this additional driving pressure. In addition, a semi-batch tubular centrifuge is discussed with either manual or automatic cake discharge. The traditional tubular uses a high length-to-diameter ratio which requires manual cake removal, whereas the more modern tubular, which takes advantage of the solid-basket centrifuge design and has length-to-diameter ratio of order unity, is designed with automatic cake discharge and more space for solid storage; consequently it can take on feed with higher-solids concentration.

### References

- [1] W.W.F. Leung, *Industrial Centrifugation Technology*, McGraw-Hill, New York, 1998.
- [2] W.W.F. Leung and R. Probst, Lamella and tube settlers: Part 1 Model and operation, *I&EC Process Des. and Dev.*, 1983.
- [3] G.V. Childs., J.M. Lloyd, G. Unabia, D. Rougeau, Enrichment of corticotropes by counterflow centrifugation, *Endocrinology*, 123:2885–2895, 1988.
- [4] W.W.F. Leung and A. Shapiro, Improved design of conical accelerators for Decanter and pusher centrifuges, *Filtration and Separation*, pp. 735–738, Sept. 1996.
- [5] W.W.F. Leung and A. Shapiro, Efficient double-disk accelerator for continuous-feed centrifuge, *Filtration and Separation*, pp. 819–823, Oct. 1996.
- [6] W.W.F. Leung, Experimental and theoretical study of flow and sedimentation of tubular centrifuge for bioseparation, AICHE Annual Conference, Cincinnati, USA, Nov. 2005.

### Problems

- (3.1) A suspension of relatively monodispersed particles settle in a vertical test tube under the Earth's gravity, it produces a sharp liquid-suspension interface that moves towards the bottom of the tube over time, while a layer of sediment builds up from the bottom of the tube to meet this liquid-suspension interface (see Figure 3.10). If the tube is inclined with respect

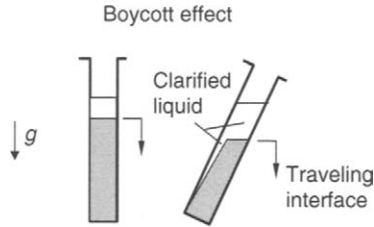


**Figure 3.10** Boycott effect

to the vertical (Figure 3.10), the liquid-suspension interface travels at a much faster rate towards the bottom of the tube. Explain this phenomenon which was first discovered by the physician Dr Boycott in the 1920s. How would this compare to the swing-out spintube and the fixed-angle spintube pair?

- (3.2) A small tubular centrifuge can attain 60,000 g when operating at an angular speed of 50,000 rev/min. What is the diameter of the tubular centrifuge? It can take a maximum feed rate of 1 L/min and allows 100–300 g of sediment deposit in the bowl. A big tubular centrifuge with 457-mm diameter bowl can attain 20,000 g. What is the angular speed at which it should operate?
- (3.3) A group of cells of comparable size of about 3 microns together with cell debris in the submicron range in a mixture need to be classified. A special reagent is added in solution to target some specific cells which absorb the reagent and swell in size to about 6–8 microns. The mixture of cell debris, regular cells, and the swollen cells (product) are fed into a special elutriating centrifuge with precision control feed rate. The density of the cells is  $1050 \text{ kg/m}^3$  and that of the suspension is  $1000 \text{ kg/m}^3$ . The viscosity of the suspension is 5 cP. The mixture enters the separation zone in the centrifuge with an equivalent centrifugal acceleration at 20,000 g and a cross-sectional area of  $0.5 \text{ cm}^2$ . In this rotor, liquid enters from the outer radius and is distributed circumferentially uniform at the separation zone with a counterflow velocity (i.e. directing toward the small radius) opposing the radial directed settling velocity. What is the eluent flow rate, expressed in mL/min, in order to keep the 3-micron cells in the separation zone of the rotor while the smaller submicron debris will be carried out and exit at the small radius outlet with the liquid, and concurrently the sedimenting swollen particles will settle out of the separation zone and exit at the large radius?
- (3.4) Referring to Problem 3.3, what is the eluent flow rate to the elutriating centrifuge if the 6-micron swollen cells are to be kept stationary in the separation zone while the 3-micron regular cell and submicron cell debris are carried by the flow to exit at the small radius? After removal of the minus 6-micron particles, buffer and wash liquid may be added to wash the 6-micron cells (product) to remove any adhered contaminants.

# Disk Centrifuge

In this chapter, the inclined plate settler concept is first introduced. Subsequently this concept of settling in short distance is extended to disk-stack centrifuges. The various types, features, and functions of disk-stack centrifuges for use in biotechnology separation will be discussed.

## 4.1 Lamella/Inclined Plate Settler

### 4.1.1 Inclined Plate Settler Principle

The distance for particle settling in a tank of height  $H$  is greatly reduced if a set of parallel plates with a tilt angle  $\theta$  with respect to horizontal is installed (see Figure 4.1). The reason for the tilt angle is simply that settled solids left on the plates can slide down by a component of the gravity so that they do not accumulate and clog the channel formed between adjacent plates.

For a particle settling at a velocity  $v_s$  in a tank of height  $H$ , the maximum time for separation is simply  $H/v_s$ . Now if the inclined plates are installed with plates spaced at an equal distance  $s$ , the distance for which

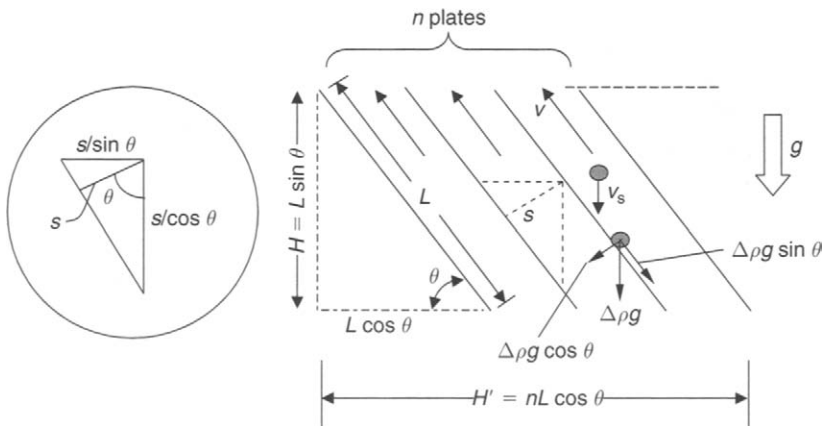


**Figure 4.1** Lamella plate sedimentation

the particle has to settle to reach the plate surface is reduced to  $s/\cos \theta$  (see inset Figure 4.1). The maximum time for particle separation is thus  $s/\cos \theta/v_s$ . The ratio of maximum time for separation for the inclined plates to that of the holding tank without the plates becomes  $(s/H) \sec \theta$ , which is independent of the number of plates  $n$ . Suppose  $s = 3 \text{ cm}$ ,  $H = 3 \text{ m}$ ,  $\theta = 60^\circ$ , this ratio is 1:50. This is equivalent to stating that the flow sedimentation capacity of the inclined settler is  $H \cos \theta/s$  times greater than the holding tank assuming other complications are not considered. This ratio is 50 times for the present example.

Another related argument to consider is the projected horizontal sedimentation area which is an indicator of the settling capacity. As shown in Figure 4.1, for the holding tank the projected horizontal sedimentation area is approximately  $(n - 1)s/\sin \theta + L \cos \theta$  whereas for the lamella plate it is  $nL \cos \theta$ . Therefore, the ratio of the lamella plate to that of the holding tank becomes  $nH \cos \theta / [(n - 1)s + H \cos \theta]$ . If  $n = 300$ , this ratio comes out to 43, which is below 50 as determined previously. As  $n$  increases to 500, this ratio increases to 45.5 and as  $n$  increases further this ratio approaches  $H \cos \theta/s$ , which is the same as that obtained previously. Indeed, both short distance and equivalent settling area arguments yield similar results.

#### 4.1.2 Complications in Inclined Plate Settler

The foregoing arguments do not account for complications that arise in real situations.

- 1 These complications include particles that can be entrained by the moving flow even if there is already sediment on the inclined surface.
- 2 Particles can accumulate to the inclined plate and may not slide down due to friction and self-cohesion between particles. As to the latter, the angle adopted for the inclined plate settler is typically at a steep angle of  $50\text{--}60^\circ$  with respect to the horizontal to ensure solids sliding down the plates and not accumulating and blocking the channels between adjacent plates.
- 3 Flow may not distribute uniformly into each channel. This is by far the most serious problem and it will be taken up later.
- 4 Fluid does not flow in one direction (primary flow) from the bottom to the top. Actually secondary flow exists at the entrance and exit as well as inside the channel [1].
- 5 Lastly, the interface between the countercurrent flow streams (i.e. primary and secondary flow) may become unstable. The instability can lead to turbulence, mixing, and resuspension of particles [2].

In any event some of these complications might reduce the capacity of the inclined channels. Instead of having a capacity ratio of inclined plate to conventional tank of 50:1, this ratio might drop to, say, 20:1 with the complications taken into consideration. Regardless, the inclined plate provides at least an order of magnitude advantage over a conventional tank.

## 4.2 Disk-Stack Centrifuge

### 4.2.1 General Disk Geometry

In this section, the inclined plate settler concept is extended to a centrifuge. Suppose the plate stack of Figure 4.1 is rotated 90° clockwise, the base  $H'$  of the tank becomes the height of the centrifuge bowl in Figure 4.2, and the inclined plates of Figure 4.1 become the axisymmetric conical disks with outer radius  $R_2$  and an inner radius  $R_1$  as depicted in Figure 4.2. When the disks rotate about the axis at high angular speed, centrifugal acceleration  $G$  is established. Heavier particles settle in the direction towards large radius while lighter fluid is displaced towards smaller radius, very much analogous to the sedimentation under gravitational acceleration shown in Figure 4.1. In a disk-stack centrifuge, particles settle on the underside of the conical disk surfaces from which a  $G$ -component,  $G \sin \theta$ , drives the particles to the peripheral of the disk.

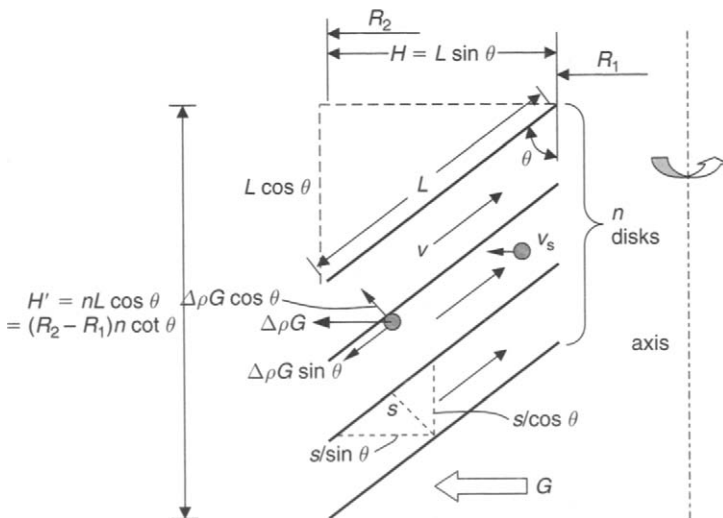


**Figure 4.2** Schematic of inclined plates (conical disks) sedimentation adopted for a rotating centrifuge

After leaving the disk stack, centrifugal acceleration further drives the particles to a temporary solids holding space at the bowl periphery.

As with the inclined plate settlers of Figure 4.1, the maximum time for separation between the rotating bowl, with disk stack versus the rotating 'chamber' bowl alone (no disk-stack centrifuge) with the annular radial extent between  $R_2$  and  $R_1$  and height  $H'$ , is significantly reduced by a factor of  $s/H/\cos\theta$ . If  $s = 1$  mm,  $L = 100$  mm,  $\theta = 40^\circ$ , this ratio comes out coincidentally to 1:50, identical with the value obtained for the inclined plate settler under  $g$ . The important point is that the separation time is much reduced irrespective of inclined plate settler under  $1g$  or disk-stack centrifuge under thousands of  $g$ . Conversely, the capacity is much increased by having the disk-stack centrifuge making separation at a high  $G$  and large surface area. Similar complications occur with the disk stack as with its counterpart – the inclined plate settler; however, there is less instability associated with countercurrent flow for the disk stack due to the strong rotating field that tends to stabilize the flow field in a two-dimensional sense (i.e. Taylor Proudman as discussed in Chapter 2). Despite this, due to relative liquid motion in the rotating frame the flow experiences further complicated Coriolis acceleration that allows a circulatory flow pattern which is represented schematically by Figure 4.3 [3].

In Figure 4.3, as liquid flows towards the small diameter (upward of paper), Coriolis acceleration directs the flow out of the paper. Vice versa, when the flow is redirected to the larger diameter (downward of paper), Coriolis acceleration directs the flow into the paper. In most designs, the undesirable Coriolis force is counteracted by the longitudinal ribs (acting as spacers between adjacent disks). These ribs, say in quantities of 4 to 6, are uniformly spaced around the circumference of the conical disk. This reduces the extent of circulatory flow and opposes the undesirable Coriolis force (see Figure 4.3a). The spacing between adjacent disks can be very small, nominally 1 mm; however, it can be reduced to 0.3 mm for low feed slurry viscosity, or as large as 1.5 to 2 mm for processing viscous feed with high solids content.

Figure 4.4 shows multiple disk-stack centrifuges installed in a plant.

### 4.2.2 Disk Angle

The inclined angle (with respect to the vertical axis) of the disks stack in a disk centrifuge is typically  $35$ – $50^\circ$ . The number of disks ' $n$ ' is anywhere between  $50$ – $200$  disks. This quantity varies between different sizes and designs of disk centrifuges. The centrifugal acceleration  $G$  ranges between  $5000$  and  $15,000g$ .

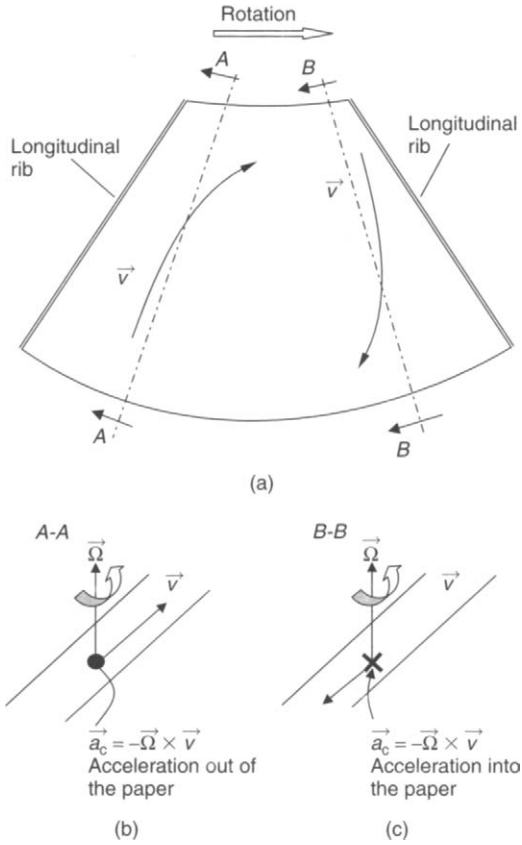


**Figure 4.3** Schematic of a segment of the angular channel showing secondary flow arises from the Coriolis effect



**Figure 4.4** Multiple disk-stack centrifuges in operation (Reproduced by permission of Westfalia Separator)

**Table 4.1** Summary of various disk centrifuges and their feed and discharge

	<i>Manual discharge</i>	<i>Dropping-bottom discharge</i>	<i>Nozzle discharge</i>
Solids discharge	Manual	Intermittent	Continuous
Percentage by volume feed solids	0–1%	0–10%	5–20%
Concentrate	Minimal	Non-flowable	Paste, flowable

### 4.2.3 Disk Spacing

The typical spacing between adjacent disks ranges from 0.32 to 1 mm. On the other hand, processing yeast with 30% by volume of feed solids needs more open spacing of 1 mm, whereas tighter spacing such as 0.5 mm is most suitable for processing *E. coli* and lysate with lower feed solids. Disk spacing of 0.32 mm can be used for processing mammalian cell broth at low feed solids with concentration of 3–4%.

Table 4.1 summarizes the different types of centrifuges in terms of feed solids and concentrate discharge.

### 4.2.4 Process Functions of Disk Centrifuge

There are several important functions in solid-liquid separation of a disk centrifuge combining the high  $G$  together with large disk areas (as discussed earlier).

#### 1 Separate suspended solids from liquid phase

The solids are removed from liquid phase.

#### 2 Clarification/Purification

The intent is to reduce the suspended solids in the liquid centrate or effluent phase to a minimum.

#### 3 Thickening or concentration

The feed slurry is concentrated to a suspension with much higher solids concentration. The solids loss in centrate is also minimized.

#### 4 Separation and washing

The solids in suspension may contain contaminants. The suspension is centrifuged first and the centrifuged concentrate is reslurried with wash liquid to dilute and dissolve the contaminants. The resulting slurry is

separated again by centrifugation to remove the spent wash liquid containing dissolved and suspended contaminants. The separation and washing process can be repeated as many times as necessary until the contaminant level of suspension reaches an acceptable level. Obviously, this should also be balanced by the economics of the process.

## 4.2.5 Feed Solids

### 1 Suspended solids

The typical feed solids in suspension, especially for biopharmaceutical applications, are 2–4% v/v (by bulk volume) for mammalian cells but can increase to 30% for yeast. The range of variation is quite large. In the future, the feed solids to mammalian cell broth might increase to 4–6% v/v and perhaps higher due to increases in solids capacity from the upstream bioreactors.

### 2 Dissolved solids

The dissolved solids in the feed consist of valuable protein product, unfortunately mixed with other contaminants, also in soluble form, that need to be removed in downstream purification.

There are three types of centrifuges according to the mode of discharging concentrate solids. Table 4.1 summarizes these three types according to the mode and nature of concentrate discharge, as well as to the percentage by volume of feed solids that these machines typically handle.

## 4.2.6 Manual Disk Centrifuge

In the manual disk centrifuge as shown in the schematic in Figure 4.5a, a space or volume in the bowl at a larger diameter is used to temporarily store the sediment from centrifugation. When this space becomes nearly full, the concentrate turns turbid due to entrainment of sediment by the incoming feed stream, at which point the feed has to be shut off and the pool liquid in the centrifuge drained, and the accumulated solids removed manually. Therefore, for practical purposes it is important that the feed solid concentration to the centrifuge should be low, otherwise there will be too much downtime due to solids discharge and cleaning. This will seriously impact on the operation.

### 4.2.6.1 Clarification of the Light Phase

A typical application of this design would be for clarifying a liquid stream with a small amount of solids. The light phase in this case is

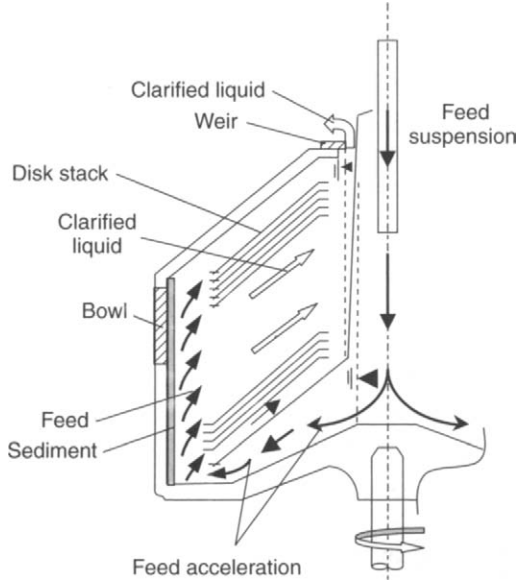


**Figure 4.5a** Schematic of a manual disk-stack centrifuge

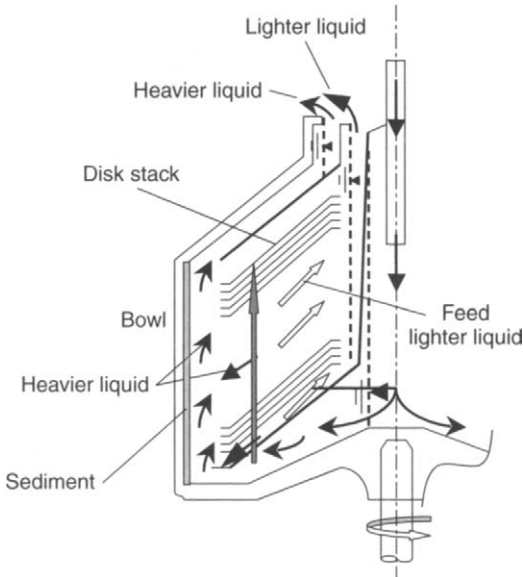


**Figure 4.5b** Schematic of a liquid-liquid-solid disk centrifuge showing the rising hole being near the periphery of the disk stack

water. Another application is to separate water droplets from continuous oil phase in which the light phase is oil. If there exists an interface located between oil and water, the centrifuge should be operated such that the interface should be located outside the disk periphery  $R > R_2$  to maximize polishing of the light phase (i.e. oil) using the conical disk area and/or residence time for settling out the dispersed heavy phase (i.e. water droplets).

#### 4.2.6.2 Separation

A common application for disk centrifuge is for liquid-liquid-solid separation, such as shown in Figure 4.5b. This is to separate a lighter liquid (such as oil), a heavier liquid (such as water) and a very small amount of suspended solids (the heaviest of all three phases). In the case where oil is lightly present in a continuous water phase, the disk centrifuge can be used to remove the oil droplets from the processed water with the provision that the disk is equipped with a set of equal-radius holes proximate to the small radius  $R_1$ . When the disks are stacked and the holes of the disks aligned, a continuous channel is formed through which the oil–water feed should be introduced. From this radius to the disk outer radius  $R_2$ , the small amount of dispersed oil droplets can be separated out from the continuous water phase. The dispersed oil droplets coalesce to form larger droplets and because of buoyancy they move to the smaller radius region and get channeled to discharge at a smaller radius, while in the clean water phase, which is heavier, they move towards the large radius where they get trapped and discharged through another liquid exit at a larger radius. This maximizes the separation of the undesired discrete lighter phase (e.g. oil droplets) from the continuous heavier phase (e.g. water). This is depicted in Figure 4.5b.

#### 4.2.7 Intermittent Discharge

For this configuration as illustrated in Figure 4.6a, accumulated solids discharge through peripheral ports, which are opened on a time-based mechanism triggered by fixed time intervals or by the increased pressure due to solids loading in the bowl. During solids discharge, the bowl bottom (a separate cover piece) drops, exposing an annular opening for discharging accumulated solids. Alternatively, the bowl bottom can drop if the ‘pressure’ due to accumulated solids exceeds a threshold. The dropping bottom can be controlled hydraulically using water, or pneumatically using inert gas with counteracting mechanical springs.

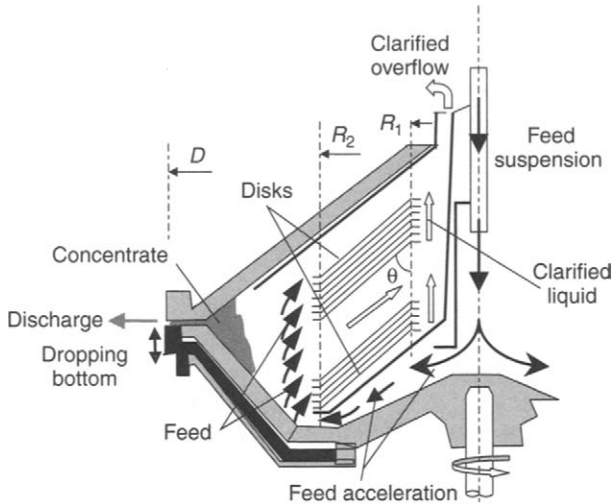


**Figure 4.6a** Intermittent discharge or dropping-bottom disk centrifuge

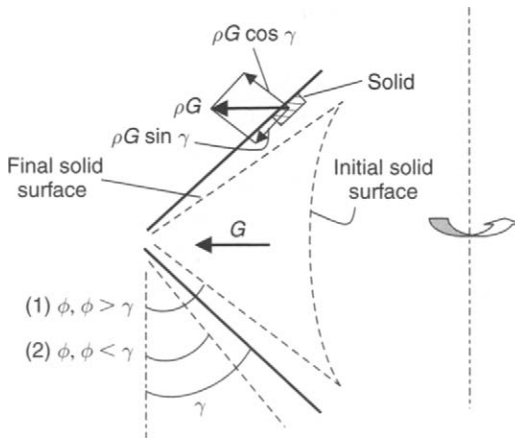


**Figure 4.6b** Schematic of discharge cone showing initial and final solid surface, and the two scenarios: (1) repose angle of solid is greater than the cone angle  $\gamma$ , and (2) repose angle of solid is smaller than the cone angle  $\gamma$ .

#### 4.2.7.1 Two Intermittent Discharge Designs

There are two types of intermittent discharge. One type uses peripheral discharge where solids are ejected radially outwards and for the other, the concentrates are directed axially at the periphery of the disk centrifuge.

The radial discharge, disk operates at a slightly lower  $G$ -force as compared to the axial discharge, which has improved mechanical integrity wherein ports in the bowl and lock ring are better positioned. As an example, the radial discharge is capable of 13,000 g, whereas the axial discharge can operate at higher speed and  $G$ s of 15,000 g. The radial discharge can process all types of solids except those with shear-thickening behavior. On the other hand, the axial discharge can process only flowable solid. This is because solids leaving the solid holding space need to travel a short axial distance towards the bowl bottom before being ejected. Some designs have a built-in pressurized air source to facilitate solid discharge for the axial-discharge disk centrifuge.

#### 4.2.7.2 *Angle of Cone for Discharge*

The angle of discharge solid holding space in a disk centrifuge depends on the repose angle  $\phi$  of the concentrate. The initial solid surface after the solid holding space in a disk centrifuge is filled, both it and the final solid surface are both shown in Figure 4.6b. The angle of repose under the  $G$ -force of the solid dictates the final solid surface. Two scenarios are shown in Figure 4.6b: the first scenario is where the repose angle of the concentrate is greater than the cone angle  $\gamma$ , and the second is where the repose angle is smaller than the cone angle  $\gamma$ . The latter is more favorable for concentrate discharge.

Even when the cone angle is smaller than the repose angle the solid will empty under  $G$ -force. The driving force component acting on the remains of solid left on the cone surface is  $\rho G \sin \gamma$ . The steeper is  $\gamma$  the greater is the  $G$ -force component  $\rho G \sin \gamma$  that helps to clear solids off the walls of the cone, see Figure 4.6b (upper part). It is also noted that the steep cone angle helps in compaction of the concentrate. Thus setting aside discharge issues, a steep cone angle results in a more concentrate solid being discharged.

#### 4.2.7.3 *Discharge Frequency*

When the following parameters are known, namely the solids hold-up volume  $V_s$  of the bowl (which typically occupies 40–50% of the entire bowl volume), feed rate  $Q_f$ , feed volume  $\phi_f$  and discharge efficiency  $\eta_d$ , the time  $t_d$  to fill up the disk centrifuge hold-up volume can then be estimated. This can be used to determine the approximate discharge frequency from which the centrifuge operation can be fine-tuned using concentrate quality; that is, suspended solids or more commonly the

turbidity of concentrate. The following example of mammalian cell broth demonstrates how the frequency of solid discharge is determined.

$$\begin{aligned}V_s &= 13 \text{ L (solids hold-up volume)} \\Q_f &= 150 \text{ L/min (volumetric feed rate)} \\ \phi_f &= 2\% \text{ (feed \% by v/v)} \\ \eta_d &= 80\%\end{aligned}$$

$$t_d = \frac{V_s \eta_d}{Q_f \phi_f} = \frac{(13)(0.8)}{(150)(0.02)} = 3.5 \text{ min}$$

The discharge time estimated above is a first initial guess. By monitoring the turbidity, further fine-tuning can be made. The discharge time (or inversely the discharge frequency) can be increased or decreased accordingly.

Processing mammalian cell culture with low solid content for clarification purposes typically requires 5–8 minutes for discharge, while processing high solid content *E. coli* broth requires the much more frequent discharge rate of about 1–2 minutes.

#### 4.2.7.4 Concentrate Solids Discharge

There are several ways to discharge concentrate solids:

- 1 Full shot with feed temporarily suspended (bowl with large part empty after vacating concentrate and contents).
- 2 Partial shot with feed temporarily suspended (bowl partially empty after vacating concentrate).
- 3 Full shot followed by buffer liquid replacing feed temporarily and feed is resumed after bowl closed (bowl mostly kept filled with liquid).
- 4 Partial shot followed by buffer liquid replacing feed temporarily and feed is resumed after bowl closed (bowl always kept filled with liquid).

The protocol for solids discharge can be as follows.

- 1 Discharge intermittently at frequency pre-determined from expected solids fill-up in solids holding space; the discharge frequency can be further fine-tuned by monitoring turbidity.
- 2 Select partial ejection (preset levels at 0.1 to 2 s), or full ejection with the solids holding volume completely emptied (10-s duration, this mode is selected especially for clean-in-place, i.e. CIP).

- 3 To avoid disturbance, feed may be momentarily stopped with buffer liquid displacing and replacing feed. Buffer liquid is subsequently discharged with concentrate/solids. To ensure the bowl is always filled, buffer liquid is continuously added to fill the bowl before resuming feed again.
- 4 To avoid too much disturbance, a flush or partial ejection after every full ejection is carried out.

#### 4.2.8 Chamber Bowl

As shown in Figure 4.7, the chamber bowl with intermittent discharge has no disk stack. The chamber bowl is similar to a tubular centrifuge but with small  $L/D$  ( $<1$ ) ratio. It is suitable for running viscous feed or feed with more concentrated solids. As stated, the clarification capacity is less than that with the disk-stack centrifuge due to a reduced settling area. However, the chamber bowl can take higher feed solids compared to disk-stack centrifuge. The feed rate usually is smaller for a chamber bowl compared to that of disk-stack centrifuge for the same bowl size.

#### 4.2.9 Nozzle Discharge

As depicted in Figure 4.8a, a nozzle disk can be used for continuous concentrate discharge. This type of machine has been used in brewing in the past. Typically, a set of nozzles are located at the periphery of the

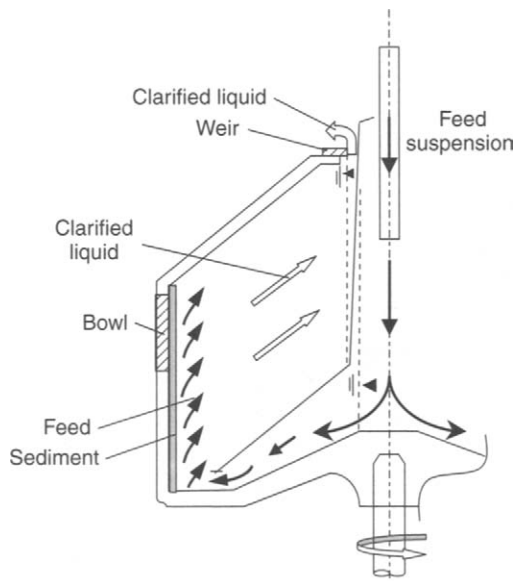


**Figure 4.7** Chamber bowl centrifuge (no disk stack)

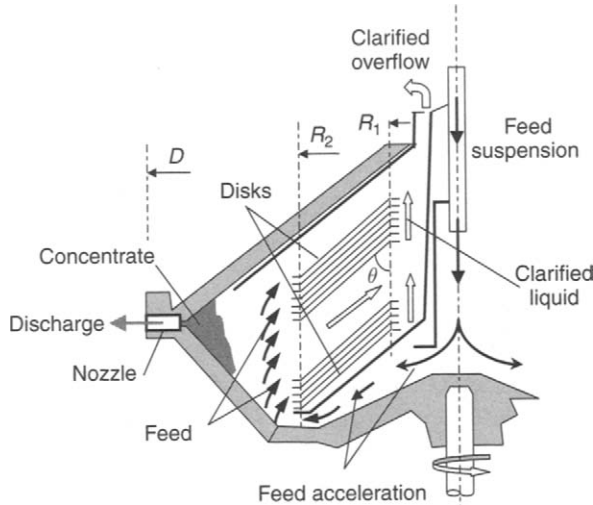


**Figure 4.8a** Nozzle discharge (continuous solids discharge) disk centrifuge

bowl or at a smaller radius (for saving power purpose) to discharge flowable solids. This feature is not shown in Figure 4.8a. The total nozzle area is selected to balance feed solids with concentrate discharge solids. For further power savings, the nozzle discharge is directed approximately along a direction opposite to rotation, which recovers part of the energy of the discharge stream.

The nozzles range in size from 0.5-mm diameter openings for use on the smaller centrifuges to 3.2 mm for the larger centrifuges. The designed number of nozzles per centrifuge, depending on its size, ranges typically from 12 to 24. For satisfactory operation, the minimum allowable nozzle size is at least twice the diameter of the largest particle to be discharged. Large particles must be removed by pretreatment such as screening. The number of nozzles is controlled by the angle of repose of the sedimenting solids and must be selected so that the accumulation of solids between adjacent nozzles does not build into the disk stack and interfere with its clarification effectiveness.

Solid concentrate that is not flowable, like yeast or yogurt, can clog the nozzles. Another design takes the flowable concentrate and redirects it to a vortex discharge located at a small diameter to further reduce energy being wasted in the discharge stream.

The pressurized concentrate discharge design also routes the concentrate at the bowl radius back to a chamber near the axis. Stationary pipes are used to skim the concentrate from the chamber and redirect it to leave the machine near the axis converting the kinetic energy from the

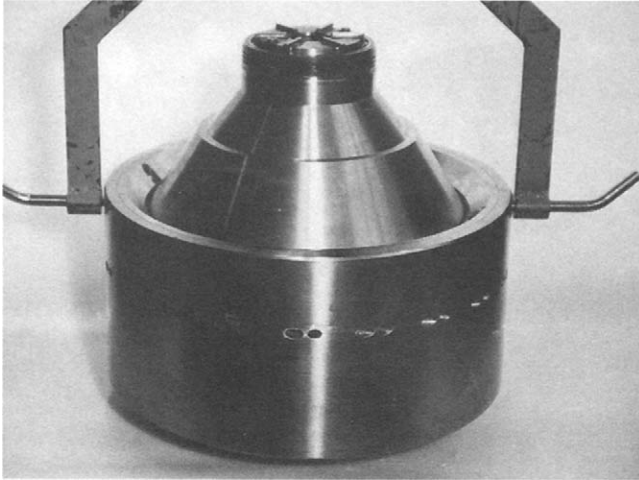


**Figure 4.8b** Rotor assembly of a nozzle disk centrifuge. The direction of rotation is clockwise. The nozzles are directed in the anticlockwise direction to save power



**Figure 4.8c** The rising channel formed by the cut-out at the periphery of the disk, forming a continuous channel for suspension feeding in the disk stack

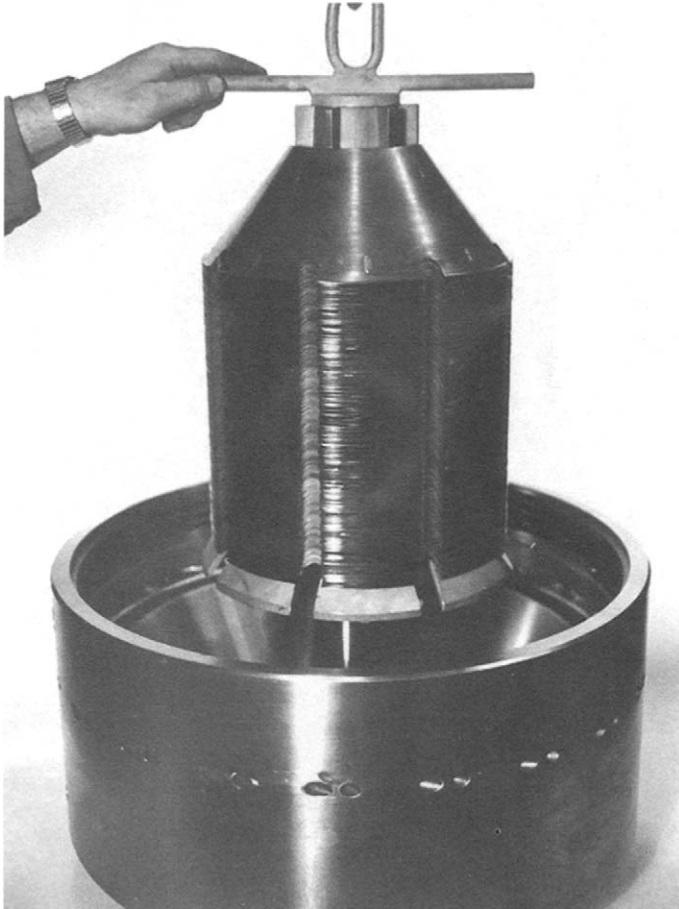


**Figure 4.8d** There are over 100 disks. The openings in the bowl with the nozzles (not shown) can be seen

rotating concentrate flow to pressure. This is similar, in principle, to the centripetal pump for discharging pressurized liquid, which is to be described next.

Figures 4.8b–4.8e are a series of photos on nozzle disk centrifuge. Figure 4.8b shows the rotor assembly of a nozzle disk centrifuge. The bowl openings for the nozzles are directed in the anticlockwise direction to save power as the rotor in the picture is rotating clockwise. Figure 4.8c shows the cut-out at the periphery of the disk forming a continuous rising channel for suspension feeding in the disk stack. More than 100 disks are used in the stack and this is shown in Figure 4.8d. Finally, Figure 4.8e shows the lower conical portion of the nozzle disk bowl.

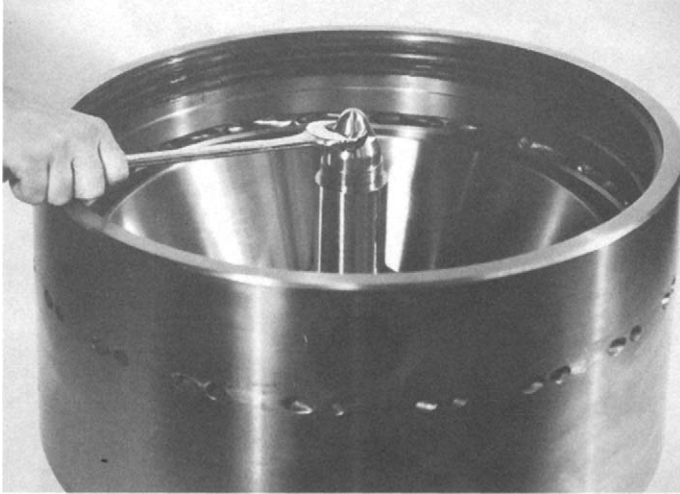


**Figure 4.8e** The lower conical portion of the nozzle disk bowl

#### 4.2.10 Liquid Discharge

Centrate or effluent liquid can be discharged by centripetal pump (also known as paring disk). The advantages with centripetal pump are a reduction of:

- energy of discharge stream
- foaming especially when liquid has dissolved protein
- contact with air.

##### 4.2.10.1 Centripetal Pump for Liquid Discharge

As shown in Figure 4.9a, a pair of stationary channels is used to skim the rotating pool. The rotating liquid enters the opening of the channels and flows past a back-pressure valve where kinetic energy is converted to pressure head. The maximum back pressure that can be established depends on the size of the pump and the rotation speed of the centrifuge (1–7 bars). In essence, this recovered pressure is of the order of magnitude as the dynamic pressure due to the rotating pool  $\rho (\Omega R_p)^2$ , with pool surface radius  $R_p$ .

Using Bernoulli's equation with energy loss for a non-rotating system assuming negligible change in elevations,

$$p_1 + \frac{1}{2} \rho v_1^2 = p_2 + \frac{1}{2} \rho v_2^2 (1 + C_{\text{loss}}) \quad (4.1)$$

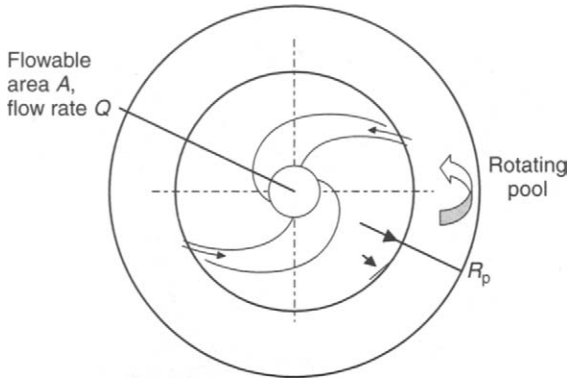


**Figure 4.9a** Centrifugal pump with rotating pool directed counterclockwise

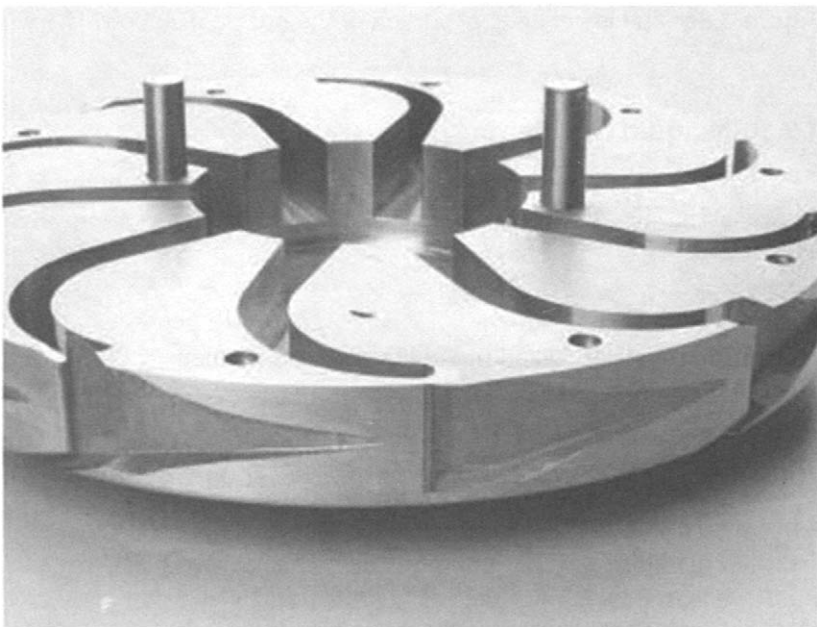


**Figure 4.9b** Stationary paring disk design (cover removed, not shown) (Reproduced by permission of Alfa Laval)

In Equation 4.1, location '1' refers to the intake slightly below the pool surface,  $p_1 \approx p_a$ , and  $v_1 \approx \Omega R_1$ , and '2' refers to a location in the collection duct.  $p_2$  is the pressure build-up at the collection duct to be determined, and  $v_2 = Q/A$  is where  $Q$  is the total centrate discharge rate and  $A$  is the total cross-sectional area of all the collection ducts.  $C_{\text{loss}}$  is

the head loss coefficient due to flow in piping and valve. This is an oversimplification of the flow loss.

$$\frac{p_2 - p_1}{\frac{1}{2} \rho (\Omega R_p)^2} = 1 - \frac{\frac{1}{2} \rho \left[ \frac{Q}{A} \right]^2 (1 + C_{\text{loss}})}{\frac{1}{2} \rho (\Omega R_p)^2} \quad (4.2)$$

If  $C_{\text{loss}}$  is relatively small compared to unity, and  $p_1$  is the atmospheric pressure, then the gauge pressure build-up  $p_2 - p_1$  at the centripetal pump becomes

$$p_2 - p_1 \approx \frac{1}{2} \rho \Omega^2 R_p^2 - \frac{1}{2} \rho \left( \frac{Q}{A} \right)^2 \quad (4.3)$$

Note that part of the pressure recovered is converted to the kinetic energy of the discharge liquid. This is the maximum pressure that can be recovered assuming the energy loss in the valve and duct of the pump is negligible, i.e.  $C_{\text{loss}} \approx 0$ . In practice, a well-designed properly-sized centripetal pump can indeed recover a large fraction of this dynamic pool pressure minus the kinetic energy of the discharge liquid. The design and size of the pump is tailored to a given flow rate and rotation speed. In contrast, without the centripetal pump the kinetic energy of the discharged liquid jet (originated from the kinetic energy of the liquid pool) would have been dissipated to heat and foam as the jet hits the wall of a stationary collector. The soluble protein product would further degrade upon impact of the liquid jet on the stationary wall. Note that the maximum pressure regain, as given by Equation 4.3, can also be expressed as the kinetic energy per unit volume of the pool liquid minus the kinetic energy of the discharge liquid.

$$KE/V = \frac{1}{2} \rho \Omega^2 R_p^2 - \frac{1}{2} \rho \left( \frac{Q}{A} \right)^2 \quad (4.4)$$

Further, if  $A$  is sufficiently large, the kinetic energy of the discharge liquid in Equations 4.3 and 4.4 can be neglected.

A paring disk with 10 inlets around the circumference is shown in Figure 4.9b. These inlets are positioned to dip slightly into the liquid pool. Note that the direction of the rotating pool is clockwise. The fluid with high tangential speed  $\Omega R_p$  is skimmed and directed through a channel to the center at a much smaller radius. This kinetic energy per unit volume of liquid is converted to pressure head after losing some kinetic energy.

#### 4.2.10.2 *Hermetic Seal Design at Liquid Discharge*

On a similar principle, a hermetic seal design can also be used in liquid discharge. The centrifuge bowl is completely filled with liquid which eliminates a liquid–air interface. When air is completely sealed off from contacting the feed and discharged liquid, this prevents oxidation and contact with airborne virus and bacteria of the protein product in the broth, leading to product denaturing and contamination.

### 4.3 Feed Inlet and Accelerator

All disk centrifuges are designed with the highest surface area and maximum  $G$  for use in a given application.

#### 4.3.1 Introduction to Low Shear

Low shear stress is required from centrifuge inlet to centrifuge exit when processing suspension with mammalian cells. At the inlet, feed suspension fills to the axis of the machine to accelerate the flow gently from the axis,  $R = 0$  with zero circumferential velocity  $v = 0$ . Also, it is important to have good feed accelerator design to impart a solid-body rotation to the feed from  $R = 0$  to the periphery of the disk stack at a larger radius  $R = R_2$ .

#### 4.3.2 Hydro-Hermetic Feed Design

Feed is delivered to the bowl from a stationary feed pipe. The surface of the liquid pool is at a radius  $R_p$  as shown in Figure 4.10a. Under solid-body rotation, the pool liquid should have a tangential velocity  $v = \Omega R_p$  in the direction of rotation. This required tangential velocity could not have been delivered by a stationary feed pipe despite the pipe opening being oriented at an angle to the pool, nor could it be readily delivered by a rotating feed pipe. The design of a rotating pipe is complicated and, most importantly, it does not help as the pipe diameter is small; therefore the imparted tangential speed is also limited. Without tangential velocity, when the feed is introduced into the pool in a solid-body rotation, there is a mismatch in tangential speed between the feed and pool liquid which leads to slip, turbulence, and mixing. With the latter, this facilitates oxidation of the cells in the pool, especially those near the pool surface and in stagnant areas which have contact with air. This is solved with the hermetic feed-seal mechanism wherein liquid pool can fill to the axis of the machine (see Figure 4.10b).

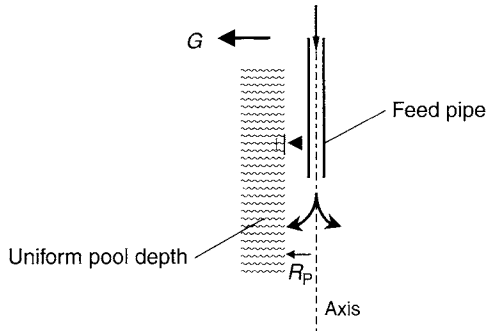


**Figure 4.10a** Pool level distribution

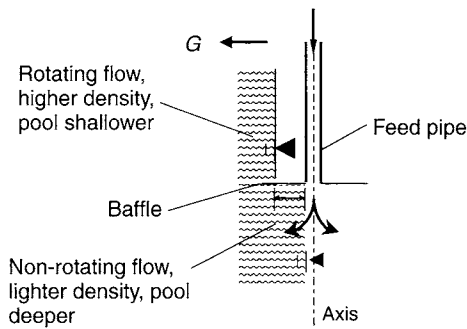


**Figure 4.10b** Pool level elevated at the pool side with less acceleration. One design uses additional accelerating vanes to ensure accelerating feed stream to solid-body rotation before feeding the disk stack

A circular baffle is installed perpendicular to the axis at the end of the pipe. The baffle protrudes into the pool separating the pool into upstream and downstream sections. Downstream of the baffle, the pool liquid is either accelerated, or somewhat accelerated, by contact with other rotating solid parts. (As an example, one design employs a set of closely spaced rotating disks acting as a disk pump to impart circumferential momentum to the local pool liquid.) On the other hand, the pool liquid upstream of the baffle is not accelerated and it appears the liquid is lighter in density when compared with the accelerated 'appeared heavier' liquid pool downstream. As a result, the upstream lighter pool liquid needs a taller liquid column in order to balance the downstream heavier liquid with a shorter liquid column. This induces a differential liquid head across the baffle, as shown in Figure 4.10b. The liquid upstream can even fill up to the axis of rotation, sealing off any air from contacting the pool, thus eliminating air and oxidation altogether. With this arrangement, feed starts to accelerate at the axis, reducing the shear due to mismatch in tangential velocity.

### 4.3.3 Power Loss

Let us consider the energy loss during feed acceleration as this provides some insight into minimizing shear, especially on processing shear-sensitive feed materials. Let the inlet be at pool surface radius  $R_p$  (i.e. entrance to the feed accelerator) and the outlet at the exit of the feed accelerator  $R_{ex}$ . The power acquired by the exit liquid stream after acceleration by the feed accelerator rotating at speed  $\Omega$  is

$$P_{out} = \frac{1}{2} \rho v^2 = \frac{1}{2} \rho \Omega^2 R_{ex}^2 \quad (4.5)$$

The power input to the centrifuge from the motor is given by the product of torque  $T$  and rotating speed  $\Omega$ . Based on Newtonian mechanics, which states that change of momentum equals to torque, the input mechanical power by the centrifuge drive can be determined:

$$P_{in} = T\Omega = \left[ \rho Q (\Omega R_{ex}) R_{ex} \right] \Omega = \rho Q (\Omega R_{ex})^2 \quad (4.6)$$

Subtracting the output power given by Equation 4.5 from the input power given by Equation 4.6, the loss power equals

$$P_{loss} = P_{in} - P_{out} = \rho Q (\Omega R_{ex})^2 - \frac{1}{2} \rho Q (\Omega R_{ex})^2 = \frac{1}{2} \rho Q (\Omega R_{ex})^2 \quad (4.7)$$

This is precisely half of the input power [3]. It is lost due to shear which is ultimately dissipated in viscous losses in feed acceleration. Consider that the feed is being accelerated quasi-steadily from the smaller radius  $R_p$  to a larger radius  $R_{ex}$ , the hydrostatic pressure  $\Delta p$  between these two radii is simply

$$\Delta p = \frac{1}{2} \rho \Omega^2 (R_{ex}^2 - R_p^2) \quad (4.8)$$

Multiplying both sides of Equation 4.8 by  $Q$ , and combining with Equation 4.7, we obtain another form on the power loss as follows

$$P_{loss} = Q \Delta p + \frac{1}{2} \rho Q (\Omega R_p)^2 \quad (4.9)$$

The first term of power loss Equation 4.9 represents frictional losses as feed with volumetric rate  $Q$  is accelerated from  $R_p$  to  $R_{ex}$  in the feed accelerator. In this process, there will be shear and pressure forces acting on the fluid from the rotating surfaces doing various mechanical work and dissipation. Fortunately these forces are not that large as they

are being spread out over a large surface area. As a result the overall power loss  $Q\Delta p$  is similar to that of flow through a ‘resistor’ where there is a pressure drop  $\Delta p$  across the flow resistance element. The second term in power loss Equation 4.9 can be minimized at the expense of increasing  $Q\Delta p$  when  $R_p$  is rendered zero or feed starts accelerating at the axis,  $R_p = 0$ . This is precisely being done in the foregoing discussion with the hydro-hermetic feed design when liquid is filled to the axis. Sealing the center core of the disk centrifuge with liquid also prevents air and oxygen coming in contact and spoiling the liquid product. These are two key advantages for the simple hydro-hermetic design.

#### 4.3.4 Feed Acceleration Visual and Quantitative Testing

An issue that is often ignored when dealing with centrifugation is whether the feed is fully accelerated before being introduced to the separation zone. This is a critical question especially pertaining to high  $G$ -centrifuge where additional speed and power is required to generate better separation. Some extensive research has been conducted on feed acceleration of a continuous liquid stream [4–12].

As shown in Figure 4.11, a simple experiment has been set up to visualize the effect of feed acceleration in a centrifuge. The bowl rotates at 1000 rev/min and is cantilevered from the support at one end. A ring weir attached to the centrifuge bowl holds a rotating liquid pool in place to prevent it overflowing. The feed is introduced to the feed accelerator via a stationary pipe at the support end. After accelerating to rotation speed, the feed stream is introduced to the pool surface. Two bowls are set up side-by-side for bench marking wherein one configuration has a conventional feed accelerator and the other has an improved feed accelerator. To help visualizing the pool, a pool meter supported on a free bearing is driven by two diametrically opposite paddles that extend 3 mm into the pool. The rotating liquid pool at the introduction of the feed stream drives the paddle of the pool meter. Tuning the flashing frequency of a

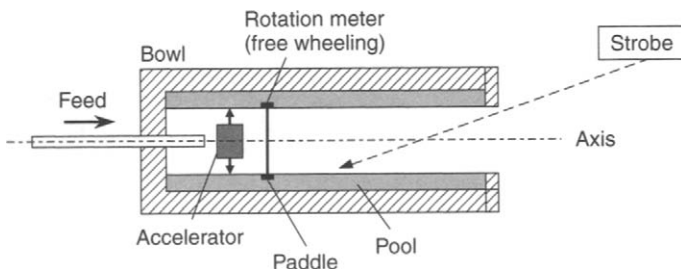


Figure 4.11 Schematic of the test rig

strobe to 'stop' or 'make it appear stationary', the rotation speed of the pool at the point of feeding can be determined. This is also the rotational velocity of the introduced feed. In addition, the pool surface where the feed is introduced can be clearly seen through the front of the bowl with strobing, as depicted by the schematic figure in Figure 4.11.

Figure 4.12a is a photo of the improved feed accelerator. The bowl is rotating at 1000 rev/min. Feed is introduced at 5 m<sup>3</sup>/h. The pool meter appears stationary when the strobe is tuned with a strobing frequency of 1000 flashes per minute, which is at the same rotation speed as the bowl. This means that the introduced feed stream has also attained an angular speed of 1000 rev/min. The pool surface appears calm with reflected color of the pool meter. If the pool surface was 'rough' or 'textured' with waves, color reflection would not have been possible. Both pieces of information confirm that the feed is indeed rotating at solid-body rotation with the bowl.

On the other hand, Figure 4.12b shows a strong contrast under the same operating condition (i.e. same bowl speed and feed rate) as before, but with the pool meter appearing to be rotating counterclockwise, i.e. backwards. By slowing down the strobing frequency, the pool meter can be made to appear stationary again. However, the angular velocity of the feed stream was determined to be only a small fraction of the full bowl speed of 1000 rev/min. This means that the feed is not at solid-body rotation with the rotating bowl. This situation further deteriorated with higher feed rate. Most strikingly, waves and turbulence showed up on the pool surface at the point where the feed was introduced. Figure 4.12c shows a close-up of this situation, revealing intense mixing due to mismatch of pool velocity with that of the feed stream. Also, there is no color reflection. The pool surface appeared like a rough sea.

The feed acceleration efficiency is defined as the ratio of the feed stream tangential speed to the tangential speed under solid-body rotation  $v_{\theta} = \Omega R$ .

$$\eta_a = \frac{v_{\theta}}{\Omega R} \quad (4.10)$$

In this case,  $R$  in Equation 4.10 refers to the pool radius  $R_p$ . Another important measure is the  $G$ -efficiency, which is defined as the  $G$ -acceleration of the feed at the pool to that of  $G$ -acceleration at the same location assuming solid-body rotation, thus

$$\eta_G = \frac{(v_{\theta}^2/R)}{\Omega^2 R} = \left( \frac{v_{\theta}}{\Omega R} \right)^2 = (\eta_a)^2 \quad (4.11)$$

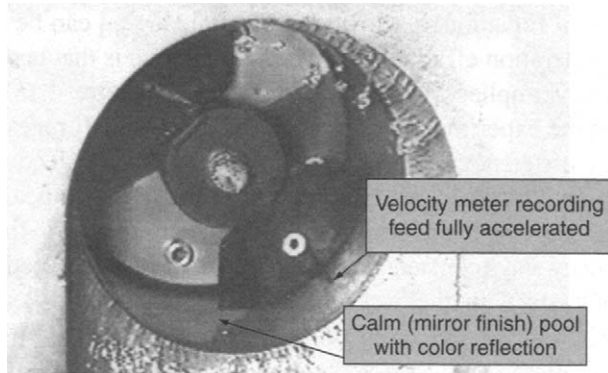


**Figure 4.12a** Improved accelerator showing quiescent pool and reflection of color from excellent feed acceleration

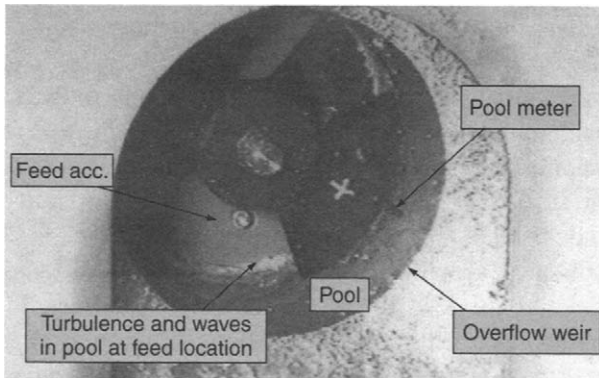


**Figure 4.12b** Conventional accelerator showing turbulence in pool from poor feed acceleration

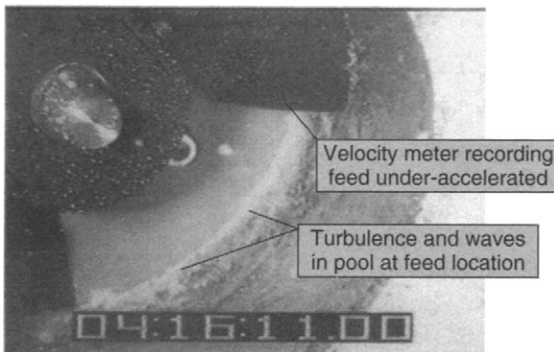


**Figure 4.12c** Close-up of conventional accelerator showing turbulence and mixing in pool from poor feed acceleration

It is clear from Equation 4.11 that the  $G$ -efficiency  $\eta_G$  can be generated from the acceleration efficiency  $\eta_a$ . The significance is that bad acceleration efficiency implies very poor  $G$ -efficiency. Figure 4.13 plots the results from the experiment described in the foregoing. It reveals that the acceleration efficiency drops sharply with increasing feed rate with the conventional feed accelerator taking feed rate in the range 0–10 m<sup>3</sup>/h. On the other hand, with the improved feed accelerator design the acceleration efficiency stays constant at 100%, independent of the feed rate. This finding contrasts with the well-known centrifugal pump performance behavior wherein the delivered pressure head typically drops off with increasing flow rate, and vice versa. Unlike a centrifugal pump, there is no trade-off in performance for an improved feed accelerator!

The  $G$ -efficiency can be generated in lieu of Equation 4.11 by taking the quadratic power of  $\eta_a$ . This is shown in Figure 4.13. As can be expected,  $\eta_G$  would be worse as it is the square of  $\eta_a$ , especially when  $\eta_a$  is less than unity. At a feed rate of 6 m<sup>3</sup>/h, if  $\eta_a = 55\%$  then  $\eta_G = (55\%)^2 = 30\%$ . This implies that the feed velocity is 55% of the solid-body rotation, whereas the  $G$ -force is only 30% of the solid-body! This is considerably disappointing given that the  $G$ -force is responsible for sedimentation and separation. In contrast, the improved feed accelerator maintains at 100% for both efficiencies  $\eta_a$  and  $\eta_G$ , independent of the magnitude of feed rate.

For a disk-stack centrifuge, a set of radial or curved vanes can be used to accelerate the feed stream from the small radius all the way to the large radius. This enforces a solid-body rotation at all radii from  $R = 0$  to near the disk stack outer radius  $R_2$ . Two improved designs and other features of the disk centrifuge are considered briefly next.

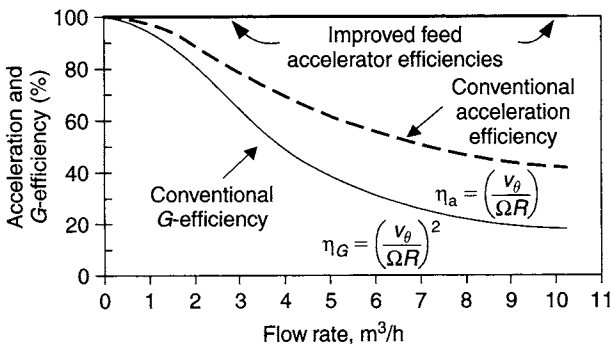


**Figure 4.13** Conventional versus improved accelerators

### 4.3.5 Improved Feed Accelerator

#### 4.3.5.1 Improved Accelerator without Smoothing Disk Section

It is important to accelerate the feed stream to speed in the most efficient manner as discussed. This also reduces temperature increase (due to intense shear leading to heat dissipation) during acceleration, as well as entrainment of air and oxygen that can adversely affect the process. In order to get feed accelerated from inlet radius  $R_1$  to an exit radius  $R_2$ , a specially designed feed accelerator can be realized, as shown in Figure 4.14. The notion on improved accelerator vane was discussed earlier [3,5]. When feed is introduced to the axis of the machine, initially it has no tangential velocity component. Suppose the direction of rotation is clockwise, and the feed is distributed into, say, four inlet channels each with a radial velocity  $v_r$  (see Figure 4.14). In the reference frame of the rotating accelerator rotating at speed  $\Omega$ , the feed is moving with a radial velocity  $v_r$  superimposed with a backward tangential velocity  $\Omega R_1$ . The resultant velocity relative to the rotating frame is then given by  $v_{1r} = (v_r^2 + [\Omega R_1]^2)^{1/2}$ . The accelerator channel shown in Figure 4.14 has an opening aligned with the orientation to the incoming feed stream receiving  $V_{1r}$ . Even if there is a departure in direction between  $V_{1r}$  and that of the channel opening, at least the 'angle of attack' is small and the energy loss during mismatch in entrance orientation (resulting in flow separation) is

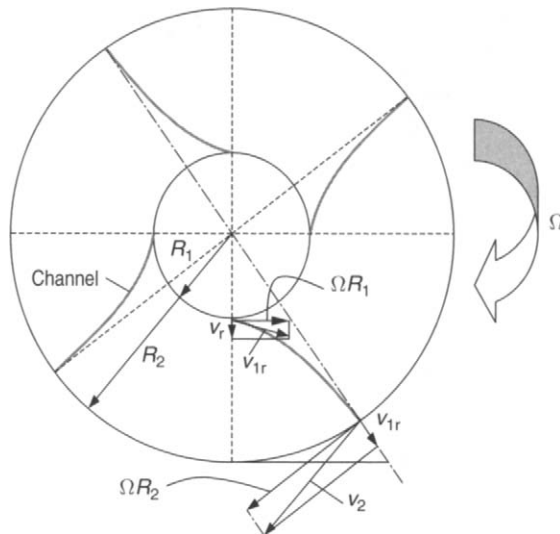


**Figure 4.14** This shows four inlet acceleration channels (gray) with the channel first curving backwards at  $R_1$  and subsequently coming out radially at  $R_2$ . The rotation is in a clockwise direction

minimized. The flow stream is accelerated with increasing tangential speed along the channel by the ‘pressure face’ of the channel to exit at  $R = R_2$ . At the exit, the channel is oriented radially and hence the flow relative to the rotating channel is also directed radially outward. However, because the disk is rotating as a solid body, the feed stream in contact should also acquire this solid-body speed  $\Omega R_2$ . The net resultant velocity in the laboratory frame (i.e. inertial reference frame) should be a superposition of the two orthogonal velocity components, relative channel velocity  $v_{1r}$  (assuming the channel cross-sectional area at exit is the same as that at entrance) and solid-body tangential velocity  $\Omega R_2$ , as depicted in Figure 4.14. The absolute velocity in the laboratory frame is thus  $v_2 = (v_{1r}^2 + [\Omega R_2]^2)^{1/2}$ .

An accelerator is shown in Figure 4.15. Here the direction of rotation for the accelerator is clockwise. It is clear from the photo that the accelerator is formed from a stack of circular disks with eight cut-outs or ‘vanes’ per disk. When the disks are stacked together and aligned, the cut-outs form accelerating channels taking and accelerating the feed to solid-body rotation to be discharged at radius  $R_2$ . Figure 4.15 shows that the outlet channels are radial oriented, as does the schematic diagram of Figure 4.14.

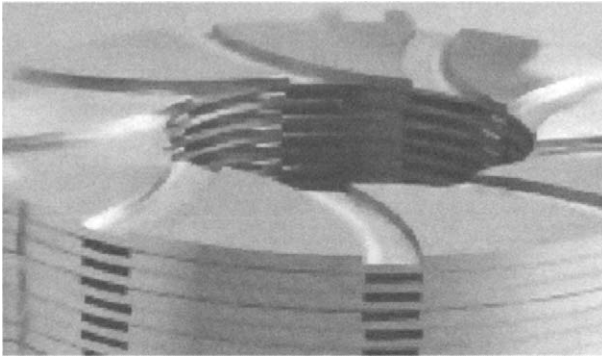


**Figure 4.15** Inlet feed accelerator design with rotating pool directed clockwise (Reproduced by permission of Alfa Laval)

#### 4.3.5.2 Improved Accelerator with Smoothing Disk Section

An improved arrangement is to have the vanes or channels at the exit radius  $R_3$  curved forward in the direction of rotation, as illustrated in Figure 4.16. Note that the exit radius of the vanes/channels  $R_3$  falls short of  $R_2$ . So between  $R_3 \geq R \geq R_1$  there are discrete vanes/channels, whereas in  $R_2 \geq R \geq R_3$  this is a smoothener without vanes/channels.

The tangential speed at exit of the accelerator at  $R_3$  would have a component in the tangential direction from the throughflow velocity

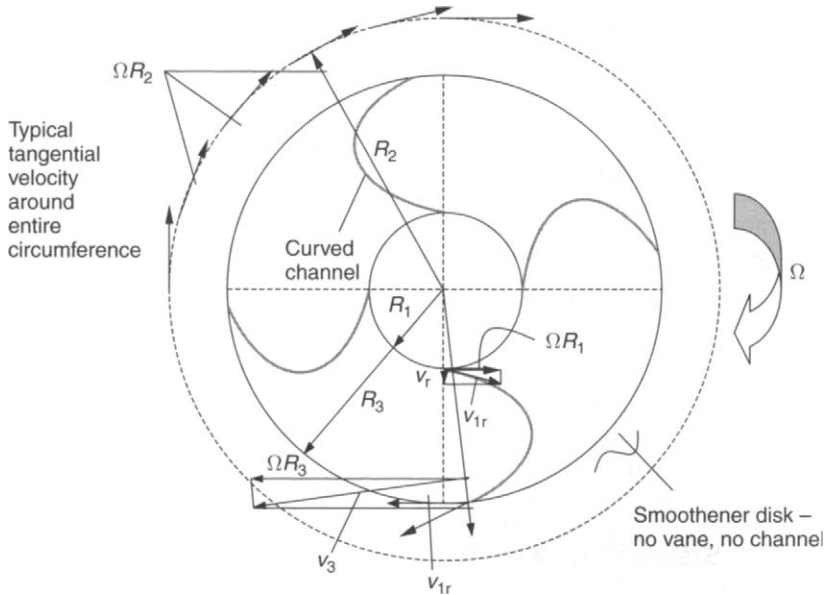


**Figure 4.16** This shows four curved inlet acceleration channels (gray) with the channel first curving backwards at  $R_1$  and subsequently curving forwards at  $R_2$  in rotation. The rotation is in a clockwise direction

$V_{1r}$ , plus the solid-body rotation tangential speed  $\Omega R_3$ . The net resultant velocity is the vector sum of the tangential component and the radial velocity (see Figure 4.16). The disk region without vanes and channels for  $R_2 \geq R \geq R_3$  can be used as a smoothener or smoothening section to reduce the tangential velocity, smoothing out the discrete streams (four discrete streams as shown in Figure 4.16) into multiple streams or a continuous sheet of fluid at radius  $R = R_2$ . Thus, uniformity and solid-body rotation can be both attained [3,5]. Also a side benefit is that the radial velocity component of the feed at  $R_2$  is reduced [5], with this design minimizing plunging of the flow radially outwards, which can disturb the sediment in the solid holding space of the bowl.

## 4.4 Other Considerations

### 4.4.1 Materials of Construction

A major challenge is that the disk is used for high-speed separation as well as processing highly corrosive suspension. Very few materials can meet this stringent requirement. High-strength stainless steel, such as duplex and higher-grade duplex, is used for the bowl and accessories construction. The liquid may contain fine particulates that are highly

abrasive. Areas that are prone to wear and tear are protected by tungsten carbide and nickel-based alloys. Special ceramic sealings are also used when in contact with the liquid containing these abrasive fines.

#### **4.4.2 Clean-in-Place**

On completing the separation process, wash liquid is circulated through the centrifuge internals and disk stack, and the connected system, with repeated full solids ejection (helps to dislodge solids and clean disk stack) to prolong operation prior to routine manual disassembling of the bowl. Wash liquid to be used for washing the bowl may be caustic, dilute acid, or appropriate chemicals. Other hygienic measures can be taken, such as using wash nozzles to spray inside of the hood and casing (stationary parts) and the outside of the rotating bowl.

#### **4.4.3 Steam Sterilization**

Steam is used to sterilize up to 130°C under 1–3 bar for 60–120 minutes duration to kill bacteria. Further sterile air is added for cooling and ‘blanketing’ until the next product run. Most processes do not require steam-in-place (SIP), therefore more disk-centrifuge models are available for selection, such as those for processing yeast in the brewing industry. As such the centrifuge for use in processing yeast has been referred to as a ‘yeast bowl’. Some users prefer a centrifuge with an SIP feature for cleaning during periodic machine maintenance and to reduce the chance of cross-contamination between runs with batches of different feeds and processes.

#### **4.4.4 Containment**

The centrifuge should be fully contained for product integrity and operator safety. There should be double-axial seals on the bowl spindle to prevent leakage. In some designs the seals are cooled and lubricated with circulating water, especially to withstand high sterilization temperature and pressure.

#### **4.4.5 Surface Finish**

The bowl should have a high-polish stainless-steel surface to ensure effective clean-in-place (CIP). There should be no ‘kink’ in the path of flow, so as to avoid unnecessary shear on shear-sensitive cells (e.g. mammalian cells).

#### 4.4.6 Temperature Control

A centrifuge bowl hood is jacketed or circulated with cooling water to ensure temperature control during solid-liquid separation.

#### 4.4.7 Water Requirements

Water is used for a cooling jacket in the bowl hood. In addition, hermetic seal designs (if present), axial seals, a cyclone with cooling jacket in certain designs, and a hydraulic actuated dropping-bottom for other designs all require water.

#### 4.4.8 Noise Level

A specially designed cooling liquid jacket is necessary to ensure noise emissions are under 80 db to meet the industrial standards.

#### 4.4.9 Explosion-Proof Design

An explosion-proof design is available with inert gas instead of air. This requires an inert gas regulating unit with valves and flow-switches for flow control. The explosion-proof control panel is an important piece of equipment for the system. Also, a solids collector should be equipped with a pneumatic pump to transport discharged solids.

### 4.5 Examples of Commercial Disk-Stack Centrifuge

Some commercially available disk centrifuges are described in this section. Figures 4.17a and 4.17b show a 12,000 g centrifuge capable of serving a separation for a 10,000–20,000 L fermenter. The solids-holding space for the disk centrifuge is 14 L. A small or a large centripetal pump is used depending on the concentrate flow rate to be covered in two possible rate ranges, 0 to 5 m<sup>3</sup>/h, or 2 to 12 m<sup>3</sup>/h.

As shown in Figure 4.17b, the solid concentrate is first routed axially and subsequently radially outwards when the bowl bottom drops using a pneumatic-mechanical (spring) mechanism for opening and closing of the bottom. A jacketed cyclone can be supplied when solids need to be cooled.

Another disk-stack centrifuge (see Figure 4.18) capable of 15,000 g is offered by another manufacturer. The centrifuge services a 5000 L to 20,000 L fermenter. The maximum solids-holding capacity in the disk centrifuge is 13 L.

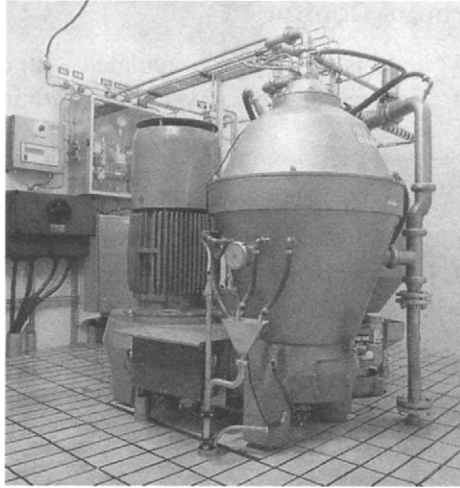


**Figure 4.17a** Model BTAX 215 disk-stack centrifuge (Reproduced by permission of Alfa Laval)

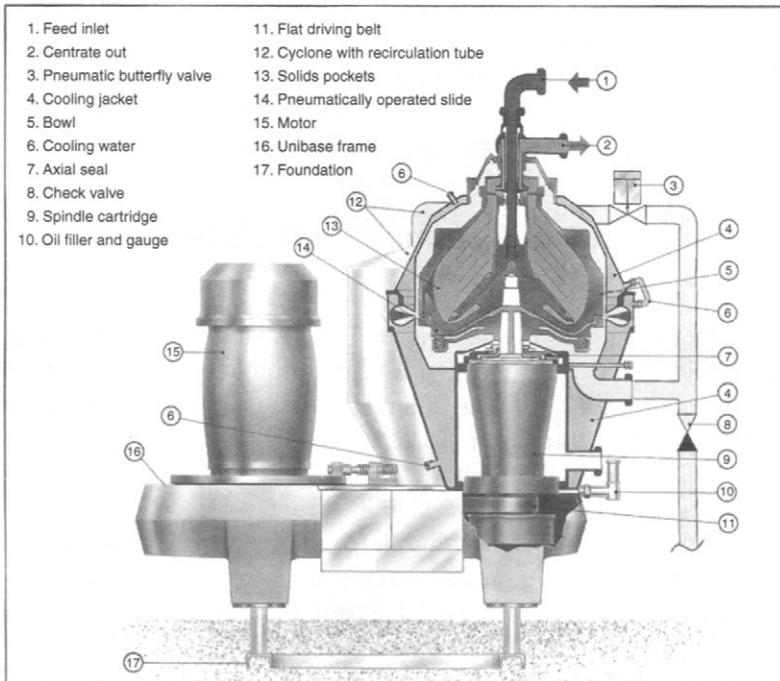


**Figure 4.17b** BTAX 215 with paring disk version and dropping-bottom mechanism using pneumatic control (Reproduced by permission of Alfa Laval)



**Figure 4.18** Model CRA 160-576 (Reproduced by permission of Westfalia Separator)

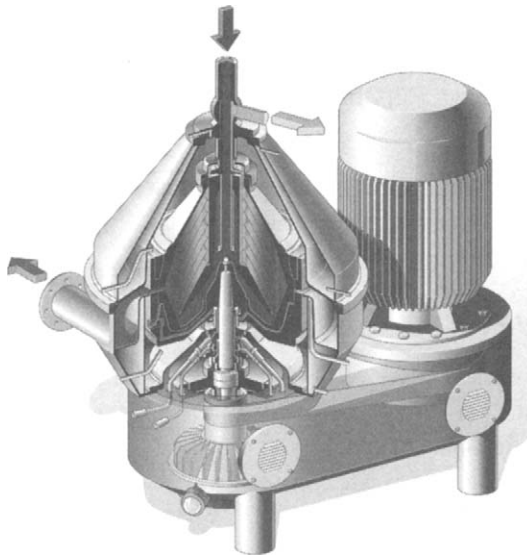


**Figure 4.19** Cut-away of model CSE disk centrifuge (Reproduced by permission of Westfalia Separator)

Finally, a picture of a steam disk-stack centrifuge is shown in Figure 4.19. Figure 4.20 shows a picture of the centrifuge with the control panels for use in SIP.

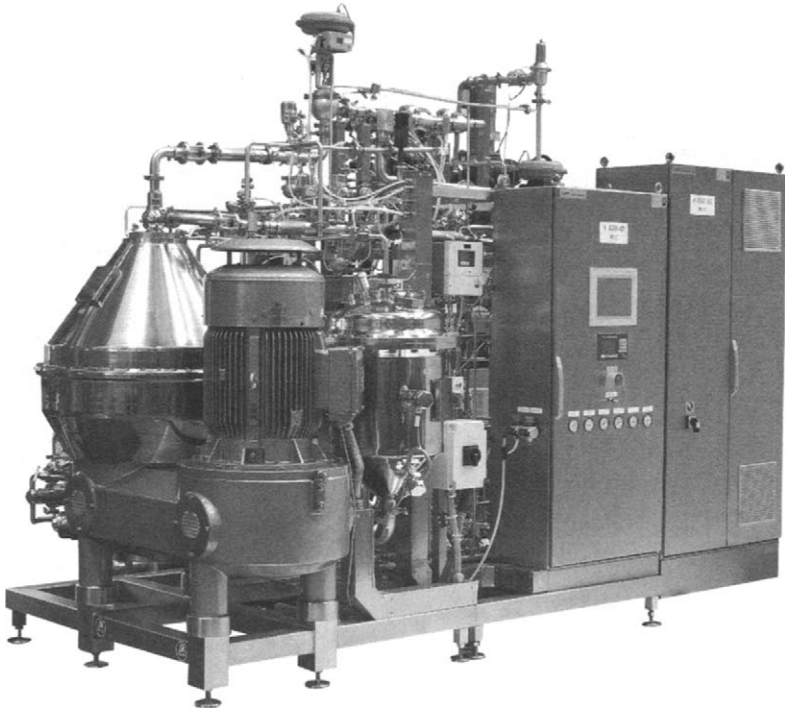


**Figure 4.20** Model CSE-170 steam disk centrifuge (Reproduced by permission of Westfalia Separator)

The past several examples are used for illustration purposes and by no means are they exhaustive.

## 4.6 Summary

In this chapter, we have reviewed the principle of inclined plate sedimentation. The same principle is extended to disk-stack centrifuge. The geometry of the disk-stack centrifuge is discussed. The adverse effect due to Coriolis acceleration can be minimized with use of spacing bars, which oppose the flow driven by Coriolis and serve as spacing elements between adjacent disks. Also manual, dropping-bottom and nozzle disks are described. Gentle acceleration of the feed stream and the means of discharging the separated liquid streams converting the kinetic energy to pressure head are both discussed. Also some illustrations on feed acceleration tests demonstrate a big contrast, both qualitatively and quantitatively, in the performance differences between a good and poor feed accelerator. Factoring into consideration the various issues discussed in this chapter,

a properly designed centrifuge can achieve good performance despite separating difficult biological cell suspensions, as it genuinely takes advantage of high centrifugal acceleration to effect separation.

## References

- [1] W.W.F. Leung and R.F. Probst, Lamella and tube settlers: Part 1 Model and operation, *I&EC Process Des. and Dev.*, 1983.
- [2] W.W.F. Leung, Lamella and tube settlers: Part 2 Flow stability, *I&EC Process Des. and Dev.*, 1983.
- [3] W.W.F. Leung, *Industrial Centrifugation Technology*, McGraw-Hill, New York, 1998.
- [4] W.W.F. Leung and A. Shapiro, An accelerating vane apparatus for improved clarification and classification in decanter centrifuges, *Transactions of Filtration Society*, vol. 1 (3), April 2001.
- [5] W.W.F. Leung and A. Shapiro, Efficient double-disk accelerator for continuous-feed centrifuge, *Filtration and Separation*, pp. 819–823, Oct. 1996.
- [6] W.W.F. Leung and A. Shapiro, Improved design of conical accelerators for decanter and pusher centrifuges, *Filtration and Separation*, pp. 735–738, Sept. 1996.
- [7] W.W.F. Leung, Feed accelerator system including feed slurry accelerating nozzle apparatus, US Patent 5,423,734, June 13, 1995, US Patent 5,651,756, July 13, 1997, US Patent 5,658,232, June 13, 1997, US Patent 5,683,343, Nov. 4, 1997.
- [8] W.W.F. Leung, A method for accelerating a liquid in a centrifuge, US Patent 5,527,474, June 18, 1996.
- [9] W.W.F. Leung and A. Shapiro, Feed accelerator system including accelerator vane apparatus, US Patent 5,520,605, May 28, 1996, US Patent 5,551,943, Sept. 3, 1996, US Patent 5,632,714, May 27, 1997, US Patent 5,769,776, June 28, 1998, US Patent 5,840,006, Nov. 24, 1998, US Patent 6,077,210, June 20, 2000.
- [10] W.W.F. Leung and A. Shapiro, Feed accelerator system including accelerator disk, US Patent 5,401,423, March 28, 1995.
- [11] W.W.F. Leung and A. Shapiro, Feed accelerator system including accelerator cone, US Patent 5,380,266, Jan. 10, 1995, US Patent 5,527,258, June 18, 1996.
- [12] W.W.F. Leung, Accelerator system in a centrifuge, US Patent 5,403,486, April 4, 1995.

## Problems

- (4.1) For a bioseparation process by sedimenting under 10,000 g, a suspension has biological cells with density of  $1100 \text{ kg/m}^3$  in a liquid with density of

- 1000 kg/m<sup>3</sup> and viscosity of 0.002 Pa-s, assuming particles have equivalent spherical diameter of 10 microns. How long does it take for the particles to settle in the spacing between adjacent disks of 1 mm in a disk-storage centrifuge?
- (4.2) Repeat Problem (4.1) but for particles of sizes 3.33, 1, and 0.33 micron, respectively.
- (4.3) Given a centrifuge with bowl volume of 8 L and 50% of which is taken up for solid storage for intermittent discharge. Using a simple approach of retention time being the remaining separation volume divided by the feed rate of 40 L/min, what is the retention time? Based on the retention time comparison with the required separation time, which of the following particle sizes, 0.33, 1, 3.33, and 10 microns, can be captured by the disk-stack centrifuge?
- (4.4) Suppose the viscosity of the fluid is increased to 0.005 Pa-s, what is the maximum feed rate that can be maintained in order to capture the 1 micron particle?
- (4.5) A centripetal pump is used to skim the liquid pool surface at a radius of 2 cm in a disk-stack centrifuge rotating at 1000/s. The centrate liquid discharge rate is 20 L/min. The centripetal pump loss coefficient  $C_{\text{loss}}$  equals to 0.4 and the cross-sectional flow area is 1 cm<sup>2</sup>. Determine the pressure that can be recovered above and beyond the ambient (a) without loss and (b) with loss.

---

# Decanter Centrifuge

For higher feed solids, decanter or solid-bowl centrifuge is a better choice for handling feed with high solids in excess of 5–10% v/v. However, the  $G$ -force that can be attained in decanter centrifuge is much lower. As shown in Figure 2.5, a large decanter can accommodate high volumetric and solid rates but the  $G$ -force is lower, whereas a smaller decanter takes a lower throughput but the  $G$ -force is higher. For example, a 750-mm diameter decanter with the length to bowl ratio of 4:1 can attain only 3000  $g$ , whereas a 150-mm diameter bowl can go up to 6000  $g$ , and higher. Some small decanter designs can actually attain 10,000  $g$  with a special support and floating bearing system. However, the  $G$ -force range is well below the maximum that can be attained by the disk-stack centrifuge. Despite this, there are some high solids feed bioprocessing applications, such as separation in ethanol processing, separation-and-re-slurrying to remove either contaminants or extracting soluble products, and dewatering of biosolids to yield dry cake, in which the decanter centrifuge is preferred.

## 5.1 Solid Bowl or Decanter Centrifuge

Figure 5.1 shows the countercurrent flow decanter, or solid-bowl centrifuge. After accelerating in the rotating feed compartment or accelerator, feed slurry is introduced to the annular pool. Under high centrifugal force, the heavier solids migrate radially outwards towards the bowl, displacing the lighter liquid to the pool surface at a smaller radius. Solids are compacted against the bowl wall to form cake by the centrifugal force. The cake is subsequently conveyed to the small-diameter solid-discharge end of the conical beach by the screw conveyor rotating at differential speed relative to the bowl. The cake is lifted above the annular pool in the 'dry beach' and liquid from the cake further drains back to the pool under  $G$ -force, resulting in discharge of dry cake.

The gear unit and/or conveyor-drive control the differential speed between the bowl and the conveyor, changing the solids retention time in the machine as necessary. The clarified liquid overflows the weirs located at the opposite end (large diameter end) of the machine. The

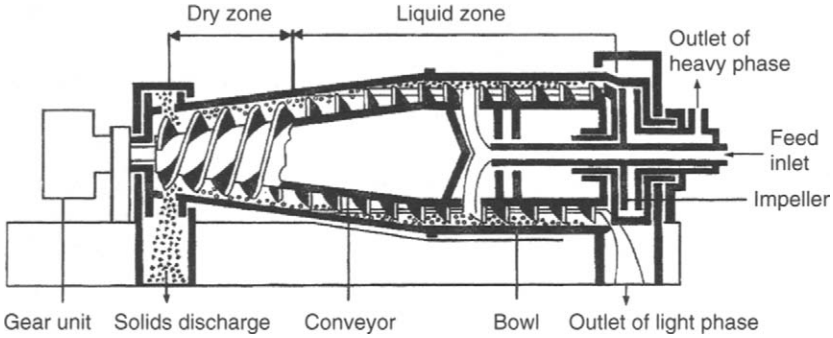


**Figure 5.1** Decanter centrifuge

pool depth is controlled by the discharge diameter of the weirs. The performance of the centrifuge depends on various operating variables, such as the feed rate, pool depth, rotation speed or  $G$ -force, and differential speed, and they should be optimized for a given process. Also, stationary centripetal pumps can be installed to skim the clarified liquid, converting the kinetic energy of the liquid to pressure. This eliminates foaming when discharging liquid with soluble protein.

## 5.2 Feed Rate

The residence time of the slurry in the bowl affects centrate clarity. Decreasing feed rate increases liquid residence time and allows more efficient settling of suspended solids. With dilute suspensions wherein solids concentration is less than 1%, gravity or cyclonic thickening upstream of the centrifuge is recommended to concentrate and reduce the total volume of feed slurry or liquid to be processed. Hydraulic loading affects the main-drive motor requirement from the point of accelerating the feed stream [1–3] while solids-loading affects the conveyor torque load.

## 5.3 Pool Depth

The proper pool depth depends on the settling characteristics of the solids in the feed slurry. By reducing the pool depth, a drier cake is normally obtained because a longer dry beach is available for cake drainage before discharge. Pool level should not be lowered to a point where centrate clarity suffers or solids conveyability is hindered. On the other hand, when the pool depth is increased the length of the drying beach is reduced. This generally results in higher cake moisture. A deeper pool

improves centrate clarity, since liquid retention time is increased, providing lighter and smaller particles with more time to settle. Increasing the pool depth also eases transport of the cake due to liquid buoyancy, resulting in improved cake conveyability, otherwise high conveying torque results and the sediment may only be discharging intermittently. This aspect will be taken up later in the chapter.

## 5.4 Rotation Speed and G-force

Higher rotation speed produces a higher centrifugal force acting on the solids in the cake and improves settling rate. The consequence is lower cake moisture and/or a clear centrate. However, this does not necessarily always hold. Some solids, especially the finer size fraction, have a density very close to that of the liquid (i.e. nearly neutrally buoyant) due to adhesion of contaminants or bubbles to the solid surfaces. They do not settle regardless of the magnitude of the centrifugal force. Some cake drains more readily under lower centrifugal force in which larger voids exist with higher cake permeability or lower specific cake resistance. While solids that form compactable cake tend to pack tightly under high centrifugal force, increasing  $G$  beyond a certain point does not warrant increasing cake dryness for the compactable cake due to equal increase in cake deliquoring resistance. For optimal operation with maximum centrate clarity, cake dryness and least power consumption, the centrifuge should be operated at the 'lowest possible' speed compatible with the process material characteristics and performance requirements. It is good practice during the initial start-up period to compare cake dryness and centrate clarity at different rotation speeds and  $G$ s using various driver and driven sheave combinations to drive the rotor, or, better still, with the machine speed controlled by variable frequency/speed drive to provide the capability of speed/ $G$  change on the fly. This allows selection of the optimum centrifugal forces for the specific application.

## 5.5 Differential Speed

By lowering the differential speed between the conveyor and the bowl, the solids residence time is increased [4]. This usually causes an increase in cake depth piling against the bowl wall with increasing compacting stress and consequential higher cake dryness. This is often accompanied by increasing conveyance torque as well [5]. Lower conveyor differential provides less turbulence and less resuspension of solids. However, too low conveyor differential speed may have the opposite effect; that the

incoming feed solids rate is higher than the solid transport rate offered by the conveyor in which untransported solids build up in the bowl, get entrained by the high-velocity clarified liquid, and eventually overflow with the centrate liquid. This imbalance in the solids feed-to-transport rate often leads to conveyance torque gradually escalating over time. Based on the foregoing discussion, there should be a balance between the solids input and removal rates to prevent loss of the centrate clarity and, more seriously, solids build-up causing plugging of the centrifuge.

Differential speed  $\Delta\Omega$  may be changed by changing the gearratio  $r$  if available for the gearbox, or changing to a different gearbox (with different  $r$ ) altogether. The differential speed is related to the bowl speed  $\Omega_b$  and the speed of the pinion shaft  $\Omega_p$  (i.e. shaft protruding from the input end of the gearbox opposite to the conveyor) by the following relation:

$$\Delta\Omega = \frac{\Omega_b - \Omega_p}{r} \quad (5.1)$$

The kinematic relationship between  $\Delta\Omega$  and  $\Omega_p$  is shown in Figure 5.2 for a bowl (with gearbox housing attached) rotating at 3000 rpm for different gear ratios  $r = 20, 40, 60, 80$  and  $100$ , respectively. A gearbox with a larger gear ratio ( $r > 100$ ) is rated at higher maximum rotation bowl speed because the differential speed is much lower, generating less friction and heat, and less dependent on lubrication to dissipate the excess heat generated compared to a gearbox with lower ratio and higher differential speed. Consider  $\Omega_b = 3000$  rpm and the pinion shaft is locked stationary,  $\Omega_p = 0$ , with a gear ratio  $r = 80:1$ . It gives a differential speed of 37.5 rpm in lieu of Equation 5.1. An alternative is to provide an electric back-drive where the pinion is driven by a DC motor, or an AC motor, which can be controlled by a variable frequency drive (VFD). A hydraulic motor-and-pump system is also used as back-drive for centrifuge. The hydraulic motor is mounted to the bowl while the hydraulic pressure actuates the conveyor scroll to rotate relative to the bowl at lower speed and high torque. By controlling the hydraulic flow rate of the oil, or tuning the frequency of the AC motor, the pinion speed is adjusted, thus changing the differential speed  $\Delta\Omega$  while the centrifuge is running. For example, using Equation 5.1, when the pinion rotates in the same direction as the bowl (positive pinion speed in Figure 5.2), respectively 1000 rpm and 2840 rpm, with the bowl speed  $\Omega_b = 3000$  rpm, the differential speed  $\Delta\Omega$  becomes 25 rpm and 2 rpm. Both values are smaller than the  $\Delta\Omega = 37.5$  rpm under the premise that the pinion is locked stationary  $\Omega_p = 0$ . The small differential speed allows longer retention time, which facilitates deliquored or dewatered

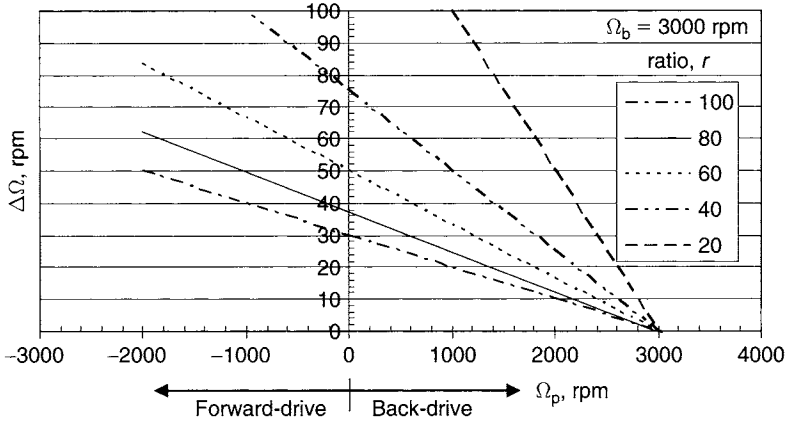


**Figure 5.2** Differential speed versus pinion speed for various gear ratios

cake to higher dryness. This can be easily accomplished by the conveyor back-drive (hydraulic or electric) which acts as a brake, slowing the pinion down without which the pinion would have rotated at the same speed as the bowl. The AC back-drive has a unique advantage in that it further regenerates power back to the main drive as needed.

On the other hand, when there are more solids loading, the differential speed needs to be accelerated to transport the cake at a faster differential rate in lieu of the foregoing discussion. Electric drive and motor can drive the pinion opposite to the rotation of the bowl, in other words the pinion speed is negative (i.e.  $\Omega_p < 0$ ). Obviously power is input into the system. For example, with  $r = 80$  and the pinion rotating at  $-1000$  rpm,  $\Delta\Omega = (3000 - (-1000))/80 = 50$  rpm. This increases the  $\Delta\Omega$  above and beyond the nominal value of 37.5 rpm when the pinion is locked. This forward conveyor drive finds important and interesting application for processing dewatering of sticky solids which causes stick-and-slip (due to momentarily high and low friction) to occur between the conveyor-cake-bowl system. There is a maximum differential speed for a given gearbox design (not shown in Figure 5.2) due to increasing heat dissipation at high differential speed.

Figure 5.3 shows the case of a fixed gear ratio  $r = 40$ , wherein different bowl speeds are considered. Equation 5.1 can be used to calculate the differential speed for a wide range of pinion speed for a fixed bowl speed. This is essentially a straight line in the  $\Delta\Omega$  versus  $\Omega_p$  plot with a negative slope, with the positive pinion speed referring to back-drive with lower differential speed compared to locked pinion, and the negative pinion speed to forward-drive with higher differential speed compared to

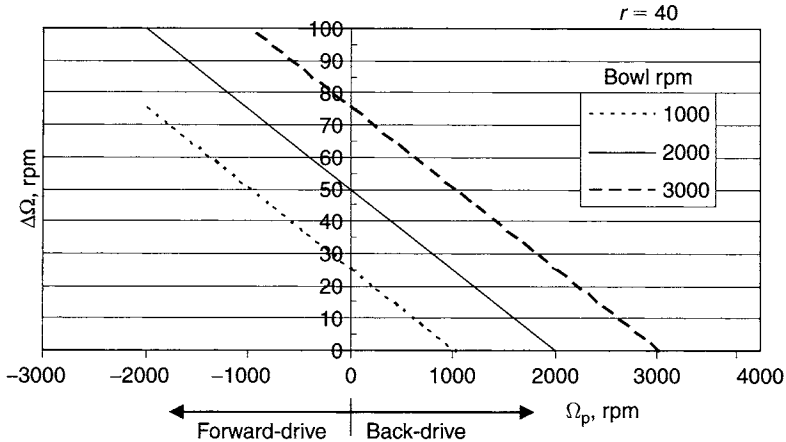


**Figure 5.3** Differential speed versus pinion speed for various bowl speeds

locked pinion. For a fixed pinion speed, higher bowl speed results in higher differential speed.

The centrifuge can be over-torqued due to plugging with unconveyed solids accumulating in the bowl. If temporary reducing or stopping of feed to the machine while continuously maintaining the differential speed between the conveyor and bowl does not clear the jammed machine, the rotation speed and thus the centrifugal force (a component of which opposes cake transport up the beach) need to be reduced to facilitate cake conveyance. Unfortunately, the differential speed also reduces, based on Equation 5.1. A centrifuge equipped with an electric or hydraulic back-drive has an advantage in that it allows the machine to adjust to the maximum differential speed to get cake conveyed out of the machine despite reducing bowl speed, or even when the bowl stops rotating.

## 5.6 Sedimentation Enhancement using Chemicals

Flocculant and/or coagulant are frequently added to the feed slurry to agglomerate fine particles and improve centrate clarity. This is frequently adopted for waste treatment in which polymer dissolved in liquid stream is of lesser concern. It is further discussed in Chapter 8. As shown in Chapter 6, flocculant is used in extracellular enzyme production. Flocculant can help both clarification of the centrate as well as dewatering of biosolids.

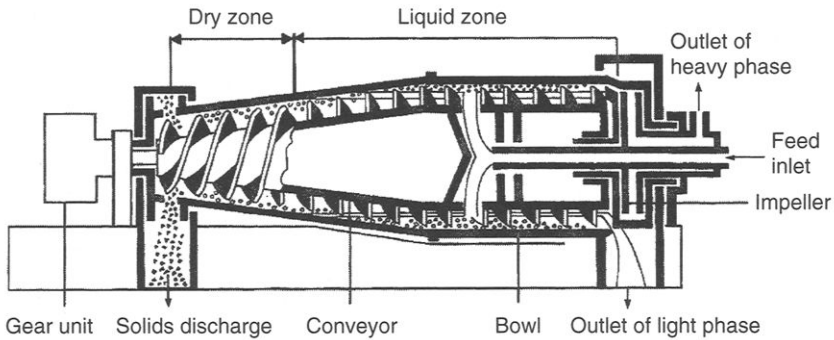


**Figure 5.4** Three-phase decanter

## 5.7 Three-Phase Separation

A machine can also be used for three-phase separation such as two liquid phases (e.g. oil and water) and biosolids. A three-phase decanter is illustrated in Figure 5.4. Two liquid phases with different densities are discharged simultaneously. Under dynamic equilibrium, liquids and solids assume their radial location in a centrifugal field with respect to the magnitude of their densities. The liquid phases are skimmed off at different radii with the lighter of the two liquids taken off at a smaller radius. Centripetal pumps or discharged weirs can be used. The centripetal pump is preferred as it reduces the kinetic energy of the lighter liquid stream, which mostly contains a predominantly oil phase, and converts it to pressure. This avoids making further emulsion, especially when the oil phase contains some water fraction. Also the pressurized discharge can be used to transport the separated liquid without additional pumping requirement.

Frequently, oil and water form an emulsion, regardless of whether it is oil-in-water emulsion or water-in-oil emulsion, depending on the percentage of each in the mixture after mixing and agitation as a result of transport and handling; chemical-treatment (emulsion-breaking chemicals) and heat-treatment (installing steam for preheating to break emulsion) are commonly used to break the emulsion prior to separation.

A flow sheet of a three-phase separation with both employment of decanter and disk is shown in Figure 5.5. The objective is to clarify waste so that the processed streams can be safely discharged or the liquid can be reused. The feed contains 50% oil, 20% water, 20% water-in-oil emulsion, and 10% biosolids, all of which are by weight basis. The mixture after addition of appropriate chemicals is sent to a heat exchanger where steam is used in the exchanger to heat up the oil to 80–90°C. A three-phase decanter is used to carry out the separation. Upon separation

by the decanter, the lighter liquid phase, being skimmed off at a smaller pool radius, contains oil and emulsion with minimal water and solids, while the discharged heavier liquid phase (water) contains less than 1% oil and solids, and the discharged cake phase contains 30–50% by weight of solids that is non-bleeding and stackable to form a pile. The light phase is further processed downstream. The oil-emulsion is reheated back to the process temperature to enhance emulsion reduction prior to downstream separation with a three-phase disk-stack centrifuge. Subsequent to separation, the oil phase (used as product) contains less than 0.1–0.5% w/w of residual solids and water, the water phase contains less than 1% w/w oil and solids that can be combined with the discharged water from the three-phase decanter in the upstream separation, and the cake contains 10–30% w/w solids which is in pumpable form.

The foregoing example demonstrates an important point about three-phase separation with separation of two liquid phases. Between the two liquid phases, one can select to have a purified phase or select to have a lesser pure phase. The lesser pure phase undergoes further treatment downstream, whereas the purified liquid product from the polishing centrifuge can be discharged or reused. Note that it is not possible to have two purified products being produced simultaneously.

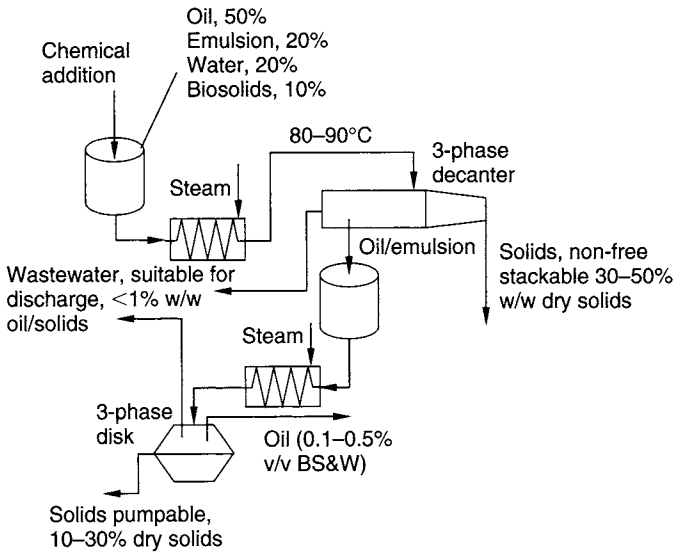


**Figure 5.5** Three-phase decanter–disk combination for clarifying oil and water streams for bioprocessing

## 5.8 Cake Conveyance

### 5.8.1 Dry Beach

When the cake gets conveyed up the beach, the path is not along the steeper beach angle  $\beta$ , nor along a helical path with helix angle  $\alpha$ , but along a climb angle  $\gamma$ , which is a combination of both angles. This is illustrated in Figure 5.6. A simple analogy is that a hiker does not walk up the mountain along the steepest slope but walks up the mountain along a zigzag, meandering road with much shallower gradient. Indeed, the climb angle can be found from geometry as shown in Figure 5.6,

$$\gamma \approx \alpha\beta \quad (5.2)$$

All angles in Equation 5.2 are expressed in radians. The differential rotation between the screw and the bowl provides the conveyance, while the resistance is offered by the component of the centrifugal gravity along the climb angle,  $\rho_{\text{eff}} G \sin \gamma$ , with  $\rho_{\text{eff}}$  being the effective density of the cake. When the cake is submerged in the pool,  $\rho_{\text{eff}}$  equals to the dry cake density  $\rho_{\text{cake}}$  after subtracting the density of the liquid pool  $\rho_L$ , i.e.  $\rho_{\text{cake}} - \rho_L$ . When the cake is above the pool,  $\rho_{\text{eff}}$  equals to the dry cake density  $\rho_{\text{cake}}$ . Therefore, at the point when the cake emerges out of the pool, the resistance force jumps by a factor of  $\rho_{\text{cake}}/(\rho_{\text{cake}} - \rho_L)$ . Consider the case of biosolids wherein  $\rho_{\text{cake}} = 1.01 \text{ g/cm}^3$  and  $\rho_L = 1 \text{ g/cm}^3$ , the ratio  $\rho_{\text{cake}}/(\rho_{\text{cake}} - \rho_L)$  becomes 101! This is very large and is typically the situation encountered for processing biosolids where  $\rho_{\text{cake}}$  and  $\rho_L$  are very close to each

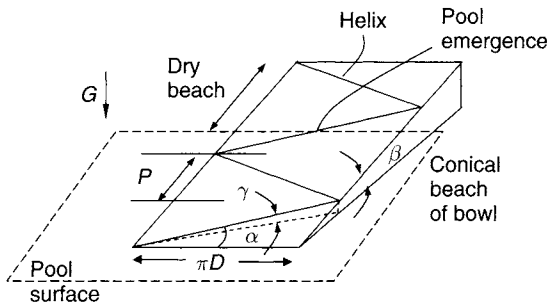


**Figure 5.6** Helix, beach and climb angle geometry in the 'unwrapped' conical beach.  $P$  is the pitch of the helix and  $D$  is the bowl diameter. The schematic is somewhat distorted as  $D$  is actually reducing up the conical beach while  $P$  can stay constant. The dashed line represents the pool surface. Resistance to cake conveyance increases significantly at the pool emergence

other. Consequently, there is a significant resistance to cake emerging out of the liquid pool. Typically, the pool is adjusted so that it is close to the spillover (i.e. pool near the conical discharge) to facilitate cake discharge.

### 5.8.2 Hydraulic Assist

If the cake does not need to be dewatered in the dry beach (out of the pool), it can be dewatered by compaction, even in the liquid pool itself. In this situation, a more innovative solution has been found. To facilitate biosolids cake discharge in lieu of the difficulty of cake transport at pool emergence as discussed in the previous section, a cake baffle or restrictive element can be used to separate the pool level across the baffle, as shown in Figure 5.7. Cake has to pass through the opening between the baffle tip and the bowl wall. The pool level downstream of the baffle is maintained by the spillover of the beach, while that of upstream is controlled by the flow resistance of the baffle which depends on the opening and the cake flow rate, which in turn depends on the feed solids rate. Thus the driving force for the flow to overcome the resistance offered by the cake baffle is  $\rho_{\text{eff}}G\Delta h$ . This is a somewhat self-regulating mechanism as higher feed rate implies higher cake rate and consequently higher driving liquid head  $\Delta h$  to drive the cake through the resistance. Given the opening of the baffle depends on the flow resistance, this opening can be made adjustable depending on the process condition; this has been demonstrated to be very useful for dewatering biosolids [6] and other applications which are shear thickening [7].

Also, an important side benefit that comes with this arrangement is that given the cake solids is highest near the bowl wall with the highest compaction stress; as demonstrated in Chapter 7, only the driest cake is admitted downstream of the baffle. Given the cake height is higher upstream of the baffle in the cylindrical bowl section of the decanter, this maximizes the cake solids concentration before cake is transported to the conical section and eventually out of the machine. This is because cake cannot dewater downstream of the baffle in the conical section, as (a) the percolated water has nowhere to go, given it cannot flow upstream

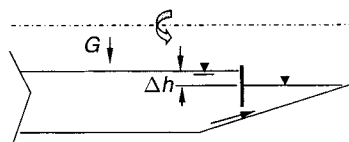


**Figure 5.7** Hydraulic assist by cake baffle

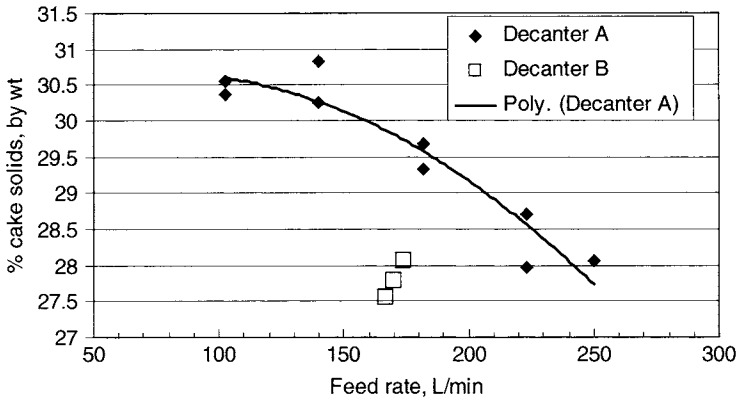


**Figure 5.8** Cake dewatering comparison between two decanters, 457-mm diameter and 445-mm diameter, dewatering biosolids

because of blockage from the baffle, and (b) the cake height is thinner in the conical section due to the conical geometry.

Figure 5.8 compares biosolids dewatering between two decanters. Decanter A is 45-mm diameter (length to diameter 3:1) whereas decanter B is 445 mm (3.5:1). Decanter A is equipped with the adjustable cake baffle technology [6] that produces high cake solids at cake discharge when compared with decanter B. At a feed rate of 170 L/min, the difference between A and B is as much as 2% by weight. This is quite significant for downstream processing. It is also noted that cake solids decrease with increasing feed rate as a result of reducing residence time of solids in the machine at higher rate.

## 5.9 Summary

The decanter is best used for high-solids separation and dewatering. Decanter can be used to classify solids of different sizes and densities, especially for a feed stream with high-solids concentration. Feed rate and bowl speed are still the key variables. In addition, pool depth adjustment by weir and differential speed adjustment (for fixed bowl speed) are two additional variables that can seriously affect centrifuge performance. Not only is the concern on making separation, the centrifuge needs to be operated with continuous feed and cake discharge. In some processes, cake discharge can present some challenges that can be overcome by understanding how the machine work and the variables that the operator can work with to circumvent the difficulty. Some of these aspects have been discussed in this chapter.

## References

- [1] W.W.F. Leung and A. Shapiro, An accelerating vane apparatus for improved clarification and classification in decanter centrifuges, *Transactions of Filtration Society*, 1, 3:61–67, 2001.
- [2] W.W.F. Leung and A. Shapiro, Improved design of conical accelerators for decanter and pusher centrifuges, *Filtration and Separation*, pp. 735–738, Sept. 1996.
- [3] W.W.F. Leung and A. Shapiro, Efficient double-disk accelerator for continuous-feed centrifuge, *Filtration and Separation*, pp. 819–823, Oct. 1996.
- [4] W.W.F. Leung and R. Havrin, High-solids decanter, *Fluid Particle Separation J.*, vol. 5, no. 1, Mar. 1991.
- [5] W.W.F. Leung, Torque requirement for high-solids centrifugal sludge dewatering, *Filtration and Separation*, pp. 882–887, Nov. 1998.
- [6] W.W.F. Leung, Dewatering biosolids sludge with varigate decanter centrifuge, *Transaction Filtration Society*, vol. 1 (2), pp. 38–44, Feb. 2001.
- [7] W.W.F. Leung, A. Shapiro, R. Yarnell, Classification of fine-particle slurries using a decanter with adjustable cake-flow control and improved feed accelerator, *Filtration and Separation*, vol. 36 (9), pp. 32–37, 1999.

## Problems

- (5.1) A 457-mm diameter decanter centrifuge is dewatering solid waste from soy bean processing and the machine is experiencing periodic high torque. Cake is also discharging only intermittently from the conical end of the machine. The  $G$ -force at the bowl wall is at 3000  $g$ , and the pool level is set 7.62 mm below the maximum pool level (i.e. at a larger radius compared to the lip for discharging the cake) and there is a dry beach in the conical section for which the cake can be dewatered with liquid draining back to the pool. What can the operator do to reduce the periodic high torque and intermittent cake discharge?
- (5.2) A decanter is running with a bowl speed of 2800 rev/min, with a gear ratio  $r = 80$ . What is the differential speed of the conveyor with respect to the bowl assuming there is no back-drive or forward-drive?
- (5.3) The differential speed is found to be too high for Problem (5.2) and it leads to wet cake. The gear ratio can be changed to another box with either  $r = 120$  or  $r = 40$ . Which ratio should be selected and what would be the differential speed with this new ratio?
- (5.4) It is desired to reduce the differential speed to 5 rev/min to get a drier cake and an AC back-drive is used to do the job. (a) What would the pinion speed be and (b) what direction should the pinion rotate (same as bowl rotation or opposite to bowl rotation)?

- (5.5) The conical beach angle is  $10^\circ$ , the helix angle can be approximated by  $L/(\pi D)$  with  $L$  being the lead/pitch, and  $D$  is the local bowl diameter. The maximum pool as set by the conical beach is 76.2 mm for a bowl with 457-mm diameter. What would be the climb angle, respectively, at the cone-cylinder junction and at the conical discharge diameter? Is the climb angle constant? Why or why not?



# Commercial Applications of Centrifugation in Biotechnology

Several commercial applications of centrifugation are commonly used in biotechnology. Products may be the biomass itself, a soluble extracellular component in liquid, or an intracellular component, either solid or liquid, residing in the cell. Since fermentation and bioreactor broth are usually very complicated, recovery and purification of the product in dilute form present a big challenge. Recovery and purification can take up as much as 50% of the expenses of the entire process. The more dilute the fermentation broth is the greater is the expense on recovery and purification [1].

In this chapter, a few process flow sheets will be discussed. The flow sheets are quite generic and they can be modified to suit a specific application. Of interest is that centrifugation plays a key separation function in the process flow sheet. Also, centrifugation may play more than one function in the flow sheet. These functions, as has been learnt from previous chapters, include separating solid from liquid, clarification of liquid to remove fines and particulates, classification of solids by sizes and densities, and washing-and-separation to remove impurities. In addition there can be multiple centrifugation stages even for the same function in the flow sheet. Finally, for the purpose of illustration, an example will be given with specific feed rate and concentration respectively of feed and effluent of a centrifuge for use in a specific application.

Many examples discussed in this chapter refer to disk centrifuge. Tubular centrifuges under high  $G$  can also be used provided the capacity of the tubular is within its limit and that semi-continuous operation of the tubular (requiring solids removal and cleaning) is factored into consideration.

## 6.1 Generic Flow Sheet of Biopharmaceutical Processing

In biopharmaceutical processing, such as shown in Figure 6.1 and Figure 1.1, there are typically three sources of protein from fermentation of yeast or bacteria and from cell culture such as mammalian cells. In fermentation of yeast or cell culture of mammalian cells, the protein is extracellularly expressed or secreted in the liquid. At harvest the suspension is sent to a centrifuge for separating yeast, followed by another centrifuge for clarification of the liquid product. In the case of mammalian cells, centrifugation is typically followed by a depth filter to clarify the liquid product (see Figure 1.1). The product can be subsequently concentrated using ultrafiltration or by evaporation, precipitation and other means for removing excess aqueous phase. The advantage of ultrafiltration is that the appropriate buffer liquid to perform buffer exchange can be added to this intermediate product. The resultant broth is purified using column chromatography. The product goes through another round of formulation such as crystallization, freeze or spray drying, and final sterile filtration. The latter is to remove viruses sized 0.2-micron and larger before the release

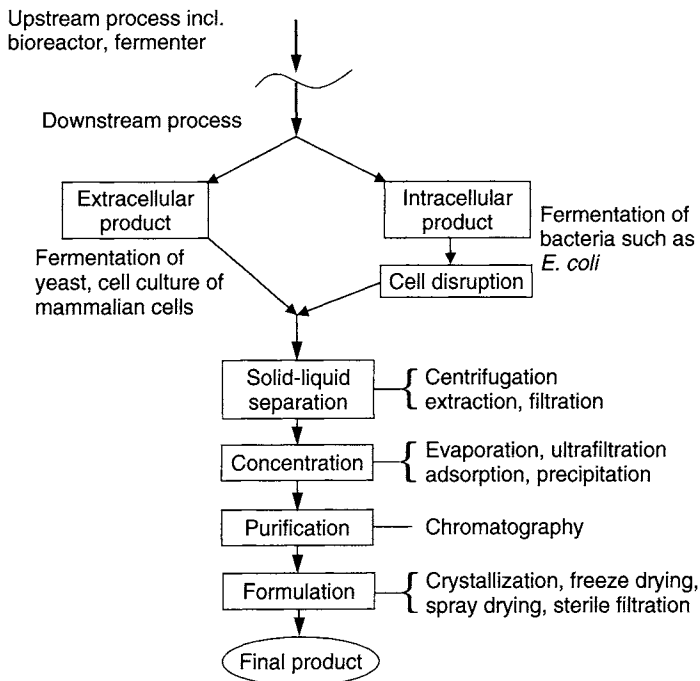


**Figure 6.1** Generic flow sheet for biopharmaceutical process

of the final product. Though not shown in Figure 6.1, it is to be noted that centrifuges are also commonly used to recover crystals downstream of crystallization, even in the formulation stage.

Antibiotics and monoclonal antibodies (MAB) are commonly processed in this manner. World sales of therapeutic antibiotics in 1991 were estimated at 15 billion dollars, which was approximately 10% of the total world pharmaceutical market. About 80% of these sales came from the five most popular antibiotics: cephalosporins, penicillins, macrolides, aminoglycosides, and tetracyclines. Sales of these five antibiotics doubled, with the exception of macrolides which tripled, in 1999 [2,3].

A microbial cell, such as bacteria, is commonly used to engineer expressed intracellular protein via fermentation. Subsequently, the bacteria are homogenized to release the inclusion bodies that contain protein. An additional separation step is required to remove the protein-bearing inclusion bodies from the lysed cell debris and liquid which may contain undesirable released intracellular materials from the lysate. This will be discussed later in the chapter.

Figure 6.2 shows three processing circuits somewhat linked together with the top diagram being the first stage immediately after the fermenter (for removal of extracellular product), followed by either removal of intracellular product in soluble form in liquid (middle diagram of Figure 6.2), or intracellular product in suspended solid form such as inclusion bodies (bottom diagram of Figure 6.2).

Referring to the top diagram of Figure 6.2, the first and foremost part is the circuit for processing extracellular product in which substrate, microorganism, and air are fed to a fermenter under prescribed mixing intensity, process temperature, pressure and time duration. At harvest, the resulting broth is sent to a disk centrifuge where the extracellular-liquid

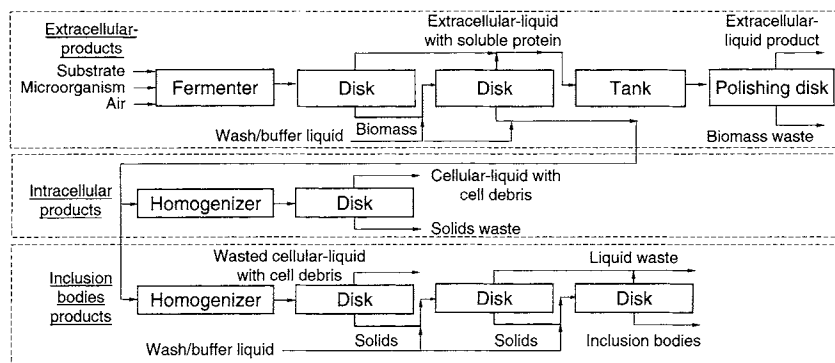


**Figure 6.2** Generic flow sheet with combined processing of extracellular and intracellular protein as well as inclusion bodies

product is removed and the biomass is further repulped to remove any liquid product that is adhered to the biomass solids. The biomass suspension is subsequently sent to a second disk centrifuge to remove the liquid (containing residual extracellular protein washed from the biomass solids). The centrate product (which has a lower concentration of soluble product) is combined with the liquid product containing enriched extracellular protein from the first-stage centrifugation. The combined liquid mixture is sent to a disk centrifuge for clarification of the liquid product, removing any suspending fines and left-over biomass solids.

The underflow or concentrate from the second centrifuge (top diagram in Figure 6.2) are reslurried with wash/buffer liquid. The biomass solid may contain some intracellular protein product (liquid or solid) that need to be recovered. The suspension is sent to a homogenizer in which the biological cells are lysed.

Referring to the middle diagram of Figure 6.2, assuming the intracellular protein product is soluble in liquid after lysing the cells of the biomass, the mixture (i.e. lysate) is fed to a disk and the liquid product is removed in the centrate while the solid concentrate is disposed as waste.

In the bottom diagram of Figure 6.2, the protein product is assumed to be in solid form such as inclusion bodies. After lysing the cells, the solid inclusion bodies (product) together with the cell debris and other suspended contaminants are released in the liquid for separation. The solid product is separated first by a disk centrifuge followed by washing-and-separation twice, using slurry tank and disk centrifuge to remove any cell debris and contaminates in the liquid stream (waste). The solid product is finally discharged in the concentrate stream of the last-stage disk centrifuge.

## 6.2 Mammalian Cell

In mammalian host cells, such as Chinese Hamster Ovary (CHO) or baby hamster kidney (BHK) cells, high-level expression from 10 to more than 100 picograms per cell per day of the recombinant protein can be delivered [4,5]. These are used as the system of choice for large-scale production of therapeutic proteins, as they represent quite a stable cell line, expressing also high levels of product proteins.

With reference to Figure 6.3a, microorganism, substrate, and air are introduced to a bioreactor. The cultivation cycle is typically relatively long. A bioreactor has lower mixing intensity, shear rate, and process temperature compared to a fermenter. At harvest, the broth is subsequently sent to a disk centrifuge for separation. The feed solid is typically 2–4%

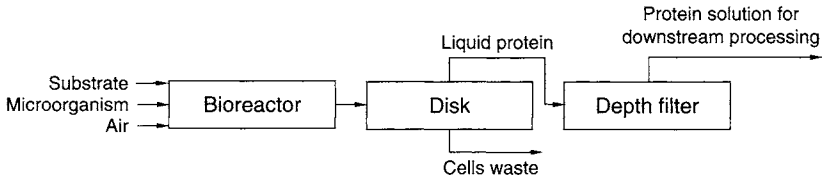


**Figure 6.3a** Mammalian cell processing

by bulk volume (from spindown in a test tube). Given that the mammalian cells, such as the CHO, have a thin membrane wall, gentle acceleration of the feed slurry is important not to rupture the cells otherwise this releases the undesirable intracellular contents which contaminate the secreted protein product in the liquid. The separated centrifuge centrate liquid (product) may still have unsettled submicron particles, which can be largely removed by a downstream depth filter. The clarified filtrate of the depth filter with minimal particulates is sent to downstream for purification. The concentrate or underflow of the disk centrifuge with remaining spent cells is disposed of. It is best to look at the centrifuge-depth filter as an ‘integrated system’ to treat mammalian cells, rather than centrifuge and filter each carrying out their own duties.

Straight batch cultures can be processed through just primary recovery by centrifugation, as the feed contains whole cells and clear fluid. As such, depth filter, as in Figure 6.3a, may not be required. However, fed-batch and perfusion culture clarification, which is the current common practice, takes two steps of separation: a primary recovery step by the centrifuge followed by a clarification step by the depth filter (see Figure 6.3a). Increased cell concentration and longer culture times, which are the current trend, typically generate more cell debris, reduce cell viability, and have more organic constituents in the liquid [6]. It is best for the centrifuge to remove the whole cells and cell debris leaving the submicron fines and colloids to the depth filter, as each equipment has their niche that works best.

Figure 6.3b (i) shows the particle size distribution in the feed with the whole cells ranging between 10 and 20 microns. The cell debris ranges between 2 and 10 microns, and the submicron colloids and fines are typically in the submicron range. The disk centrifuge should be able to remove all the whole cells and cell debris, making a cut size of about 2 microns, see Figure 6.3 (ii). The submicron colloids and fines can then be reported to a depth filter. Modern depth filters are equipped with two layers in series, with the first layer of depth filter having an open-pore permeable structure and the second layer having a tighter pore structure. In addition, some designs are further equipped with a 0.1-micron

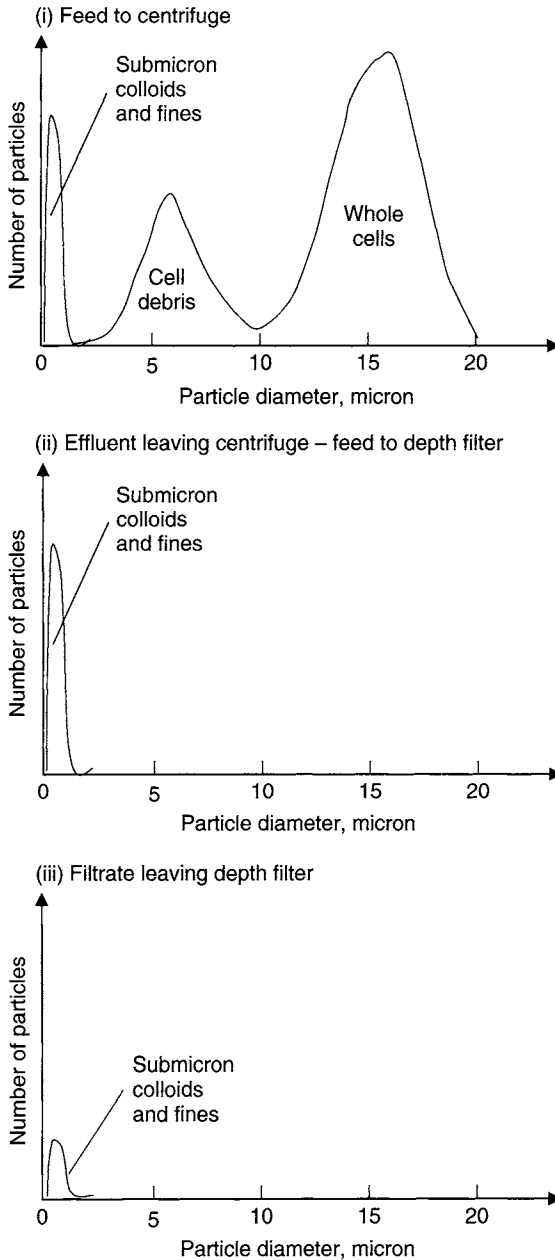


**Figure 6.3b** Particle size distribution of suspension going through a system with centrifuge for primary recovery followed by depth filter for secondary recovery: (i) feed to centrifuge, (ii) effluent leaving centrifuge and feed to depth filter, and (iii) filtrate leaving depth filter

microporous membrane backed up by a porous support downstream of the second depth filter. Not only does the microporous membrane provide a last defense filtration, it also provides back-pressure so that the incoming feed distributes uniformly over the two-layer depth filter without short-circuiting the depth filter. Figure 6.3b (iii) shows the depth filter removing a large part of the submicron particulates leaving a much lower number of submicron particles to escape uncaptured.

While the aforementioned makes use of size exclusion for trapping slightly larger particles, smaller particles can also be trapped with the filter, as discussed in the following. The cellulose fibers of the depth filter are electrically charged. Filter aids, such as diatomaceous earth, are adsorbed to the pores by the electrical charges of the cellulose fibers. The filter aid improves the permeability of the filter. The fines and colloids, especially RNA, DNA, mammalian cell (such as CHO) proteins and lipids, can be attracted by electrical forces, or simply by Van der Waals' attractive force to the pores. This certainly enhances the capture capability of submicron fines and colloids.

### 6.3 Yeast Processing

The experience of processing yeast as a biotech source of protein is quite extensive [7] as it lends itself to the long-established practices of the brewing industry. Figure 6.4 shows a schematic of a yeast processing flow sheet. At harvest, the suspension contains fine yeast cells of 0.5–1 micron in size, and liquid with the extracellularly expressed protein is sent to a centrifuge for separation. An example is given below with some specific values on the processed streams.

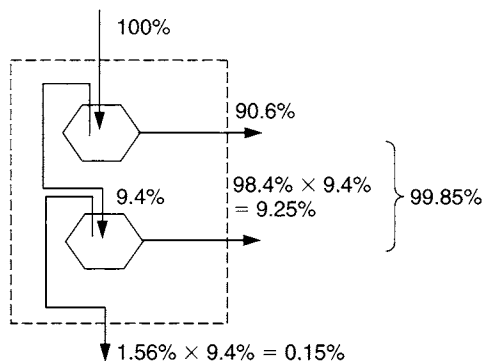


**Figure 6.4** Dual-stage centrifugation, with separation in first stage followed by clarification

**Example 6.1**

A centrifuge is used to separate yeast cells from the valuable liquid containing extracellular protein. Suppose the feed contains 30% by bulk volume of solids and the centrifuge is processing a feed rate of 30 L/min, the centrate turbidity is determined to be 300 NTU, which for this example corresponds to 4.5% v/v solids. The centrate flow is monitored to be 18.8 L/min.

The material balance on the solids and volumetric balance of the three respective streams require

$$\begin{aligned} Q_f c_f &= Q_e c_e + Q_s c_s \\ Q_f &= Q_e + Q_s \end{aligned} \quad (6.1a,b)$$

$Q_f$ ,  $Q_e$ , and  $Q_s$  are the suspension volumetric rates respectively of feed, centrate, and concentrate.  $c_f$ ,  $c_e$ , and  $c_s$  are the suspended solid concentrations (i.e. yeast for the present example) respectively in feed, centrate, and concentrate. Solids recovery refers to the amount of feed solids that are recovered in the concentrate stream, i.e.

$$R_s = \frac{Q_s c_s}{Q_f c_f} = \frac{1 - (c_e/c_f)}{1 - (c_e/c_s)} \quad (6.2)$$

Equation 6.2 is obtained from manipulating Equations 6.1a and 6.1b. If  $Q_e$ ,  $Q_f$ ,  $c_e$  and  $c_f$  are known while the concentrate solids  $c_s$  is not measured, it is best to use these variables as illustrated in the following.

$$R_s = \frac{Q_s c_s}{Q_f c_f} = \frac{Q_f c_f - Q_e c_e}{Q_f c_f} = 1 - \left( \frac{Q_e}{Q_f} \right) \left( \frac{c_e}{c_f} \right)$$

Using the present example

$$R_s = 1 - \left( \frac{18.8}{30} \right) \left( \frac{4.5}{30} \right) = 90.6\%$$

This means that 90.6% of the feed solids are captured by centrifugation in the concentrate stream while the centrate contains 9.4% of the unsettled solids. The centrate broth is sent to a holding tank for further processing. A slip stream at a rate of 15 L/min from the tank is fed to another disk centrifuge for clarification. The feed is at a solids concentration equivalent to a turbidity value of 300 NTU (4.5% solids) and the centrate

leaving the clarifying centrifuge drops down to 10 NTU, which is about 0.15% v/v. The centrate flow rate is at 7 L/min. The solids recovery is thus

$$R_s = 1 - \left( \frac{7}{15} \right) \left( \frac{10}{300} \right) = 98.44\%$$

This means that 98.44% of solids are recovered by centrifugation and 1.56% of solids leave with the product centrate.

The separation and clarification can be combined in a dual-stage centrifugation process, as shown in Figure 6.4. The first stage recovers 90.6% of solid yeast and 9.4% solids overflow to the second stage. The second stage recovers a further 9.25% of the total solids feeding into the system in Figure 6.4. In other words, the combined dual-stage centrifuges remove 99.85% of the feed yeast solid and 0.15% of solid yeast leaves with the centrate product containing protein. Typically, separation has a slightly poorer recovery with high volumetric rate and higher solids loading, while clarification deals with lower feed solids and higher solid recovery with less solids escaping in the centrate. For this example, the solid recovery in the first-stage centrifugation, carrying out separation and with higher feed solid concentration, is 90.6%, while that of the second-stage centrifugation, carrying out clarification and with lower feed solid concentration, is increased to 98.4%.

Figure 6.5 shows a complete circuit for yeast processing. Downstream of the dual-stage centrifugation, the centrate may be sent to a depth filter depending on the amount of suspended solids before being routed to a chromatography column. After the protein solution is purified, it is concentrated by crystallization or precipitation. The protein crystals are washed and separated by centrifugation. The solids recovery of this step is very important as the solids now contain valuable protein and any loss of solids in the centrate represents losing the valuable product. The concentrate is frozen for further processing. When the frozen product is taken out at a later time, it is reslurried with appropriate buffer liquid and the process of purification, concentration, and separation repeats until the product meets the requirement for downstream processing.

## 6.4 Hormones Processing

Hormones are chemicals in the bodies that regulate and control the metabolism and organ functions. Working with the nervous system, they coordinate all essential functions of the body. A common hormone, such as insulin, regulates the blood glucose of the body. Separation by centrifugation has been widely used to process insulin for use by diabetic

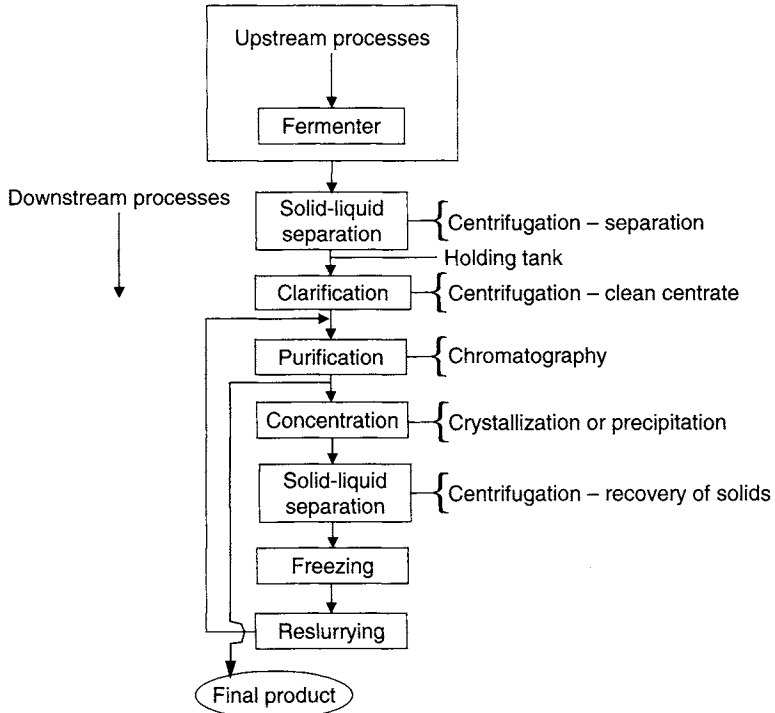


**Figure 6.5** Yeast processing flow process

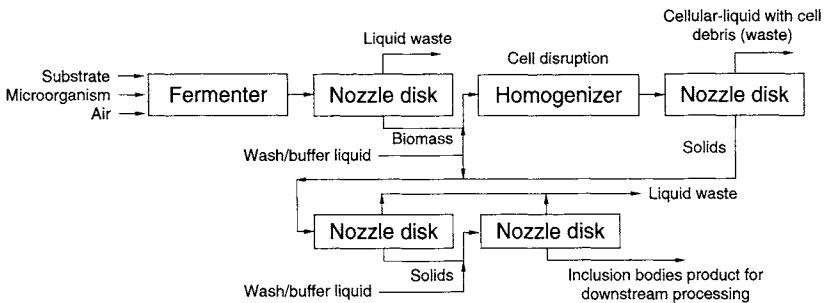


**Figure 6.6** Hormones processing flow sheet

patients. Figure 6.6 shows a generic process of separating and related processing of hormones. Microorganism, substrate, and air are, typically, ingredients to the fermenter. After fermentation, the broth is fed to a nozzle disk where the liquid phase is removed as waste stream, and the separated biomass concentrate discharges continuously through the nozzles. Subsequently, the biomass after being resuspended in wash/buffer liquid is sent to a homogenizer for cell disruption, releasing the solid inclusion bodies. The cellular liquid, with cell debris typically in the submicron

sizes, is classified by another nozzle disk in the centrate with moderate  $G$ -force. As shown in Figure 6.6, the concentrate with solid inclusion bodies containing contaminants is reslurred and separated by centrifugation sequentially in two stages. The inclusion bodies free from contaminants are sent downstream for further processing.

## 6.5 Insulin Production

Insulin is an important hormone controlling the glucose level of blood in humans. A generic insulin production sheet is shown in Figure 6.7. First the bacteria, such as *E. coli* bacteria, are genetically modified to express a specific protein under fermentation. The bacteria go through a fermentation process where temperature, agitation rate, and physiological conditions are closely monitored to ensure the process is well controlled and optimal protein is released in solution. During harvesting, the bacteria cells are lysed and the protein in solids is recovered by centrifugation followed by depth filtration. The pre-insulin is treated with buffer liquid to activate to tertiary form. An enzyme trypsin is used for cleavage. The product solution is purified with chromatography column. The protein is further concentrated by crystallization, washing, and centrifugation. This process is repeated several times until the desired purity is reached. The resulting product is frozen to maintain freshness prior to finish processing.

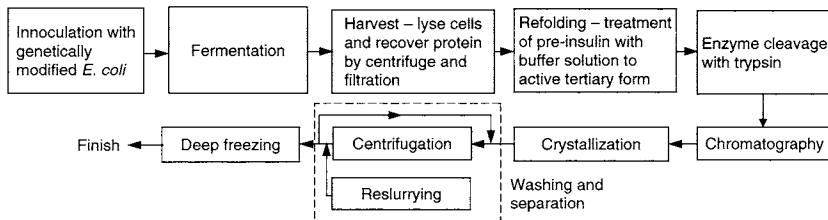


**Figure 6.7** Generic insulin flow sheet using centrifugation

## 6.6 Biotech Separation of Inclusion Bodies

A suspension with *E. coli* bacteria cells, after being engineered and fermented (usually relatively short cycle), is sent to be homogenized so that the cells are lysed to release the inclusion bodies. This is shown in Figure 6.8. Typically, it is about 10–20% v/v (spun solids). The *E. coli* is typically 3.5 microns by 1 micron and the inclusion bodies are about 0.8 micron by 0.8 micron. The SG (specific gravity) of the inclusion bodies is about 1.2 and the SG of cell debris after lysing about 1.05. The cell debris is typically less than 0.4 to 0.5 micron. Here the inclusion bodies, 0.8–1.2 micron

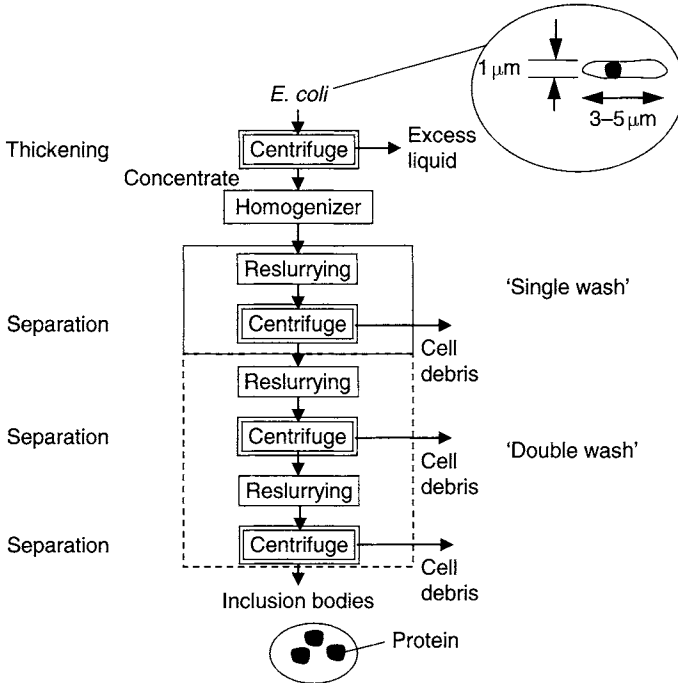


**Figure 6.8** *E. coli* and inclusion bodies

( $SG = 1.2$ ), are separated from the cell debris,  $0.4-0.5$  micron ( $SG = 1.05$ ). The lighter smaller cell debris reports to the centrate, whereas the heavier larger inclusion bodies report to the concentrate.

On the other hand, if the cell debris also has the same  $SG$  as  $1.2$ , then the effective size is more like  $0.2 (= 0.4 [(1.05 - 1)/(1.2 - 1)]^{1/2})$  to  $0.25 (= 0.5 [(1.05 - 1)/(1.2 - 1)]^{1/2})$  after making density correction. One can simplify this problem as classification only by size (and not both by size and density difference). The larger inclusion bodies  $0.8-1.2$  micron is separated from the cell debris  $0.2-0.25$  micron. The overflow rate of the centrifuge is tuned so that there is minimal cell debris settle in the concentrate and almost all cell debris leave with the centrate.

The dual process of reslurring–centrifugation is repeated until little debris is left behind in the centrate. Frequently two to three rounds of the dual process are required for removing the contaminants.

## 6.7 Vaccines Processing

There are two types of vaccines: a concentrated cell-based solid product and a serum liquid product, both of which can be processed by centrifugation.

### 6.7.1 Concentrated Cell-Based Product

The starter culture and air are introduced to a prefermenter as depicted in Figure 6.9. The virus culture from the prefermenter is sent to the main fermenter where additional air and nutrient solution are added. Afterwards, the virus culture is taken to a downstream disk centrifuge for separation. The excess liquid in the overflow is steam sterilized before discharge. The raw vaccine (concentrate from centrifugation) is sent to a downstream mixing tank where additives are added. These additives include the following:

- 1 Suspending fluid (e.g. sterile water, saline, or protein solution)
- 2 Preservatives and stabilizers (e.g. albumin, phenols, and glycine)
- 3 Adjuvants or enhancers that help vaccine improve its function.

After adequate mixing, the mixture is sent to a freeze dryer wherein excess water is removed in overflow centrate, leaving the concentrated vaccine product in the underflow.

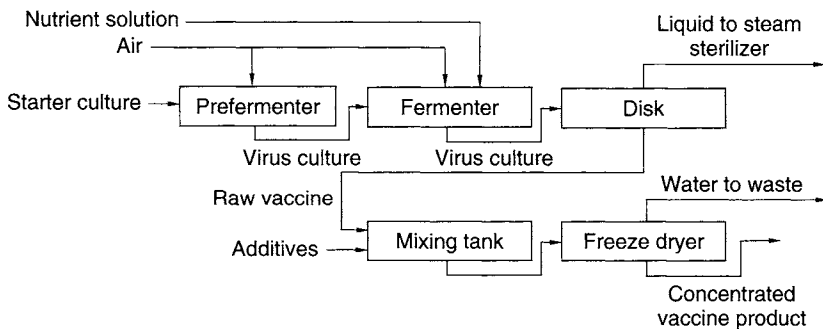


**Figure 6.9** Vaccine concentrated product flow sheet

### 6.7.2 Serum Product

As shown in Figure 6.10, a common production of vaccine in the form of serum liquid follows a similar flow sheet to that illustrated in Figure 6.9, though the fermentation and process condition may be different. After two fermentation stages, the virus culture is sent to a disk centrifuge. The serum product is in the centrate liquid which requires further processing downstream, and the biomass captured in the concentrate is starved and deprived of food and air in a killing tank, with the dead biomass subsequently disposed.

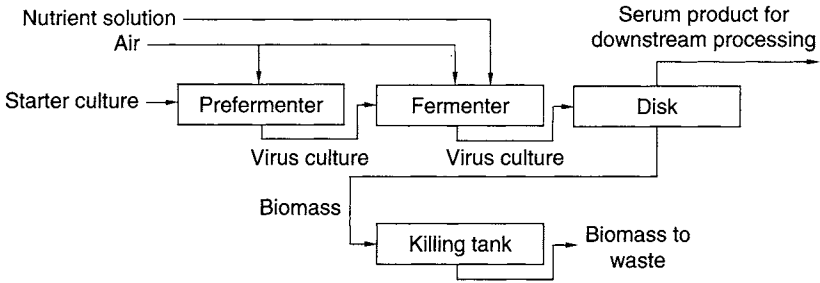


**Figure 6.10** Vaccine serum flow sheet

## 6.8 Enzymes Processing

There are two types of enzymes: extracellular enzymes and intracellular enzymes [8,9]. The processing of both processes is described below, especially where centrifugation plays an important role.

### 6.8.1 Extracellular Enzymes

Biological enzymes play a key role in expediting a given biological–chemical process. Enzymes can be produced from raw materials – substrate, microorganism, and air in the fermenter – at suitable temperature and physicochemical condition. With reference to Figure 6.11, at harvest the fermentation broth, after the addition of appropriate flocculant to agglomerate all the fine biological solids, is separated by a disk or decanter centrifuge to a centrate liquid containing extracellular liquid product and a concentrate with the biomass.

The separated biomass is reslurried in buffer or wash liquid to recover additional protein product (that could have been lost with the solids), and the resulting suspension is separated under centrifugation (disk or decanter) one more time. The overflow of the centrifuge contains diluted liquid product from washing, and the underflow biomass is disposed of. Both centrate streams coming out of the two-stage centrifuges (the first-stage centrifuge centrate containing enriched extracellular protein and the second-stage centrifuge centrate containing diluted recovered protein) are combined before routing to storage. A slip stream of the liquid from the storage tank is sent to a polishing disk centrifuge to remove suspended submicron particles. The clarified extracellular enzymes liquid product is discharged in the centrate of the disk centrifuge for downstream processing. The removed solids in the concentrate are wasted. Flocculant is required for use with both disk and decanter for the first-stage separation as the biological solids are quite fine and can easily escape with the centrate product. Flocculant is not used for the second-stage separation.

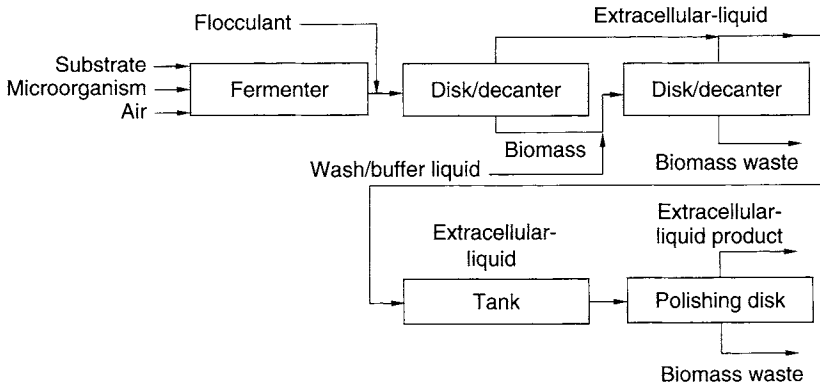


**Figure 6.11** Extracellular protein processing flow sheet

Typically, decanter works best for high feed solids while disk centrifuge works best for lower feed solids. The disk centrifuge should be used for the third-stage centrifugation, which is for clarification of the liquid product.

## 6.8.2 Intracellular Enzymes

As shown in Figure 6.12, a mixture of microorganism and substrate is introduced with air to the fermenter. The broth is thickened or concentrated by centrifugation, with liquid overflowing to waste and the concentrate biomass further reslurried with wash liquid. The resulting suspension of biomass is sent to a homogenizer for cell lysing to release the intracellular liquid product. The liquid stream containing cell debris and liquid (with intracellular protein) is separated by a high- $G$  centrifuge to isolate the protein product in the centrate liquid while the solids and cell debris are removed in the concentrate for wastage.

The foregoing shows various flow sheets demonstrating various combinations of processing extracellular and intracellular protein, nevertheless these bioseparation processes encompass one or a combination of the following:

- 1 Separation of the mixture to liquid phase and concentrated solid phase.
- 2 Washing of solid phase to remove contaminants or recovery of liquid product.
- 3 Classification to remove cell debris in the overflow.
- 4 Clarification or polishing to remove any fine solids in the product liquid stream.

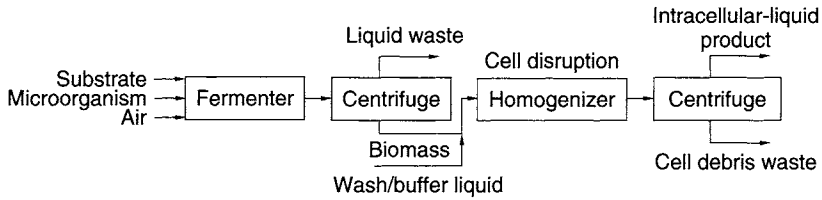


**Figure 6.12** Intracellular protein processing flow sheet

## 6.9 Ethanol Production

In the final example, the more traditional bioprocessing [10,11], whereby ethanol is produced for biofuel by the dry mill corn process, is discussed. Ethanol is ethyl alcohol and is produced and stored on site. It is a fuel component made primarily from corn and various other grains. It can be used for (a) an octane enhancer in fuels, (b) a non-petroleum-based gasoline extender, and (c) an oxygenated fuel additive that can reduce carbon monoxide vehicle emissions. Typically, ethanol is employed in its primary form for blending with unleaded gasoline and other fuel products.

The ethanol production process is illustrated by the schematic in Figure 6.13. Corn is metered to the hammermill by a computer-controlled weigh belt feeder, then ground and pneumatically conveyed to the tank in the form of slurry for further enzymatic processing. The addition of heat, water, and enzymes further breaks down the ground corn into fine slurry. The slurry is heated for sterilization and is pumped to a liquefaction tank where other enzymes are added to convert the starches into glucose. The processed corn is transferred to the fermenter, into which yeast is added for a 50-hour fermentation process.

A vacuum distillation system can be used to separate the mash from the alcohol derived from fermentation. It is routed to the dehydration equipment, wherein 145-proof alcohol is produced from the distillation stripper. This intermediate product is passed to the rectifier from which 190-proof alcohol is produced. It is further dried to 200-proof alcohol by the molecular sieve. Gasoline (5%) is added to provide a mixture of 200-proof denatured ethanol product.

The mash streams from the distillation stripper are sent to decanter centrifuges for dewatering. The aqueous phase (thin stillage), separated from the decanter, is pumped to a steam driven evaporator. A thick syrup remains after evaporation. The wet cake from the centrifuge is transported to a rotary dryer to dry the moisture of the wet cake, producing golden

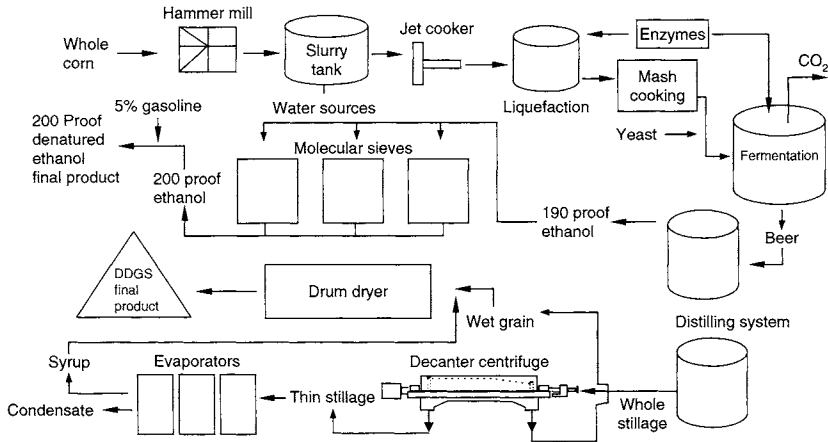


**Figure 6.13** Dry corn mill process

dried distillers grains with solubles (DDGS). One pass through the rotary dryer produces a 50% moisture product, while repeated passes produces a 10% moisture product. The drier product can be pneumatically transported to storage to cool and ready for shipment, while the heavier wetter product is shipped by trucks.

## 6.10 Other Biotech Processing

### 6.10.1 Recovery of Coagulation Factors from Blood Plasma

Coagulation factors can be purified from outdated plasma containing other highly abundant proteins, such as albumin, immunoglobulin, and fibrinogen. Plasma, after centrifugation to remove its cellular components, including erythrocytes, leukocytes and platelets, is typically in a buffered solution based in trisodium citrate. Barium chloride solution is added to the citrated plasma, which subsequently induces the precipitation of barium citrate. Dissolved coagulation factors (including factors II, V, VII, X and XI) will be absorbed onto the barium citrate precipitate. The resultant mixture is sent to a centrifuge to separate the barium citrate precipitate on to which the coagulation factors are absorbed. Relatively low centrifugal gravity, such as 1000 g, is needed for the separation for a period of 10–20 minutes at 4°C. This avoids over-compacted solids forming under high G, which would be difficult for subsequent dissolution. After removing the supernatant or centrate in continuous operation,

the centrifuged solid or pellet is redissolved in buffer (usually the equilibration buffer for the ion-exchange column downstream) before buffer exchange and subsequent ion-exchange chromatography downstream for selective partial purification of the coagulation factors. At the right set of ion-exchange resins and conditions, such as pH and ionic strength, coagulation factors will remain bound to the column while highly abundant contaminants, such as albumin, immunoglobulin, and fibrinogen, will flow through the chromatographic column. Serial elution of the coagulation factors from the ion-exchange column is usually done with a buffer containing high salt.

### **6.10.2 Tissue from Animal Cells**

Proteins of interest in cells from animal tissue can be isolated and studied in the laboratory. One technique involving centrifugation is to homogenize the tissue before centrifuging the lysate. Insoluble cell membrane and debris will be collected at the bottom of the spintube while the intracellular contents (i.e. proteins in the cytosolic fraction) left in the supernatant can be processed to recover the valuable soluble protein. (This is identical to the process as delineated in the middle diagram of Figure 6.2.) The cell membrane left as pellet in the centrifuge spintube can be reslurried and washed several times or as many times as practical until the contaminants are removed. At the end, detergent such as Tween 20 or NP-40 can be added to dissolve the membrane containing phospholipid. The resultant solution can be analyzed using standard laboratory techniques.

### **6.10.3 Laboratory Concentration and Buffer Exchange using Centrifugal Filter**

The centrifugal filter (see Figure 6.14), as described in Chapter 1 and modeled in Chapter 14, is used commonly in the laboratory for concentration and buffer exchange which replaces the traditional concentration and dialysis steps. For example, a protein in buffer A solution is fed to the centrifugal filter equipped with the appropriate MWCO (molecular weight cut-off) membrane. (The centrifugal filter, as shown in Figure 6.14, has a low MWCO of only 5000.) Protein with a molecular weight larger than the MWCO is retained and concentrated by the centrifugal filter (membrane) with removal of buffer A in the filtrate. Buffer B is added to the centrifuged proteins left on the membrane to displace any residual buffer A liquid, and the mixture is centrifuged again. This washing-and-centrifugation process is repeated several times until the protein is practically in buffer B as the suspending medium.

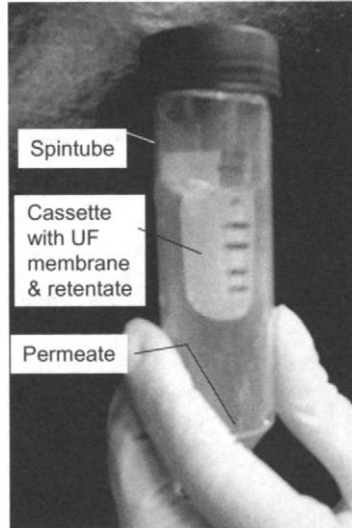


**Figure 6.14** Centrifugal filtering a protein in buffer solution

## 6.11 Summary

In closing, centrifuges have been used for various separation functions and processes from the traditional ethanol production to recovery of high-valued therapeutic protein production. These include hormones, insulin, vaccines, and enzymes, to cite just a few. It is also used in blood fractionation and various biotech separations in small and large scales. The applications discussed in this chapter are by no means exhaustive. Some examples are used to demonstrate the typical flow processes for separation of extracellular- and intracellular-expressed proteins. Other biotech processes, such as recovery of concentration factors in blood or recovery of certain red blood cells and/or white blood cells, are also of interest and of great commercial value. Other applications, such as cell tissue characterization and concentration and buffer exchange, are also carried out routinely in biotechnology, and they are all of great interest.

## References

- [1] M. Shuler and F. Kargi, *Bioprocess Engineering, Basic Concepts*, 2nd edn, Prentice Hall, Upper Saddle River, NJ, 2002.
- [2] W.R. Strohl, Industrial antibiotics: today and the future, *Biotechnology of Antibiotics*, 2nd edn, pp. 1–47, Marcel Dekker, New York, 1997.
- [3] D. Lowe, Antibiotics, *Basic Biotechnology*, C. Ratledge and B. Kristiansen (eds), 2nd edn, Cambridge University Press, 2002.

- [4] M. Butler (ed.), *Mammalian Cell Biotechnology. A Practical Approach*, Oxford University Press, New York, 1991.
- [5] R.E. Spier (ed.), *The Encyclopedia of Cell Technology*, John Wiley, New York, 2000.
- [6] M. Pailhes, C. Lambalot, and R. Barloga, Integration of centrifuges with depth filtration for optimized cell culture fluid clarification processes, *BioProcessing J.*, May/June, 2004.
- [7] K. Wolf, *Non-conventional Yeasts in Biotechnology*, Springer-Verlag, Berlin, 1996.
- [8] T. Godfrey and S. West (eds), *Industrial Enzymology*, 2nd edn, Macmillan Press, London, 1996.
- [9] R.N. Patel (ed.), *Stereoselective Biocatalysis*, Marcel Dekker, New York, 1999.
- [10] M.C. Flickinger and S. W. Drew (eds), *Encyclopedia of Bioprocess Technology: Fermentation, Biocatalysis and Bioseparation*, John Wiley, New York, 1999.
- [11] A.L. Demain, Small bugs, big business: The economical power of the microbe, *Biotechnol. Adv.*, 18:499–514, 2000.

## Problems

- (6.1) A yeast broth containing 20% suspended solids (under upset condition as the norm is more 25–30%) is sent to a disk centrifuge for separation at a rate of 25 L/min. The centrate liquid leaves the disk centrifuge at a rate of 13 L/min with 3% suspended solids. (a) Determine the solids recovery of this first-stage centrifugation. The centrate is sent to a holding tank, a slip stream of 12 L/min is sent to a disk centrifuge for clarification. The centrate leaving the clarifier centrifuge is at a flow rate of 5 L/min with turbidity of 1 NTU. Assuming 1% suspended solids is equivalent to 66.7 NTU as a rough calibration, (b) determine the solids recovery of the second-stage centrifugation as well as (c) the solids recovery or capture for the entire process.
- (6.2) Design a flow sheet where protein is expressed in a bioreactor intracellularly in the cell liquid/plasma. The processed protein needs to be in a buffer liquid A.
- (6.3) Figure 6.3b refers to mammalian cells with larger cell sizes. Design a flow process with all the appropriate separation steps if yeast (6–8 microns), cell debris (2–5 microns) and submicron colloidal particles are all present in the broth and the whole yeast cells need to be separated from the debris and colloids.
- (6.4) Design a separation flow sheet for a biofuel other than ethanol.

# Concentrating Solids by Centrifugation

## 7.1 Introduction

With a dropping-bottom disk centrifuge as shown in Figure 7.1, the solids accumulate in the solids-holding space during the period in between solids discharge. The accumulated solids become more concentrated under centrifugal force near the larger radius and concurrently liquid percolates oppositely towards the small radius. In Chapter 4, we discussed how the conical angle in the solids-holding space of a disk centrifuge may affect the discharge as well as the compaction of solids.

There are several benefits associated with discharging a concentrated shot. When the valuable protein product is in the liquid, it should be directed to the centrate and not in the concentrate or underflow. If the concentrate becomes too wet it is losing the valuable product in the rejected concentrate. In addition, handling of a very wet concentrate may be problematic as it sticks to walls and is difficult to convey unless by reslurrying.

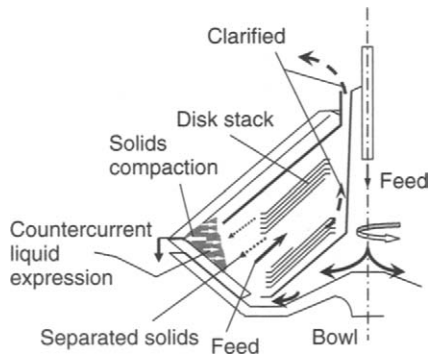


**Figure 7.1** Concentrate piling against solids-holding space in a dropping-bottom disk-stack centrifuge

## 7.2 Concentrating Underflow

In the foregoing, the importance of concentrating the underflow is discussed. One of the key benefits of separation with extracellular protein product in the liquid centrate is that it can increase the protein yield. The following example illustrates this point.

### Example 7.1

Consider a fermentation broth with 5000 L, of which after spindown the solid represent 3% v/v (bulk volume). This suspension after all contains 4850 L liquid with protein product and 150 L of solids (bulk volume). Assuming a total discharge volume of 214 L from the concentrate end of the machine with a 70% v/v, this implies 150 L of solids v/v and an additional 64 L of liquid carryover in the concentrate. The carryover liquid contains the valuable protein product. The product yield is the ratio of the liquid leaving the centrate 4786 L (= 4850 L – 64 L) to the original 4850 L in the feed, thus the yield is 98.7%. Table 7.1 shows additional calculation of what the expected outcome is with improved compaction from 70% successively to 90% in increments of 5%, translating to a product yield increase from 98.7 to 99.6%.

Also, if the concentrate is too watery, it does not discharge properly and tends to hang or stick onto the walls of the bowl, and possibly to the walls of the container outside the rotor. This may present problems when handling the wet concentrate downstream.

There are two mechanisms that are responsible for concentrating solids in the hold-up space of a disk centrifuge. They are compaction of grains and expression or percolation of liquid in the porous bed, both taking place simultaneously, as depicted in Figure 7.1 for a disk-stack centrifuge.

**Table 7.1** Example of compaction affecting product yield showing concentrate discharge volume and composition

<i>Concentrate discharge, L</i>	<i>% v/v solid</i>	<i>Bulk solid, L</i>	<i>Liquid carryover, L</i>	<i>Yield (%)</i>
214	70	150	64	98.7
214	75	161	54	98.9
214	80	171	43	99.1
214	85	182	32	99.3
214	90	193	21	99.6

### 7.3 Compaction

Compaction can be understood through a simple analogy. Imagine four acrobats standing on top of each other building up a ‘human ladder’, as shown in Figure 7.2. The top acrobat has no weight imposed upon him from above, the second acrobat bears the body weight of the top acrobat, the third bears the weight of the two above, and the fourth supports the three above. Assuming the weight of each acrobat is the same, the loading would then be evenly increasing from top to bottom in the direction of the gravitational acceleration. Likewise, it is expected that the equivalent ‘hydrostatic pressure’, or more precisely the compaction pressure, increases nonlinearly with increasing thickness of the concentrated layer in the holding space in the disk-stack centrifuge. This increase in pressure translates to an increase in solids concentration through compaction and rearrangement of solids grains in the bed. The solids concentration at the bowl wall increases, first rapidly with increasing pressure, but then gradually with diminishing rate, until it finally levels off to an asymptote.

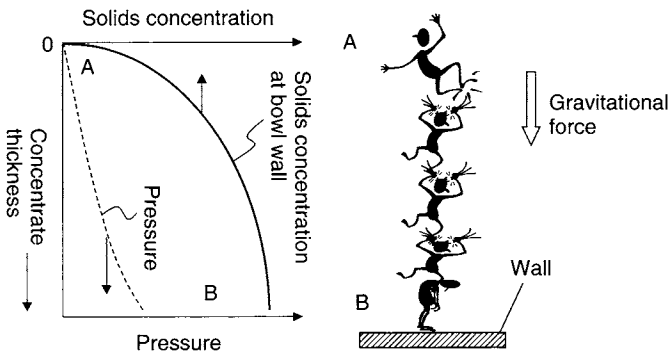


**Figure 7.2** Schematic of a human pile, one standing on top of another

### 7.4 Expression or Percolation

Liquid flows through a porous medium under the influence of a pressure gradient. According to Darcy’s law, the superficial fluid velocity in a porous medium is proportional to the driving pressure gradient and is inversely proportional to the viscosity of the fluid. (Note that the superficial velocity is basically the flow rate divided by the cross-sectional area of bed, ignoring the fact that fluid flows in the porous path between grains of the bed.) Thus

$$v = \frac{Q}{A} = -\frac{K}{\mu} \frac{dp}{dz} \quad (7.1)$$

The fluid can be either gas or liquid. The proportionality constant  $K$  of Equation 7.1 is the permeability of the porous medium and has a unit of  $m^2$ . The permeability of porous medium can span quite a wide range, from  $10^{-10}m^2$  for unconsolidated porous media to  $10^{-16}m^2$  or below for low-permeability consolidated medium. Referring to Figure 7.3, the pressure drop has to be smaller in the direction of flow or increasing  $z$  (i.e. toward the screen).

Let us examine a slice of the concentrate medium in the holding space as represented in Figure 7.4, where the centrifugal acceleration  $G$  is directing solid compaction towards the bowl wall (similar to  $g$  compacting the ‘acrobat ladder’ towards the ground). The solids will be packed more towards the wall in the direction of  $G$ -force, and likewise packed less in the direction opposite to the  $G$ -force. The hydrostatic liquid pressure is therefore highest near the wall, approximately  $\rho Gh + p_a$ , where  $p_a$  is the overburden pressure acting on the surface of the porous medium/cake and  $h$  is the concentrate thickness. Applying Darcy’s law, Equation 7.1, to determine the liquid flux  $v$

$$v = \frac{Q}{A} \approx -\frac{K}{\mu} \frac{(p_a - [p_a + \rho Gh])}{h} = \frac{K}{\mu} \rho G \tag{7.2}$$

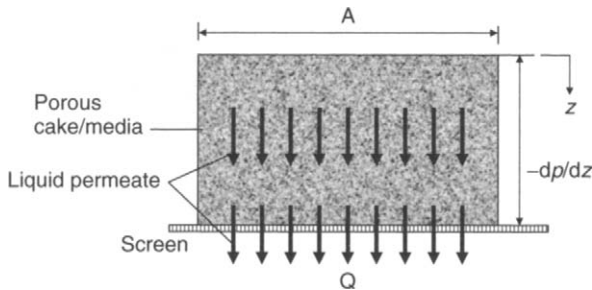


**Figure 7.3** Darcy’s law on percolation

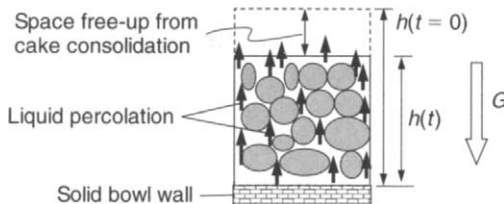


**Figure 7.4** Darcy’s law on percolation and concurrent compaction

It can be seen that the liquid flux  $v$  is independent of the overburden pressure  $p_a$  as this pressure is present at both the medium surface as well as at the bottom of the medium. The pressure gradient, being the difference of the pressure at these two locations, becomes independent of  $p_a$ . Let  $t$  be the time for liquid to percolate across the concentrate, treated herein as a packed porous bed with thickness  $h$ . Thus, the velocity of percolation is of the order

$$v \approx \frac{h}{t} \quad (7.3)$$

Combining Equation 7.2 and Equation 7.3, the time of percolation or expression of liquid can be estimated as

$$t \approx \frac{\mu h}{\rho K G} \quad (7.4)$$

It can be inferred from Equation 7.4 that higher concentrate/porous-bed permeability, higher centrifugal gravity  $G$ , lower liquid viscosity and smaller concentrate/porous-bed thickness all lead to shorter time for liquid percolation. Example 7.2 illustrates the use of Equation 7.4.

### Example 7.2

The concentrate is semipervious with the following properties:

Kinematic viscosity $\mu/\rho$ , cm <sup>2</sup> /s	0.05 (5 × water at room temp)
$h$ , cm	5
$G/g$	10,000
$g$ , cm/s <sup>2</sup>	981
$K$ , cm <sup>2</sup>	$10^{-10}$
$t$ , min	4.25

(Note 1 D (Darcy) =  $10^{-8}$  cm<sup>2</sup>)

Thus it takes over four minutes for the viscous liquid to percolate through the bed. If the discharge frequency of the disk centrifuge is much faster than this timeframe, the liquid has yet to percolate through to the surface of the porous bed and the solid underflow/concentrate would have carried this additional moisture and got very wet. This also implies that the protein yield (in liquid) in the concentrate is reduced. The time for compaction, as measured by reduction in  $h(t)$  over time  $t$ , for biological solids is usually faster compared to the time for liquid percolation. This can be determined in the laboratory using the procedure as described below. It should be noted that the above analysis is a conservative estimate on the time scale for “expression” as the concentrate layer thickness  $h$  is deposited over time and this has not been accounted for.

## 7.5 Compaction Testing

As shown in Figure 7.5, a specially designed spintube [1] has been used to determine the compaction and expression of a concentrated biological suspension. The diameter of the spintube is about 30 mm. The tube can be spun at different times,  $G$ -level, and feed solids consistency to establish various concentrate thicknesses. The large-diameter end of the spintube is equipped with a removal cap. After the cap is removed, the concentrated cake sample can be pushed out of the spintube using a plunger. The sample should remain intact during removal and it can be dissected in segments along the radial direction to determine the solids concentration of each segment as a function of radius from which solids pressure/stress under centrifugal loading can be inferred.

Figure 7.6 shows a general behavior of solids concentration  $W_s$  of the biosolids, which can be concentrated by centrifugation under increasing compaction stress  $p_s$  and increasing time. For a given time  $t$ , the solids  $W_s$  increases with increasing  $p_s$ . Likewise, for a given level of  $p_s$ , increasing time increases both consolidation and liquid expression.

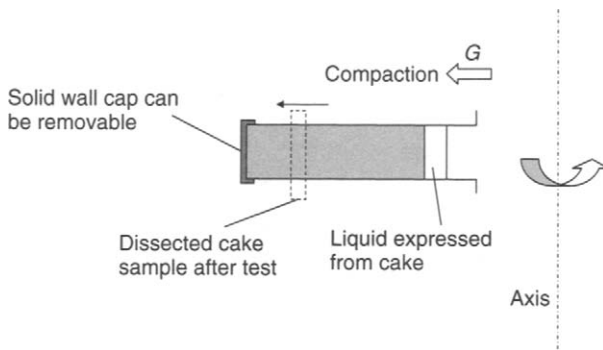


**Figure 7.5** Bucket test in determining compaction and percolation

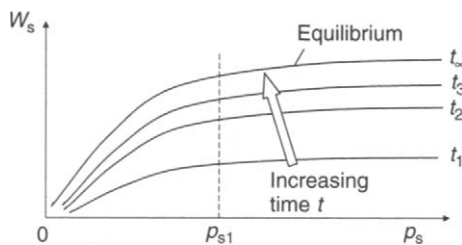


**Figure 7.6** Solids concentration  $W_s$  under compaction stress and increasing time

Figure 7.7 shows some results from testing a biological sample from a wastewater treatment plant under large compaction time (i.e. under equilibrium where the kinetics have died out). Both thin cake samples, with thickness 13–28 mm, and thick cake samples, with thickness 66–94 mm, have been tested. The tests were conducted with and without lubricating (grease lubricant) the bucket wall. It was found that the effect of lubrication was negligible.

### 7.6 Compaction Pressure

As the concentrate media is compacted, force is transmitted from solid grain to solid grain, as depicted in Figure 7.8. A loose structure with

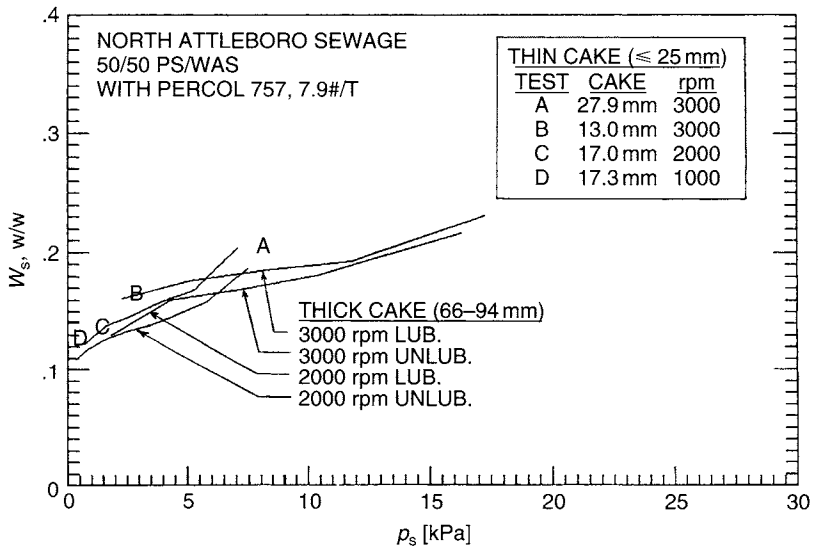


Figure 7.7 Test data on biological materials in a bucket centrifuge

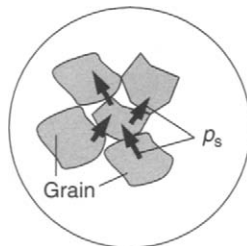


Figure 7.8 Solid pressure/stress transmitted across grain-to-grain contact

wide open pores can be compacted under body force to a much tighter structure with less porosity and lower flow permeability.

Accounting for the buoyancy effect due to the overlying expressed liquid on top of the concentrate or cake, the solids stress/pressure  $p_s$  can be expressed as an integral

$$p_s(R) = (\rho_s - \rho_L) \int \Omega^2 R \phi_s(R) dR \quad (7.5)$$

with

$\phi_s(R)$  = solids volume fraction in cake at radius  $R$

$\Omega$  = rotational speed

$\rho_s$  = solids density

$\rho_L$  = liquid density

The integral Equation 7.5 can also be approximated by a finite sum

$$p_s(R) \approx (\rho_s - \rho_L) \Omega^2 \sum_i R_i \phi_{si} \Delta R \approx (\rho_s - \rho_L) \phi_{sa} Gh \quad (7.6)$$

where

$\phi_{sa}$  = average solids volume fraction in cake column

$G = \Omega^2 R_a$

$h$  = cake height

$R_a$  is the average radius. The solids pressure has been determined for the data displayed in Figure 7.7 via Equation 7.6, and the data is found to be well-correlated by a power law as depicted in Figure 7.9. Thus

$$\frac{W_s}{W_{so}} = \frac{\phi_s}{\phi_{so}} = p_s^n \quad (7.7)$$

where  $n = 0.23$  for the data set shown in Figure 7.9. Note that this correlation does not depend explicitly on the cake thickness and  $G$  or rotation speed  $\Omega$ .

Solids concentration by weight as a function of compaction pressure has been obtained for some cake samples from a continuous-feed decanter processing biosolids [2]. The results for two different test runs using respectively 2000 g and 2500 g have been charted in Figure 7.10. As can be seen, the cake solids (different from those considered in Figures 7.7 and 7.9) indeed follow a trend of diminishing increase with increasing solids pressure. Figure 7.10 shows that the cake solids can also be approximated by a power law, Equation 7.7, with an exponent  $n$

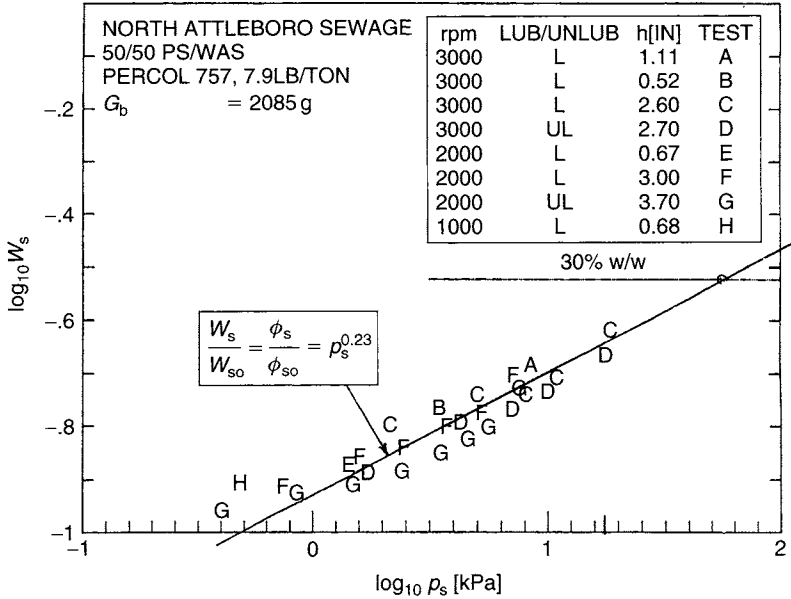


Figure 7.9 Biosolids by weight versus compaction pressure

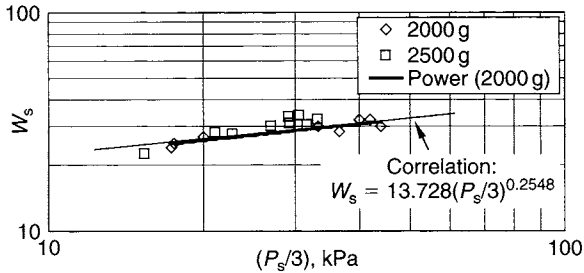


Figure 7.10 Cake solids by weight versus compressive solids pressure/stress from cake sample obtained from a continuous-fed 460-mm diameter decanter on biological sludge

of 0.26. This is close to the bench testing with  $n = 0.23$ , despite being for different biosolids and using different test equipment.

### 7.7 Recommendations for Increasing Solids Concentration in Underflow

There is a good basis for reducing solids concentration in the concentrate: one reason is to reduce loss of valuable liquid product; the other

reason is to reduce liquid content, thus reducing the bulk volume for downstream processing, especially if the concentrate is the product. The following are recommendations and concerns for increasing the concentrate solids:

- Increase solids residence time for thicker drier cake to effect compaction and liquid expression.
- Concentrate depth should not be too deep, such that it interferes with the separation zone (disk stack or pool surface for tubular centrifuge).
- Concentrate cannot be too concentrated, such that it presents discharge problem and plugs the openings of the discharge port of the centrifuge.
- Concentrate does not distribute unevenly around the circumference leading to unbalance and mechanical vibration.

The tubular centrifuge allows the solids to be compacted as more settled solids from the incoming feed are added until the bed becomes thick. The solids adjacent to the bowl wall become concentrated due to (a) liquid expressing out of the layer and moving away towards the small radius, (b) increasing compaction pressure from thicker concentrate  $h$ . Feeding stops when the concentrate layer becomes too thick and close to the feed stream, leading to entrainment of solids to the effluent. The liquid pool is subsequently drained off and the concentrate is removed by mechanical plough or a plunger. The drainage of pool liquid prevents the latter from mixing and further wetting the drier concentrate.

A special disk centrifuge without disk stack also operates in a similar way to a tubular centrifuge. After cake has built up to a certain thickness, feeding stops. The centrifuge is slowed down and the pool liquid is subsequently drained. Nitrogen can be used to blow-dry the concentrate to provide sterilization. Subsequently, the centrifuge ramps up to speed again to establish the  $G$ -force and the bowl bottom opens to discharge the concentrate. The cycle time is longer than a regular disk centrifuge without draining the pool. The concentrate discharge is drier without any pool liquid and with special provision as described.

## 7.8 Summary

The need for discharging a concentrated underflow is demonstrated in terms of recovery of extracellular expressed protein, otherwise the valuable protein is lost with the liquid in the underflow or concentrate stream.

In other words, a high yield on protein should be maintained. The underlying physics on cake compaction and percolation is explained. Once the  $G$ -forces of a given machine are selected and the process determined, the kinetics of dewatering dictates whether there is enough time in between shots to drain the liquid trapped in the pores between cake solids. Some designed cake compaction and percolation experiments can be carried out to determine the kinetics of dewatering. Under steady state, cake compaction and percolation depend on the cake solid stress, which in turn depends on the  $G$ -force and the concentrate thickness. There is general increase in solids concentration with increasing solids stress initially, fairly linearly, and subsequently at a rate of diminishing return. On one end, the underflow should not be too compacted, otherwise it might have discharge difficulty, and also this might increase the concentrate turbidity or solids.

## References

- [1] W.W.F. Leung, *Industrial Centrifugation Technology*, McGraw-Hill, New York, 1998.
- [2] W.W.F. Leung Dewatering biosolids sludge with varigate decanter centrifuge, *Transaction Filtration Society*, vol. 1 (2), pp. 38–44, Feb. 2001.

## Problems

- (7.1) Sediment after being separated in a disk stack operating at 5000  $g$  gets compacted in the solid holding space of a dropping-bottom disk-stack centrifuge. The concentrate thickness is 3 cm. The viscosity is 0.03 P. The density of the biosolids is  $1 \text{ g/cm}^3$ . The permeability of the sediment is  $8(10^{-11}) \text{ cm}^2$ . What is the time for liquid percolation across the concentrate? If the time between adjacent discharges is 4 minutes, would this be sufficient? Why or why not?
- (7.2) The concentrate thickness remains 3 cm as with Problem (7.1). The viscosity is increased to 0.1 P due to an increase in the soluble matters. The density of the biosolids is  $1 \text{ g/cm}^3$ . The permeability of the sediment is  $8(10^{-11}) \text{ cm}^2$ . What is the rotational speed in rev/min to operate a 500-mm diameter disk centrifuge such that the time in between shots is equal to the percolation time across the concentrate of 5 minutes?
- (7.3) A compaction testing under an angular speed 300/s has been conducted. This is similar to the one described in Section 7.6. The density difference between the biosolid and liquid is  $0.1 \text{ g/cm}^3$ . The concentrate has been dissected along the radius in 2 cm increments. Table 7.3 shows the test results.

**Table 7A** Example of compaction affecting product yield

<i>Sample</i>	<i>R (cm)</i>	$\phi_s [-]$	$\Delta p_s$	$p_s$
1	5	0.05		
2	6	0.07		
3	7	0.08		
4	8	0.085		
5	9	0.088		

- (a) Determine the relationship of the solids volume fraction versus the compaction pressure. Plot in log-log scale the solids volume fraction  $\phi_s$  versus the compaction pressure  $p_s$ . (b) How does this result compare with that shown in Figure 7.9? (c) What is the exponent if the correlation is made based on a power law relationship between  $\phi_s$  and  $p_s$ ?

---

# Laboratory and Pilot Testing

In this chapter, the objectives of centrifugal separation are reviewed. This is followed by discussion of characterization of solids, liquid, and suspension. Bench-scale and pilot tests will be presented for biotechnology separation.

## 8.1 Process Objectives

There are five process objectives in biotechnology separation.

- 1 *Separation* Suspended solids are separated from the liquid phase. The solid phase can be the valuable product being recovered in the concentrate and the liquid a waste, or the solid phase can be the waste while the liquid is the product recovered in the concentrate or overflow.
- 2 *Clarification* The liquid phase or broth is the product and as such the amount of suspended solids should be minimized. This application may take place wherein the concentrate from the first-stage centrifugation is sent to the second-stage centrifugation to further remove fine dispersed suspended solids. For example, a suspension with solids concentration 300–1000 ppm can be centrifuged (in the second-stage centrifugation) with concentrate reduced to 10–20 ppm.
- 3 *Dewatering/deliquoring of concentrate* This is to remove additional liquid in the concentrate. Some processes require ultra-dry concentrate for special processing.
- 4 *Washing or repulping concentrate* This can be used to strip off valuable protein adhered to the solids (cells or crystals) in an effort to increase the protein yield of the separation process, but this increases the liquid amount for downstream processing as shown in certain flow sheets in Chapter 5.
- 5 *Classification of debris* from the released inclusion bodies after bacteria (such as *E. coli*) is lysed. The inclusion bodies need to be recovered in the concentrate while the finer cell debris should be removed in the concentrate/overflow. There are other applications where separation of particles can be both accomplished by difference in particle sizes and/or difference in densities.

## 8.2 Solid, Liquid and Suspension Properties

It is important to characterize the properties of solids, liquid, and suspension as a whole.

### 8.2.1 Solids Properties

- 1 The density of solids density is not important. What is more important is the difference in density between the solid and liquid. The greater the density difference is, the greater impact it has on separation. The specific density of biosolids does not differ greatly from that of water, hence the driving force is very small. Centrifugation with high  $G$  can certainly compensate to a large extent on such small density difference.
- 2 The shape of the solid also plays an important role in settling and consequently separation. Solid is typically amorphous, yet thin elongated-shaped solids have some interesting and peculiar settling properties, with the long axis settling much faster than that of the short axis.
- 3 When solids are suspended in liquid, charges can be induced on the solid surface from ions present in the liquid. The Zeta potential provides a measure of the electrical charges on the solid surface.
- 4 The particle size distribution (PSD) is extremely important. The sedimentation rate of particles in a stationary liquid varies as to the square power of the particle size. While larger particles are no problem to separate, small particles are difficult to separate. Hence, it is important to know in what sizes the particles are populated.

### 8.2.2 Mother Liquid Properties

- 1 The density of mother liquid affects separation. Typically, the liquid in biotech separation is largely aqueous or water-based.
- 2 The viscosity of liquid, as shown in Chapter 2, is a function of temperature. Increasing temperature often reduces the viscosity and enhances the separation rate. Viscosity of the liquid can be increased with increase in soluble intracellular materials from cell lysate, such as RNA and proteins.

### 8.2.3 Feed Slurry Properties

- 1 The viscosity of suspension depends on the viscosity of the liquid and the concentration of suspended solids. Increasing the concentration of suspended solids and/or higher liquid viscosity leads to higher suspension viscosity.

- 2 In addition, the pH or hydrogen ion concentration of the suspension affects the acidity (or alkalinity) of suspension.
- 3 The ionic strength of suspension affects the charges (Zeta potential) of particles and consequently particle–particle interaction in the concentrate.

## 8.3 Bench-Scale Testing

### 8.3.1 Separability

The separability of solids in a suspension is of great interest. Does the sample separate? If so, how much time and under what  $G$ -force would the solid phase be separated from the liquid phase? Further, is the supernatant (i.e. centrate or overflow) cleared of suspended solids? How much suspended solids are recovered? What is the concentration in the concentrated underflow and how does it compare to that of the feed? What is the factor of concentration? As discussed in Chapter 3, spintubes are common centrifuges used for laboratory testing. The time duration that it takes to fill up the solids-holding space for intermittent discharged centrifuge can be easily estimated from spintube testing. This determines the discharge frequency for the dropping-bottom disk centrifuge.

### 8.3.2 Flocculant and Coagulant in Bench Tests

In some bioprocesses, especially when the protein product is in the liquid, flocculant can be used to assist agglomerating finely dispersed biological solids. Flocculants are polyelectrolytes with long chain polymers with charges in the chains serving as an agglomeration agent or ‘mop’ from which fine particulates, which are difficult to separate, can be attached. The flocculants can be anionic (negatively charged), cationic (positively charged), or even non-ionic. The polymer is selected that is compatible with the liquid solvent without adverse effect on the dissolved protein, enzyme, and downstream processing.

On the other hand, coagulants are simple electrolytes – acids, bases, and salts. Upon dissolution, the inorganic ions from these electrolytes, such as sodium ion, magnesium ion or aluminum ion, can be used to neutralize outstanding charges (typically negative that stay on particle surfaces) and allow particles to agglomerate due to the attractive Van der Waals’ force. Most particles and colloids carry negative charges, consequently positive ions from these electrolytes are very effective in neutralizing the charges from these particles. In essence, upon charge neutralization the ‘charged double layer’ surrounding and keeping the

particles in repulsion collapses. The effectiveness of these ions is in the order as stated because ions with large positive charges, such as the  $\text{Al}^{+3}$  ion, can neutralize more outstanding charges than a smaller  $\text{Mg}^{+2}$  ion, which in turn is better than an  $\text{Na}^+$  ion, which carries less positive charge. At times, coagulants followed by flocculants are both used. Flocculants have been used in separating extracellular enzymes (see Chapter 6) in which fine solids are collected by these long chain flocculants to report to the underflow, leaving the product enzyme free from suspended solid.

In the laboratory it is of interest to determine what type of flocculant and coagulant are appropriate for the process and at what polymer dosage (measured by kg of flocculant per tonne of solids) to be treated? A systematic series of spintube testing can address the above issues. Selection of coagulant and flocculant depends on the type of solid, pH, ionic strength of liquid, and process temperature. Through systematic experimentation, optimal coagulant or flocculant dosage can be derived to obtain reasonably sized flocculated solids (commonly referred to as flocs) that are strong enough to withstand shear forces in a centrifuge. In this process, proper mixing is required to provide the needed energy for flocculation. Also, proper dilution of flocculant is important, especially if in solid or condensed emulsion form. The polymer is folded up and needs to be appropriately diluted with liquid (typically water) so that the polymer chain and functional groups are stretched out to effectively capture the biosolids and fines. It is best to follow the manufacturer's specifications, with some laboratory dilution trials for fine-tuning.

In carrying out spintube tests, different  $G$ 's and  $t$ 's and chemical dosages on coagulant or flocculant, should be tried. Some extreme values of  $G$ ,  $t$ , and chemical dosage should also be tested to determine operation and performance outside the normal range.

### 8.3.3 Test Variables

The variables in spintube testing comprise the following:

- Centrifugal gravity  $G$
- Time duration  $t$
- Feed solids concentration  $c_f$
- Flocculant type (anionic, cationic, non-ionic) and dosage  $D$ , and coagulant type and dosage  $D$ .

$G$  and  $t$  are the most readily tested variables, as all modern bench centrifuges can allow a readily programmable manual to adjust these two

variables. Feed solids can be varied by either dilution with the appropriate buffer liquid or by concentration by filtration. Both coagulant and flocculant types and dosage require trial-and-error using a standard mixing device, with several bench mixing devices running concurrently for making comparison.

### 8.3.4 Material Balance

The separation efficiency or solid capture efficiency  $R_s$  depends on  $G$ ,  $t$ ,  $D$ , and  $c_f$ . The solids recovery is a function of these four variables. Furthermore, the solid recovery under steady state can be expressed as a function of the feed solid concentration  $c_f$ , centrate solids concentration  $c_e$ , and concentrate solid concentration  $c_s$ . The  $c$ 's are the concentration of solids by bulk volume. The commonly used method to determine the bulk volume is by spindown of the sample (feed, centrate/supernatant, or concentrate) under 10,000 g for 3–5 minutes. Note that the separation test referred to below has a much shorter time of centrifugation as it is supposed to determine if the sample, which has much shorter residence time than 3–5 minutes in the machine, can be separated despite the  $G$ 's, and can be comparable. Alternatively,  $c$ 's can also represent number of biological cells per unit volume in which a totally different measurement needs to be carried out, and not by spindown of the sample.

#### 8.3.4.1 Material Balance Consideration for Bench Scale

With reference to Figure 8.1, before spinning the entire tube is homogeneous with suspension, with solids  $c_f$  occupying  $V_f$ . After spinning, there are two separated phases, a lighter phase with volume  $V_e$  with solids  $c_e$ , and a heavier phase adjacent to the bottom of the tube with volume  $V_s$  and with solids concentration  $c_s$ . Balancing total volume and solids respectively before and after spinning

$$V_f = V_e + V_s \quad (8.1a)$$

$$V_f c_f = V_e c_e + V_s c_s \quad (8.1b)$$

Rearranging Equations 8.1 and 8.2, the volumetric recovery (i.e. volume recovered in concentrate versus original feed volume  $V_s/V_f$ ) becomes

$$\frac{V_s}{V_f} = \frac{c_f - c_e}{c_s - c_e} \quad (8.2)$$

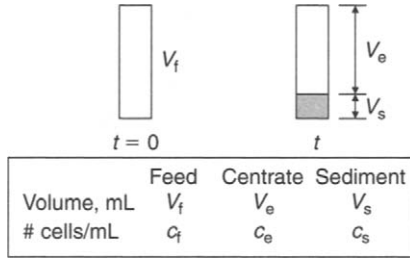


**Figure 8.1** Material balance of a spintube before and after spinning

The solids recovery  $R_s$  becomes

$$R_s = \frac{c_s V_s}{c_f V_f} = \frac{c_s}{c_f} \frac{c_f - c_e}{c_s - c_e} = \frac{1 - c_e/c_f}{1 - c_e/c_s} \tag{8.3a}$$

Also when the centrate concentration is very much smaller than that of the concentrate

$$R_s \approx 1 - c_e/c_f \quad (c_e \ll c_s) \tag{8.3b}$$

The concentration factor CF becomes

$$CF = \frac{c_s}{c_f} \approx \frac{V_f}{V_s} \tag{8.3c}$$

$$\text{as } \frac{V_f}{V_s} = \frac{c_s - c_e}{c_f - c_e} \approx \frac{c_s}{c_f} \quad (c_e \ll c_s \text{ and } c_e \ll c_f)$$

Typically, when the sample is spun at 10,000 g for  $t = 3$  to 5 min, one can determine  $V_f/V_s$  which also equals the concentration factor CF.

For a given  $G$ , the solids recovery increases with increasing centrifugation time. For a fixed time, the recovery increases with increasing  $G$ . This is illustrated in Figure 8.2a. Vice versa, when  $R_s$  is plotted against  $G$  with  $t$  as a parameter, as shown in Figure 8.2b, similar behavior results. In fact,  $R_s$  can be well correlated with the multiplication product  $Gt$  [1], as depicted in Figure 8.2c. Flocculant may be used in applications in which the product is the liquid phase and solid the waste. The solid-recovery curve is plotted versus  $Gt$  for a fixed flocculant dosage. A set of curves can be generated readily respectively for different flocculant

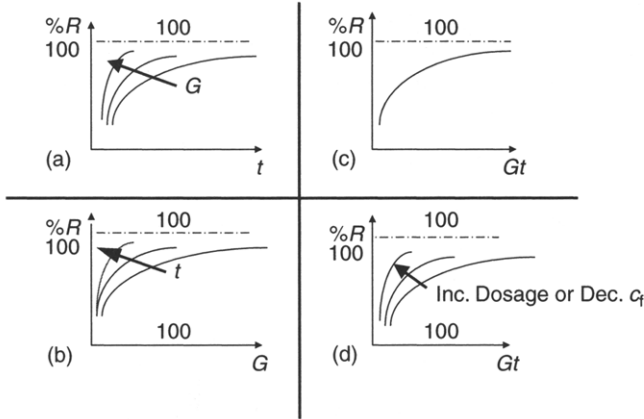


**Figure 8.2 (a)–(d)** Centrifugal behavior

dosages. Increasing flocculant dosage generally increases the solid recovery, as illustrated in Figure 8.2d.

### 8.3.5 Acceleration and Deceleration Time Duration

Despite using a powerful motor drive, it takes some elapse time to get the centrifuge rotor to speed because of inertia of the rotor. Some specially designed bench centrifuges can get up to 10,000 g in 2 s, however most other spintube centrifuges can only accelerate to, say, 3000 g in a matter of 15 s, and it may take another 20 s, or longer, to coast down with pneumatic/hydraulic brakes and other electrical retardation mechanisms. Suppose we have the operating speed  $\Omega_o = 3500$  rev/min and it takes an elapse time  $t_a = 10$  s to get to the operating speed  $\Omega_o$ . Assuming a linear increase of angular speed over time  $t_a$ , the integral of  $G$ - $t$  is simply

$$\int_0^{t_a} G dt = \int_0^{t_a} \left( \frac{\Omega_o t}{t_a} \right)^2 R dt = \frac{1}{3} G t_a \quad (8.4a)$$

Likewise, if  $t_d$  is the time elapse for deceleration, the  $G$ - $t$  integral for deceleration is

$$\int_0^{t_d} G dt = \int_0^{t_d} \left( \frac{\Omega_o [t_d - t]}{t_d} \right)^2 R dt = \frac{1}{3} G t_d \quad (8.4b)$$

The total effective time for the test run, including both acceleration and deceleration and assuming  $t$  is the operating time duration at steady rotation speed  $\Omega_o$ , should then be

$$(Gt)_{\text{total}} = Gt + \frac{1}{3}G[t_a + t_d]$$

An example is used in the problems at the end of this chapter to illustrate the importance of making this correction, otherwise the test data would be incorrectly interpreted.

### 8.3.6 Settling Velocity

The settling velocity of a particle depends on size, shape, solid concentration, and other variables. Thus far, the Stokes law has been used to calculate the settling velocity with correction of hindered sedimentation from concentrated suspension by the hindered settling factor  $\lambda (= v_s/v_{s0})$ .

#### 8.3.6.1 Apparatus for Visualizing Sedimentation Behavior

A special spintube arrangement can be set up whereby both  $v_{s0}$  and  $v_s$  (or  $\lambda$ ) can be measured. Suppose the spintube is rotated to the position as shown in Figure 8.3. It is illuminated by a set of focused light sources spaced closely apart and aligned in a radial direction (top of Figure 8.3).

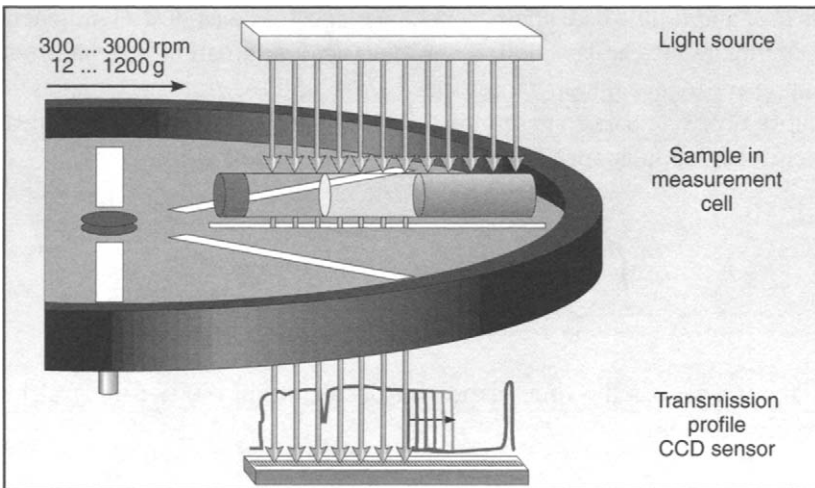


**Figure 8.3** Special spintube setup equipped with light transmission and CCD sensor to detect the transmission of light through the suspension (Reproduce by permission of LUM GmbH)

The light source can be either near infrared or ultraviolet light depending on the suspension. The transmitted light is measured by the CCD sensor located on the opposite side of the spintube (bottom of Figure 8.3). From the transmission profile measured, both along the radius and over time, the location of the interfaces (liquid-suspension interface and the cake-suspension interface) and the solids concentration at a given location may be inferred. Eight to twelve spintubes can be used at any time during a test run and measurement of the transient transmission profile on each spintube is stored for subsequent data retrieval and analysis.

### 8.3.6.2 Sedimentation Behavior for Monodispersed Suspension

Figure 8.4 shows a sketch of the transmission profile for a suspension with monodispersed particles. The liquid-suspension interface is very distinct as all particles of the same size settle at the same velocity. The liquid-suspension interface increases with time at a relatively constant rate, but this rate can actually increase as it moves to a larger radius due to increasing  $G$ , as  $G$  is proportional to radius. After a certain time, the interface reaches the bottom, intercepting the sediment-suspension interface

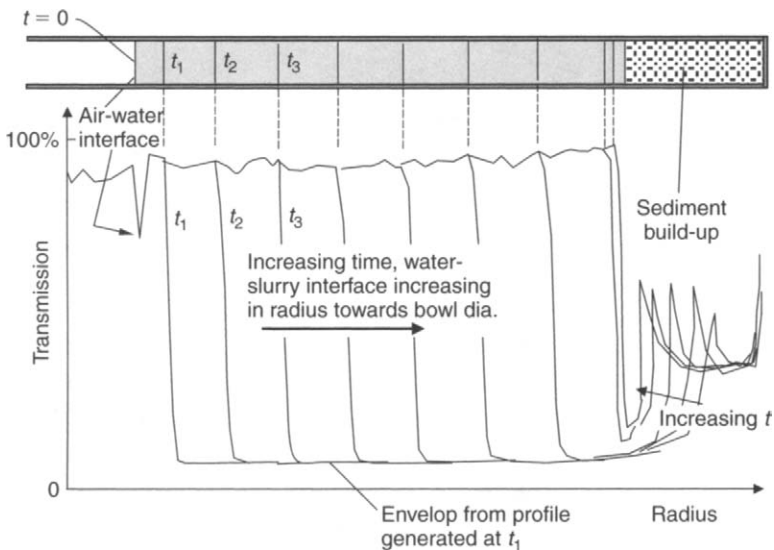


**Figure 8.4** Typical spintube air-water interface position (top) and transmission profile over time for a monodispersed suspension with distinct suspension-water interface moving from small to large radius; also sediment is building up concurrently from large to small radius

moving radially inward. For monodispersed particles, the cake forms a regular structure and the cake-suspension interface is also very distinct.

### 8.3.6.3 Sedimentation Behavior for Polydispersed Suspension

In contrast, there is no distinct liquid-suspension interface when the particle size distribution in suspension is polydispersed, as depicted in Figure 8.5. Larger particles settle faster followed by smaller particles, down to the colloidal size in the submicron range settling very slowly. At any instant, the larger particles may be located close to the large radius of the tube, while the smaller ones are still at the small radius close to the air-water interface. These slow-settling fine particles reflect, scatter, and absorb the light-reducing light transmission. Consequently, there is a gradual increase over time in light transmission from the small radius to the large radius as these fines settle (see Figure 8.5). This is a slow process and the behavior is very different from that of the monodispersed suspension sedimentation shown in Figure 8.4.

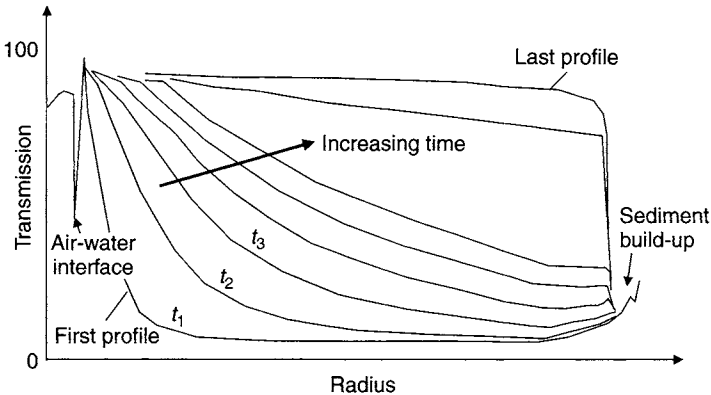


**Figure 8.5** Typical spintube air-water interface position (top) and transmission profile over time for a polydispersed suspension; no distinct suspension-water interface moving from small to large radius; also sediment is building up counter-currently from large to small radius

### 8.3.6.4 Sedimentation Behavior for Monodispersed Suspension with Hindered Settling

For sedimentation with monodispersed suspension, there is a distinct liquid-suspension interface that can be traced over time. A plot for such a real suspension is shown for feed solids 5.5–19.55% v/v (bulk volume basis). They all exhibit a linear increase first, followed by a horizontal

line (where sediment builds up to meet the liquid-suspension interface). Note that for feed solids concentration 5.5–10.2%, they all show a slight concave upward behavior instead of a linear increase, due to increasing settling velocity at a large radius, as discussed. The slope (or average slope of the curve) represents the average settling rate over the period, and it decreases with increasing feed solids. Particles do not contact each other; however, they do feel the hydrodynamic effect of settling of neighboring particles. (Imagine someone driving a small car on the motorway who feels the effect of a bigger car passing by despite there being no physical contact.) At a bulk solid concentration of 39.2%, the particles form a network and there could be physical contact during sedimentation. As can be seen in Figure 8.6, the curve exhibits a convex upward shape (due to increasing  $G$  with  $R$ ) followed by a concave downward shape until the liquid-suspension interface meets the growing sediment.

The specially designed bench centrifuge shown in Figure 8.3 can provide useful measurement of the settling rate of a given suspension for particles with various sizes, shapes, and densities. Also, the concentration effect can be quantified, i.e. the hindered settling factor can be measured instead of using correlation. In addition, it can also measure the sedimentation not only for dispersed particles but also for flocculated particles.

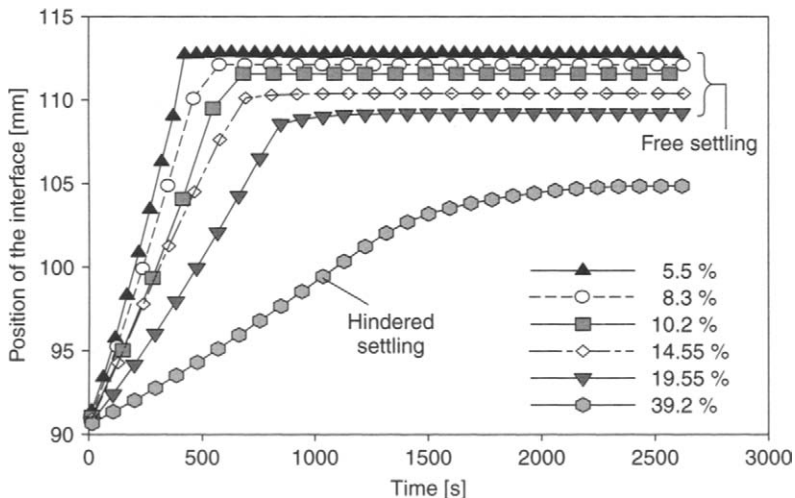


**Figure 8.6** Radius of suspension-water interface for monodispersed suspension with different feed solids concentration showing free settling and hindered settling behavior (Reproduced by permission of LUM GmbH)

## 8.4 Pilot Testing

Pilot testing is absolutely essential as it takes a viable bench technology to a demonstration phase where 'biotech materials' can be produced on a semi-continuous small-scale basis. It is one of the most critical phases. Often problems arise which are not encountered in bench-scale testing. This could be due to many factors, among which are the absence of flow dynamics with inflow and outflow which is not present in bench testing, and larger amounts of feed materials and discharge materials (centrate or concentrate) for handling compared to a bench scale, which is handled manually. This addresses whether the scale-up is appropriately carried out from laboratory bench-scale to pilot-scale tests on the bioprocess in question. Even sample (i.e. feed, centrate, and concentrate) handling, such as transport, becomes quite different between a continuous pilot test operation and a bench test. Prior to discussing pilot testing, a discussion of basic concepts on material balance with continuous flow is in order.

### 8.4.1 Material Balance Consideration for Pilot/ Production Scale

#### 8.4.1.1 Material Balance by Volume Fraction

Our discussion on material balance is not limited to pilot-scale tests; it can also apply to production trials or full production.

In pilot or production tests, continuous feed and discharge streams have to be dealt with. Balancing the volumetric rate  $Q_s$  and the solids concentration individually for feed, concentrate, and centrate, material balance equations can be obtained similar to Equations 8.1a,b, and as such similar results can be obtained.

$$Q_f = Q_e + Q_s \quad (8.5a)$$

$$Q_f c_f = Q_e c_e + Q_s c_s \quad (8.5b)$$

from which

$$\frac{Q_s}{Q_f} = \frac{c_f - c_e}{c_s - c_e} \quad (8.6)$$

The solids recovery  $R_s$  becomes

$$R_s = \frac{c_s Q_s}{c_f Q_f} = \frac{c_s}{c_f} \frac{c_f - c_e}{c_s - c_e} = \frac{1 - (c_e/c_f)}{1 - (c_e/c_s)} \quad (8.7a)$$

Also, when the centrate concentration is very much smaller than that of the concentrate

$$R_s \approx 1 - \frac{c_e}{c_f} \quad (c_e \ll c_s) \quad (8.7b)$$

One immediate application of the result is to determine the solids recovery in the continuous pilot and production tests. Another use is to back-out the time for the intermittent discharge of the concentrate.

Given  $V_s$  is the solids-holding volume of the disk centrifuge, the time to fill the space  $t_s$  can be determined from the definition with the use of Equation 8.7a

$$t_s = \frac{V_s}{c_s Q_s} = \left[ \frac{V_s}{Q_f} \right] \frac{(1 - c_e/c_s)}{c_f(1 - c_e/c_f)} \quad (8.8a)$$

In the test,  $V_s$  is given by the geometry of the test centrifuge,  $Q$  is fixed by the operating feed rate, and the  $c$ 's are measured for the test conditions on all three streams.

Frequently, operators ignore the concentration of centrate solids, i.e. assuming  $c_e \ll c_f$ , thus, this also implies  $c_e \ll c_s$ . Taking  $c_e/c_f \approx 0$  and  $c_e/c_s \approx 0$

$$t_s \approx \frac{V_s \eta_d}{c_f Q_f} \quad (8.8b)$$

This discharge time is a rough estimate anyway and is used as an initial point for adjusting discharge.  $c_f$  can be measured from the bench test and, given  $V_s$  and  $Q_f$  are both readily obtained,  $t_s$  can be estimated. Once the machine is set to discharge at this initial guess, subsequently the discharge time can be better tuned (either longer or shorter) once the turbidity is monitored in-line with the discharged centrate liquid.

It is to be noted that concentrate discharge efficiency  $\eta_d$  is added to Equation 8.8b to account for the possibility that solids may adhere to the space in between the openings of the intermittent discharge disk centrifuge.

#### 8.4.1.2 Material Balance by Mass Fraction

Instead of examining the concentration as expressed by the number of biological cells per unit volume or by bulk volume concentration, one

can also examine the solid weight fraction  $W_i$  of a given species 'i' and the mass flow rate  $M_i$  of that species. The species i can be the feed f, centrate e, or solid s. Balancing the mass rate of liquid and solid in feed, centrate, and solid, as well as balancing the biological material (excluding liquid) of the feed, liquid, and solid

$$M_f = M_e + M_s \quad (8.9a)$$

$$M_f W_f = M_e W_e + M_s W_s \quad (8.9b)$$

Again, Equations 8.9a,b follow very much like Equations 8.1a,b and 8.5a,b. The results should be the same but with appropriate change in variables.

Solids recovery by weight is thus

$$R_s = \frac{W_s M_s}{W_f M_f} = \frac{W_s}{W_f} \frac{W_f - W_e}{W_s - W_e} = \frac{1 - (W_e/W_f)}{1 - (W_e/W_s)} \quad (8.10a)$$

Ignoring the centrate concentration in relation to that of the concentrate

$$R_s \approx 1 - W_e/W_f \quad (W_e \ll W_s) \quad (8.10b)$$

### 8.4.2 Product (Protein) Yield

In what follows, all quantities and relationships that are required to determine protein yield are examined (see Figure 8.7). A key assumption to simplify the mathematics is that we ignore the suspended solids in the centrate.

Let  $\phi_f$  be the 'actual' (not bulk) volume fraction of solids in feed, and  $\phi_s$  the volume fraction of solids in cake. Material balance on volumetric rate and liquid rate are given in Equations 8.11a,b, respectively.

$$Q_f = Q_e + Q_s \quad (8.11a)$$

$$Q_f(1 - \phi_f) = Q_e + Q_s(1 - \phi_s) \quad (8.11b)$$

Subtracting Equation 8.11a from Equation 8.11b, and after rearranging

$$\frac{Q_f}{Q_s} = \frac{V_f}{V_s} = \frac{\phi_s}{\phi_f} \quad (8.11c)$$

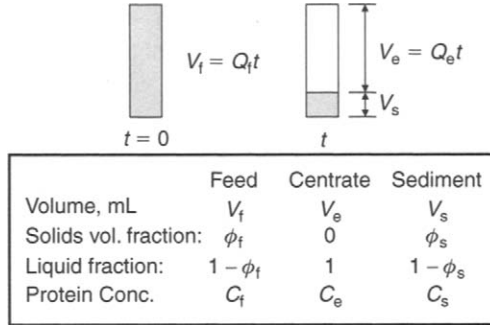


**Figure 8.7** Schematic of a spintube before and after centrifugation, assuming no suspended solids in concentrate. This is the basis for calculating yield of protein in product centrate

Note in Equation 8.4 that the  $Q$ 's refer to the rate respectively of feed slurry and concentrate flow in a continuous centrifuge, whereas  $V$ 's refer to the volume respectively of feed slurry and concentrate in a spintube, such as shown in Figure 8.3.

From Equations 8.11 a,b

$$\frac{Q_e}{Q_f} = 1 - \frac{\phi_f}{\phi_s} \quad (8.11d)$$

Further,  $C_f$ ,  $C_e$ , and  $C_s$  are the concentration of dissolved protein in liquid for feed, centrate, and cake solids, balancing the protein in the three streams, so that

$$Q_f(1 - \phi_f)C_f = Q_e C_e + Q_s(1 - \phi_s)C_s \quad (8.11e)$$

Protein yield  $Y_1$  can be defined as the ratio of protein in the centrate to that of the feed, so that

$$\begin{aligned} Y_1 &= \frac{C_e Q_e}{C_f Q_f (1 - \phi_f)} = \frac{C_e}{C_f} \frac{1 - \phi_f / \phi_s}{1 - \phi_f} = \frac{C_e}{C_f} \frac{1 - V_s / V_f}{1 - \phi_f} \\ &= \frac{C_e}{C_f} \frac{1 - (1/CF)}{1 - \phi_f} \end{aligned} \quad (8.12)$$

The yield of protein can be determined from Equation 8.12. It requires the solids volume fraction  $\phi_f$ , concentration factor  $CF = V_f/V_s$ , and concentration ratio of protein  $C_e/C_f$ . When  $\phi_s \approx 0$ ,  $CF \gg 1$ , then yield depends

primarily on the concentration of protein in the centrate and feed,  $Y \approx C_e/C_f$ . The concentration factor can be obtained from the spintube.

It is clear from Equation 8.11e that if the concentrate has little liquid content, i.e.  $\phi_s \approx 1$ , then the protein yield approaches 100%. This makes it impossible to completely remove the liquid in the concentrate. In practice, the concentrate leaving the centrifuge is repulped and goes through a second-stage centrifugation to remove as much protein as possible in the centrate of the second stage, or subsequent stages for that matter, by dilution followed by separation.

Suppose the concentration ratio  $CF_2 = (Q_f/Q_s)_2 = (V_f/V_s)_2$ . Then the yield  $Y_2$  from the second-stage centrifugation (based on the protein feed from the feed of the first stage) becomes

$$\begin{aligned} Y_2 &= \frac{C_s Q_s}{C_f Q_f (1 - \phi_f)} \left( 1 - \frac{1}{CF_2} \right) \left( \frac{C_e}{C_f} \right)_2 \\ &= \left( 1 - \frac{C_e Q_e}{C_f Q_f (1 - \phi_f)} \right) \left( 1 - \frac{1}{CF_2} \right) \left( \frac{C_e}{C_f} \right)_2 \\ &= (1 - Y_1) \left( 1 - \frac{1}{CF_2} \right) \left( \frac{C_e}{C_f} \right)_2 \end{aligned} \quad (8.13)$$

Total yield from the two-stage centrifugation becomes

$$Y_{\text{total}} = Y_1 + (1 - Y_1) \left( 1 - \frac{1}{CF_2} \right) \left( \frac{C_e}{C_f} \right)_2 \quad (8.14)$$

### Example 8.1

$$\phi_f = 0.05$$

$$CF_1 = CF_2 = 7$$

$$(C_e)_1 = (C_f)_1; (C_e)_2 = (C_f)_2$$

$$Y_1 = \frac{C_e}{C_f} \frac{1 - (1/CF)}{1 - \phi_f} = \frac{1 - (1/7)}{1 - 0.05} = 0.902$$

$$Y_2 = (1 - 0.9022)(1 - 1/7) = 0.0838$$

$$Y_{\text{total}} = Y_1 + Y_2 = 0.9022 + 0.0838 = 0.986$$

The protein yield from the first stage is 90.2% and in the second stage there is an addition of 8.4%, giving a 98.6% protein yield from the two stages.

### 8.4.3 Pilot Test Factors

Pilot test centrifuges can be used for confirming production of product protein. Pilot disk centrifuge of nominal diameter 180 and 240 mm are used for testing and feasibility study. Also, pilot tubular centrifuge of nominal diameter 150 mm is used for testing.

A picture of the 180-mm pilot disk-stack centrifuge is shown in Figure 8.8. Also, Figure 8.9 shows the back end of the pilot disk-stack centrifuge with the turbidity meter for monitoring centrate clarity.

#### 8.4.3.1 Monitored Variables in Pilot Tests

The monitored variables in the pilot test include the following:

- *rpm/G centrifuge* The rotational speed or centrifugal gravity of the centrifuge should be monitored with a tachometer or comparable speed-measurement device. The set rotational speed should be adjusted to adapt to the process need. Given that centrifugal acceleration varies

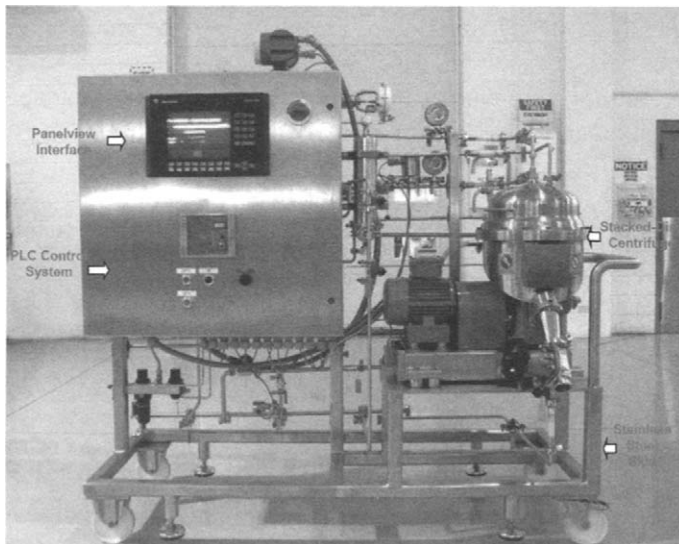


**Figure 8.8** Skid-mounted pilot disk centrifuge showing the front view and the control panel (Reproduced from Rohr and Teebe's paper (2002) by permission of the American Filtration and Separation Society)

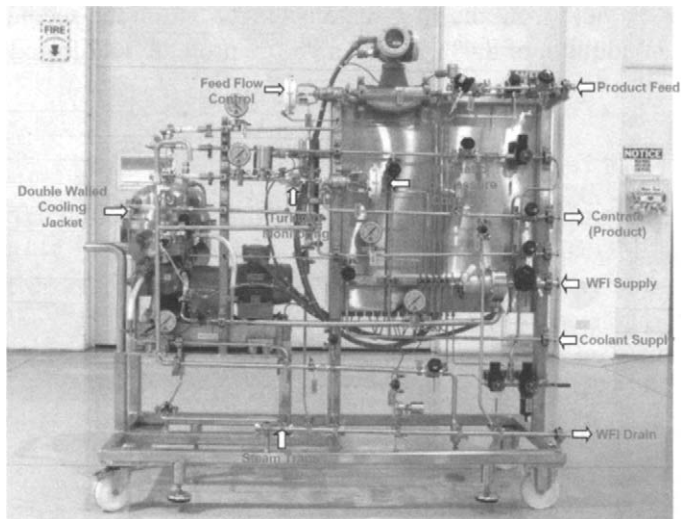


**Figure 8.9** Skid-mounted pilot disk centrifuge showing the back view with back-pressure control, turbidity monitoring, centrate, and feed ports (Reproduced from Rohr and Teebe's paper (2002) by permission of the American Filtration and Separation Society)

to the second power of the rotation speed and solid-liquid separation is typically a strong function of  $G$ , the speed is one of the key controlling parameters. The test range should be made at a wide range of  $G$ 's with a nominal mean value selected for constant operation. Also higher and lower  $G$ -force should be tested to check cost-benefit effects.

- *Flow rate of feed and centrate* Another readily adjustable parameter is the feed rate. The feed and centrate rates should be closely monitored. Other than the nominal feed rate having to be tested, higher and lower feed rates should be tested for use in scale-up.
- *Centrate solids and turbidity* The centrate solids should be monitored, for example using turbidity as a monitoring index on a continuous basis as it is the key gauge variable measuring performance. This is especially so when the centrifuge is performing clarification or polishing. Also individual or 'grab' samples should be taken periodically to measure the percentage by weight or percentage by bulk volume (after being centrifuged for 2–3 minutes under 10,000 g). With low solid concentration, it may be difficult or inaccurate to measure based on percentage by weight, as the tare weight is large compared to the sample weight.

- *Solids concentration in feed and underflow* Both feed and underflow concentration should also be monitored. The former measures the solids loading and the latter measures the concentrate concentration and handling. Also, the latter measures the yield of the protein product – loss of liquid protein in reject concentrate. The solids concentration is best measured using percentage by weight or percentage by bulk volume (after centrifugation in a spintube). Occasionally, if the feed contains a low amount of solids, as with clarification application, turbidity monitoring should be conducted on the feed stream.
- *Cell concentration* The number of concentration cells per mL in feed, centrate, and underflow (continuous discharge) are monitored for, say, mammalian cells (such as the popularly used Chinese Hamster Ovary). Also, the lysed cells are closely monitored using, say, LDH technique, especially when lysed cells can generate undesirable intracellular substances released in the liquid that contaminates the expressed protein product.
- *Flocculant dose* Flocculant is used for extracellular enzyme processing. Most other bioprocesses do not use flocculant due to (a) solid being the product, and (b) liquid being the product, however the polymer dissolved in solution might affect the liquid product. For the extracellular enzyme application, a suitable flocculant is selected such that it is compatible with the liquid product.
- *PSD of feed and centrate* The particle size distribution of feed and centrate should be monitored. Given that sedimentation rate varies as the second power of particle size, particle size distribution with a large fine fraction in submicron range may experience difficulty of separation.
- *Protein concentration in feed, centrate, and underflow* Protein concentration in all three streams should be monitored to accurately determine the yield.
- *Process temperature* plays a key role in the viscosity of the liquid and hence that of the suspension. Liquid viscosity is reduced by higher temperature but there is a limit on the process temperature due to (a) protein may denature at certain elevated temperature, (b) increase in corrosion, and (c) economics.
- *Viscosity* may be monitored using commercially available viscometers that come in different geometry, such as coaxial, capillary, and cone-and-plate etc. Occasionally in-line viscometers can be used as most of these provide only relative measurement on viscosity.
- *pH* should be monitored to keep protein in solution and avoid precipitation or dissolution of solids due to high solution acidity (low pH) or alkalinity (high pH).

- *Mechanical and electrical conditions* should all be monitored to ensure that the machine is running under normal conditions. These encompass:
  - mechanical vibration to ensure the masses in the rotor are evenly distributed without unbalance
  - torque to ensure it is within the limit preventing torque overload
  - electrical current to ensure again the loading and associated power drawn is within limit
  - bearing temperature that is within limit and the lubrication system of the rotating parts is working properly.
- Other pertinent process parameters for the process should also be monitored and controlled.

#### 8.4.3.2 Metrics of Pilot Tests

Several parameters below are used to gauge the performance. Some are more important than others.

- *Centrate clarity (solids percentage by weight or turbidity in NTU)*  
The centrate clarity or suspended solids are most commonly used to gauge separation. Too high centrate solids lead to overload of downstream depth filter in the case of processing mammalian cells. High turbidity is another way of measuring poor separation as turbidity and suspended solids are closely correlated for low solid concentration. Also, turbidity/centrate suspended solids usually increase gradually with increasing volumetric feed rate. At very high feed rate, turbidity/centrate solids can increase sharply with a small increment of rate, as depicted in Figure 8.10. This is due to concentrate accumulating in the disk-stack solid holding space, which has increased between concentrate discharges or shots. Some solids get entrained by the feed stream and start migrating to the disk stack and are carried by the fast-moving centrate flowing up the disk channels.
- *Solids recovery  $R_s$  in concentrate* is another measure of centrate clarity. As with the centrate suspended solids which depend on the feed solids concentration, the solid consistency in the concentrate also depends on the feed solids. The solids can get entrained in the disk channel and cause a sudden precipitous drop in solids recovery.
- *Yield  $Y$  (soluble product in centrate versus feed)* is usually in the high 90%. It is an important measure of not losing protein during separation of solids from the suspension.
- *Cell viability* should be maintained at a maximum. Moreover, cell viability should not be significantly decreased between feed and the

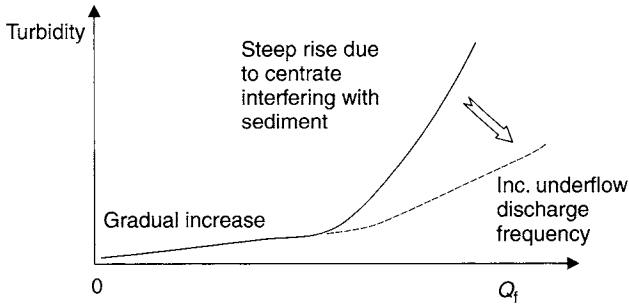


**Figure 8.10** Turbidity as a function of volumetric feed rate

concentrate, otherwise the centrifuge would act unintentionally as a homogenizer. It can be measured by conventional laboratory tests, such as LDH-release assay or multiplex cytotoxicity assay.

- *Solids throughput/capacity* should be maintained. This means that the volumetric feed rate should be maintained constant if feed solids concentration is relatively constant.

The frequency distribution of feed particle size affects separation as bigger particles settle much faster than smaller ones, by virtue of Stokes' law as discussed in Chapter 2. Figure 8.11 shows two different common size distributions expressed as cumulative size distribution. These two size distributions are, respectively, monodispersed and polydispersed particle size distribution. In the frequency distribution (not shown), the curve for the monodispersed distribution appears as a spike in the narrow size range where most particles reside. Outside this range, the frequency of occurrence is practically very small to nil. In the cumulative distribution, as illustrated in Figure 8.11, this appears as a discrete step

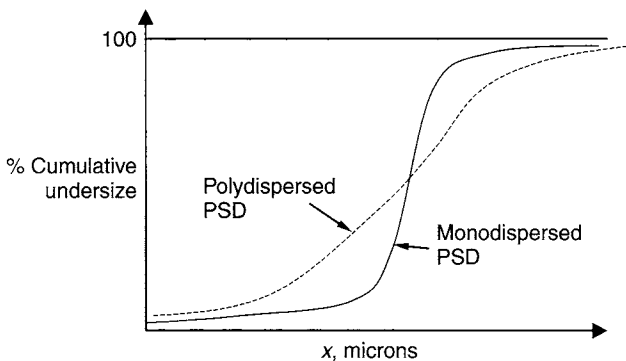


**Figure 8.11** Particle size effect

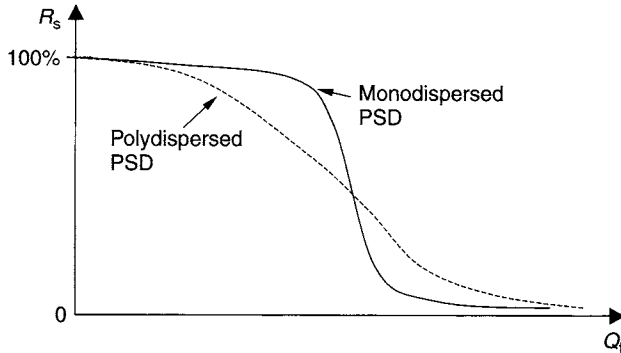


**Figure 8.12** Solid-recovery curve

where the particle size resides. Below this size, the cumulative distribution is virtually 0%, and above this size range, the cumulative distribution approaches 100%. On the other hand, the curve for the polydispersed distribution appears as a broad spectrum that spans a wide range of particle sizes. In the cumulative plot the polydispersed distribution, as illustrated in Figure 8.11, appears as a gradual increase from the small size at 0% all the way up to the larger sizes until it reaches 100%.

As shown in Figure 8.12, the solids-recovery percentage  $R_s$  depends importantly on the feed particle size distribution. The recovery curve is almost a mirror image of the particle size distribution of Figure 8.11. For monodispersed size distribution, the solid recovery stays close to 100% at small feed rates, and after a critical feed rate has been reached, the solids recovery drops off precipitously with any marginal increase to a very low value. For polydispersed size distribution, the solids recovery drops gradually with increasing feed rate, and increases gradually with reduction in feed rate, as illustrated in Figure 8.12.

#### 8.4.3.3 Flocculant and Coagulant in Pilot Tests

Screening tests should be conducted, initially, to determine the appropriate coagulant and flocculant that work best for the specific biological solution under investigation. In pilot testing of coagulant and flocculant, usually higher dosage is needed above and beyond that of the laboratory dosage due to flow dynamics (primarily believed to be shear) that are absent in spintube testing.

Also certain adjustments need to be made in pilot testing, such as mixing time, so that there is sufficient time and energy from the mixing to form sizable floc sizes. This holds especially for the flocs that have

slow kinetics. In pilot testing, coagulants and flocculants are added tens of meters away from the centrifuge, usually by piping the feed and chemical stream to meet at an angle, or  $T$ -junction, to deliberately generate mixing and turbulence when the two streams meet. The combined stream is sent to the centrifuge 5 to 20 meters away. The turbidity of the concentrate is monitored and the polymer dose is adjusted accordingly to minimize the turbidity at a reasonable dosage of chemicals.

## 8.5 Summary

Process objectives, feed properties, bench-scale testing, and pilot-scale testing have been discussed in this chapter. Material balance is used to back-calculate the variables that are difficult to measure accurately, but are required as part of the measuring indices or metrics. Laboratory spintube testing can be made to determine the separability and the  $G$ 's and  $t$ 's to make separation. It can also be used to determine whether chemical additives, coagulants, and flocculants are required to enhance separation. A special designed spintube centrifuge system, equipped with optical transmission measurement, provides sedimentation behavior of the suspension (monodispersed versus polydispersed particles, and unflocculated versus flocculated suspension) over time and space. Pilot testing is a necessary programme once a bench-scale test demonstrates the viability of the separation process. Various parameters in controlling and monitoring pilot centrifuge testing are discussed.

## Reference

- [1] W.W.F. Leung, Separation of dispersed suspension in rotating test tube, *Separation and Purification Technology*, vol. 38, issue 2, pp. 99–119, Aug. 2004.

## Problems

- (8.1) A spintube is spun to a maximum speed of 3500 rev/min. The acceleration time  $t_a$  is 10 s, and the deceleration time  $t_d$  takes 20 s from 3500 rev/min to a stop despite a pneumatic brake being used. The geometric mean radius of the suspension is at 6 cm. (Use this geometric radius instead of the bowl radius at the bottom of the tube as it should be more accurate [1]. The geometric mean radius is the geometric mean of the bowl/tube radius and the radius of the suspension-water intersurface.) The following are the test

data collected from an experiment on sedimentation characteristics of a biological suspension:

**Table 8A**

<i>t, s</i>	<i>Solids recovery (%)</i>
0	Nil
5	33
10	40
20	55
30	66
40	73
50	79
60	82

The data in the table are the centrifugation time duration at 3500 rev/min without accounting for either acceleration or deceleration times. Determine the performance of this test set by calculating  $(Gt)_{\text{total}}$  (a) without and (b) with accounting for acceleration and deceleration using Equation 8.5. What is the difference between the two results?

- (8.2) In a spintube test, the feed is solid and determined to be 4% v/v, centrate solids at 0.5% v/v, and sediment at 15% v/v. What is the solids recovered (a) in the sediment and (b) in the centrate?
- (8.3) A small pilot disk has a bowl volume of 3 L, 50% of which is used to store sediment in between shots. For a yeast feed at 20% v/v and with a feed rate of 4 L/min and discharge efficiency of 80%, what is a reasonable initial guess on time duration in between shots?
- (8.4) Design a pilot test using a tubular centrifuge to run broth from a 200 L fermenter. What are the parameters that should be controlled and monitored?

# Selection and Sizing of Centrifuges

This chapter discusses selection and sizing of centrifuges which are both very important and pertinent in practice, especially for applications in biotechnology which require hands-on work. We will discuss selection of centrifuges based on the process requirements. A unified approach on scale-up of all centrifuges based on the dimensionless Le number is presented.

## 9.1 Selection

### 9.1.1 Introduction

Both disk and tubular centrifuges have been used for separation of microbial cells or bacteria, yeast, and mammalian cells, especially in biopharmaceutical production. In the other extreme, spintubes are commonly used respectively to carry out separation in the feasibility study of a process, and ultracentrifuges are used to determine analytically the properties of a sample in the laboratory, as well as other analytical separation which requires precision and high  $G$ .

Centrifugal separation of microbial cells uses higher  $G$  for separation, especially with smaller particles. On the other hand, centrifugal separation of mammalian cells with slightly larger particles, over ten microns, uses slightly lower  $G$  for separation. Mammalian cells are more susceptible to shear and damage due to lack of cell wall. This is especially the case when accelerating feed stream ineffectively to high speed. When under-accelerated feed is in contact with the pool liquid which is already at solid-body rotation (i.e.  $v = \Omega R$ ), there is a significant difference in velocity mismatch that leads to turbulence and mixing, which have already been discussed in Chapter 4. This may lead to undesirable lysing of cells, inadvertently releasing smaller cell debris that is difficult to separate, and undesirable intracellular contaminates.

### 9.1.2 Tubular Centrifuge Selection

Tubular centrifuge is advantageous to processing lower rate applications using a single unit. It has a cyclic process of loading, separation, liquid drainage, concentrate discharge, cleaning, and rinsing. Concentrate in tubular centrifuge has solids consistency that can withstand shear by unloading a knife or a plunger during concentrate discharge. When sizing the tubular centrifuge, the entire cycle needs to be factored into the capacity calculation. This is unlike a nozzle or intermittent discharge disk centrifuge in which concentrate discharge is continuous or semi-continuous and there is no downtime required for the operation.

### 9.1.3 Disk Centrifuge Selection

When steam-in-place (SIP) is not required, a centrifuge manufacturer can offer disk models for yeast separation from brewing applications with clean-in-place (CIP) features. The costs of these brewing centrifuges are lower (from the disk centrifuge to the control panel) and there are more choices for serving the fermenter size of interest. Also, it would be useful to plan out any possible expansion in the next five years, or longer if possible, so that existing equipment does not run out of capacity in a hurry. When sizing the manual disk, as with the tubular centrifuge, the entire cycle needs to be factored into the capacity consideration. If the downtime becomes unacceptable and the feed solid is high, then the nozzle or intermittent discharge disk centrifuge should be considered. The nozzle or the intermittent discharge disk is selected based on the nature of the concentrate to be discharged as well as the feed solids concentration.

### 9.1.4 Centrifuge Comparison

Table 9.1 summarizes the various types of disk and decanter centrifuges with the typical range of feed solids and sediment handling. It is noted that manual discharge handles low solid feed in the range of 0 and 1% by bulk volume of solids. The intermittent axial-channel (concentrate path at bowl diameter as discussed in Chapter 4) disk can go up to 0.01–10% v/v feed solids. The intermittent discharge (radial slot) takes up higher feed solids of 0.2–20% v/v. The nozzle disk can process 1–30% v/v feed solids, provided that the concentrate is in flowable form (concentrate not stackable with large angle of repose). All large centrifuges can process at upward of 400 L/min feed rate.

Table 9.2 compares the advantages and disadvantages of the centrifuges. The tubular bowl has high  $G$ , typically 5000  $g$  to 20,000  $g$  with

**Table 9.1** Basic types of centrifugal separators

	<i>Sediment</i>	<i>Solids content in feed (% v/v)</i>
Automatic tubular	Remains in bowl	0–4
Manual disk	Remains in bowl	0–1
Intermittent discharge (axial channel)	Discharge through axial channels	0.01–10
Intermittent discharge (radial slot)	Discharge through radial slots	0.2–20
Nozzle disk	Continuous discharge through nozzles	1–30
Decanter	Screw conveyed discharge continuously	5–80

the exception of one small bench unit that can attain 62,000 g (Table 3.2). It has reasonably good dewatering characteristics, simple to disassemble, and easy to clean. Traditional tubulars with large  $L/D$  ratio have limited storage, with the exception of the small  $L/D$  ratio tubular with large diameter bowl. Further, the removal of solids is inconvenient, with the exception of the new modern tubular with low  $L/D$  ratio, as discussed in Chapter 3 where solids are discharged by plunger or with an unloading knife during the solid-unloading cycle. The key disadvantage is the downtime required for either manual or automatic concentrate discharge.

The chamber bowl has good clarification and dewatering characteristics, and large temporary space to hold solids. As with the tubular, it requires downtime for solids unloading translating to lower overall capacity. The concentrated solids unloading is manual. Depending on the nature of the solids, it might be of concern for some process materials as it requires human interface with the process materials. Also, cleaning of the bowl is even more difficult than with the tubular.

For disk centrifuge, there are various forms of solids discharge, as discussed in the foregoing, and there is quite a lot of flexibility for selection, depending on process requirements, budget, availability, and delivery. Liquid is discharged using a centripetal pump to reduce foaming. Also, various forms of hermetic seals are available for both feed and liquid discharge to avoid the liquid product having contact with air, which can cause oxidation and spoilage. The key disadvantages are poor dewatering and the difficulty of cleaning, especially the disk stack.

**Table 9.2** Advantages and disadvantages of various types of centrifuges

<i>Centrifuge type</i>	<i>Advantages</i>	<i>Disadvantages</i>
Tubular bowl	<ul style="list-style-type: none"> <li>(a) High <math>G</math></li> <li>(b) Good dewatering</li> <li>(c) Simple dismantling of rotating assembly</li> <li>(d) Easy to clean</li> </ul>	<ul style="list-style-type: none"> <li>(a) Limited solids storage</li> <li>(b) Recovery of solids manually and difficult (loss of solids if product)</li> <li>(c) Foaming unless centripetal pump used</li> <li>(d) Downtime during cake removal cleaning</li> </ul>
Chamber bowl	<ul style="list-style-type: none"> <li>(a) Clarification efficiency stays constant until solid holding space gets filled</li> <li>(b) Large solids-holding capacity</li> <li>(c) Good dewatering</li> <li>(d) Bowl cooling possible</li> </ul>	<ul style="list-style-type: none"> <li>(a) No solid discharge</li> <li>(b) Cleaning more difficult than tubular bowl</li> <li>(c) Recovery of solids manually and difficult (loss of solids if product)</li> <li>(d) Downtime during cake removal and cleaning</li> </ul>
Disk centrifuge	<ul style="list-style-type: none"> <li>(a) Solids discharge possible</li> <li>(b) Liquid discharge under pressure eliminates foaming</li> <li>(c) Bowl cooling possible</li> </ul>	<ul style="list-style-type: none"> <li>(a) Poor dewatering</li> <li>(b) Difficult to clean</li> </ul>
Decanter	<ul style="list-style-type: none"> <li>(a) Continuous solids discharge</li> <li>(b) High feed solids concentration</li> </ul>	<ul style="list-style-type: none"> <li>(a) Lower <math>G</math></li> <li>(b) Less surface area for clarification compared with disk stack</li> </ul>

Decanter centrifuge provides a continuous cake discharge and continuous feed. It has good dewatering capability. The key advantage it has among all centrifuges is that it can take much higher feed solids concentration. The drawbacks are that it has lower  $G$  compared to the tubular and disk centrifuges and less surface area compared with the disk centrifuges, rendering the clarification and separation of biosolids

less desirable, unless flocculants are used to increase the feed solids sizes, as with processing extracellular enzyme (see Chapter 6).

## 9.2 Centrifuge Sizing

### 9.2.1 Sizes and Rates

Figure 9.1 shows a schematic of a disk centrifuge. It is expected that the larger the fermenter or bioreactor is, the larger is the centrifuge required. Figure 9.2a shows that a 1-L bowl can handle the 50-L bioreactor, a 3-L bowl disk centrifuge serves the 100–1000 + L fermenter, a 20-L bowl serves the 2500–10,000 L fermenter, while a 25–30 L bowl serves the 5000–20,000 L fermenter. This information is also tabulated in Table 9.3 for ease of reference. As can be seen, the centrifuge bowl size increases linearly with the fermenter size. Figures 9.2b and 9.2c show two different commonly used fermenter sizes, respectively, a 50-L and a 2000-L bioreactor or fermenter. The maximum and minimum feed rates of respective tubular and disk centrifuges are shown in Figure 9.3. The feed rate varies approximately as the third power of the bowl diameter from the hydraulic capacity consideration. This is much lower from the process viewpoint and the specific feed rate depends on the requirements of a given process.

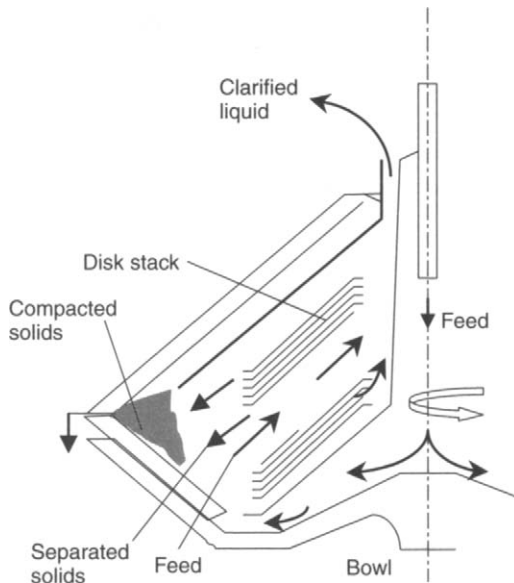


**Figure 9.1** Schematic diagram of a disk

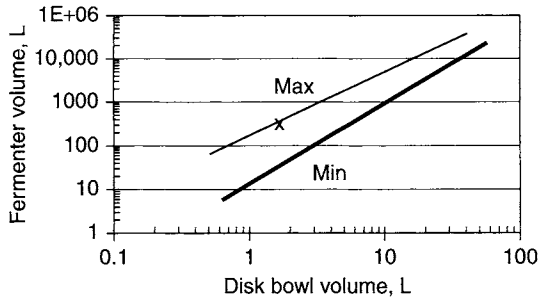


**Figure 9.2a** Fermenter size versus disk bowl volume

**Table 9.3** Fermenter volume

<i>Fermenter size (L)</i>	<i>Disk bowl volume (L)</i>
100–1000+	3
2500–10,000	20
5000–20,000	25–30

### 9.2.2 Dimensionless Le Number

A new dimensionless Leung number (hereafter abbreviated as ‘Le’) has been developed for spintube, disk, tubular, and decanter centrifuges as used for separation and clarification sizing. The Le number was used successfully in many applications for fine particle sedimentation (0.1–100  $\mu\text{m}$ ) [1,2,3]. Le is directly correlated with the cut size, i.e. the maximum size in the supernatant, or the minimum size in sediment. Despite this, one might argue that there is no cut size that provides a sharp demarcation of the minimum size of cake/concentrate sample and the maximum size of the concentrate due to various complexities (entrainment of sediment etc.), yet this provides a concept whereby one can quantitatively size or scale-up centrifuges. Most importantly, the approach presented herein provides a unified approach for sizing different types of centrifuges.

Le depends on centrifuge design geometry and properties of suspended particles (size distribution and density) and liquid (density and viscosity). The Le number has been developed for batch sedimentation (spintube) and continuous-feed centrifuges (disk, chamber bowl, tubular, and decanter centrifuges).

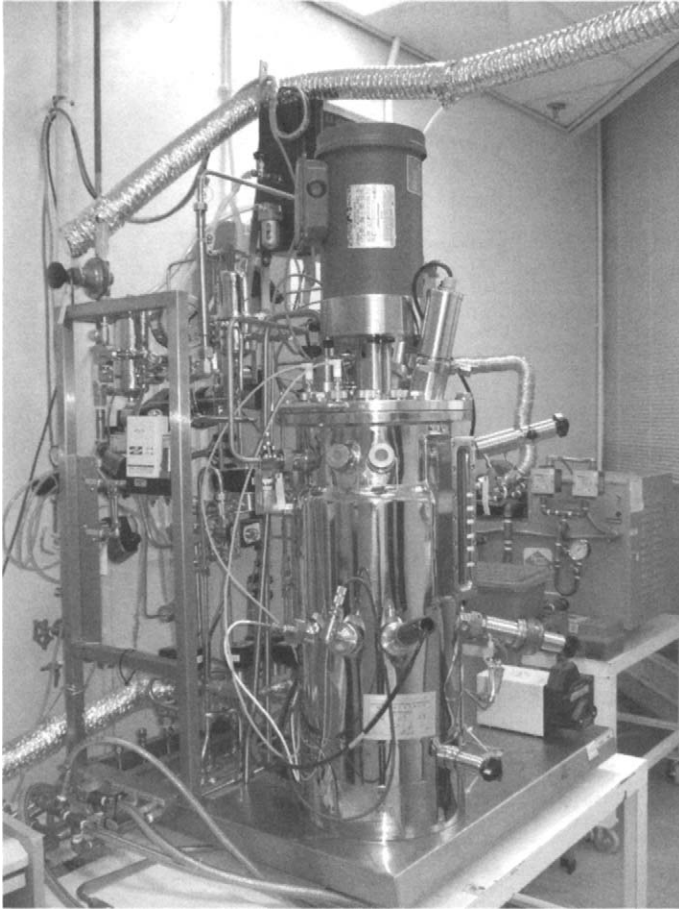


**Figure 9.2b** 50-L bioreactor/fermenter

### 9.2.3 Spintube (bottle) Centrifuge

As discussed in Chapter 3, spintube centrifuges have been widely used in the laboratory, a schematic of which is shown in Figure 9.4. A new analytical procedure of separating a given suspension of well-defined particle size distribution (PSD) to the desired particle capture has been developed [1].

The dimensionless  $Le$  number for the spintube incorporates several key geometric and operation parameters: suspension height  $H$ , centrifugal acceleration  $G$ , time duration  $t$ , and suspension viscosity  $\mu$ , density difference between solid and suspension  $\Delta\rho$ , hindered settling factor  $\lambda (<1)$ , which depends on the concentration of suspended solids  $\phi$ ,

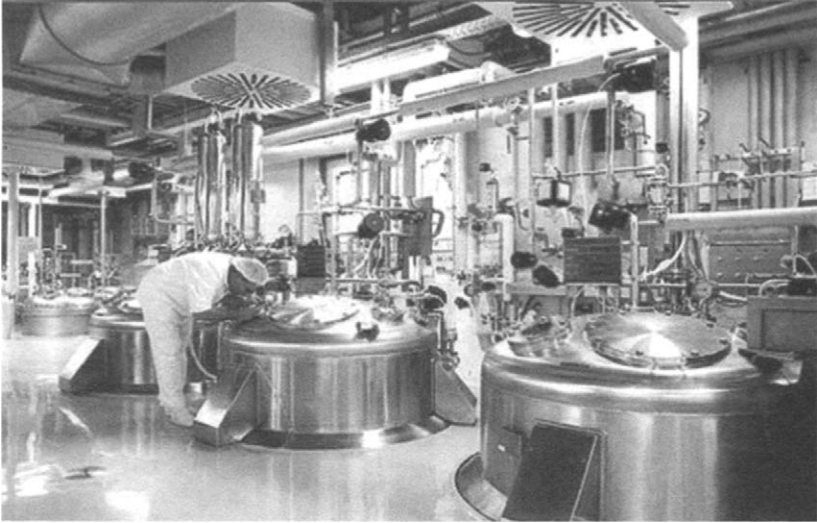


**Figure 9.2c** 2000-L bioreactor/fermenter

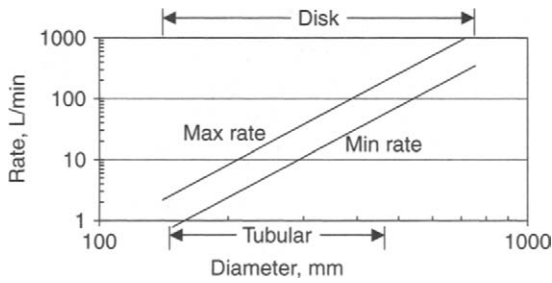


**Figure 9.3** Disk and tubular size versus feed rate, with maximum rate limited by the hydraulic capacity

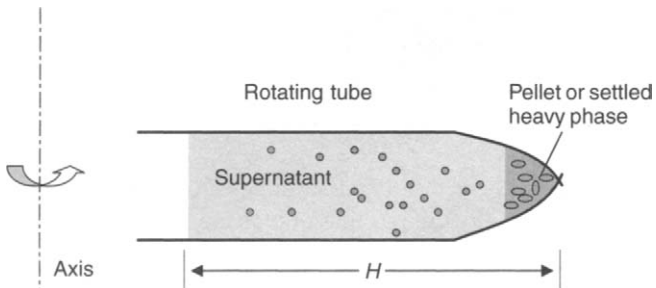


**Figure 9.4** Spintube schematic

efficiency of spin-up  $\eta$ , and the characteristics particle size  $x_o$ . The Le number is defined as

$$\text{Le} \equiv \sqrt{\frac{2\pi\mu H}{\Delta\rho\lambda(\phi)\eta Gtx_o^2}} = \sqrt{\frac{2\pi\mu' H}{\Delta\rho Gtx_o^2}} \quad (9.1)$$

$$\mu' = \frac{\mu}{\lambda(\phi)\eta} \quad (9.2)$$

$$\frac{x_c}{x_o} = \left( \frac{3}{\sqrt{\pi}} \right) \text{Le} = 1.693\text{Le} \quad (9.3)$$

In the above equations,  $\mu'$  is the effective viscosity defined as a ratio of liquid viscosity divided by the product of  $\lambda$  and  $\eta$ . This definition also accounts for hindered settling in the spintube as well as efficiency of spin-up and non-ideal radial geometry.

### Example 9.1 Le calculation – yeast yell ( $7 \times 10 \mu\text{m}$ )

$$H = 4 \text{ cm}$$

$$\mu'/\rho = 0.01 \text{ cm}^2/\text{s}$$

$$\Delta\rho/\rho = 0.05$$

$$g = 981 \text{ cm/s}^2$$

$$G/g = 3000$$

$$t = 240 \text{ s (4 min)}$$

$$\left( \frac{G}{g} \right) t = 720,000 \text{ s}$$

$$x_o = 1 \mu\text{m}$$

$$\text{Le} = 0.844$$

$$x_c = 1.69 \text{ Le}, x_o = 1.43 \mu\text{m}$$

Note that the cells to be separated are between 7 and 10 microns. If the spintube is operated such that the largest particle in the centrate is below  $1.43 \mu\text{m}$ , then particles in the 7–10 micron range would certainly settle out in the sediment. In other words, the spintube is operated with cut size equal or smaller than the cell size that is intended to be removed in suspension. For a given  $G$ ,  $H$ , and other parameters, increasing time duration

$t$  certainly reduces  $Le$  and cut size. This also compensates for the lack of high  $G$ -force for some centrifuge designs, or in some processes  $G$  needs to be lowered to avoid over-compaction of the pellet/sediment leading to difficulty for downstream processing (e.g. dissolution).

Let us consider various biological cells to be separated by centrifugation, as listed in Table 9.4. In the table, it shows the commonly practised  $G$  and  $t$  of centrifugation for separating various cell sizes. As can be seen, the cut size should always be smaller than the cell size in order to remove the cells by sedimentation from the suspension. Figure 9.5 delineates a log-log graph of cell size plotted against cut size for the data in Table 9.4. A 45° line can be drawn through the graph. As depicted in Figure 9.5, given that the cut size should be smaller than the cells to be separated, all the data lies above the 45° line as they should.

The same exercise can be carried out on small organelle. A tabulation of nuclei, mitochondria, ribosomes, and lysosomes is given in Table 9.5. The organelles are indeed very small biological organisms with diameters

**Table 9.4** Biological cells

Cells	$G/g$	$t$ min	Cut size ( $\mu$ )	Cell size ( $\mu$ )
Cell debris	40,000	30	0.14	$0.2 \times 0.2$
Bacteria	10,000	10	0.49	$1 \times 2$
Yeast	3000	4	1.43	$7 \times 10$
Mammalian	200	2	7.82	$10 \times 40$
Plant	200	1	11.1	$100 \times 100$

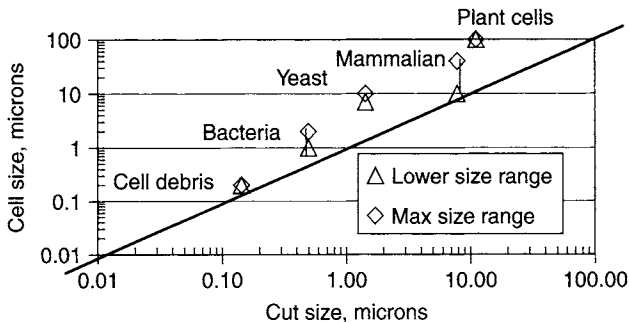


**Figure 9.5** Biological cells

**Table 9.5** Smaller-size organelle

<i>Organelle</i>	<i>Diameter (<math>\mu</math>)</i>	<i>Density (g/cc)</i>
Nuclei	5–10	1.4
Mitochondria	1–2	1.1
Ribosomes	0.02	1.6
Lysosomes	1–2	1.1

ranging between 0.02 and 10 microns. The density of the small organelle is also listed in Table 9.5.

Table 9.6 shows the typical time and  $G$  adopted to make separation based on laboratory experiences of these applications. Again, from separation consideration, these biological particles should get settled when the cut size is smaller than the particle size. Analogous to Example 9.1, calculations on the cut size can be conducted; the results are shown in Table 9.5. Figure 9.6 compares the cut size drawn from Table 9.6 with the cell size drawn from Table 9.5 for the various processes. As expected, all the data lie above the  $45^\circ$  line, indicative that the cut size is smaller than the cell size that is required to be separated by centrifugation.

**Table 9.6**  $G$  and  $t$ 

<i>Organelle</i>	$G/g$	$t$ (min)	$Le$	$x_c$ (microns)
Nuclei	1000	1	1.03	1.75
Mitochondria	10,000	20	0.146	0.25
Ribosomes	100,000	100	0.008	0.014
Lysosomes	10,000	20	0.146	0.25

### 9.2.4 Sizing for Disk Centrifuge

With reference to Figure 9.7, the dimensionless  $Le$  number for a disk-stack centrifuge incorporates the feed rate  $Q$ , the angle of the disk stack with respect to the vertical  $\theta$ , the inner disk radius  $R_1$ , the outer disk radius  $R_2$ , the slant length of disk  $L$ , the projected area parallel to the axis of the machine  $L_p$ , the number of disks  $n$ , the liquid viscosity  $\mu$ , the density difference  $\Delta\rho$ , and the characteristics particle size  $x_o$ .

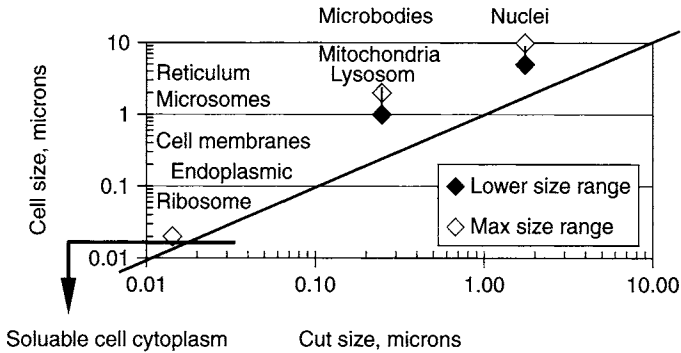


**Figure 9.6** Cut size comparison between theoretical and observed

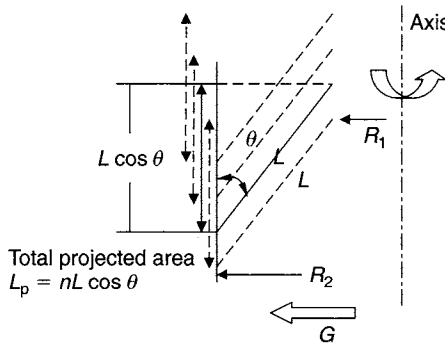


**Figure 9.7** Projected area of disk centrifuge

The Le number for the disk centrifuge is given by

$$Le = \frac{\sqrt{\frac{Q}{L_p} \frac{\mu}{\Delta\rho}}}{\Omega R' x_o \eta} \tag{9.4a}$$

$$R' = \left[ \frac{R_2^2 + R_2 R_1 + R_1^2}{3} \right]^{1/2} \approx R_1 \left( 1 + 0.5536 \left[ \frac{R_2}{R_1} - 1 \right] \right) \tag{9.5}$$

$$L_p = nL \cos \theta \tag{9.6}$$

In the above, an effective radius  $R'$  is related to  $R_1$  and  $R_2$  as expected. Equation 9.4a is very similar to that of the decanter centrifuge, except that  $R'$  replaces the pool radius  $R_p$  for the case of a decanter.  $R'$  can be

approximated by a linear relationship. It is also shown in Chapter 12 that  $Le$  can be expressed in a more compact form as follows:

$$Le = \frac{\sqrt{\left(\frac{3Q}{n}\right)\left(\frac{\mu}{\rho_s - \rho_L}\right)\frac{\tan \theta}{(R_2^3 - R_1^3)}}}{\Omega x_o \eta} \quad (9.4b)$$

It is to be noted that both Equations 9.4a and 9.4b yield identical results in the calculation of the  $Le$  number.

The results from the investigation of settling in a lamella or an inclined plate under the Earth's gravity show that there are two modes of operation when feed suspension is introduced from the top of the channel. With reference to Figure 9.8, the first is a subcritical mode whereby the feed layer fills more than half of the channel width-wise and the feed expands to occupy the entire channel, with the exception of a thin clear layer rapidly flowing up against the underside of the channel. The second mode is a supercritical mode whereby the feed layer occupies less than half of the channel and contracts as it is introduced into the channel. Most of the channel is occupied by the clear layer. In contrast, when the feed is introduced at the bottom of the channel, only the subcritical mode is realized [4].

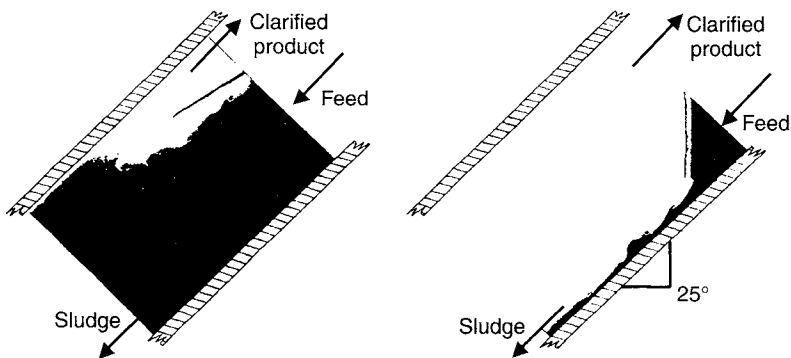


**Figure 9.8** Subcritical mode (left photo) and supercritical mode (right photo) of inclined plate settler

The aforementioned description applies only to a single channel. On the other hand, if there are multiple channels all lining up in parallel, the feed introduced at the bottom might not distribute uniformly into each channel, as demonstrated by the numerical simulation results in Figure 9.9. It is seen in the figure that not all channels get the same amount of feed suspension. The channel adjacent to the main feed stream gets most, whereas the channel to the farthest side from the main feed gets the least. In

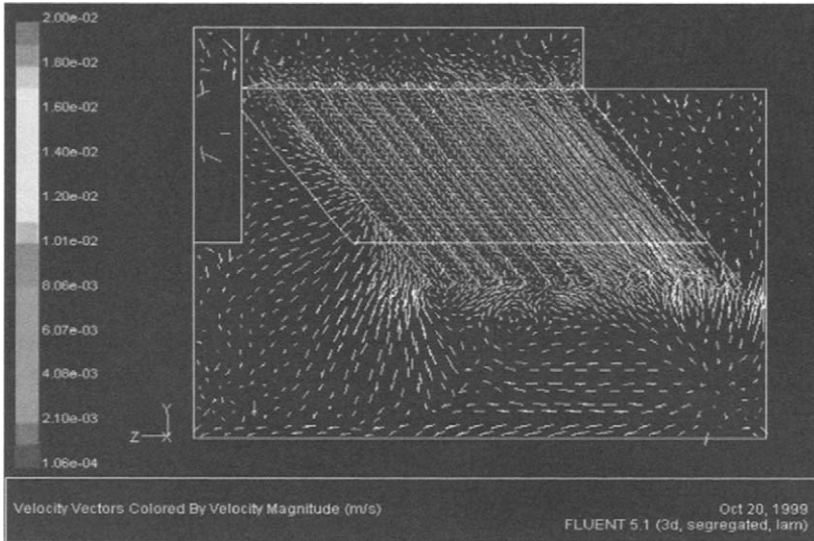


**Figure 9.9** Non-uniform distribution of inclined plate settler, feed inlet on left of figure (generated from commercial computational fluid dynamics)

between there is recirculation and other complicated secondary flow patterns. The flow pattern for a disk stack is similar to that of a lamella settler with non-uniform feed distribution from channel to channel. This shortcoming of non-uniformity is accounted for by using an efficiency index,  $\eta$  in Equation 9.1.

#### 9.2.4.1 Efficiency $\eta$ in Le Number

There are actually several deficiencies that are all lumped into an overall efficiency factor:

- Non-uniform distribution of feed into each channel, as discussed
- Feed not fully accelerated
- Entrainment of sediment by high-velocity liquid stream in disk stack.

Given these complexities, it would still be desirable to maintain a high efficiency factor.

A few qualitative implications can be summarized from Equations 9.3–9.5. Good separation requires small cut size  $x_c$  or small Le, low feed rate  $Q$ , high rotation speed  $\Omega$ , large disk-stack area  $A$ , and low suspension viscosity  $\mu$ , and vice versa for poor separation. Below is an example to illustrate the point.

### Example 9.2 Disk centrifuge

Centrifuge bowl diameter  $D = 400$  mm

Disk outer diameter  $2R_2 = 300$  mm

Disk inner diameter  $2R_1 = 177$  mm

Disk angle  $\theta = 40^\circ$  from vertical

Density difference/density  $\Delta\rho/\rho = 0.1$

Viscosity  $\mu = 5$  cP

$G = 12,000$  g (7270 rpm);  $G = 6000$  (5140 rpm)

$n = 100$  disks

Overall efficiency = 70%

Figure 9.10 shows the linear relationship of Equation 9.3 where the ratio of the cut size to the reference size is linearly proportional to the Le number. The reference size  $x_o$  is fixed at 1 micron.

The cut size is the largest particle that remains in the liquid centrate or the smallest particle in the sediment under a given operating condition. It is therefore also the separated cell size by centrifugation in the sediment. For the above set of parameters in Example 9.2, we can relate these parameters using Equations 9.3, 9.4a, 9.5 and 9.6.

$$R_1 = 8.85 \text{ cm}$$

$$R_2 = 15 \text{ cm}$$

From Equation 9.5

$$R' = \left[ \frac{15^2 + (15)(8.85) + 8.85^2}{3} \right]^{1/2} = 12.06 \text{ cm}$$

$$L_p = (R_2 - R_1)/\tan \theta = 7.33 \text{ cm}$$

$$nL_p = 733 \text{ cm}$$

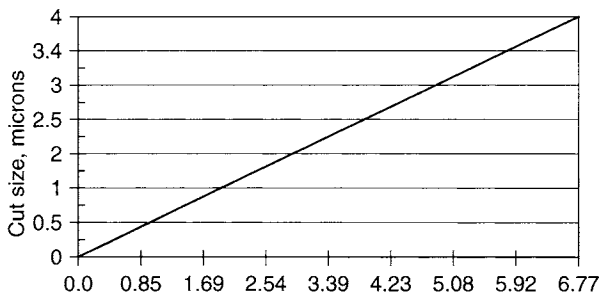


**Figure 9.10** Cut size is linearly proportional to Le

From Equation 9.4a

$$\text{Le} = \frac{\sqrt{\frac{Q}{733} \frac{1000}{60} \frac{0.05}{0.1}}}{(5140\pi/30)(12.06)(1 \times 10^{-4})(0.7)} \quad (9.7)$$

$Q$  in the above is in L/min. From Equation 9.3

$$\frac{x_c}{x_o} = \frac{3}{\pi^{1/2}} \text{Le} = 1.693 \text{Le}$$

Note that  $x_o$  is set equal to  $1 \mu\text{m}$ . Combining Equations 9.3 and 9.7, we obtain Equation 9.8a for the  $G$ -level of 6000 g. Also, for the 12,000 g case, 7270 rpm can be used in place of 5140 rpm in Equation 9.7; this leads to Equation 9.8b.

$$\begin{aligned} Q(L/m) &= 6.34 \left( \frac{x_c}{x_o} \right)^2 & G &= 6000 \text{ g} \\ Q(L/m) &= 12.68 \left( \frac{x_c}{x_o} \right)^2 & G &= 12,000 \text{ g} \end{aligned} \quad (9.8a,b)$$

Given  $Q \propto \text{rpm}^2 (x_c/x_o)^2$  and  $G \propto \text{rpm}^2$ , the coefficient in Equations 9.8a and 9.8b doubles when the  $G$ -level is doubled. This is illustrated in Table 9.7.

These results are plotted in Figure 9.11. Equations 9.8a,b are linear in a log-log plot. As the cell size to be separated decreases, the feed rate drops off as the second power of the separated cell size, which is quite sensitive. Therefore, it pays off to increase the particle size through

**Table 9.7** Processed rate for two different  $G$ 's

Separate cell size $x_c$ , (micron)	Processed feed rate $Q$ (L/min)	
	6000 g	12,000 g
0.5	1.6	3.2
1	6.3	12.7
2	25.3	50.7
3	57.0	114.1

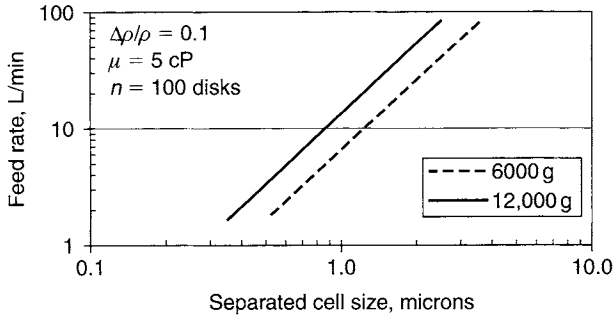


**Figure 9.11** Performance of a disk for a feed suspension with 5 cP

agglomeration of fine biological materials, such as the addition of flocculant to the feed suspension when separating intracellular enzyme.

When the viscosity is increased by 100 times to 5 P, the particle size needs to be increased by 10 times in order to keep the feed rate the same as before. This is illustrated in Figure 9.12. A 10-micron particle can be removed in a suspension of 5 P at the same feed rate processed (about 6–7 L/min) as with a 1-micron particle at 5 cP. Without considering the 10 times increase in the particle size, the feed rate would have to be reduced by a factor of 1/100. Consequently, highly viscous suspension can be very difficult to separate with low capacity and require high centrifugal acceleration.

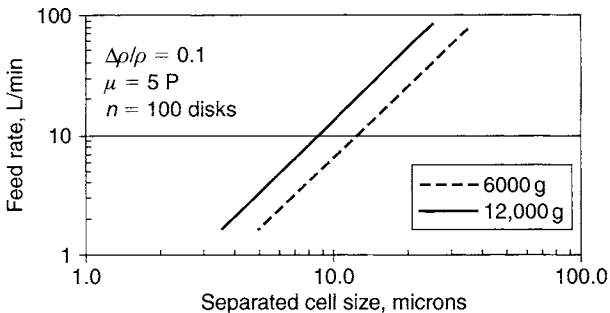


**Figure 9.12** High feed viscosity (5 Poise) and solids concentration

### 9.2.5 Sizing for Tubular, Chamber, and Decanter Centrifuge

The sizing of tubular and chamber centrifuge is also given by the Le number. Figure 9.13 shows a schematic of a tubular centrifuge with a bottom feed.

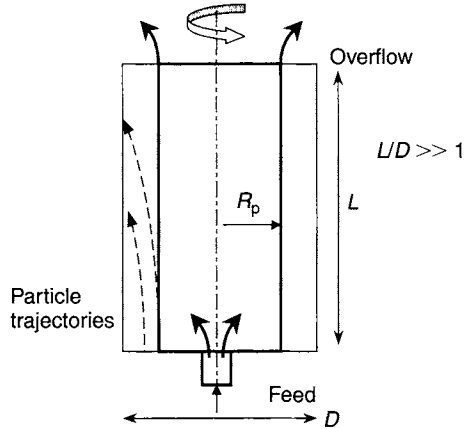


**Figure 9.13** Tubular centrifuge

The  $Le$  number can be defined for a tubular, chamber and decanter centrifuge as

$$Le = \frac{\sqrt{\frac{Q}{L} \frac{\mu}{\Delta\rho}}}{\Omega R_p x_o \eta} \quad (9.9)$$

where

- $Q$  = volumetric feed rate
- $L$  = clarifier length
- $\mu$  = suspension viscosity
- $\Delta\rho$  = density difference
- $\Omega$  = angular speed
- $R_p$  = inner pool radius
- $\eta$  = feed acceleration efficiency

As evident, the  $Le$  number for tubular centrifuge is very much similar to that of the decanter [2]. As discussed, this also applies to chamber bowl centrifuge geometry but without a disk stack. This is illustrated by the example below.

### Example 9.3 Tubular centrifuge

Centrifuge diameter  $D = 300$  mm

Length  $L = 457$  cm

$R_b = 300/2 = 150 \text{ mm}$   
 $h_p = 35.7 \text{ mm}$   
 $R_p = R_b - h_p = 114.3 \text{ mm}$   
 Density difference/density  $\Delta\rho/\rho = 0.1$   
 Viscosity  $\mu = 5 \text{ cP} = 0.05 \text{ P}$   
 $G = 20,000 \text{ g}$  (10,920 rpm); or  
 $G = 5000$  (5460 rpm)  
 Overall efficiency = 80%

Using Equations 9.3 and 9.9 for this numerical example, it can be easily shown that

$$\begin{aligned}
 Q(L/m) &= 0.51 \left( \frac{x_c}{x_o} \right)^2 & G = 5000 \text{ g} \\
 Q(L/m) &= 2.04 \left( \frac{x_c}{x_o} \right)^2 & G = 20,000 \text{ g}
 \end{aligned}
 \tag{9.10a,b}$$

Equations 9.10a,b are plotted in Figure 9.14, for  $G/g = 5000$  and  $20,000$  respectively. For removing a 1-micron particle, the centrifuge at  $5000 \text{ g}$  needs to operate at a feed rate no more than  $0.5 \text{ L/min}$ , whereas at  $20,000 \text{ g}$  it can be operated at  $2 \text{ L/min}$ . Likewise, when the viscosity increases by 100 times to  $5 \text{ P}$ , these feed rates can be maintained if the particle is 10 times bigger, i.e. 10 microns instead of 1 micron. This is illustrated in Figure 9.15.

### 9.3 Feed Particle Size Distribution

The performance that has been discussed considers the separation of a single biological cell or particle in the feed (thick solid line in Figure 9.16).

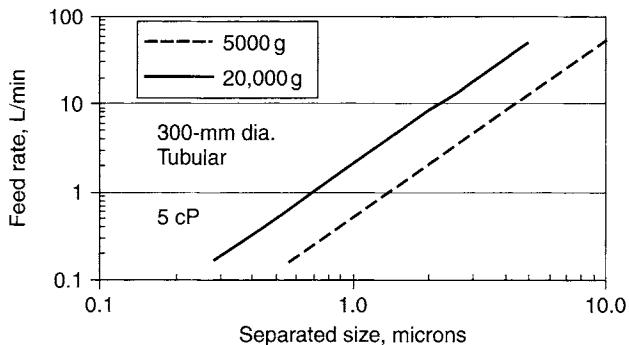


**Figure 9.14** Tubular centrifuge for a feed with viscosity of  $5 \text{ cP}$

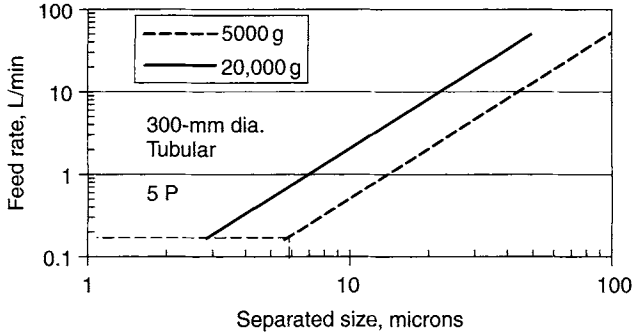


**Figure 9.15** Tubular centrifuge for a feed with high viscosity of 500 cP and high feed solids

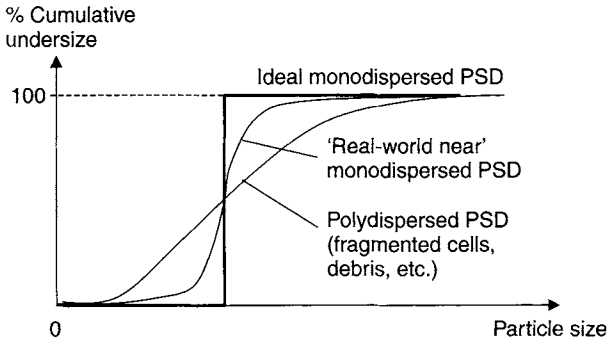


**Figure 9.16** Size distribution of feed

A near ideal monodispersed particle size distribution is shown as a thinner curve in Figure 9.16 as there is no monodispersed size in reality. There is always a dispersed distribution around the most populated size. A broader range of particle sizes, i.e. polydispersed particle size distribution (PSD), is frequently encountered (see Figure 9.16). Regardless of whichever scenario, what is most interesting is that separation performance depends on the feed PSD. Figure 9.17 sketches the behavior of various forms of solids recovery or solids capture by centrifugation corresponding to their counterpart feed size distribution in Figure 9.16.

For monodispersed PSD, the solids recovery is usually very high for a small  $Le$  number, and it can drop off precipitously at a large  $Le$ . On the other hand, for a polydispersed PSD, the solids recovery spreads out across a wider range of particle sizes and there is no critical threshold  $Le$  as with monodispersed particles, for which there is a sudden change in solids recovery. It is understood that after the feed rate exceeds a critical rate all the particles cannot settle for a monodispersed PSD, this leads to a rapid degrading poor performance.

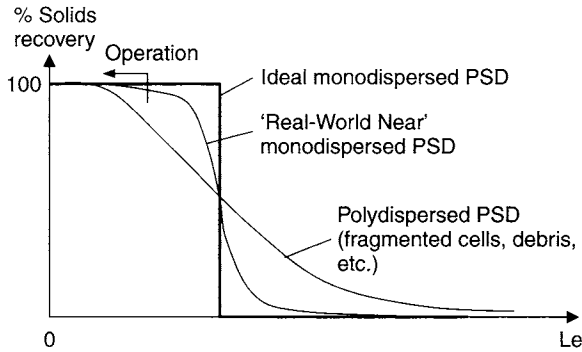


**Figure 9.17** Separation behavior in accordance to the different particle size distribution

Finally, Figure 9.18 shows a combination of several tubular centrifuge test results [5], all plotted with a parameter which is proportional to the governing  $Le$  number, despite the abscissa having a variable  $c(Le)$  and  $c$  being a constant. This does not change the shape were the data in Figure 9.18 plotted against  $Le$  instead of  $c(Le)$ , as this amounts to a parallel translation in the abscissa, given that this is a log plot. What is most important is that all the test data from different geometry, design, feed rates, speed or  $G$  are all correlated by the  $Le$  number. The left ordinate scale of Figure 9.18 refers to recovery in the centrate,  $R_c$ , whereas the right ordinate scale refers to recovery in the concentrate (or sediment),  $R_s$ .

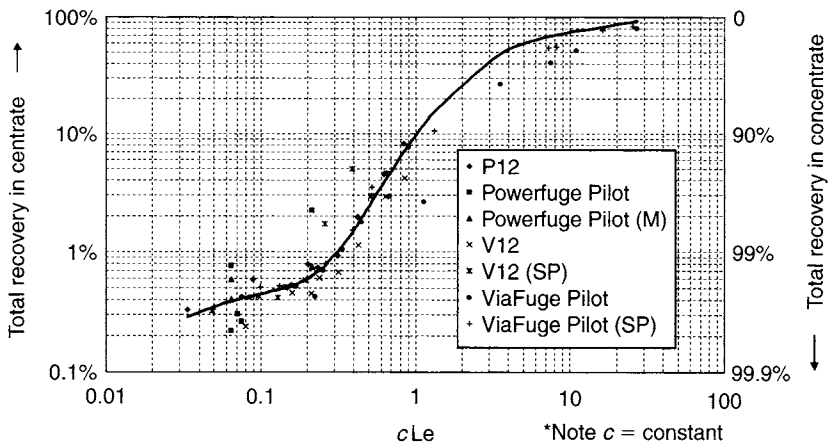


**Figure 9.18** Scale-up of tubular centrifuge tests with  $Le$  number (From T Simpson's paper [5]. Reproduced by permission of the American Filtration and Separation Society)

$$R_e = \frac{M_e w_e}{M_f w_f} = \frac{1 - (W_s/W_f)}{1 - (W_s/W_e)} = 1 - R_s \quad (9.11)$$

$R_e$  and  $R_s$  are based on measurements under steady state of solids concentration in the three streams feed  $W_f$ , centrate  $W_e$ , and concentrate  $W_s$ . Equation 9.11 is derived based on material balance assuming all test data are taken at the steady state.

The test results in Figure 9.18 demonstrate clearly that a large  $Le$  is associated with high centrate recovery, or poor solids recovery, and vice versa. This is independent of the specific tubular centrifuge design, as long as the feed PSD is the same.

## 9.4 Summary

Selection and sizing of centrifuges for biotech applications have been considered in this chapter. The theory behind the sizing will be dealt with in later chapters. An important result is that all centrifuges – spintube, disk stack, tubular, chamber bowl, and decanter – can be scaled by the appropriate dimensionless  $Le$  number. However, the  $Le$  number depends on the specific set of geometric and operating parameters for each type of centrifuge. Based on this, one can determine the separated size of cell particles – the cut size. The cut size which depends on the operation and geometry of the machine should be smaller than the size of cell that needs to be separated. If there are any changes in viscosity (from temperature change) or solids concentration, this affects the  $Le$  number from which the feed rate and  $G$ -force need to be modified, otherwise the cut size would be different and affect the separation outcome. Sizings have been made on centrifuges for use in small organelles (0.1–1 micron) and relatively larger biological cells (1–20 microns and bigger).

## References

- [1] W.W.F. Leung, Separation of dispersed suspension in rotating test tube, *Separation and Purification Technology*, vol. 38, issue 2, pp. 99–119, Aug. 2004.
- [2] W.W.F. Leung, *Industrial Centrifugation Technology*, McGraw-Hill, New York, 1998.
- [3] W.W.F. Leung and R. Probststein, Lamella and tube settlers: Part 1 Model and operation, *I&EC Process Des. and Dev.*, 1983.
- [4] W.W.F. Leung, *Plant Design Handbook for Mineral Processing*, pp. 1262–1288, *Soc. of Min. Eng.*, 2002.

- [5] T. Simpson, Semi-continuous centrifuges, characterization, modelling, and scale-up, Proceedings of the American Filtration and Separation Society Annual Conference, Galveston, USA, 19–22 April, 2002.

## Problems

- (9.1) An application in-hand is a fermentation broth with slightly higher feed concentration of 35% v/v solids. Based on the size of the fermenter, the feed rate to the separation and recovery phase immediately downstream is 50 L/min. The objective is to remove as much yeast as possible with no more than 1.0% of the feed yeast escaped with the centrate that contains the valuable intracellular protein. What equipment would be recommended for this application?
- (9.2) A suspension contains 10% solids and the valuables in liquid need to be recovered to have a high yield of at least 90%. Some of the valuables may be adhered to the solids that require washing. What are the flow sheet and equipment required to do the job if the feed rate is 60 L/min?
- (9.3) A feed suspension of yeast has a mean particle size of 8 microns. The spintube is loaded with suspension with a liquid depth of 0.04 m. The viscosity of the suspension is 6 cP and the density of liquid is  $1000 \text{ kg/m}^3$ , while that of the solids is  $1010 \text{ kg/m}^3$ . The spintube is operated at 3000 g for 4 minutes. What is the Le number for this process separation? What is the cut size in microns? How would this compare to the yeast that needs to be separated by centrifugation?
- (9.4) The same yeast suspension is tested in another spintube with a 0.045 m depth suspension. The maximum centrifugal acceleration for this centrifuge is only 2500 g. What should be the centrifugation time so as to remove the yeast with the same recovery or capture of the cells as in Problem (9.3)?
- (9.5) Another application is to fully recover mammalian cells in a broth from harvesting the bioreactor. The minimum particle size in the broth is 9.6 microns and the maximum size 20.5 microns. A high-speed spintube capable of operating at 5000 g with a sample depth of 0.03 m is used. The broth viscosity is 50 cP and liquid density  $1000 \text{ kg/m}^3$ . The solids density is  $1050 \text{ kg/m}^3$ . What is the minimum centrifugation time in order to fully recover the mammalian cells in the pellet of the spintube?
- (9.6) The process separation and requirements are identical to Problem (9.5). The small-distance separation such as what takes place in a disk stack, where the disks are spaced only by 1 mm or less, is simulated with this exercise. Using a spintube, the smallest possible liquid depth that can be tested with meaningful results is 0.01 m, and the high-speed centrifuge hosting the spintube is capable of accelerating up to 12,000 g. All the process properties are identical to Problem (9.5). What is the minimum centrifugal acceleration one can operate in order to make separation in, say, 20 s?

- (9.7) A 400-mm diameter disk with a disk-stack geometry with 100 disks having an inner disk radius of 8.85 cm and an outer disk radius of 15 cm, capable of operating at 10,000 g, is used in the pilot demonstration. The conical disk makes an angle  $40^\circ$  with the vertical and the overall efficiency of the disk-stack centrifuge is 80%. The unit is used to run the mammalian cell broth of Problem (9.5) with 100% recovery of all the cells. What is the maximum feed rate to the disk-stack centrifuge?
- (9.8) The very same centrifuge of Problem (9.7) is used to process yeast suspension upon harvest. The density of yeast is  $1080 \text{ kg/m}^3$ , while that of liquid is  $1000 \text{ kg/m}^3$ . The viscosity of the liquid is 20 cP. The minimum yeast particle in suspension is 6 microns. Determine the maximum feed rate to the centrifuge.
- (9.9) A tubular bowl has a diameter of 300 mm and length of 457 mm. The pool depth is measured at 3.57 mm from the inner bowl radius. The feed solid has a density of  $1050 \text{ kg/m}^3$ , while that of liquid is  $1000 \text{ kg/m}^3$ . The viscosity of the suspension is 50 cP. The operating G is 20,000 g. At a feed rate of 5 L/min, (a) what is the dimensionless Le number for the tubular centrifuge? (b) What is the smallest cell size to be captured by centrifugation?
- (9.10) The same tubular centrifuge as described in Problem (9.9) is used to process mammalian cell suspension. The tubular needs to capture or recover even the smallest mammalian cell within the population, with sizes ranging between 9.6 microns and 20.5 microns. What is the maximum feed rate to the tubular centrifuge that can still capture the finest cell to achieve a high solids recovery?

# Troubleshooting and Optimization

Troubleshooting and optimization of production centrifuges are often dealt with hand in hand. A centrifuge that has a troubleshoot for various mechanical and process problems may often require process optimization. On the other hand, optimization can be made on a centrifuge that has been performing well to provide process fine-tuning.

## 10.1 Troubleshooting

### 10.1.1 Timescale of Occurrence

It is important to identify a problem as to the timescale for which it occurs. In most cases it would be sufficient to know if the problem is due to long-term degradation (i.e. the condition degrading over a long period of time, such as several months) or it happens quickly in a few days or few hours. Knowing the timescale often allows one to diagnose the root cause of the problem and come up with the solution.

For example, a centrifuge may operate fine one day but fail to perform the next day. The centrifuge after all is a mechanical device; it takes what is being fed and reacts to the feed accordingly! So it might very well be the feed slurry that causes the centrifuge to produce off-spec outputs – centrate or concentrate – and this has nothing to do with the machine. So the characteristic of the feed suspension to the centrifuge needs to be monitored constantly at all times, whether the machine is performing well or not. This enables an operator to rule out a change due to the process or a change due to a mechanical fault.

### 10.1.2 Mechanical or Process Problem

As mentioned briefly in the foregoing, problems can be divided into two types: mechanical-related or process-related. If a problem can be clearly identified as one or the other, a solution can be developed promptly. On

the other hand, these two types of problems can be coupled in a complicated way; a problem that appears to be process-related is actually caused by a mechanical component failing, or a mechanical-related problem is actually due to process problems. This is unlike an independent mechanical problem, such as a missing or loose bolt causing mechanical vibration, or an independent process problem, such as a concentrated feed leading to the build-up of solids rapidly at the solid-holding area that further triggers frequent concentrate solid discharge/shots. In this situation, it would still be constructive to determine which of the two is the root cause of the problem, and to come up with an appropriate remedial plan to solve it.

### 10.1.3 Process Problems

#### 10.1.3.1 High Centrate Turbidity

##### 1 High feed solids throughput causing high centrate turbidity

This is measured by increasing the dry weight of solids per unit time (kg/h DS). This may be due to higher concentration of suspended solids from a bioreactor or fermenter. The operator should reduce the feed rate (if possible), or increase  $G$ -force. Another possibility of higher feed solids throughput may be due to higher volumetric feed rate. The speed of the centrifuge or  $G$ -force should be increased (if possible) for this case. Obviously, the electrical power drawn will increase as  $P \propto \rho\Omega^2Q$  where  $\rho$  is the density of suspension,  $\Omega$  is the angular speed, and  $Q$  is the feed rate; and all three quantities are increasing.

When either the feed rate increases and/or the feed suspended solids concentration increases, these lead to higher viscosity and more hindered settling, therefore the dimensionless  $Le$  number increases (see Equation 8.1 in Chapter 8). The operating point ( $Le$ ,  $R_s$ ) will shift along the curve towards the increasing  $Le$  direction from point  $Le_1$  to point  $Le_2$ . The solids recovery decreases from  $R_{s1}$  to  $R_{s2}$ . This is illustrated by Figure 10.1. If the speed or  $G$ -force increases and/or feed rate decreases,  $Le$  can be dropped back to the original  $Le_1$ , as shown in Figure 10.2.

##### 2 Finer feed solids causing high centrate turbidity

An increase in fine suspended particles from reactor or fermenter often occurs as a result of debris, upset, and other unfavorable conditions. This condition can be detected by monitoring the PSD of the feed to centrifuge. Under this condition, it is best to increase  $G$  if possible or reduce the feed rate. Figure 10.3 shows the performance curve ( $R_s$  vs.  $Le$ ) for both (1) nominal feed and (2) upset feed.

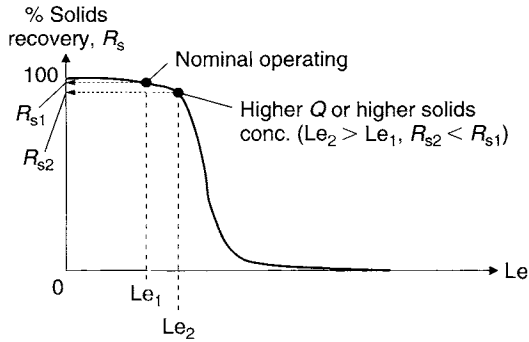


**Figure 10.1** Increase feed rate or solids concentration

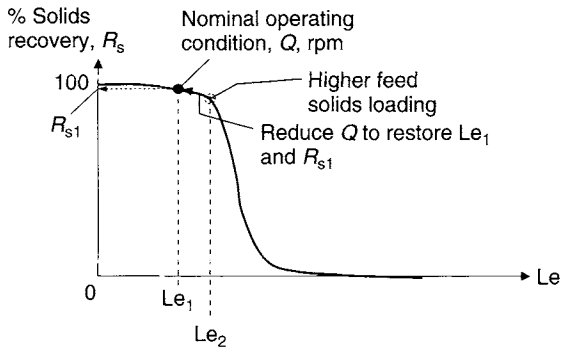


**Figure 10.2** Compensating for upset condition by restoring solids recovery at  $Le_1$

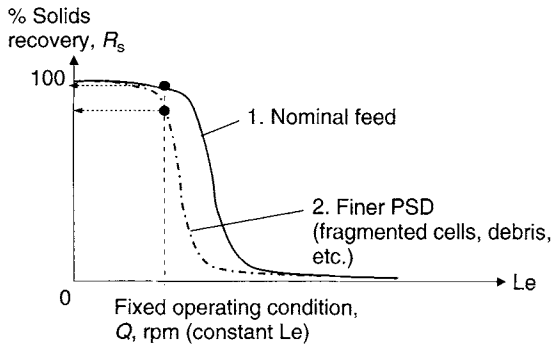


**Figure 10.3** Feed particle size effect for nominal condition and upset condition with finer particle size distribution

By reducing  $Le$  such as by increasing  $G$  or by reducing feed rate, one can boost up to the same solids recovery as with the previous nominal feed. This is illustrated in Figure 10.4.

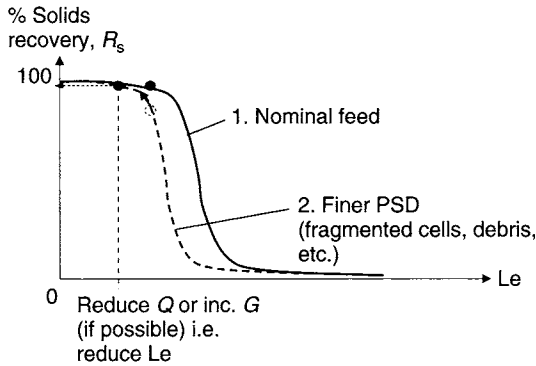


**Figure 10.4** Compensating for upset condition by restoring solids recovery at even lower  $Le$  compared to initial condition

### 3 Concentrate not discharging causing high centrate turbidity

If concentrate is not discharging fast enough, the first symptom is cloudy to dirty centrate due to entrainment of solids. If the problem is more severe, this leads to accumulation of solids in the disk stack, causing vibration if solids are not uniformly distributed around the circumference. Some remedial measures may be to (a) increase frequency of concentrate ejection, (b) increase duration in each ejection for disk, (c) check to ensure the automatic control unit, if available, for sensing turbidity and controlling ejection is working, and (d) confirm turbidity meter is working and flow tubing is free from adhered solids causing a false reading.

### 4 Lower process temperature and higher viscosity causing high centrate turbidity

For the case of lower operating temperature which results in elevated suspension viscosity, the operator may compensate for this shortcoming by increasing operating temperature, increasing  $G$  or rotation speed as necessary, and/or decreasing feed rate if possible.

#### 10.1.3.2 Wet or High-Moisture Concentrate

High moisture means a loss of product protein in the liquid discharged with the solids in underflow stream/concentrate. This is undesirable in biopharmaceutical processing of mammalian cells and yeast, or for any other

process wherein protein are expressed in the liquid. If the concentrate is too wet, concentrate may stick to the bowl wall, leading to incomplete discharge of concentrate in the solid-holding space of dropping-bottom disk centrifuge. There are several ways of fixing the problem:

- Reduce the frequency of discharge; this allows the build-up of thicker 'cake' near the bowl wall, facilitating compaction and percolation.
- Reduce duration of concentrate ejection, allowing only the driest cake adjacent to the bowl wall (peripheral of the bowl) to be ejected.
- A higher operating  $G$  and speed if possible; this improves compaction and percolation.

## 10.1.4 Mechanical Problems

### 10.1.4.1 High Vibration

Vibration is due to the mechanical unbalance of distributed masses in a centrifugal field. It is a very common problem in centrifugation. When the laundry goes through a blow-dry cycle while the washing machine is spinning, a little mal-distribution of the laundry around the drum can lead to mechanical vibration (i.e. shaking) and loud noise from the washing machine. The washer can be momentarily stopped, the laundry can be redistributed, and the drying cycle can be resumed. The washer would then run smoother, with reduced vibration and noise.

Some vibrations can be of short duration, in which case after a short transient the vibration goes away. However, it would be undesirable if a large vibration (vibration amplitude or speed that reaches or exceeds manufacturer's limit) persists for a long time. It causes component damage in the machine, which undermines and damages the supporting structure. Dangerous situations, such as losing or detachment of rotating parts, can occur under severe conditions.

As discussed, vibration is due to unbalance in the rotor. If the machine is vibrating in dry condition and it has not run any process, either some components or parts (such as nuts and bolts) are loose or missing.

On the other hand, if the machine has run a process in the past and it is supposedly clean (no residual solids) yet it is running with high vibration, then another thorough cleaning cycle needs to be carried out to ensure that there is no residual solid left in the rotor. For example, a piece of residual solid of mass 10 g located at the periphery of the disk machine (near discharge port), operating at 10,000 g, can lead to an unbalance force  $F_u = ma = (0.01 \text{ kg})(10,000)(9.8) = 980 \text{ N}$ . This can give rise to impressive vibration that catches attention, especially when

the machine ramps up in speed and  $G$ -force. Note that both the unbalance force and vibration increase to the second power of rotation speed. If the vibration becomes excessive, the machine should be stopped immediately and it should go through a cleaning cycle to ensure that there are no residual solids left in the rotor. Cleaning inside and outside the rotor may involve, generically, the following procedure.

- Flush the machine with water, or specially prepared cleaning liquid, thoroughly. Eject periodically for dropping-bottom disk, or continuously for nozzle disk, to remove any accumulated solids.
- Run flush water at lower rpm (without establishing centrifugal field with an annular liquid pool) as this allows liquid to be sloshed in the machine at a much lower rotation speed, providing effective cleaning.
- Flush and clean the outside of the rotor for any residual solid deposit (from carry over).

Repeat several cycles of cleaning until the vibration reduces to an acceptable level.

If vibration occurs over time (i.e. not over a short duration, such as overnight), the operator needs to conduct a proper mechanical diagnostic according to the centrifuge supplier's instruction in order to rule out all possible causes of vibration (e.g. unbalance due to misalignment, worn bearing, drag on rotor from interference with stationary parts, etc.). An historical maintenance record of operation, especially for vibration, voltage, current, and other pertinent parameters, is desirable.

#### *10.1.4.2 Other Mechanical Problems*

Other non-vibration problems, such as bearing overheating, excessive wear due to abrasive materials, and high acoustic emission, are not uncommon. The overheating problem may be related to appropriate lubricant not being used or the correct lubricant not being replenished after being consumed, or it may be due to worn balls or rollers in bearings that need to be replaced. Overheating can also be related to misalignment of the rotor, which causes excessive generation of heat from Coulomb friction. If there are areas showing excessive wear from the process stream, these areas need to be covered with abrasive resistant material, such as tungsten carbide, silicon carbide tiles or other wear-resistant materials. High acoustic emission may be due to vibration as a result of unbalance of rotating parts or poor acoustic isolation design.

## 10.2 Optimization

There are two forms of optimization. Optimization means that the centrifuge needs to meet targeted metrics of separation and to run most effectively and efficiently within the set metrics. Optimization also implies process-wise robustness. The centrifuge should be more forgiving to upstream variations from upsets yet providing consistent (with striving improvement) output results for downstream processes (i.e. filters, concentration/buffer exchange step, purification, sterile filter, etc.).

### 10.2.1 Separation Metrics

There are several process metrics.

#### 1 Yield $Y$ of soluble protein (in liquid product)

Drier solids in concentrate stream would boost the yield. Yield is typically in excess of 90%. Repulping and separation of concentrate can further improve the yield but at the expense of additional operating and capital costs.

#### 2 Clarification: Separation of suspended solids in liquid

High recovery  $R_s$  of solids in sediment/concentrate infers less solids leaving the overflow or centrate. The suspended solids in centrate (% ss w/w) are also commonly monitored more subjectively using optical methods such as turbidity.

#### 3 Feed rate or throughput

The volumetric feed rate or solid throughput of centrifuge, respectively expressed as L/min or kg/h, is most important for a production plant.

#### 4 High cell viability (for cell culture, e.g. mammalian cells)

This is an important consideration for processing and separating mammalian cells. Referring to Figure 10.5, if the cells get lysed inadvertently, undesirable intracellular protein is further released from the cells, contaminating the liquid containing the valuable expressed protein. This cross-contamination implies that an additional separation step may be required using membrane to separate the valuable protein

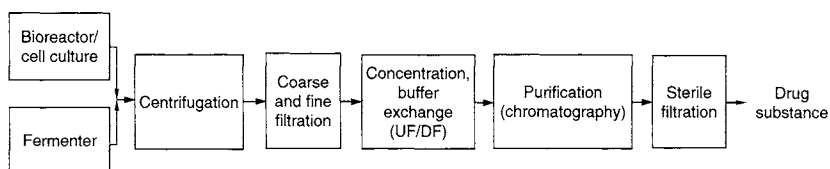


**Figure 10.5** Generic biopharmaceutical processing leading to drug substance

from other intracellular protein released from the lysate, and to carry out the difficult purification by the chromatography column downstream. The worst case may also result in wasting of the entire batch.

In centrifugation, the variables can be divided into monitored and controlled variables. Measurements are made continuously or periodically based on these monitored variables, to ensure that they are within the limits.

### 10.2.2 Monitored Variables

The following are the monitored variables.

- rpm/G
- Flow rate of feed and centrate
- Centrate solids and turbidity
- Solids concentration in feed and underflow
- Cell concentration – cells/mL respectively in feed, centrate, and underflow (continuous discharge)
- PSD of feed and centrate (these are less common measurements and should be monitored where possible as they provide good insight into operation and optimization)
- Protein concentration in feed, centrate, and underflow
- Process temperature
- Viscosity
- pH
- Mechanical and electrical conditions (vibration, torque, bearing temperature, acoustic emission, voltage, current, power, etc.)
- Other pertinent process parameters.

Some of the monitored variables listed can be controlled.

### 10.2.3 Controlled Variables

The following are variables that can be controlled.

- *Rate  $Q$*  This may not be an option due to production demand.
- *Speed  $\Omega$  or centrifugal gravity  $G$*  This impacts on power consumption and should always be under the recommended limit. Also high  $G$ /speed often results in more wear-and-tear or shorter operation time between maintenance.
- *Feed suspended solids (adjustable through dilution)* A desirable feed consistency is needed. There seems to be a growing trend for increasing feed solids concentration in bioprocessing. For example, there is

a tendency for increasing feed solids concentration (by bulk volume) from 4% to a higher concentration, such as 6%, to improve capacity and to optimize bioreactor operation.

- *Increasing particle size upstream of centrifuge* (see Figure 10.5) via flocculation if possible, such as in enzyme processing.

## 10.2.4 A Simple Optimization Scheme

Granted that solids separation as measured by solids recovery or capture is a primary function of the dimensionless number  $Le$ , a relatively simple optimization is discussed in the following to illustrate the general approach of using  $Le$  as an index. If  $Le$  is kept constant during operation, the performance should remain the same. This immediately leads to designing simple schemes for optimization. In Chapter 9 it has been demonstrated by Equation 9.1 for spintube, Equation 9.4a,b for disk stack, and Equation 9.9 for tubular, chamber bowl, and decanter centrifuge, that

$$Le^2 = c \frac{Q\mu}{\Omega^2} \quad (10.1a)$$

$$Le^2 = c \frac{Q\mu}{\Omega^2} \quad (10.1b)$$

$c$  in Equations 10.1a and 10.1b is a constant independent of  $Q$ ,  $\Omega$  and  $\mu$ .

Assuming  $Le$  being constant, taking the logarithm and subsequently the differential of Equation 10.1b leads to the following.

$$\log Q = \log \left( \frac{Le^2}{c} \right) + 2 \log \Omega - \log \mu \quad (10.2a)$$

$$\frac{dQ}{Q} = 2 \frac{d\Omega}{\Omega} - \frac{d\mu}{\mu} \quad (10.2b)$$

$$\frac{\Delta Q}{Q} \approx 2 \frac{\Delta \Omega}{\Omega} - \frac{\Delta \mu}{\mu} \quad (10.2c)$$

### 10.2.4.1 Optimizing Centrifuge (Increased $Q$ )

When the feed rate  $Q$  (more precisely  $\Delta Q/Q$ ) needs to be increased by a ratio, the operator can increase the rotation speed  $\Omega$  (i.e.  $\Delta \Omega/\Omega$ ) in accordance with Equation 10.2c to compensate for the feed rate increase.

**Example 10.1**

When  $\Delta Q/Q = 20\%$ , one needs to increase  $\Delta\Omega/\Omega = 10\%$  (as viscosity remains constant) to maintain  $Le$  being constant, thus ensuring  $R_s$  is the same.

Note that the speed increase should not be excessive for mammalian cell separation, otherwise this may lead to cell damage.

**10.2.4.2 Optimizing Centrifuge (Increased Viscosity  $\mu$ )**

When feed solids concentration increases and viscosity also increases, an increase in  $\Omega$  and/or decrease in  $Q$  in combination, in accordance with Equation 10.2c, would negate the effect of increasing viscosity. Rewriting Equation 10.2c

$$\frac{\Delta\mu}{\mu} \approx 2 \frac{\Delta\Omega}{\Omega} - \frac{\Delta Q}{Q} \quad (10.3)$$

**Example 10.2**

When  $\Delta\mu/\mu$  increases by 30%, feed rate is decreased by 10% so that  $\Delta Q/Q = -10\%$ , and the rotation speed only needs to increase by 10%, i.e.  $\Delta\Omega/\Omega = 10\%$ . On the other hand, if the feed rate is not allowed to change, the rotation speed needs to be increased by 15%, or  $\Delta\Omega/\Omega = 15\%$ . Again, one needs to pay heed to the same considerations as other possible adverse effects incurred during speed increase for mammalian cell separation.

The solids recovery is a function solely of  $Le$ , which in turn is a function of the centrifugal acceleration  $G$  (or rotational speed  $\Omega$ ) and feed rate  $Q$ . By changing  $G$  (or  $\Omega$ ) and/or  $Q$ ,  $Le$  may be changed, and so is  $R_s$ . A plot of  $R_s$  versus  $1/G$  (or  $1/\Omega$ ) and  $Q$  results in a three-dimensional surface of  $R_s$ , as shown in Figure 10.6. One can work with various  $G$  and  $Q$

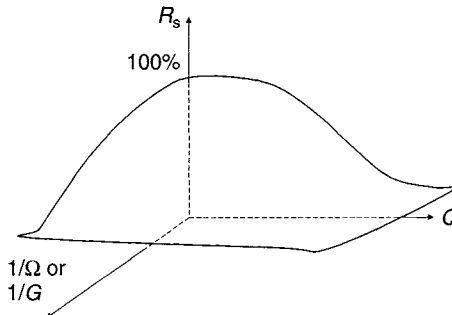


**Figure 10.6** Solids recovery versus speed/ $G$  and feed rate

to get  $R_s$  within the operating limits ( $R_{s\min}$ ,  $R_{s\max}$ ). There could be equal- or iso-recovery (constant  $R_s$ ) lines on such a surface, which also corresponds to iso-Le (constant Le), given  $R_s$  is a function only of Le.

### 10.3 Summary

Both mechanical and process problems and troubleshooting factors have been discussed in this chapter. Process problems for disk centrifuge include, but are not limited to, centrate with too much suspended solids or turbidity or concentrate that is too wet. Mechanical problems include vibration, acoustic emission, wear and tear, etc. It is important to have a sense of the timescale when problems have occurred. To that end, day-to-day mechanical and process monitoring, as well as recording or logging, are important. Some monitored and control variables have been reviewed. A simple optimization strategy based on feed rate and angular speed gauging on the solids recovery (or centrate solids) is presented.

### Problems

- (10.1) After shutting down over the weekend, a tubular centrifuge is experiencing excessive vibration on Monday morning; when it is rotating to speed and when running feed suspension, the vibration does not go away. The machine is flushed a couple of times with wash liquid but it does not help. The machine went through maintenance just two weeks ago and has been running smoothly since. What can you recommend to eliminate the vibration?
- (10.2) A dropping-bottom disk-stack centrifuge processing yeast is experiencing high turbidity in the centrate. The feed rate is at 40 L/min and 10,000 g, and the time duration between shots is 4 minutes. What can you recommend to reduce the centrate solids without penalizing the throughput?
- (10.3) A new decanter centrifuge is not discharging cake on the first maiden run despite the machine having a continuous feed input for the first 20 minutes with a rate of 200 L/min and feed solids at 3%. The liquid is discharging over the weirs at the large end of the machine. Torque seems to be building up slowly initially, but also seems to pick up at a decent rate. What can be done to get cake discharge?
- (10.4) A lab-scale spintube centrifuge after accelerating to speed keeps reverting to coast down, decelerating on its own without reason. What can the operator do to fix the problem?
- (10.5) A dropping-bottom disk-stack centrifuge is vibrating noisily as it is discharging and the amount of wet solids do not seem to be much. In fact, the concentrate seems to be on the wet side and sticks onto the container that it is discharging into. What can the operator do to alleviate the problem?

- (10.6) A decanter centrifuge, dewatering waste of the biotech process, is discharging wet cake, and the flocculant dosage increased to keep the cake in a handleable form. The valuable is in soluble form that escapes with the moisture in the cake. What can the engineer recommend to tackle the problem of having a more handleable cake and reducing loss of valuable?
- (10.7) In the simple optimization scheme as proposed in Section 10.2.4, if the viscosity increases by 20% and the rotational speed can at best be increased by 7%, what can the operator do to maintain the same concentrate quality without loading downstream processes with extra suspended solids leaving the centrifuge?

# Flow Visualization and Separation Modeling of Tubular Centrifuge

A tubular centrifuge model will be presented in this chapter. Prior to this, it will be instructive to visualize the flow pattern associated with a tubular centrifuge. A schematic of the tubular is shown in Figure 11.1. This is similar to the one shown in Figure 11.3. In the sectional view of Figure 11.1, there are two possible configurations: one that has annular baffle rings stretching radially from the inner bowl wall to the pool surface, and one that does not have baffle rings.

Despite this, there is quite a large annular area for flow. It will be demonstrated later that the flow actually takes place in a much smaller annulus just below the pool surface. The depth of this moving, or boundary, layer has been presented first by Leung [1], see Figure 11.2. The depth of the moving layer  $h$  is thin yet relatively constant in thickness along the axial direction. The moving layer is above a more quiescent thicker layer which occupies almost the entire annular pool.

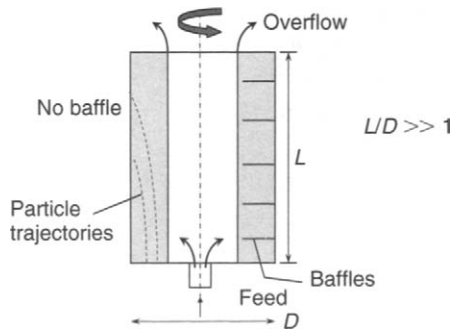


**Figure 11.1** Schematic of tubular centrifuge showing baffles arrangement on right side and no baffle arrangement on left side

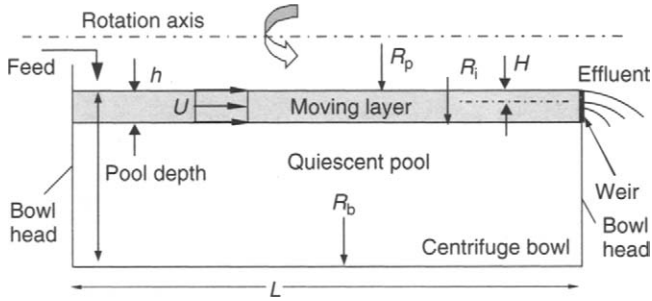


**Figure 11.2** Schematic of tubular centrifuge showing moving layer flowing over an otherwise stagnant pool

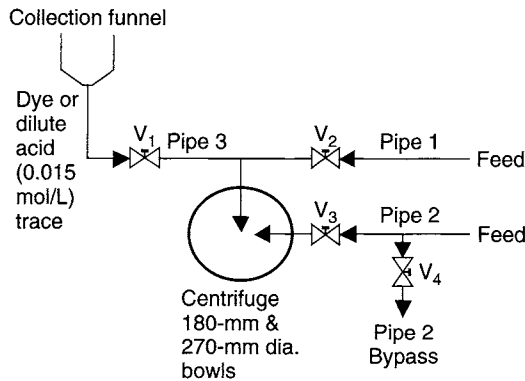


**Figure 11.3** Arrangement of dye injection before and after filling the bowl

## 11.1 Flow Visualization

In this section, a useful experimental setup is discussed, followed by various techniques introduced to visualize and quantify the flow of a moving layer in a rotating pool with continuous feeding.

An experiment is set up to visualize the flow pattern of tubular centrifuge. There are two concurrent feeding channels to the bowl, as shown in Figure 11.3. It allows (a) dye to be injected prior to introducing the 'normal' liquid flow, (b) dye to be injected subsequent to normal flow, or (c) a background dye to fill up the pool followed by a different dye injection.

Figure 11.4 shows one possible setup wherein water was first introduced into a rotating bowl at 150 g with a pool depth of 45 mm measured radially from the bowl wall (i.e. bowl inner radius). At the start of the experiment  $t = 0$ , the red dye introduced immediately stretched longitudinally

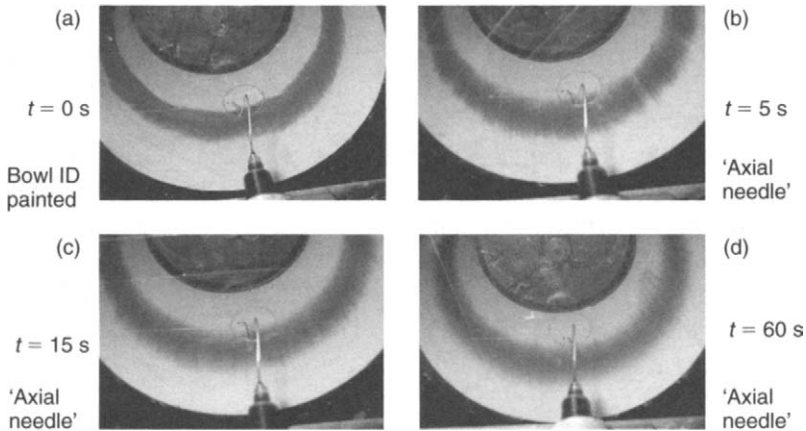


**Figure 11.4** Bowl inner diameter painted white for visualization. Red dye introduced to a fully accelerated pool at 150 g and 45-mm pool depth: (a)  $t = 0$ , (b)  $t = 5$  s, (c)  $t = 15$  s, and (d)  $t = 60$  s

like a needle showing the Taylor Proudman column [2], or more generically in rotating flow as exhibiting a two-dimensional flow pattern. This needle-like pattern was aligned with the axis of the rotating bowl and lasted for about 60 s in the experiment until diffusion took over and started smearing the flow pattern.

Another flow visualization experiment is described in the following with results captured in the photos of Figure 11.5 (a) and (b). The pool was initially filled with black ink and after filling and accelerating to speed, the feed was changed to water feed. A white pillar attached to the rotating bowl wall showed that a portion of the pillar close to the pool surface (covered by a thin transparent water layer) is exposed without

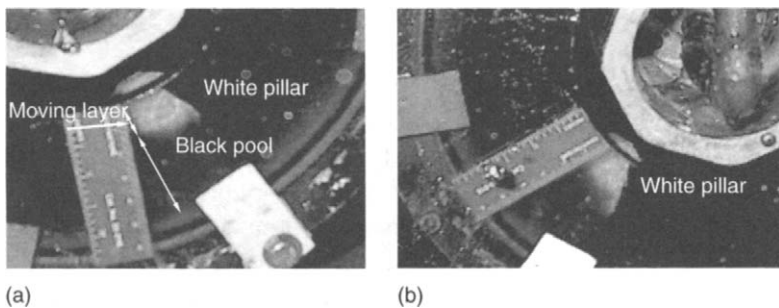


**Figure 11.5** Water introduced to an otherwise 'black' pool of liquid. Moving layer is observed by white pillar co-rotating with bowl serving as background: (a) ruler placed at 5:30 position on the front stationary cover, and (b) ruler placed at the 8:40 position

being darkened by the initial 'black' pool. This layer thickness for a given  $G$  and feed rate can be measured by placing a ruler on the Plexiglas weir and sighting, without parallax, the pillar using a strobe to stop the rotating motion.

Alternatively, florescent dye was introduced instead of water as a continuous feed. Using an ultraviolet light, an annular ring of bright color reflected from the florescent light was visible, as depicted in Figure 11.6 (a) and (b). Strobe light was not used for visualization and the moving layer appears as a florescent circular ring with infinite images overlaying each other, wrapping around  $360^\circ$ . This ring thickness can be measured and is shown in Figure 11.6.

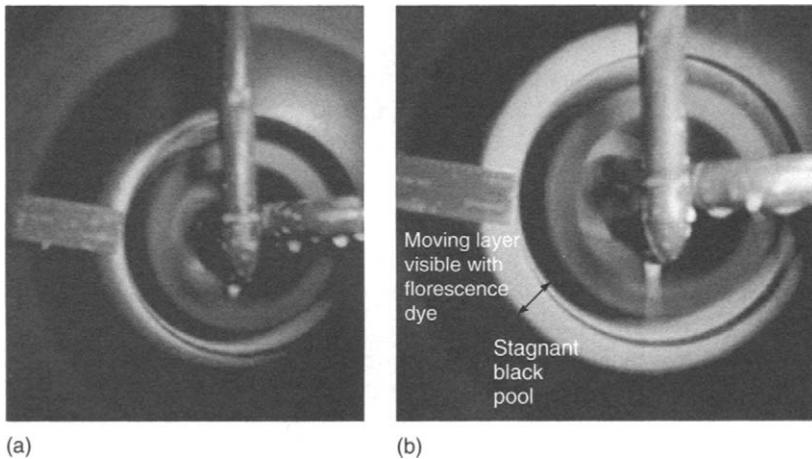


**Figure 11.6** Florescent dye illumination: (a) far view showing pool depth, (b) close-up of moving layer

Finally, one more experimental configuration has been set up that facilitates quantitative measurements. Instead of using dye, an acid pool was introduced into a rotating bowl. After filling, the acid feed was immediately replaced by water at  $t = 0$ . The conductivity of the effluent liquid leaving the centrifuge was monitored starting at  $t = 0$ . One of the typical results is shown in Figure 11.7. The conductivity or acid strength in the effluent liquid decreases over time as the pool of acidic liquid is flushed out from the rotating bowl. After two pool volumes, the conductivity of the effluent drops to the base level and stays there, even for as much as  $30\times$  pool volumes. The feeding of the bowl with water stopped and the bowl was allowed to decelerate until the pool collapsed with a lot of sloshing and mixing of the liquid inside the bowl. The conductivity level of the effluent liquid rose up to 0.6 units despite it having been practically at

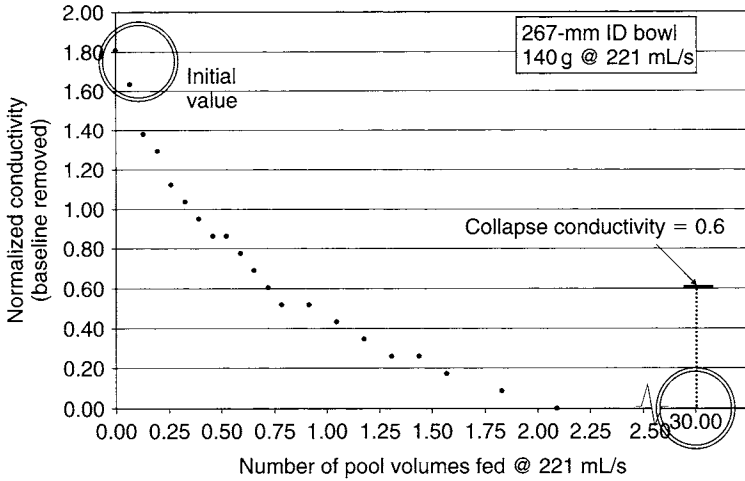


**Figure 11.7** Acid or conductivity versus the number of pool volumes feeding the centrifuge bowl

zero after feeding two pool volumes of water. The results of this experiment strongly suggests that the flow is in the form of a moving layer with little interaction between the moving layer (water without acid) and the rest of the rotating pool (acidic liquid), as represented by Figure 11.2. Assuming a moving layer model as depicted in Figure 11.2, the equivalent moving layer thickness can be deduced, based on the initial and final conductivity of the effluent, provided there was thorough mixing between the moving layer and the rest of the ‘stagnant’ pool during pool collapse. Figure 11.8 compares test results on the florescent dye technique and the conductivity technique for several feed rates of a given test bowl geometry

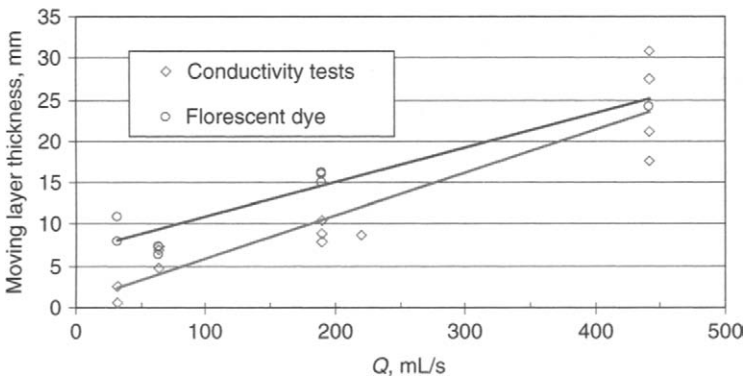


**Figure 11.8** Comparing moving layer by, respectively, conductivity test and florescent dye

under a fixed  $G$ -force. There is reasonable agreement between the two techniques. Based on this, a moving layer model has been adopted similar to the one originally [1], but with further enhancement in that the feed particles are initially distributed across the entire moving layer and not concentrated at the surface (i.e. at one radial position) of the moving layer.

## 11.2 Improved Moving Layer Flow Model

In the improved model [3], instead of lumping all the suspended solids at the pool surface, a more reasonable and likely assumption is that solids are distributed uniformly across the moving layer, despite the thickness of the moving layer being very thin. This moving layer, dictates that separation is at the pool surface  $R_p$ . Particles or solids settle across the moving layer to a relatively quiescence zone and form sediment adjacent to the bowl wall, while feed in the moving layer continues to flow towards the overflow weir.

To simplify the analysis, consider initially the case where the moving flow layer has over its entire length  $L$  (see Figure 11.9  $u = U$  profile and note the exaggerated vertical scale) a uniform thickness  $h$  and a uniform velocity profile,  $u(y) = U$ . Later, it will be shown that the uniform velocity profile, as sketched on the left side of Figure 11.9, gives the same results as the more general velocity profile  $u(y)$ , as sketched on the right side of Figure 11.9. Furthermore, it will be demonstrated that the longitudinal changes in thickness  $h$  and the mean speed  $U$ , caused by viscous friction, have very little effect upon the results.

The spatial variable along the axis of the bowl is designated as ' $s$ '. As mentioned above, the concentration of solids is taken to be uniform at the entrance, where  $s = 0$ . The volume concentration of solids is further assumed to be small, such that each solid particle settles independently of the others. Therefore, one can consider each particle size separately, using Stokes' law of drag for the settling speed in the centrifugal field.

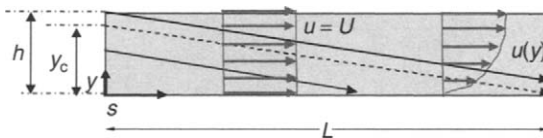


**Figure 11.9** Schematic of moving layer without underlying pool with trajectory of particles (dotted line shows limiting trajectory) in the moving layer

In Figure 11.9, the three slanted lines represent the trajectories of particles of a particular size  $x$ , starting at different levels in the flow layer. Since both the forward speed and the settling speed remain constant, the trajectories are straight lines. The lowermost trajectory is for a particle that is captured, the uppermost for one that escapes to the centrate.

The dashed line is the trajectory of a particle starting at the level  $y_c$  at the inlet to the moving layer that is just barely captured to the cake. Since all particles starting below  $y_c$  are captured, and the velocity and entering concentration are both uniform, the fraction going to the sediment is

$$Z_s = \frac{y_c}{h} \quad (11.1)$$

Again, since both the speed  $u = U$  and the settling speed  $v_s$ , are uniform, simple geometry requires that

$$\frac{y_c}{L} = \frac{v_s}{U} \quad (11.2)$$

Now Stokes' law for a spherical particle is

$$v_s = \frac{1}{18} \frac{G(\Delta\rho/\rho)x^2}{(\mu/\rho)} \quad (11.3)$$

and the total volume rate of flow may be expressed as

$$Q = 2\pi R_p h U \quad (11.4)$$

After combining Equations 11.1, 11.2, 11.3, and 11.4, and noting that the pool area  $A = 2\pi R_p L$ , thus

$$Z_s = \frac{v_s A}{Q} = \frac{\pi}{9} \frac{R_p L G(\Delta\rho/\rho)x^2}{(\mu/\rho)Q} \quad (11.5)$$

Of course, the value of  $Z_s$  cannot be greater than 1.0, so Equation 11.5 must be truncated at the value of  $Q$ , which exceeds this value. Then, denoting  $Q_{100}$  as the maximum flow, at which 100% of the particles of size  $x$  are captured to the cake, Equation 11.5 may be written as

$$Q_{100} = \frac{\pi}{9} \frac{R_p L G(\Delta\rho/\rho)x^2}{(\mu/\rho)} \quad (11.6)$$

Take further note that when

$$Q \leq Q_{100} \quad Z_s = 1 \quad (11.7)$$

Equation 11.6 may alternatively be interpreted as

$$Q = \frac{\pi R_p LG(\Delta\rho/\rho)x_c^2}{9(\mu/\rho)} \tag{11.8}$$

Here,  $x_c$  is the minimum size for which 100% recovery of a given size  $x$  to the cake is possible when the flow rate is  $Q$ .

Now one may express the fractions to the cake and the effluent with the further proviso that  $Z_s$  cannot exceed 1.0 as

$$Z_s = 1 - Z_e = \frac{Q_{100}(x)}{Q} = (x/x_c)^2; \quad x < x_c \tag{11.9a,b}$$

$$Z_s = 1 - Z_e = 1; \quad x \geq x_c$$

$$x_c = \frac{3}{\sqrt{\pi}} \sqrt{\frac{(\mu/\rho)Q}{\Delta\rho/\rho(\Omega R_p)^2 L}} \tag{11.9c}$$

Given a particular flow rate, Figure 11.10 illustrates how the fractions to the cake and the centrate vary with the particle size.

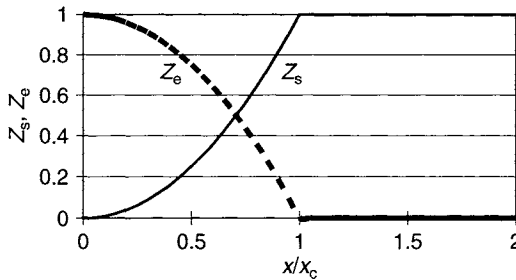


**Figure 11.10** Capture fraction for different size  $x$

### 11.3 Effect of Velocity Profile

The dotted curved trajectory shown in Figure 11.9 (right side of schematic) is for a particle that starts at the location  $s = 0, y = y_c$ , and ends at  $s = L, y = 0$ . It represents the particle size  $x$  that just barely gets captured in the moving layer. Assuming as before that the particles are

uniformly distributed in the incoming stream of the moving layer, the fraction recovered to the sediment is thus given by

$$Z_s = \frac{\int_0^{y_c} u \, dy}{\int_0^h u \, dy} \quad (11.10)$$

The equation for the particle trajectory

$$\frac{dy}{ds} = \frac{-v_s}{u(y)} \quad (11.11)$$

may be integrated between the starting and end points of the trajectory to give

$$\int_0^{y_c} u \, dy = |v_s| L \quad (11.12a)$$

Note  $v_s$  in Equation 11.11 is negative as defined in Figure 11.9. The total volume rate of flow within the layer may be expressed as

$$Q = 2\pi R_p \int_0^h u \, dy \quad (11.12b)$$

Putting together Equations 11.10, 11.11, 11.12a, and 11.12b one gets exactly the result expressed by Equation 11.5. Consequently, the results for the improved model do not depend upon the particular velocity distribution within the flowing surface layer.

## 11.4 Effect of Friction within the Flow Layer

Viscous stresses acting in the liquid layer as it flows over the stationary fluid in the pool cause an increase of speed and a decrease of the flow layer thickness as the liquid proceeds toward the centrate overflow. While this will affect considerably the flow pattern and the particle trajectories, the effects on the results worked out above are believed to be actually quite small for the following two reasons.

Remarkably, the values of  $Z_s$  and  $Z_e$  derived above are determined only by the total flow rate,  $Q$ , and *do not depend upon the particular values of thickness*.

The thinning of the flow layer is accompanied, of course, by a downward velocity of the liquid in the layer. But this also carries the particles down with the liquid, and it is only the Stokes' law of settling speed relative to the liquid that determines the relative position of the particle within the layer at any longitudinal location.

## 11.5 Dimensionless Le Parameter

With introduction of the dimensionless Le number, which is defined as

$$\text{Le} = \frac{\sqrt{(Q/L)}\sqrt{\Delta\rho/\mu}}{\Omega R_p x_o \eta_a} \quad (11.13a)$$

from Equation 11.9c, the cut size can be written as

$$\frac{x_c}{x_o} = \frac{3}{\sqrt{\pi}} \text{Le} \quad (11.13b)$$

The significance of the Le number and the cut size in mineral separation/processing has been discussed [4,5,6,7].

## 11.6 Quantitative Prediction

### 11.6.1 Total Solids Recovery in Cake

The total solids captured in the cake is determined using the cumulative undersize fraction of the feed  $F_f(x)$  from which the frequency of occurrence  $f_f(x)$  of size  $x$  can be determined. The following relationships are derived from the size distribution and Equations 11.9a and 11.9b:

$$\begin{aligned} R_s(\text{Le}) &= \int_0^{\infty} f_f(x) Z_s(x) dx = \frac{1}{x_c^2} \int_0^{x_c} f_f(x) x^2 dx + \int_{x_c}^{\infty} f_f(x) dx \\ &= 1 - F_f(x_c) + I(x_c) \\ F_f(x) &= \int_0^x f_f(x) dx \quad (11.14a-d) \\ I(x) &= \frac{1}{x_c^2} \int_0^x x^2 f_f(x) dx = \frac{1}{x_c^2} \int_0^x x^2 dF_f \\ I(x_n) &\approx \frac{1}{4x_c^2} \sum_{k=1}^n (x_{k-1} + x_k)^2 (F(x_k) - F(x_{k-1})) \end{aligned}$$

### 11.6.2 Total Solids Recovery in the Centrate

The total solids recovery in the centrate is simply the complement of that of the cake, from Equation 11.14a

$$R_e(\text{Le}) = 1 - R_s = F_f(x_c) - I(x_c) \quad (11.15)$$

### 11.6.3 Particle Size Distribution of Supernatant/Overflow

The particle size  $x_k$  in the product centrate (i.e. overflow of centrifuge) becomes

$$\begin{aligned} F_e(x_k; \text{Le}) &= \frac{\int_0^{x_k} f_f(x) \left[ 1 - \left( \frac{x}{x_c} \right)^2 \right] dx}{\int_0^{x_k} f_f(x) \left[ 1 - \left( \frac{x}{x_c} \right)^2 \right] dx} = \frac{F_f(x_k) - I(x_k)}{F_f(x_c) - I(x_c)} \\ &= \frac{F_f(x_k) - I(x_k)}{R_e(x_c)} \end{aligned} \quad (11.16)$$

The centrate cumulative size distribution  $F_e$  is a function of the size  $x_k$  and the cut size  $x_c$ , which is a function of  $\text{Le}$ . Note that the PSD of the feed is required to evaluate the above through  $I(x_k)$  and  $R_e(x_c)$ , where  $R_e(x_c)$  is given by Equation 11.15.

Particle size  $x_k$  can be considered as a tracer wherein the fraction of particles with a size less than  $x_k$  in the effluent is being tracked as a function of the separation condition, more precisely  $\text{Le}$ .

### 11.6.4 Cumulative Size Recovery

In the size range between 0 and  $x_k$ , the size recovery (SR) in the product centrate as a fraction of that in the feed suspension can be determined by

$$\text{SR}(x_k; \text{Le}) = \frac{\int_0^{x_k} f_f(x) \left[ 1 - \left( \frac{x}{x_c} \right)^2 \right] dx}{\int_0^{x_k} f_f(x) dx} = 1 - \frac{I(x_k)}{F_f(x_k)} \quad (11.17)$$

Note that SR is a function of  $x_k$  and Le through  $F_f(x_k)$  and  $I(x_k)$ . In the classification of fine-particle slurry, it is clear that the feed PSD plays a vital role in size distribution, size recovery, and total solids recovery in the product centrate.

## 11.7 Sedimentation Tests

### 11.7.1 Experiments on Sedimentation in Rotating Bowl Centrifuge

For these tests, a 1% by weight suspension of 1–10  $\mu$  silica ( $x_{50} = 3\text{--}4 \mu\text{m}$ ) was fed to the centrifuge under different feed rates and rotational speeds, and the recovery was quantified by solids analysis on the three streams, respectively the solids by weight of the feed  $W_f$ , effluent  $W_e$ , and the sediment  $W_s$ . Based on the material balance on the centrifuge under steady state, the solids recovery  $R_s$  can be deduced from the respective three weight concentrations

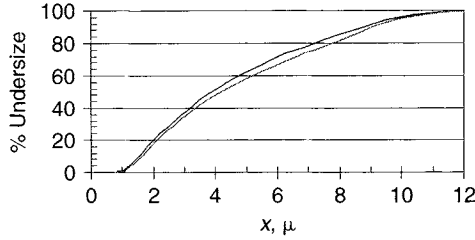
$$R_s = \frac{1 - (W_e/W_f)}{1 - (W_e/W_s)} \quad (11.18)$$

The cut-off was determined by comparing the particle size distribution (PSD) of the feed and effluent for each sample.

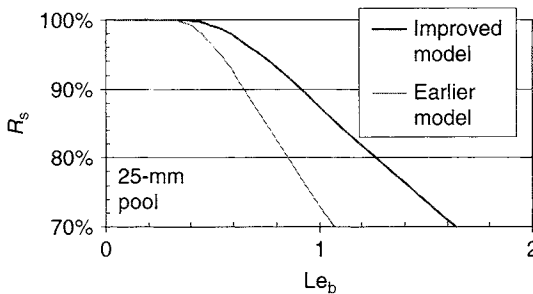
Tests were carried out on the 178-mm diameter tubular bowl using, respectively, 13-mm and 25-mm ring weirs (measured radial inwardly from the bowl wall). The rotational speed was 2947 rev/min, corresponding to 863 g measured at the bowl inner diameter. Five different feed rates, respectively, of 32, 95, 189, 379, 536 mL/s were tested. The viscosity of the slurry is about 1 cP and the density difference  $\Delta\rho/\rho = 1.6$ . The results are recast in  $Le_b$  based on the bowl radius  $R_b$  instead of the pool  $R_p$  as in Equation 11.13a, so that the dimensionless  $Le$  is independent of pool depth. Further, the effect of the pool radius parameter  $R_p/R_b$  can be examined separately. In fact,  $Le_b/Le = (R_p/R_b)$ .

Figure 11.11 shows both the range of feed PSD measured (coarse and fine) using a laser diffraction particle analyzer.

Before comparing it with the test, the earlier model prediction is compared with the improved model prediction in Figure 11.12 using the same feed PSD as given by Figure 11.11 (for finer PSD feed). As seen, the solids recovery is higher for the improved model (bold curve) as compared to the earlier model (thin curve). The earlier model assumes that all feed solids are located at the surface of the pool  $R = R_p$ , whereas the improved model assumes a spread out of solids across the radial



**Figure 11.11** Fine (lower curve) and coarser (upper curve) feed PSD of silica suspension



**Figure 11.12** Comparing earlier model (lower curve) with present improved model (upper curve)

zone  $R = R_p$  to  $R = R_p - h$ , and thus the settling distance for the earlier model is the same, which equals the thickness of the moving layer. On the other hand, in the improved model solids of all sizes are assumed to be uniformly distributed across the moving layer, solids closer to the bottom of the moving layer  $R = R_p - h$  settle immediately, whereas solids at the surface of the layer  $R = R_p$  take a longer time. As such, the total solids recovery should be higher for the improved model, and this difference is obvious for the two curves depicted in Figure 11.12.

The test results corresponding to the 13-mm pool run are compared with the corresponding model prediction in Figure 11.13. Note that the tests were repeated under identical conditions to confirm the reproducibility of the data, which seems to be pretty good. Comparing prediction with test results, the model over-predicts the solids recovery at a low rate and low  $Le_b < 1$  by as much as 5%. However, the agreement is relatively good for  $Le_b > 1$ .

The results for the 25-mm deep pool are depicted in Figure 11.14. Three sets of tests were carried out to confirm reproducibility. The PSD in the feed has been changed in the third test to a coarser particle size distribution, as shown in Figure 11.11. Thus, prediction is made for the

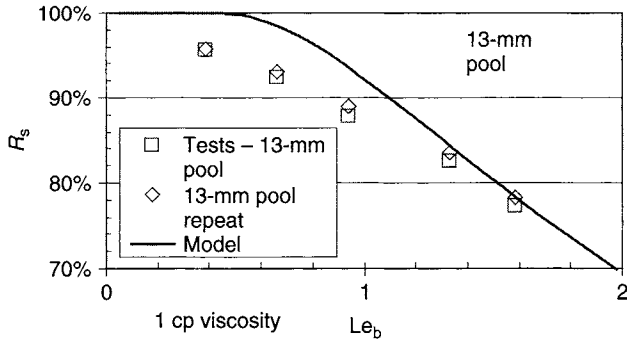


**Figure 11.13** Comparing analytical prediction with experiments for 13-mm pool

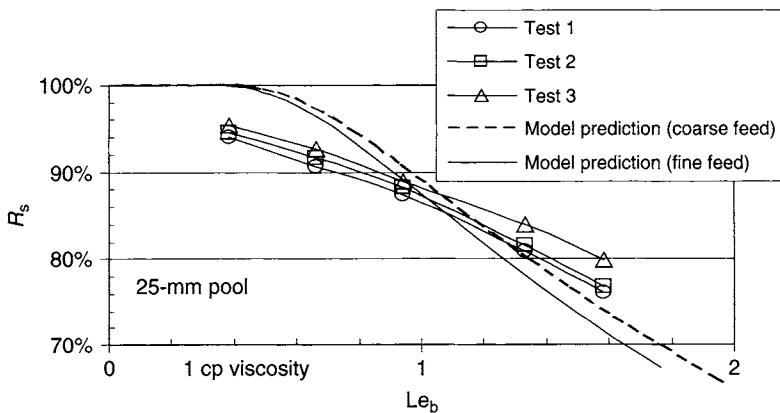


**Figure 11.14** Comparing analytical prediction with experiments for 25-mm pool

nominal finer PSD and the coarser PSD. Both predictions (coarse and fine feeds) are compared with all three tests in Figure 11.14. The coarser PSD leads to higher solids recovery as expected. At lower  $Le_b$ , the prediction is higher than the measurement, yet at much larger  $Le_b$ , the prediction is below the measure.

Possible explanations for the discrepancy between theory and test data, as seen in Figures 11.13 and 11.14, are due to other factors not being considered in the improved model:

- 1 Prediction is based on the PSD as measured subjectively using the PSD analyzer, which uses laser diffraction which is an indirect measurement, and the measurements are recast in equivalence to spherical particles.
- 2 Entrainment and resuspension of the sediment by the complicated Ekman flow on the exit ring weir may present the effect which may be

more pronounced at a high sedimentation rate or low  $Le_b$ . This leads to a solid capture shy away from 100%.

- 3 The very fine submicron silica particles may stay in suspension due to the double-layer electrical forces present and also would not settle under the relatively lower  $G$  (860 g) in the tests.
- 4 Other secondary flows which negatively affect separation are unaccounted for in this model.

In any event, the model predicts within 5% the performance of a rotating tubular bowl centrifuge. Useful insights are obtained from a very extensive flow visualization study of a rotating bowl with continuous feed in which the moving layer is demonstrated and quantified for the first time. To a first approximation, the thin moving layer thickness does not enter into the equation, which is quite remarkable. Finally, the improved model approximates reasonably well the sedimentation tests.

## 11.8 Summary

In this chapter a comprehensive flow visualization program is presented for the first time on a rotating bowl centrifuge. Both dye and tracer were used and revealed a thin moving layer present at the pool surface above a stagnant dead pool. The moving layer is a function of the feed rate and the centrifugal acceleration. Due to the strong rotational effects, the flow exhibits two-dimensional behavior which agrees with the understanding on rotating flow. The sedimentation in a centrifugal field is dictated by a dimensionless governing  $Le$  parameter.

A refined model is presented to quantify separation and classification. The model is an improvement over the model presented earlier, which assumed that all the particles stay at the surface of the moving layer. The improved model actually provides higher solids recovery compared to the earlier model for the same condition.

Experiments on sedimentation of fine silica slurry with  $x_{50} = 3$  to 4 microns using a test centrifuge are presented. Predictions from the improved model agree reasonably well with test results.

## References

- [1] W.W.F. Leung, *Industrial Centrifugation Technology*, McGraw-Hill, New York, 1998.
- [2] H. Greenspan, *The Theory of Rotating Fluids*, Cambridge University Press, London, 1968.

- [3] W.W.F. Leung, Experimental and theoretical study of flow and sedimentation of tubular centrifuge for bioseparation, AICHE 2005 Annual Conference, Cincinnati, USA.
- [4] W.W.F. Leung, Centrifugal sedimentation and filtration for mineral processing, *Plant Design Handbook for Mineral Processing*, pp. 1262–1288, Society of Mineral Engineering, 2002.
- [5] W.W.F. Leung, Scale-up of sedimenting centrifuges, in R. Wakeman (ed.), *Filtration Processes – Equipment Scale-Up*, pp. 375–441, Elsevier, Oxford, 2005.
- [6] W.W.F. Leung, Centrifugal classification of fine-particle suspension, Plenary Lecture at Filtration Society Japan Association-INCHEM 2003 Conference, Tokyo, 2003.
- [7] W.W.F. Leung, Centrifugal classification of drill mud, presented at 9th World Filtration Congress, 18–24 April, 2004, New Orleans, USA.

## Problems

- (11.1) It has been revealed and backed up by experimental findings that feed is distributed in a tubular centrifuge in a thin moving layer flowing from the feed end to the concentrate discharge end at the opposite side. This contrasts with the conventional wisdom of a plug flow where feed is uniformly distributed in the angular space from the bowl wall to the pool surface and sweeps through the bowl while heavier solids settle out. (a) What phenomenon is this moving layer due to? What is the implication from a process standpoint of the moving layer instead of the plug flow – is the machine doing better or worse having the moving layer?
- (11.2) Which is the most sensitive parameter among the several parameters listed in Equation 11.13a for the  $Le$  number? Sensitive refers to a small increase in the parameter which results in a large increase in  $Le$ , whereas insensitive refers to a large increase in the parameter which results in a small increase in  $Le$ . Which are the parameters that are difficult to determine in the  $Le$  number? What is the basis of introducing a dimensionless number?
- (11.3) What are other effects, if any, that have not been taken into account in the tubular model?

## Disk Stack Modeling

In this chapter, the separation performance of a disk-stack centrifuge will be modeled. A schematic of the dropping-bottom intermittent discharge disk centrifuge is shown in Figure 12.1. The model discussed in this chapter is also applicable to the nozzle disk and the manual discharge disk. The model will be validated with results from a pilot test on a disk-stack centrifuge. As will be shown in Chapter 13, the disk model can be used to simulate performance of disk-stack centrifuge of different sizes operating at various feed rates and rotational speeds applicable to various bioprocess and biotech applications.

A suspension of particles is continuously fed to the disk centrifuge. Under centrifugal acceleration  $G$ , heavier solids settle to the lower surface of the annular disk channel formed between two disk surfaces, displacing lighter liquid phase towards the small radius. The collected sediment slides down the upper surface of the disk under the longitudinal component of

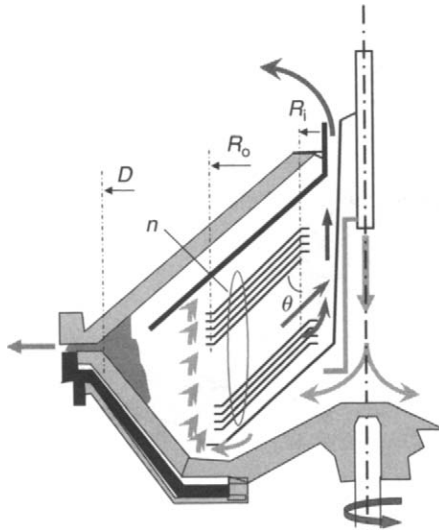


**Figure 12.1** Schematic of a disk-stack centrifuge

the  $G$ -force until it leaves the disk stack and is collected at the solid holding annular space of the bowl.

## 12.1 Disk Model

In the simple model [1] presented herein, the following assumptions are made:

- 1 The solid concentration is relatively dilute, such that the presence of solids does not affect the flow field.
- 2 The aspect ratio of the channel (longitudinal length to the channel height or spacer height between adjacent disks) is very large and the details of the entrance and exit geometry respectively at both ends can be ignored. For modeling purposes, the triangular region at the inlet of the disk channel can be eliminated; likewise the triangular region at the exit of the disk channel can be added (see Figure 12.2), so that the channel has an inlet area and exit area exactly perpendicular to the longitudinal direction of the channel. By virtue of the large aspect ratio and the strong rotational field at high rotation speed, the flow develops quickly (i.e. for an entrance distance equivalent to several channel spacing) to a steady velocity profile.
- 3 The flow is uniformly distributed across all the ' $n$ ' channels. This assumption is very weak, as will be seen later. As such, only a single channel is considered.
- 4 The flow field in each channel (e.g. see Figure 12.3) is independent of particle sedimentation; however, the reverse holds in that the sedimentation of a particle depends on the velocity profile in the channel. This statement holds for dilute suspension and where particles are relatively small compared to the channel spacing.
- 5 The velocity profile in the suspension is assumed to be relatively constant across the entire channel within a given channel, despite the

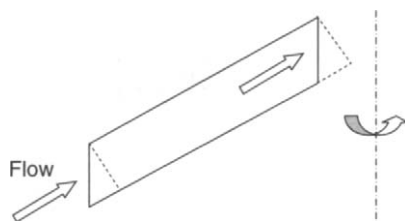


**Figure 12.2** Entrance and exit channel region (annulus) being ignored

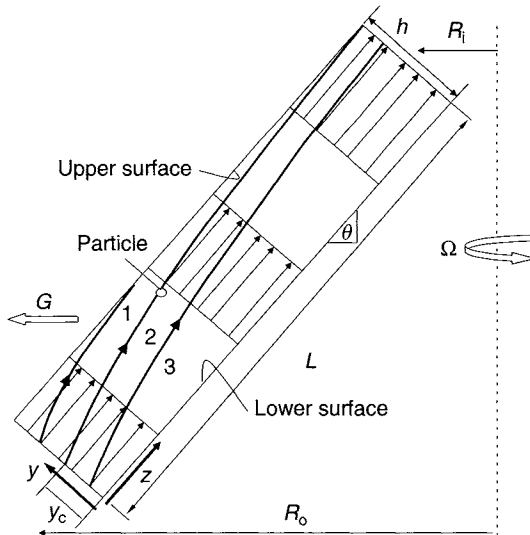


**Figure 12.3** Velocity profiles and trajectory of particles in the disk channel

possibility of an Ekman layer flow adjacent to the upper or lower surfaces of the disk surfaces and also a thin clear liquid flowing on the upper surface of the disk channel analogous to the lamella settler [2].

Referring to Figure 12.4, a particle in the channel is subject to convection from the main flow along  $z$ -direction, as well as relative motion due to sedimentation under  $G$ . Uniform distribution in Figure 12.3 implies that the flow rate to each channel is identical and only a single channel needs to be modeled. We will separately consider the continuum phase (which is the suspending liquid) and the particles (the dispersed phase).

### 12.1.1 Continuous Phase

The continuity and momentum balances (without considering the settling particles) imply the following.

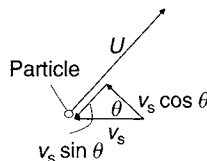


**Figure 12.4** Particle velocity in the channel

## 1 Continuity

The flow rate per unit channel is equal to the overall feed rate  $Q$  divided evenly among  $n$  channels in  $n + 1$  disks, thus

$$Q = 2\pi nRUh \quad (12.1)$$

where  $R$  is the radius,  $U(z)$  is the local longitudinal velocity in the  $z$ -direction,  $y$  is the transverse coordinate measured from the upper surface of the disk channel, and  $h$  is the channel height, i.e. distance between adjacent disks (see Figure 12.3). This equation holds from the feed entrance  $R = R_o$  along increasing  $z$  to the disk channel exit at the small radius  $R_i$ .

2  $z$ -momentum:

Despite the above, we have assumed  $U$  being constant, independent of the transverse coordinate  $y$ . To satisfy continuity or mass conservation, Equation 12.1, the longitudinal velocity has to increase with reducing radius.

$$U(z) = \left( \frac{Q/n}{2\pi h} \right) \frac{1}{R} \quad (12.2)$$

### 12.1.2 Dispersed Phase

The dispersed phase is sufficiently dilute such that the presence of particles does not affect the flow field, rather the rate of deposition and removal of them depend on the main flow. The relative velocity of settling particles in relation to the liquid (in relation to the surrounding liquid under steady-state) with negligible acceleration and deceleration is given by Stokes' law, as discussed in Chapter 2. Given  $x$  being the particle size (equivalent spherical diameter), Stokes' law in a centrifugal field states

$$v_s = \frac{(\rho_s - \rho_L)Gx^2}{18\mu} \quad (12.3)$$

The above holds under  $0 \leq x < \infty$ ,  $0 \leq y \leq h$ ,  $0 \leq z \leq L$ . The frequency  $f(x)$  of a particle residing in a given size range is the derivative of the cumulative undersize  $F(x)$

$$f(x) = \frac{dF(x)}{dx} \quad (12.4a)$$

$$F(x) = \int_0^x f(x) dx \quad (12.4b)$$

The frequency size distribution  $f(x)$  or cumulative size distribution  $F(x)$  are assumed to be known from measurement.

The trajectory can be determined for a given particle located at transverse location  $y$  at the inlet (i.e.  $z = 0$ ) in a flow field, as illustrated in Figure 12.3. The approach is to determine if the particle intercepts the collecting surface of the channel (i.e. upper surface of the disk channel) prior to traveling through the channel length,  $z = L$ . Consider a particle, with size  $x$  starting at  $z = 0$  and taking on trajectory 1, which gets settled as it travels through the disk channel. If the particle had been positioned differently at the inlet and had taken trajectory 3, it would have escaped from being settled. With reference to Figure 12.3, trajectory 2, with particle at channel inlet  $z = 0$  and  $y = y_c$ , is the critical trajectory wherein particle with size  $x$  barely gets captured as it traverses through the disk channel (see Figure 12.4). Therefore, the fraction captured in the sediment  $Z_s$  for particle size  $x$  is

$$Z_s(x) = \frac{h - y_c}{h} \quad (12.5)$$

where  $h$  is the channel height as set by the spacer between adjacent disks. Assuming particles of all sizes are initially distributed uniformly across the inlet of the channel from the limiting trajectory, the solids recovery or size capture can be determined. Another important point is to determine the cut size, i.e. the particle positioned at the inlet lower corner of the channel  $z = 0$  and  $y = 0$  (see Figure 12.3) that undertakes the critical trajectory as shown by path 2. With the above information, the fraction captured for particles of all sizes can be schematically represented by Figure 12.5.

As stated, the particle settling velocity is Stokes' velocity relative to the moving liquid under the influence of the  $G$ -acceleration (see Figure 12.4). There are two velocity components that should be considered: one component is perpendicular to the underside of the disk surface in which a particle is settling towards a velocity  $v_s \cos \theta$ ; another is the longitudinal component,  $v_s \sin \theta$ , which is in the negative direction of the streamwise direction. This second component should be superimposed with the streamwise flow with velocity  $U(R)$ , i.e.  $U - v_s \sin \theta$ . Let us

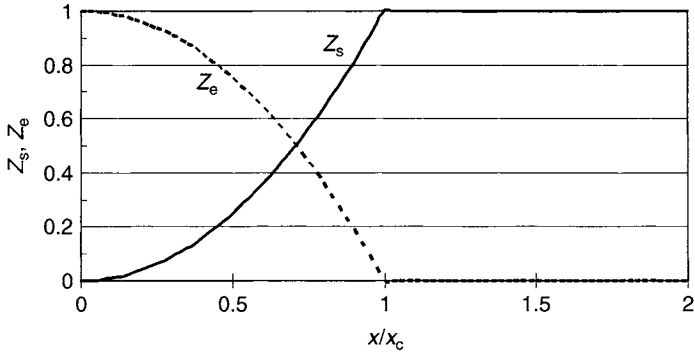


**Figure 12.5** Capture fraction for different particle size  $x$

consider a small incremental path ( $dz, dy$ ) along the particle trajectory. Thus it follows that

$$dt = \frac{dy}{v_s \cos \theta} = \frac{dz}{U - v_s \sin \theta}$$

or

$$\frac{dz}{dy} = \frac{U - v_s \sin \theta}{v_s \cos \theta} \quad (12.6)$$

From Equation 12.3, by virtue of the geometry

$$R = R_0 - z \sin \theta \quad (12.7)$$

It follows that  $dR = -\sin \theta dz$  and substituting this in Equation 12.3

$$-\frac{1}{\sin \theta} \frac{dR}{dy} = \frac{b/R - aR^2 \sin \theta}{aR^2 \sin \theta} \quad (12.8)$$

where

$$a = \frac{1}{18} \frac{\Delta\rho}{\mu} (\Omega x)^2 \quad (12.9a)$$

$$b = \frac{Q/n}{2\pi h} \quad (12.9b)$$

Note that the coefficient  $a$  is derived from Stokes' law, whereas coefficient  $b$  is from continuity Equation 12.2. Integrating Equation 12.5

along the critical trajectory where particle initially at  $y = y_c$  just barely gets captured. The two limits have to be respectively  $R = R_o$  to  $R - R_i$ , and  $y = y_c$  and  $y = h$ . Also, for all practical purposes the component of the Stokes' velocity is assumed to be much smaller than the streamwise velocity component, thus  $aR^2 \sin \theta \ll b/R$ .

$$-\int_{R_o}^R \frac{aR^2 \sin \theta}{b/R - aR^2 \sin \theta} = \int_{y_c}^h dy \quad (12.9c)$$

Rearranging and with substitution of  $a$  and  $b$  respectively from Equations 12.9a and 12.9b, we get

$$h - y_c = \frac{a \cot \theta}{b} \frac{1}{3} (R_o^3 - R_i^3) = \frac{\pi \Delta \rho \Omega^2 h \cot \theta}{27 \mu} \frac{\Omega^2 h \cot \theta}{\mu Q/n} (R_o^3 - R_i^3) x^2 \quad (12.10)$$

Assuming uniform particle concentration across the entire channel, the fractional capture of particle with size  $x$  from Equation 12.5 is then

$$Z_s = \frac{h - y_c}{h} = \left[ \frac{\pi \Delta \rho \Omega^2 \cot \theta}{27 \mu} \frac{\Omega^2 \cot \theta}{Q/n} (R_o^3 - R_i^3) \right] x^2 = \left( \frac{x}{x_c} \right)^2 \quad (12.11)$$

From Equation 12.11, the dimensionless Le number that governs the settling behavior of the disk stack can be defined as

$$\text{Le} = \frac{\sqrt{\left( \frac{3Q}{n} \right) \left( \frac{\mu}{[\rho_s - \rho_L]} \right) \frac{\tan \theta}{(R_o^3 - R_i^3)}}}{\Omega x_o \eta} \quad (12.12)$$

where  $n$  is the number of disks,  $R_o$  is the radius of the outer disk and  $R_i$  is that of the inner disk,  $\theta$  is the angle subtended between the disk surface and the vertical axis,  $\mu$  is the suspension viscosity,  $\rho_s$  is the solid density,  $\rho_L$  is the liquid density,  $\Omega$  is the angular velocity,  $\eta$  is the acceleration efficiency. The cut size is thus given by

$$\frac{x_c}{x_o} = \frac{3}{\sqrt{\pi}} \text{Le} \quad (12.13)$$

As  $n$  is very large in excess of 100,  $n$  channels in  $n + 1$  disks are nearly the same value, as such it will be taken simply as  $n$ . The rest of the governing

equations are identical to the ones (i.e. solid recovery etc.) that have already been presented in Chapter 11, given that the  $Z_s$  function is identical with the tubular model.

## 12.2 Model Validation

It would be useful to validate the model with some experimental results [3]. A suspension of cell culture contains viable mammalian cells 10–20 microns, non-viable cells 5–10 microns, and cell debris which is less than 5 microns. The size distribution in terms of number of particles is shown in Figure 12.6. The suspension was separated in a pilot disk-stack centrifuge with a bowl diameter of about 190 mm. The cell debris and non-viable cells are removed in the centrate and the viable cells are captured in the concentrate. Figure 12.7 shows the centrate solids by volume after spindown at 14,000 g for 10 minutes of a spintube containing a centrate sample. The solid curve is the model prediction and the data points are results from the experiment [3]. The two agree extremely well with each other. It is clear that the centrate solids increase with increasing feed rate. When the feed rate reaches 10 L/min the centrate solids shoot up dramatically. For this example, the cut size  $x_c$  is determined to be at 11.4 microns, and this is within the range of the mammalian cells (see Figure 12.6). When the centrifuge is operating at this high rate, some of the particles that were intended to be captured also escape in the centrate. In this case, the feed rate should be maintained below 6–7 L/min.

Another measure is to examine the solids recovery as a function of increasing feed rate, which is given by Figure 12.8. As can be seen, the

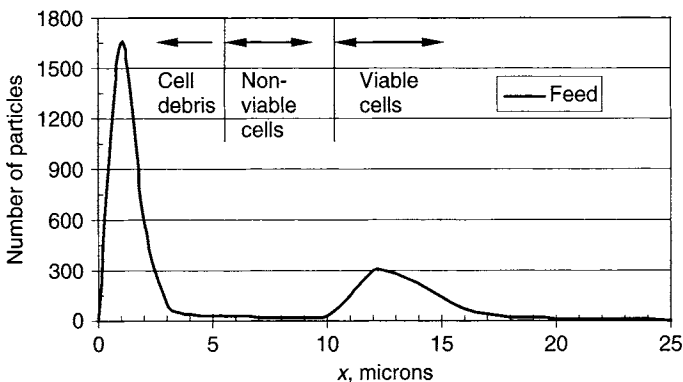


**Figure 12.6** Particle size distribution of feed suspension [3] (Reproduced with permission from the American Filtration and Separations Society)

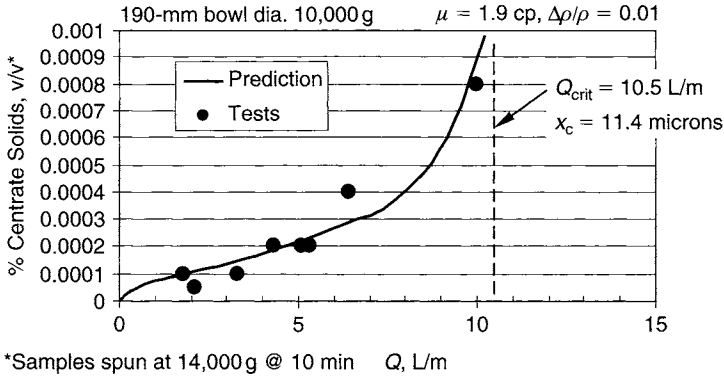


**Figure 12.7** Centrate solids from a 190-mm disk centrifuge (Test results [3] reproduced with permission from the American Filtration and Separations Society). Solid curve is prediction from the present model

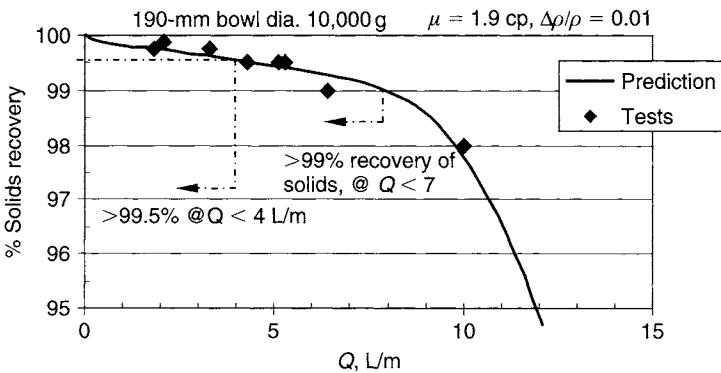


**Figure 12.8** Solids recovery versus feed rate. Solid curve is predicted from the present model and test data are derived from Figure 12.7

solids recovery drops gradually initially at a low rate and when the feed rate reaches 10 L/min, the solids recovery drops precipitously, even with a small increase in feed rate. Note that the model prediction compares very well with the test data.

### 12.3 Complications

One key complication is that the feed may not distribute uniformly to all the channels. Figure 9.9 shows a computational fluid dynamics simulation of flow into a stack of plates under the Earth’s gravity, wherein a complicated flow pattern occurs near the entrance of the channels. This

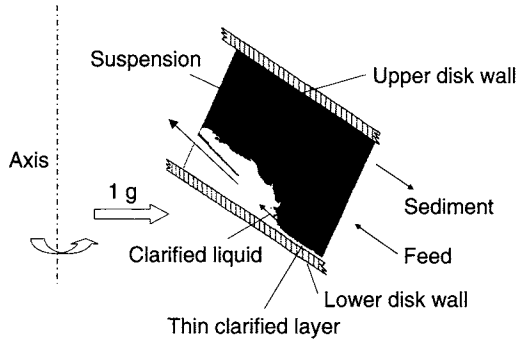


**Figure 12.9** Flow of thin clarified layer and thick suspension layer in a simulated disk channel under the Earth's gravitational acceleration

is perceived to happen also with disk-stack centrifuge. The non-uniformity will be accounted for by the efficiency  $\eta$  in the Le number. Low efficiency implies a larger Le number which is undesirable.

Another complication is that the separated clarified liquid stays on the upper side of the disk and flows rapidly up the channel by buoyancy force. Because it is lighter in density compared with the surrounding suspension, the velocity of the clarified layer is very high and can entrain particles from the suspension adjacent to it. In fact there could be instability between the two liquid layers [4]. This is simulated under 1g using an inclined plate settler, as shown in Figure 12.9. Presumably, similar phenomena also occur for high-speed centrifugation.

One last complication is that the flow might not have been fully accelerated when it reaches the entrance of the disk stack in which the feed experiences lower centrifugal acceleration  $G = v^2/R$ , which may be less than that of the solid-body acceleration  $G = \Omega^2 R$ . The efficiency factor accounts to some extent for this effect and indeed produces a Le number which is much larger than it should have been if the feed were 100% accelerated.

## 12.4 Summary

A simple trajectory model on particle deposition in a disk-stack centrifuge has been presented. The flow in each channel formed between adjacent disks is assumed as a plug flow. The model has been validated against an experiment on cell separation using a disk-stack centrifuge. The model presented herein will be used to simulate conditions that may not have experimental results or extend to conditions where experimental results are limited or lacking. The simulation is discussed in the next chapter.

## References

- [1] W.W.F. Leung, Simulating centrifugal recovery of protein in biopharmaceutical production using AT-SPIN simulator, presented at the American Filtration and Separations Society Annual Conference, 2005, Atlanta, USA.
- [2] W.W.F. Leung and R. Probst, Lamella and tube settlers – Part 1 Model and operation, *I&EC Process Des. and Dev.*, 1983.
- [3] M. Rohr and H. Tebbe, Clarification of mammalian cells by stacked disk centrifugation, presented at the American Filtration and Separations Society Annual Conference, 2002, Galveston, USA.
- [4] W.W.F. Leung, Lamella and tube settlers: Part 2 Flow stability, *I&EC Process Des. and Dev.*, 1983.

## Problems

- (12.1) Why are the streamlines shown in Figure 12.3 curved? Can the particles influence the fluid streamlines?
- (12.2) Why can one ignore  $v_s \sin \theta$  in comparison with the throughflow velocity  $U$ ? (Hint: Make an estimate on their orders of magnitude.)
- (12.3) Show that Equation 12.12 is identical to Equations 9.4a, 9.5, and 9.6. What is the rationale for Equations 9.4a, 9.5, and 9.6. (Hint: Compare Equation 9.4a with Equation 9.9.)
- (12.4) For larger particles ( $>100$  microns) in which inertial effect of the particle becomes important, would the trajectory model still work? Why not?



# Performance Projection of Centrifuges in Bioseparation

Mathematical models have been developed respectively for various types of centrifuges: disk, tubular, chamber bowl, decanter, and spintube centrifuges. Performance simulations have been made [1–4] for disk, tubular, decanter, and spintube centrifuges and some of these will be presented in this chapter. The results of the simulation will also be discussed.

## 13.1 Disk Centrifuge

In Chapter 12, a model for disk-stack centrifuge has been established. The model has been validated by test results on separation of a broth from a bioreactor. Below various examples on biotechnology processing will be used to demonstrate the use of numerical simulation on practical problems. Specifically, the performance of disk centrifuge can be projected for various operating conditions from uncontrollable feed upsets to optimization of the process.

First, some discussion of the numerical simulator is in order. A schematic of the disk centrifuge simulator is illustrated in Figure 13.1. The following lists the key features of the simulator.

- 1 *Geometry*: The basic dimensions are bowl diameter  $D$ , disk stack inner radius  $R_1$ , disk stack outer radius  $R_2$ , number of disks  $n$ , and angle  $\theta$  of disk surface with respect to the axis.
- 2 *Feed properties*: These include volume percent after spindown, weight percent/weight fraction of suspended solids  $W_f$ , solid density  $\rho_s$ , liquid density  $\rho_L$ , suspension viscosity  $\mu$ , and cumulative particle size distribution  $F_f(x)$ .
- 3 *Operating variables*: The operating variables are feed rate  $Q_f$ , rotation speed  $\Omega$ , and feed acceleration efficiency  $\eta$ .

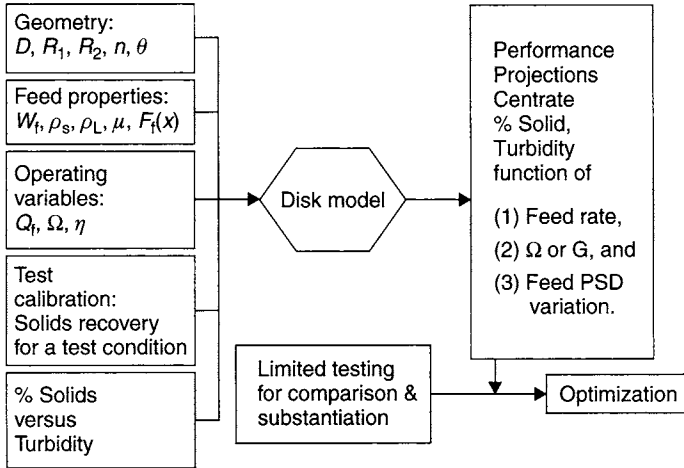


**Figure 13.1** Disk-centrifuge model

4 *Calibration*: Some preliminary test data are required to calibrate the model, especially the acceleration efficiency. An initial efficiency value is assumed for use in the simulation to generate process results that can be compared with test data. The efficiency value is then adjusted through iterations until the simulation prediction matches that of the test data. Also, the turbidity should be calibrated with suspended solids of known concentration for several solid concentrations to ensure the validity of calibration.

With reference to Figure 13.1, for given feed properties (i.e. given particle size distribution and feed solids concentration), feed rate, and  $G$ -force, the numerical model can predict turbidity and centrate/effluent suspended solids. Alternatively, it can predict either the feed rate or rotation speed/ $G$  to meet the limits set on centrate turbidity or suspended solids concentration, which may be more useful. Based on predictions from the model on a given centrifuge processing various feed size distribution, feed solids concentrations, rotation speeds, and feed rates, the optimal condition can be selected.

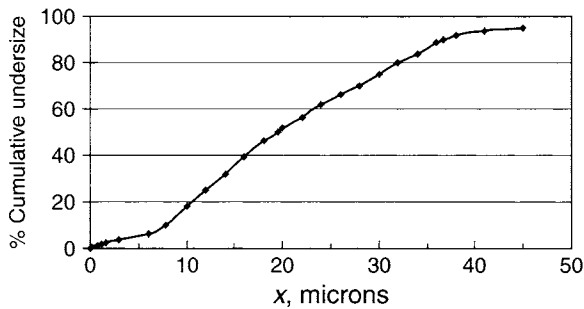
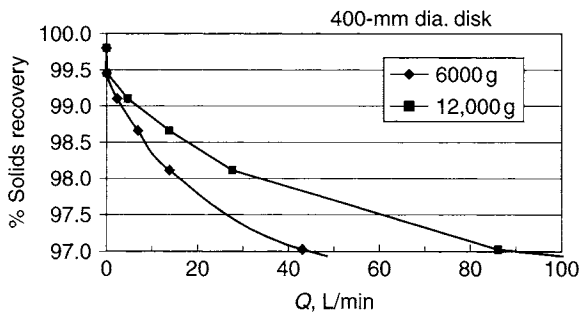
Table 13.1 lists the basic parameters for a 400-mm diameter disk centrifuge for use in the simulations in Sections 13.1.1 and 13.1.2.

### 13.1.1 Baseline Case (400-mm Disk)

A feed suspension from the mammalian cell culture with the cell size expressed in terms of the cumulative undersize distribution is given by Figure 13.2. As shown in the figure, the median size is 20 microns and 90% of cell size is less than 40 microns.

**Table 13.1** Performance prediction – disk

Centrifuge bowl diameter	400 mm
Disk outer diameter	304 mm
Disk inner diameter	178 mm
Number of disks	100
Efficiency	85%
$\Omega_1, G_1$	5139 rpm, 6000 g
$\Omega_2, G_2$	7268 rpm, 12,000 g
Density difference., $\Delta\rho/\rho$	0.1
Viscosity $\mu$	5 cP

**Figure 13.2** Cumulative distribution of particles sizes for the examples in Sections 13.1.1–13.1.4**Figure 13.3** Solids recovery of disk centrifuge

Shown in Figure 13.3 is the simulated solids recovery for the disk stack with geometry and physical parameters listed in Table 13.1. When the centrifuge is operating at 12,000 g and with feed rate at 40 L/min, the numerical simulator predicts solids recovery at 97.8%. The predicted solids recovery drops to 97% when the feed rate leaps more than

double to 86 L/min. On the other hand, when the centrifuge is operated at lower  $G$ -force – 6000 g maintaining the recovery at about 97.1% – the feed rate is limited to 40 L/min. It can be inferred that for a constant performance of the centrifuge (in this case constant solids recovery) doubling the  $G$ -force also doubles the feed rate, provided torque and power are not limiting as both increase with increasing speed and feed rate.

### 13.1.2 Effect of Fine Size Distribution (400-mm Disk)

Suppose the bioreactor is at upset condition generating off-spec particle size distribution (dash curve) with smaller  $d_{50\%}$  at 13 microns instead of 19.5 microns, as illustrated in Figure 13.4, the numerical simulator can be used to predict centrifuge performance under the upset condition. The solids recoveries as predicted by the numerical simulator for

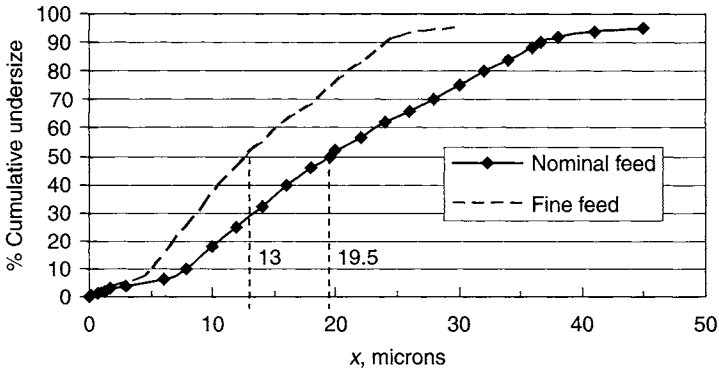


**Figure 13.4** Feed particle size distribution

the 400-mm centrifuge on processing finer feed, respectively, at 6000 g and 12,000 g are shown as the two dotted curves in Figure 13.5.

By comparing with the nominal feed results, it is obvious that the fine feed produces a lower solids recovery at 12,000 g by as much as 1% at high feed rate, whereas at 6000 g the difference exceeds 1% at the high rate. For example, at 40 L/min, the simulator predicts solids recovery of 97% (fine feed) instead of 97.8% (normal feed) at 12,000 g. For the same feed rate with the fine feed, the simulator predicts solids recovery of 96.3% (fine feed) instead of 97.1% (normal feed) at lower centrifugal gravity of 6000 g. At increasing feed rate, such as at 100 L/min, the difference between the nominal and fine feed widens to 1.4% for the 6000 g and more at a higher feed rate (see in Figure 13.5 where the two curves between nominal and fine feed at 6000 g diverge). It is presumed that the finer feed condition may not persist for long and the feed

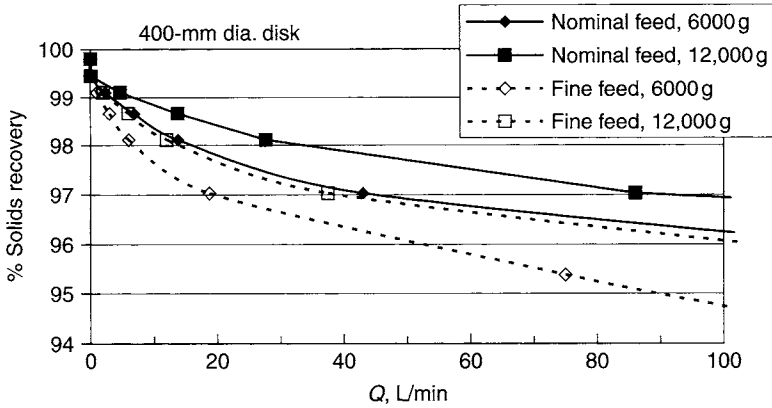


**Figure 13.5** Effect of fine feed on recovery

condition may be restored back to the nominal condition, otherwise the centrifuge performance would be poor in response to the fine feed.

For the two examples used herein, the feed solid concentration is at 3% and the concentrate at 50%, both from a spindown test at 10,000 g. A given value of the solids recovery also infers a certain value of the concentrate suspended solids concentration. High solids recovery or higher solids capture is equivalent to low concentrate suspended solids. As will be explained later, a look-up chart can be provided showing the relationship between concentrate solids and solids recovery when specific feed and concentrate solid concentrations are given. In Figure 13.8, a chart of the aforementioned is prepared with solids concentration for feed and concentrate identical to the ones used in our present example.

### 13.1.3 Effect of G-Force (580-mm Disk)

The two key adjustable parameters in centrifugation are feed rate and centrifugal gravity. We have examined the effect of feed rates, now the effect of  $G$  is to be studied next. The effect of different  $G$ -forces, respectively, at 4000 g, 6000 g, 12,000 g, and 15,000 g can be simulated for a large centrifuge with a 580-mm bowl diameter. The simulated solids recovery is shown in Figure 13.6. It can be seen that both 4000 g and 6000 g results are very much below 12,000 g. When the  $G$ -force increases to 15,000 g, the performance increases only slightly above that of 12,000 g. For example, with a fixed feed rate at 80 L/min, at 4000 g the solids recovery is 97.0%; at 6000 g it is 97.4%, at 12,000 g the solids recovery jumps to 98.1%, while at 15,000 g it increases only slightly to 98.25%.

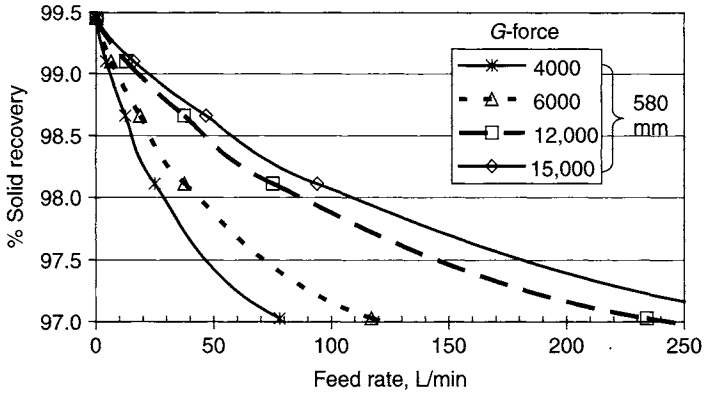


**Figure 13.6** 580-mm disk performance effect of  $G$ -force

The performance of the two centrifuges with bowl diameters 400-mm and 580-mm at various  $G$ -forces is compared in Figure 13.7a. At a fixed recovery of 97.5%, the feed rate that can be attained is respectively 25 L/min (6000 g) and 51 L/min (12,000 g) for the 400-mm bowl; and respectively 72 L/min (6000 g), and 143 L/min (12,000 g) for the 580-mm bowl. At this condition, the scale-up factor on feed rate between the large and small centrifuges is about 2.8 times at the same  $G$ . Also, the feed rate doubles when the  $G$  doubles for a given centrifuge. At 4000 g and for the same solids recovery of 97.5%, the rate for the larger machine is 47 L/min, which is nearly that of the smaller machine but at a higher centrifugal acceleration 12,000 g. On the other hand, at 15,000 g and for the same solids recovery of 97.5%, the 580-mm bowl can accommodate a feed rate of 182 L/min.

Instead of expressing results in terms of solids recovery, centrate suspended solid is often used as the metric. For the foregoing example, the simulation results can also be expressed in centrate solids, as in Figure 13.7b. (Note that all the solids concentrations referred hereafter are on a bulk volume basis from spindown of samples in a tube for 5–10 minutes.) At a fixed centrate solid of, say, 0.08%, the feed rate that can be attained for the two  $G$ -forces and the two different sizes are identical, as already stated with solids recovery at 97.5%. This is because for this example, 0.08% centrate solid is equivalent to 97.5% solids recovery when feed solids concentration is at 3% and concentrate solids concentration is at 50%.

On the other hand, when the centrate solid is relaxed to 0.1% v/v, the feed rate would be even higher. It can be seen that, depending on the metric either on solids recovery or centrate solid, the operating feed rate

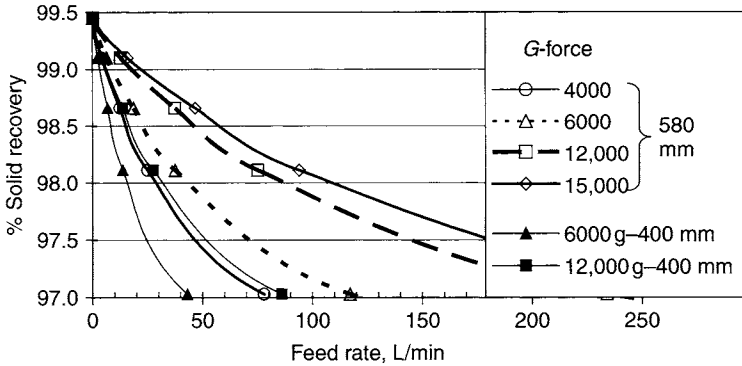


**Figure 13.7a** Comparing 400-mm and 580-mm solids recovery

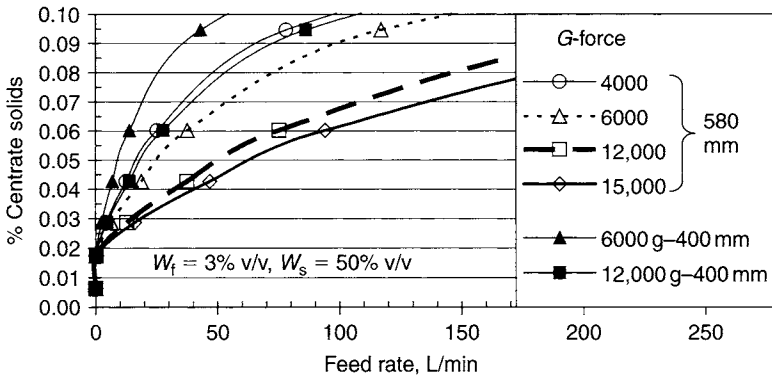


**Figure 13.7b** Comparing 400-mm and 580-mm with feed solids, 3% v/v (spindown)

can be different unless the two metrics correspond with each other. There is a one-to-one correspondence between the two metrics. Indeed, from material balance consideration, the centrate solids  $W_e$  can be expressed in terms of solids recovery  $R_s$ , the feed solid  $W_f$ , and concentrate solids  $W_s$ , as in Equation 13.1.

$$W_e = W_f \frac{1 - R_s}{1 - R_s \frac{W_f}{W_s}} \tag{13.1}$$

Figure 13.8 shows the relationship of  $W_e$  versus  $R_s$  with feed solids at 3% and concentrate solids at 50%.

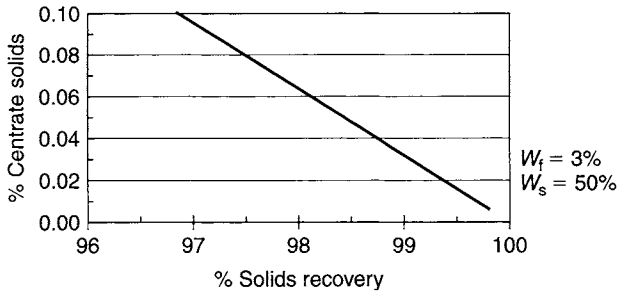


**Figure 13.8** Centrate solids versus solids recovery for feed solids at 3% and cake solids at 50%

### 13.1.4 Effect of Efficiency $\eta$ (580-mm Disk)

The efficiency  $\eta$  includes more than just acceleration efficiency. It also accounts for:

- non-uniform distribution of feed into each disk channel
- feed not fully accelerated when it is introduced to the disk-stack periphery
- entrainment of sediment to centrate by high-velocity liquid stream in disk stack.

Different efficiencies, respectively 60%, 70%, 80%, and 90%, are assumed in the numerical model for a 580-mm bowl diameter centrifuge operating at 12,000 g and using the same feed size distribution as depicted in Figure 13.2. Again, the viscosity is taken to be 5 cP while the ratio of density difference to that of liquid density is 0.1. The simulation results on centrate solids are shown in Figure 13.9. If there is a calibration between centrate solids and turbidity, the simulation result can be converted to turbidity, in NTU, quite easily.

The message conveyed in Figure 13.9 is clear. Suppose at a spec centrate of 0.06%, various efficiencies 60–90% allow a feed rate of 55–125 L/min. On the other hand, suppose 0.08% centrate solid is acceptable, this allows a higher feed rate of 110–240 L/min, depending on the specific efficiencies. Higher centrifuge and separation efficiency  $\eta$  allows much higher feed rate to the same centrifuge operating at the same condition. This is certainly a value-added benefit in designing centrifuge that maintains high efficiency and low shear. Shear should be kept minimal, especially for separating mammalian cell suspension.

Another complementary measure is given by the solids recovery. The calculation of solids recovery depends on the value of the solids concentration of the concentrate and the feed. Figure 13.10 shows the

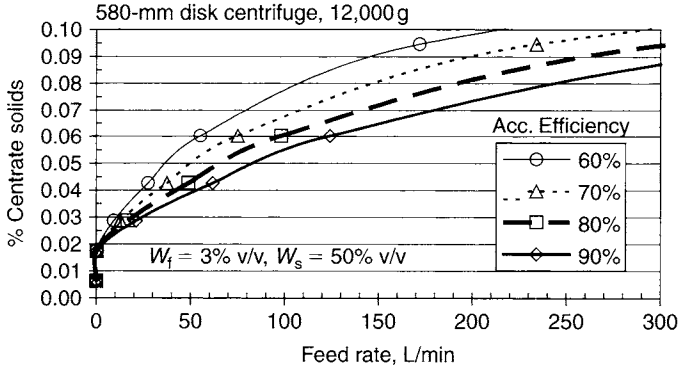


**Figure 13.9** Solids in centrate as a function of feed rate for four efficiencies for a 580-mm diameter centrifuge

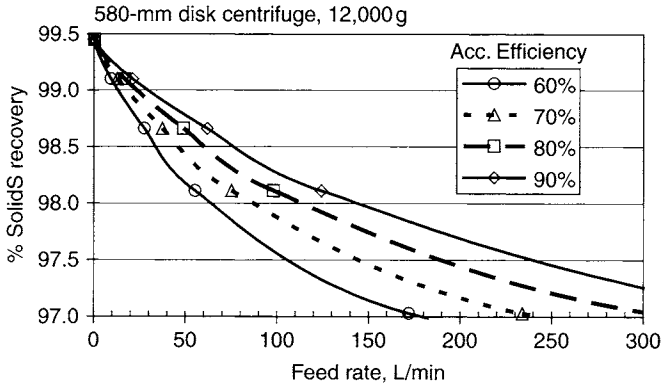


**Figure 13.10** Solids recovery as a function of disk-centrifuge efficiency

solids recovery for the 580-mm bowl as a function of feed rate. Higher feed rate results in lower solids recovery. Higher efficiency also results in higher solids recovery. For the simulation results shown respectively in Figures 13.9 and 13.10, the feed solids concentration is taken at 3% v/v, and the concentrate at 50% v/v.

The efficiency  $\eta$  in Le number is used to calibrate a model prediction as discussed. A range of different efficiencies can be assumed as input to the disk simulator, just like the sensitivity study in the past example. The prediction result can be compared with the test results to back-out the efficiency of the actual disk centrifuge (see illustration in Figure 13.11) used in the test, and this efficiency value is used for future prediction with the simulator. Figure 13.12 illustrates this point for the numerical simulator.

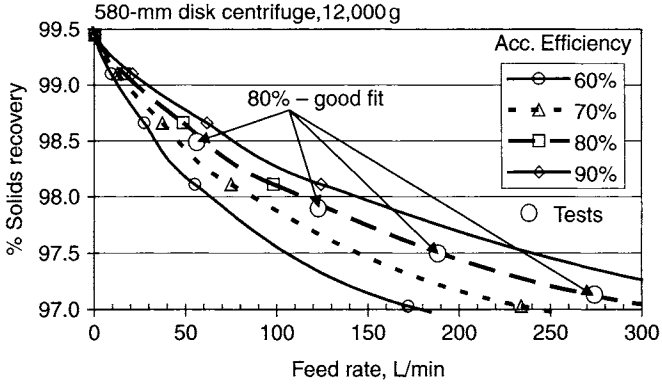


**Figure 13.11** Effect of efficiency – calibrate against tests to determine actual efficiency for use in simulator

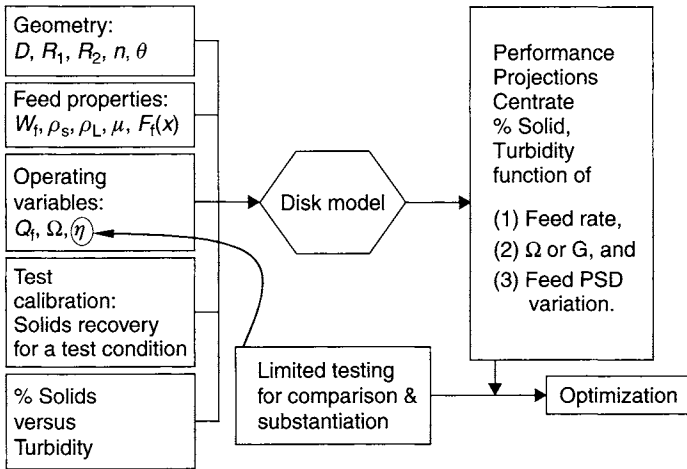


**Figure 13.12** Disk-centrifuge model requiring calibration

### 13.1.5 Disk Centrifuge for Yeast Processing (500-mm Disk)

Upon harvest, a suspension of yeast cell and liquid containing valuable expressed therapeutic protein is sent to a disk stack for separation wherein the valuable protein liquid is separated from the yeast cells. Unlike mammalian cells, yeast is much finer in particle size, and for this example the median size is at 8.5 microns. The frequency and cumulative undersize distributions of the feed yeast suspension are depicted respectively in Figure 13.13. The objective is to make separation and clarification all in one step. The gauge of the process is that the centrate suspended solids should not exceed 8 NTU (turbidity unit), and under

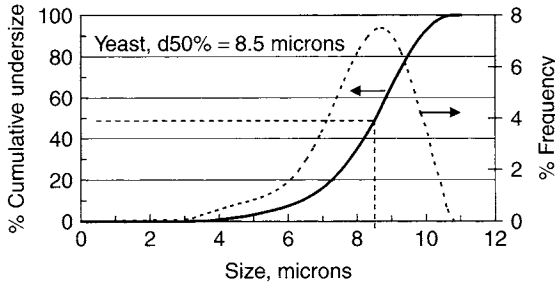


**Figure 13.13** Frequency distribution of feed yeast to centrifuge for separation

no circumstance should it be more than 10 NTU. A large 500-mm diameter disk stack is used for the separation step and the simulation results are shown in Figure 13.14. It is clear that increasing feed rate, which reduces retention time of the suspension, leads to much higher loss of solids, which contaminates the centrate liquid containing the dissolved protein product. The solids need to be further removed either by a second-stage centrifuge or by a depth filter. In order to stay below 8 NTU and to avoid another downstream separation, the feed rate to the 500-mm disk centrifuge needs to stay below 138 L/m. The operating range for the centrifuge is recommended at 122–138 L/min with centrate turbidity at 6–8 NTU. This is depicted in Figure 13.14.

### 13.1.6 Disk Centrifuge for Inclusion Body Separation (260-mm Disk)

As discussed in Chapter 6, bacteria such as *E. coli* are engineered so that they can express a specific type of therapeutic protein in their

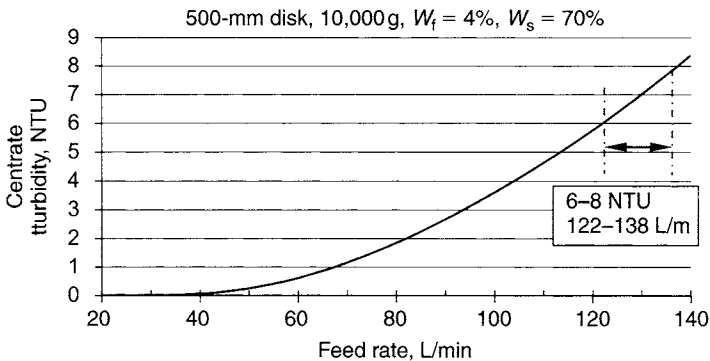
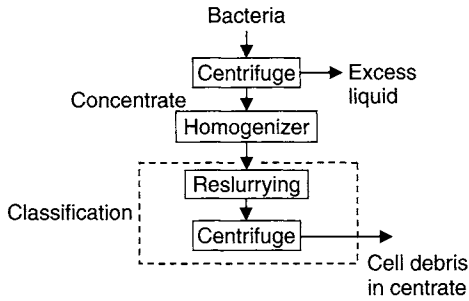


**Figure 13.14** Centrate turbidity as a measurement index for controlling operation of yeast bowl

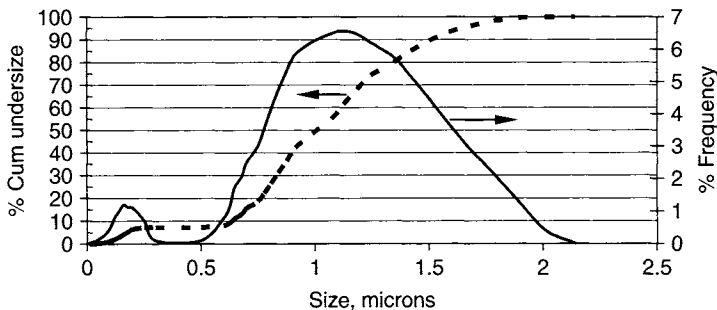
inclusion body in the bacteria. Upon harvesting, a suspension with the harvested bacteria is first sent to a centrifuge for removing excess liquid. Subsequently the concentrate from the centrifuge is lysed in the homogenizer. The resulting suspension contains the valuable inclusion bodies with size less than a micron, much finer cell debris, and liquid with unwanted intracellular fluid. The next step is to recover the inclusion bodies and remove cell debris and undesirable intracellular fluid by using a series of repulping and classifying steps by centrifugation. This is schematically represented by Figure 13.15.

Figure 13.16 shows the particle size distribution in both frequency and cumulative distribution. As can be seen in Figure 13.16, the frequency distribution is bimodal, with a small population of cell debris located around 0.1 to 0.3 micron and a majority population of inclusion bodies between 0.5 microns and larger, with maximum size at 1 micron.

Figure 13.17 shows the result from simulation using a 260-mm disk-stack centrifuge operating at 12,000 g on a repulped suspension. The centrate solids show a very interesting behavior in that they increase rapidly with initial increase in feed rate ( $Q_f$  less than 1 L/min) and that the centrate solids concentration subsequently increases only slightly between feed rate of 1.3 and 4 L/min. As the feed rate increases beyond



**Figure 13.15** Repulping and classifying inclusion bodies



**Figure 13.16** Size distribution of bacteria lysate feeding the centrifuge

4 L/min, the centrate solids concentration once again increases at a fast rate. This behavior is typical of classification of a suspension with bimodal particle size distribution. The initial rise is due to removal of the fine cell debris (less than 0.5 micron) in the centrate liquid, while the second steep rise at feed rate beyond 4 L/min is due to losing the valuable inclusion bodies in the centrate. As such, in order to remove the cell debris but not to lose the inclusion bodies, it is best to operate the centrifuge between 1.5 and 4 L/min.

The effect of various  $G$ -levels on the classification process is given by the simulation results plotted in Figure 13.18. Four  $G$ -levels have been employed in the simulation: 8000, 10,000, 12,000 and 14,000  $g$ , respectively. It is quite remarkable that there is not much difference, due to the various  $G$ -levels when operating at feed rate less than 2.5 L/min. Subsequently, different  $G$ -levels yield different maximum feed rate. At 8000  $g$ , the maximum feed rate is 2.5 L/min before any significant

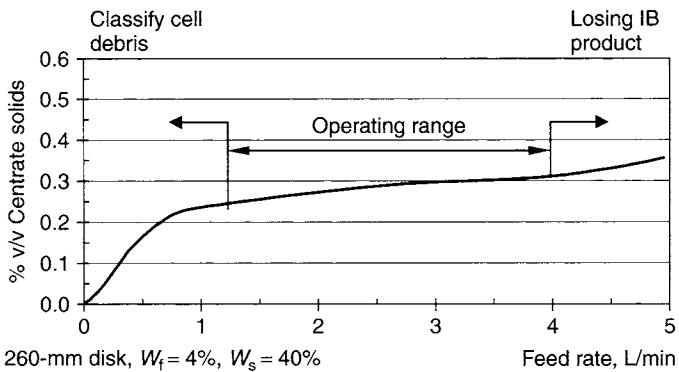


**Figure 13.17** 260-mm disk centrifuge operating at 12,000  $g$  to separate lysate cells

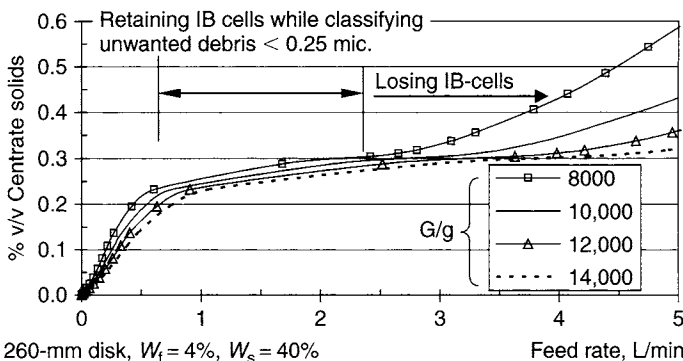


**Figure 13.18** Effect of  $G$ -force on classification of inclusion bodies

increase in the centrate solids; at 10,000 g it is 3.1–3.2; at 12,000 g, it is 4 L/min; and, finally, at 14,000 g it is at 4.5 L/min. Indeed  $G$ -level has significant impact on the maximum allowable feed rate to prevent losing the valuable inclusion bodies in the centrate during classification.

It is also of interest to review the accompanied chart – the solids-recovery behavior – which is depicted in Figure 13.19. This figure is almost a mirror image of Figure 13.18 on the centrate solids concentration behavior. High recovery implies low centrate solids concentration and vice versa. All the description pertaining to the centrate is applicable to the solids recovery without repeating it.

### 13.1.7 Enzymes (580-mm Disk)

A 580-mm diameter disk stack is used to process extracellular enzymes. As shown in Figure 13.20, the solids are quite fine with 50% = 20 microns. Suppose the process from a given biopharmaceutical plant demands a high feed rate yet the centrate solids cannot be more than

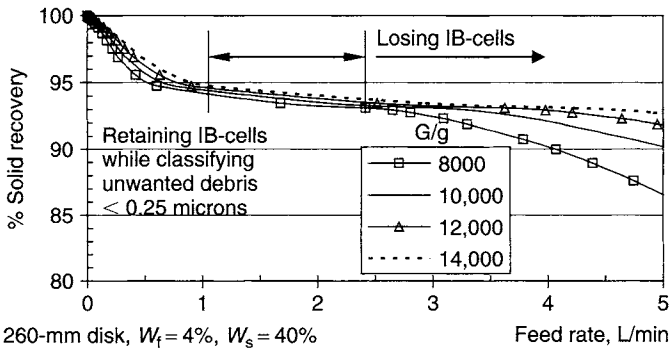


Figure 13.19 Effect of  $G$ -level on solids recovery

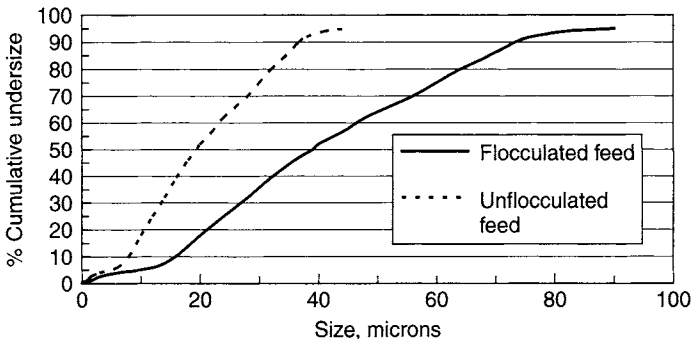
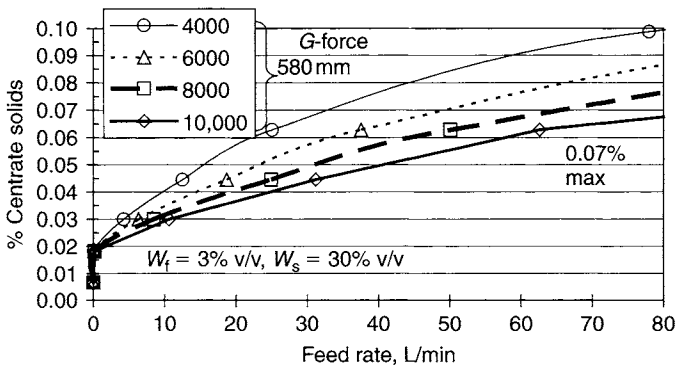


Figure 13.20 Unfloculated feed in enzymes process

0.07%, otherwise the product has to be polished downstream with a depth filter.

With unflocculated feed, the simulator generated a series of projected centrate suspended solids for 4000, 6000, 8000 and 10,000 g, respectively (see Figure 13.21). The feed is at 3% v/v, while the sediment discharge is about 30% v/v. The ratio of the density difference between solid and liquid to the liquid density is 0.1, while the viscosity is 5 cP. In order to maintain centrate solids 0.06–0.07%, a 580-mm diameter disk stack operating at 8000 g allows a maximum feed rate of 45–65 L/min.

On the other hand, flocculants are introduced so that large flocculated solids form. Assuming that after the flocculated solids enter into the disk stack and accelerate, the effective size of the floc doubles the original particle size (conservative estimate); see Figure 13.20 on the size distribution of a flocculated feed; the solids concentration of the centrate leaving the centrifuge is given by Figure 13.22. At 8000 g, the maximum feed rate that the 580-mm disk machine can accommodate is



**Figure 13.21** Centrate solids for unflocculated feed to centrifuge

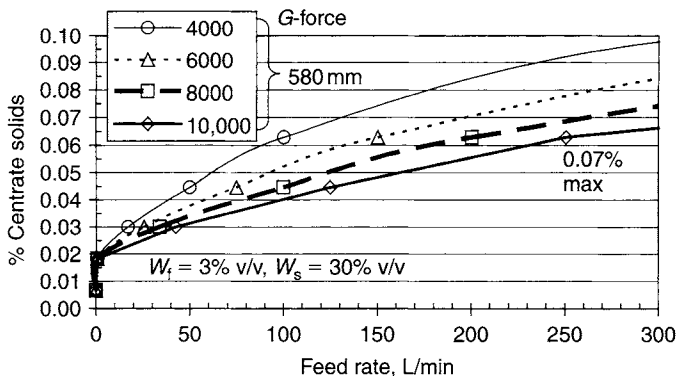


**Figure 13.22** Centrate solids from a flocculated feed

180–260 L/min; this is four times the rate for an unflocculated feed suspension which is quite dramatic. Also, the product is the liquid and the flocculant selected should be compatible with that of the product without any side-effect on the process. It is quite remarkable that numerical simulation can bear out the benefit of flocculation. Obviously, one has to make a judicious assumption that the feed size distribution changes, but in a reasonable way so that the simulation results are reasonable and compare well with test results.

## 13.2 Tubular Centrifuge

A tubular centrifuge simulator can be set up similar to that of the disk. Figure 13.23 shows a schematic of other types of centrifuges, including tubular, decanter and spintube. The logistics of the process flow are similar to that of the disk-stack centrifuge. Two types of tubular centrifuges with their respective ranges of  $G$ -forces will be simulated.

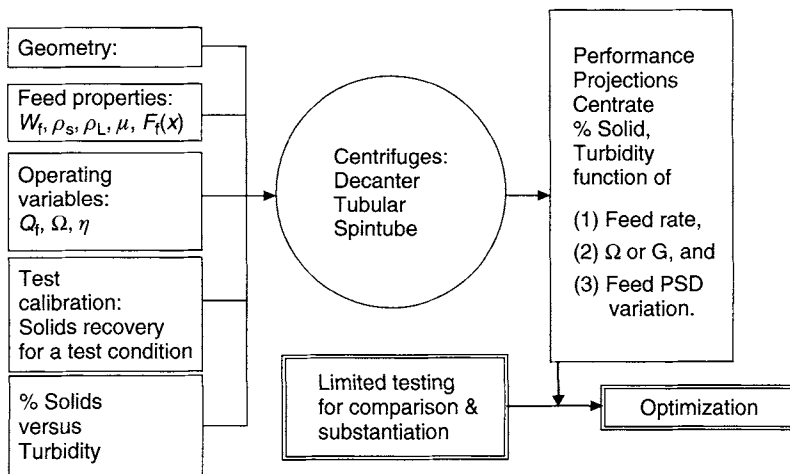


**Figure 13.23** Other centrifuges (decanter, tubular, and spintube) simulators

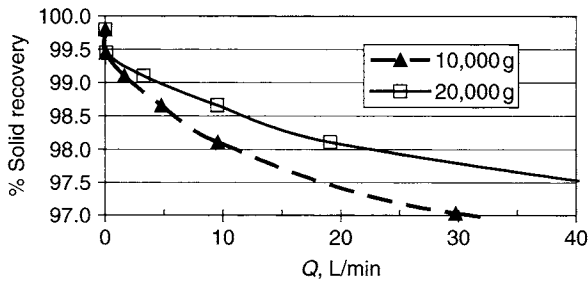
### 13.2.1 High- $G$ Tubular (150-mm and 300-mm)

The bowl diameter, bowl length, and pool diameter define the needed geometry of tubular centrifuge for numerical simulation. As an example, a high-speed tubular bowl of 457-mm diameter and of length 610 mm, with a pool depth of 45 mm, is used. The feed particle size distribution is the same as Figure 13.2. The geometry and physical parameters used for the simulation are tabulated in Table 13.2.

**Table 13.2** Performance prediction of tubular

Centrifuge bowl diameter	457 mm
Centrifuge bowl length	610 mm
Pool diameter	366 mm
Efficiency	95%
$\Omega_1, G$	6255 rpm, 10,000 g
$\Omega_2, G$	8846 rpm, 20,000 g
Density difference, $\Delta\rho/\rho$	0.1
Viscosity	5 cP

The results of the simulation are shown in Figure 13.24. For example, at a specification of  $R_s = 97.5\%$ , the feed rate for the centrifuge operating at 10,000 g is 19 L/min, and at 20,000 g it is 40 L/min. On the other hand, for a more stringent higher recovery 98.5%, the maximum feed rate is 6 L/min at 10,000 g and 12 L/min at 20,000 g. This demonstrates that the feed rate is directly proportional to the  $G$ -level, as with the disk centrifuge.

**Figure 13.24** Solids recovery of tubular centrifuge

### 13.2.2 Lower- $G$ Tubular (150-mm and 300-mm)

Two smaller tubular centrifuges are also used for performance simulation, both with maximum  $G$ -force of 5000 g. This will simulate the performance, for example, of the submerged hub design tubular as discussed in Chapter 3.

#### 1 150-mm Tubular

The first is a 150-mm diameter centrifuge that processes mammalian cell broth with PSD, as depicted in Figure 13.2. The results are shown in Figure 13.25a for the centrate solids and in Figure 13.25b for the solids recovery. As evident, much lower centrate solids and higher solids recovery

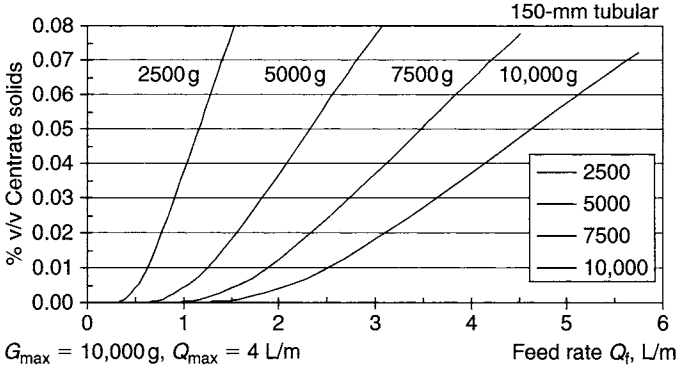


**Figure 13.25a** Centrate solids of a 150-mm diameter pilot tubular centrifuge with four different  $G$ 's

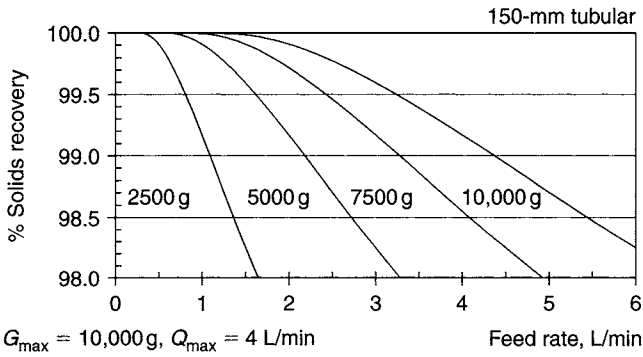


**Figure 13.25b** Solids recovery of a 150-mm diameter pilot tubular centrifuge with four different  $G$ 's

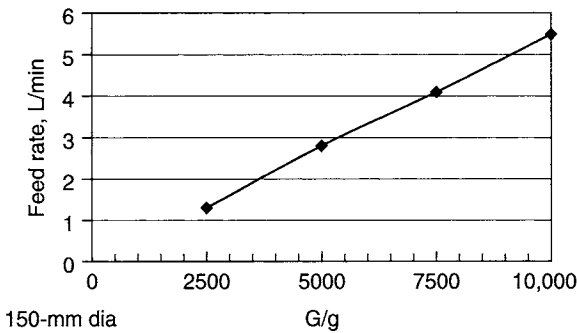


**Figure 13.25c** Feed rate versus  $G$ -force for a 150-mm pilot tubular centrifuge with same centrate quality for 0.07%

can be obtained for higher  $G$ -level at a fixed feed rate. On the other hand, for a fixed performance (fixed centrate solids concentration/solids recovery) a higher feed rate is obtained with higher  $G$ . For example, to obtain no more than 0.07% centrate solids corresponding to 98.4% solids recovery, the feed rate of 1.3, 2.8, 4.1, 5.5 L/min can be attained, respectively, for 2500 g, 5000 g, 7500 g, and 10,000 g. This linear proportionality relationship is shown in Figure 13.25c.

## 2 300-mm Tubular

The second example is a 300-mm diameter centrifuge that processes mammalian cell broth with PSD, as depicted in Figure 13.2. The results are shown in Figure 13.26a for the centrate solids and in Figure 13.26b for the solids recovery. Similar conclusions can be drawn as with the pilot centrifuge. Assuming both centrifuge discharge suspended solids at 0.07% with a solids recovery of 98.4% for a 150-mm diameter centrifuge operating at 5000 g the feed rate can be maintained at 2.85 L/min

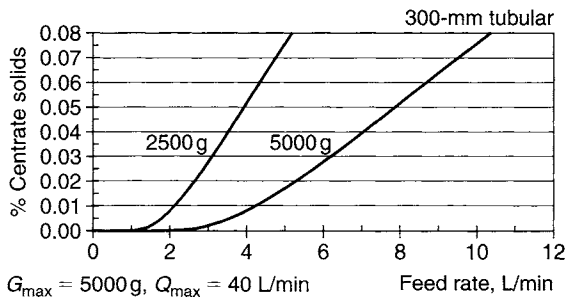


**Figure 13.26a** Centrate solids of a 300-mm tubular diameter centrifuge with two different  $G$ 's

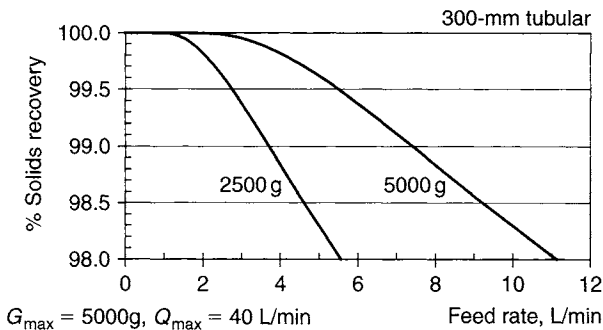


**Figure 13.26b** Solids recovery of a 300-mm diameter tubular centrifuge with two different  $G$ 's

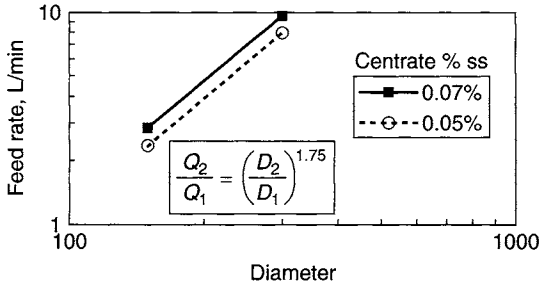


**Figure 13.26c** Feed rate as a function of tubular centrifuge diameter. Note that 0.07% v/v corresponds to 98.4% solids recovery, and 0.05% v/v corresponds to 98.5% solids recovery

(not shown), and for a 300-mm diameter centrifuge it is 9.6 L/min. If the centrifuge is restricted to discharge a tighter metric, only 0.05% suspended solids with a solids recovery of 98.85%, the rate for the 150-mm diameter centrifuge would have been lower, to 2.35 L/min (not shown), and that for the 300-mm diameter centrifuge lower, to 7.95 L/min. Indeed, the feed rate that can be processed by the tubular centrifuge varies approximately as the 1.75-power of the centrifuge bowl diameter, as shown in Figure 13.26c. This is different from that of the disk-stack centrifuge, where it was found from simulation that  $Q \sim D^{2.8}$ . One obvious reason is the use of the disk stack, resulting in more sedimentation area for the centrifuge.

### 13.3 Decanter

A decanter centrifuge simulator is used to simulate a process to separate flocculated biosolids with a specification that the feed is about 10% and the cake is 30%. The feed PSD is given by Figure 13.27. As can be seen, the  $d_{50}$  is slightly above 60 microns. A 460-mm diameter capable of 4000 g is used to perform the task. The solids recovery as a function of feed rate for various  $G$ -levels, respectively 2000 g, 2500 g, 3000 g and 3500 g, are shown in Figure 13.28. The centrate solids leaving the decanter centrifuge is shown in Figure 13.29. The objective is to limit the centrate solids to be no more than 0.16–0.29%, which corresponds respectively to 98–99% solids recovery. The details of the geometry and  $G$ -levels are detailed in Table 13.3. At the lower specification of 0.16% centrate solids (or 99% solids recovery), a 2000 g machine can provide a maximum feed rate of 140 L/min, while a 3500 g machine can boost this up to 255 L/min. At the upper specification of 0.29% centrate solids (or 98% solids recovery), a 2000 g machine can provide a maximum

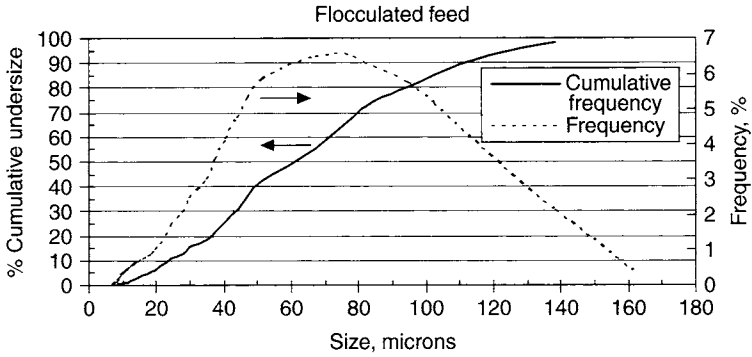


**Figure 13.27** Frequency and cumulative undersize distribution for feed to decanter

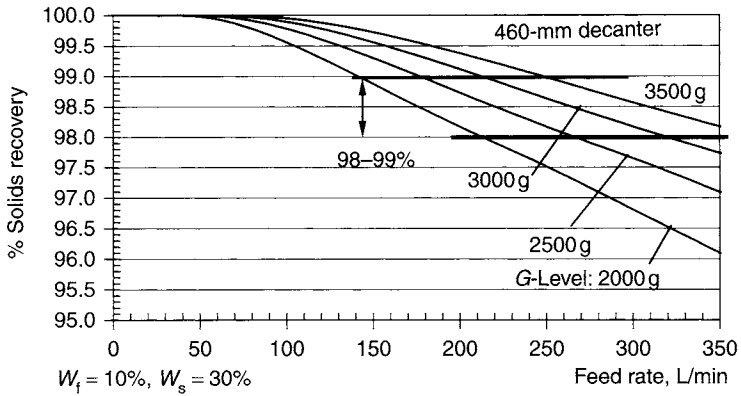


**Figure 13.28** Solids recovery as function of feed rate for four different  $G$ 's

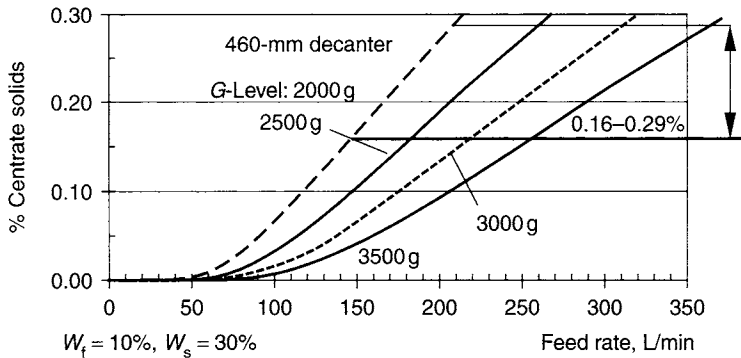


**Figure 13.29** Centrate solids as a function of feed rate for four different  $G$ 's

**Table 13.3** Performance prediction of decanter

Centrifuge bowl diameter	457 mm
Length/Diameter	4
Pool depth	75 mm
Efficiency	90%
$\Omega_1, G$	2797 rpm, 2000 g
$\Omega_1, G$	3127 rpm, 2500 g
$\Omega_1, G$	3426 rpm, 3000 g
$\Omega_2, G$	3700 rpm, 3500 g
Density difference, $\Delta\rho/\rho$	0.03
Viscosity	2 cP

feed rate of 205 L/min, while a 3500 g machine can boost this up to 370 L/min.

In this chapter the simulation of decanter centrifuge is not as well illustrated as is disk and tubular centrifuges. In fact, we have not discussed the modeling of decanter other than referencing it to the tubular model presented in Chapter 10. Except for processing intracellular enzymes and some other niche bioprocessing applications, decanter is not as widely used compared to the disk-stack centrifuge, due to lower  $G$ -force, lesser surface area, and relatively lower feed solids for bioseparation.

### 13.4 Spintube

A spintube centrifuge simulator has also been developed. An example is used on laboratory testing of a feed suspension from the flue gas desulfurization process. For illustration, we will compare laboratory test results with that of the simulator. The feed particle size distribution of the suspension is shown in Figure 13.30.

The solids recovery from simulation for different  $G$ 's and time durations are shown in Figure 13.31. The solid curves are just trends for the test data. Increasing centrifugation time increases solids recovery for a given  $G$ -force. Increasing  $G$ -force increases recovery for a given centrifugation time. The results of the test data (five sets of different  $G$ -forces and time durations) are best 'normalized' and well correlated by the dimensionless Le number (see Equations 9.1 and 9.2) in Figure 13.32. The solids recovery drops sharply with increasing Le number. The prediction of the simulator is shown by a single solid curve in the figure. As can be seen, the test data compare well with the prediction demonstrating the prediction accuracy of the simulator and the scale-up capability of the model.

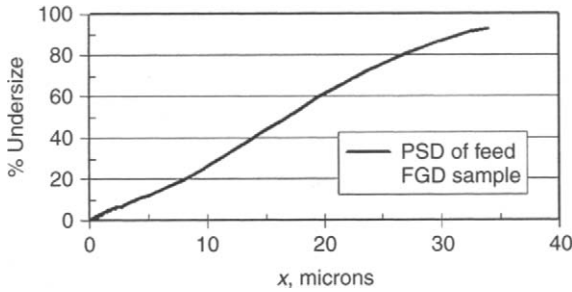


**Figure 13.30** Particle size distribution in a suspension of flue gas desulfurization solids

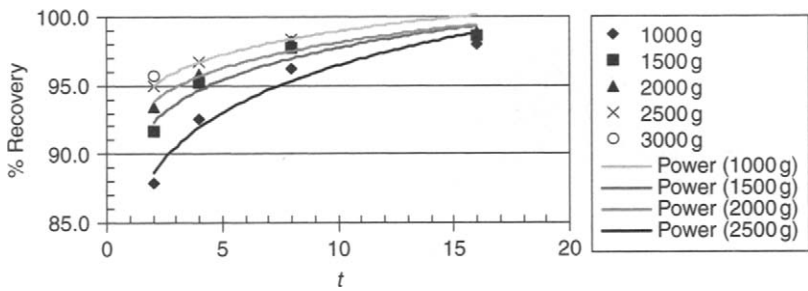


**Figure 13.31** Spintube tests results

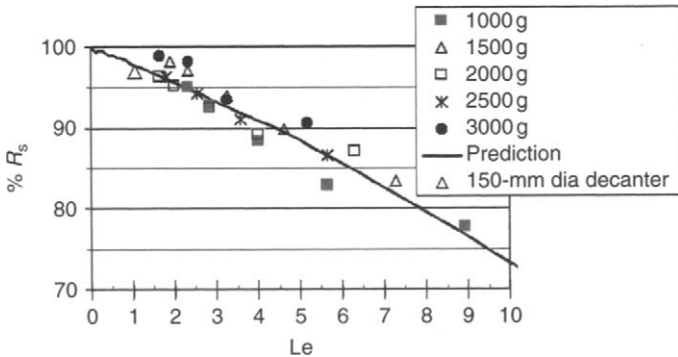


**Figure 13.32** Normalized solids recovery versus Le number

### 13.5 Strategy of Developing Drug using Numerical Simulations

Centrifugal separation is known to be complicated and exhibits non-linear responses not readily amendable to prediction and scale-up as



## 13.6 Summary

The numerical simulator developed, respectively, for disk, tubular, decanter, and spintube centrifuges can be used to predict performance using both geometry and physical parameters as inputs to the simulation. The governing dimensionless  $Le$  number for a given centrifuge depends on the geometry and operating condition of the centrifuge. The simulator can be used to predict solids recovery, centrate solids for a given feed rate, speed/G, and a given feed size distribution. Alternatively, it can be used to predict the maximum allowable feed rate to meet the centrate solids concentration limit. The simulator can also be used in all phases of drug development from bench-scale laboratory feasibility study phase, piloting, clinical manufacturing, large-scale production, and even back to small-scale testing. Several examples have been used in this chapter to demonstrate the capabilities of numerical simulation. Numerical simulation should not be used alone; it has to be complemented with experimental or production results to reliably forecast or project results above and beyond what is already known. Numerical simulation can provide a vast amount of results for different scenarios. The simulation results should be interpreted and used with caution like any other numerical simulations, as the outputs are, at best, as good as the inputs.

## References

- [1] W.W.F. Leung, Performance prediction and scale-up for disk centrifuge for bioseparation, American Chemical Society Annual Conference, Anaheim, USA, Mar. 2005.
- [2] W.W.F. Leung, Small feasibility study to pilot and production scale-up of primary recovery separation by AT-SPIN simulation, Filtech Europa, Wiesbaden, Germany, Oct. 2005, and American Filtration and Separations Annual Conference, Atlanta, USA, April 2005.
- [3] W.W.F. Leung, Experimental and theoretical study of flow and sedimentation of tubular centrifuge for bioseparation, AIChE Annual Conference, Cincinnati, USA, Nov. 2005.
- [4] W.W.F. Leung, Flow visualization and modeling of separation and classification of suspension in continuous-feed centrifuge–surface flow, paper presented at 9th World Filtration Congress, New Orleans, USA, 18–24 April, 2004.

## Problems

- (13.1) In Figure 13.26c, it is shown that the scale-up factor for the example of tubular centrifuge is  $Q \sim D^{1.75}$  assuming constant performance in

terms of centrate solids and solids recovery. Is there any rationale behind why the index power is 1.75 and not as high as 2 or 3? Please explain.

- (13.2) In Section 13.1.3, the example illustrates that the scale-up factor between the 400-mm diameter disk and the 580-mm diameter disk is 2.8, given the clarification performance being equal. Let  $Q \sim D^n$ , what would be the index  $n$  for the disk centrifuge in this example? Why is it higher/lower than that of the tubular, see Problem (13.1)?
- (13.3) Derive the centrate solids concentration given by Equation 13.1 given that feed solids and cake solids concentration, as well as the solids recovery, are known and the process condition is under steady state?

# Rotating Membrane in Bioseparation

Separation, impurities removal, concentration, buffer exchange, and purification are vital in biotechnology to process a valuable bioderived product so that it can be best utilized downstream for drug formulation or other bioprocesses. A generic flow sheet for bioseparation is shown in Figure 6.1. The objectives of the process flow sheet are to achieve both high recovery and high purity of valuable component at the maximum production capacity.

The processing needs to be carried out in a most effective yet efficient manner. One promising innovation is to combine the selectivity and multifunction features of membrane separation [1] and process (such as purification etc.), together with the centrifugation and other benefits due to rotation, to effect separation and the process. In this chapter, the technology of bioseparation using stationary membrane is briefly reviewed first. This is followed by a discussion of rotating effects on membrane filtration. Two distinct cases are identified and discussed separately. The first concerns using the rotation effect under steady state to generate a boundary-layer flow that can scour the membrane surface reducing concentration build-up of solids on the membrane surface. The second concerns using rotation to generate a centrifugal pressure that drives membrane filtration under transient condition. A rotating disk membrane and a small-scale spintube equipped with membrane module are discussed and modeled mathematically, the results of which are compared with experiments.

## 14.1 Membrane

Reverse osmosis (RO), nanofiltration (NF), ultrafiltration (UF), and microfiltration (MF) are popular filtration processes used to filter, respectively, molecular and ionic sized, nanosized, and macromolecules solutes, while microfiltration is used to remove soluble large macromolecules and proteins, as well as insoluble micron-sized solids.

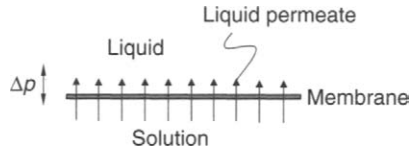


**Figure 14.1** Liquid permeation through membrane

### 14.1.1 Osmotic Pressure Resistance

As shown in Figure 14.1, membrane filtration is a process wherein a pressure gradient  $\Delta p$  is applied across a semi-permeable membrane. The latter allows liquid to permeate through the membrane, while the large macromolecules are retained by the membrane. The size of macromolecules that the membrane retains is specified as the molecular weight cut-off (MWCO) for the membrane. Under a pressure gradient superimposed across the membrane, liquid and small molecules are forced through the pores of the membrane while larger solutes or suspended particulates that cannot percolate through the pores are retained by the membrane. The pressure gradient needs to overcome flow resistance in the membrane as well as the osmotic pressure, that drives liquid to flow from the 'liquid permeate' side to the 'concentrate' side of the membrane to balance the concentration difference of solute across the membrane. The higher the solute concentration in solution the greater is the osmotic pressure that needs to be overcome to force liquid to the concentrate or solution side.

The membrane selected for a given separation process depends on permeability of liquid flow and selective rejection of a given solid specie. Unfortunately, high liquid permeability often implies poor selectivity of solute, while high selectivity implies low membrane permeability. Small-molecule solutes (e.g. sodium chloride) give rise to higher osmotic pressure than large-molecule solutes (e.g. protein). The pressure required for membrane filtration depends on the process, and it is highest for RO, NF, UF, and MF in that order, as most resistance comes from osmotic pressure when operating under the condition below 'gelling' (to be explained later) on the membrane, and RO deals with smaller solute size than NF, NF smaller than UF, and UF smaller than MF.

The membrane is characterized by pressurizing saline water through the membrane and measuring the water permeation through the membrane for a given imposed pressure gradient. As shown in Figure 14.2, a linear trend (labeled 'water flux') of permeate flux ( $\text{cm}^3/\text{cm}^2/\text{s}$ ) versus applied pressure gradient results from such testing. The greater the slope of the linear line the higher is the membrane permeability.

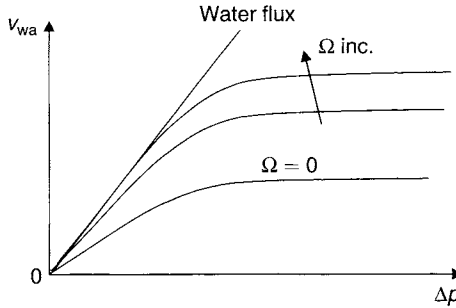


**Figure 14.2** Flux versus applied pressure for stationary ( $\Omega = 0$ ) and rotating ( $\Omega \neq 0$ ) membrane

(The flux that has been loosely referred to is the average flux  $v_{wa}$  over the membrane area, i.e. total permeate liquid collected per unit time per total membrane area, and not the local flux  $v_w$  at a given radius.) This will be more carefully dealt with later, for now we just refer to it as flux. When the membrane has been reused repeatedly for filtration over some time, the membrane permeability drops due to fouling with deposition and clogging from deposits of inorganic and organic compounds. This is represented by a decrease in membrane permeability or decrease in the slope of the linear trend, as in Figure 14.2.

### 14.1.2 Gel Resistance

Using a protein solution for filtration instead of a saline solution, the permeation flux  $v_w$  increases with applied pressure, but stays below the water flux line. The increase in  $v_w$  slows down at high  $\Delta p$  and it reaches a point at which  $v_w$  becomes independent of  $\Delta p$ , as depicted by the horizontal portion of the filtration curve shown in Figure 14.2.

With high transmembrane pressure  $\Delta p$ , more macromolecules are transported and get retained by the membrane, building up a solids concentration that can reach the solubility limit of the solute. Under this condition, dissolved solids start precipitating to form a gel layer [2] on the membrane surface. This gel layer significantly increases the resistance to filtration. This is known as concentration polarization. Increasing  $\Delta p$  results in an equal increase in flow resistance, with the consequence that there is no increase in permeation flux. The constant flux under concentration polarization is referred to as the limiting flux. This is one serious concern in separating biological solids. One measure to alleviate concentration polarization is to operate below the critical flux, the point at which the flux curve starts departing from the linear water flux line.

Under concentration polarization, the resulting limiting flux depends on a number of factors: flow condition (laminar or turbulent flow, with and without eddy promoter, and with or without rotation), membrane module design and geometry, and the physicochemical condition of solution (pH, ionic strength, and protein concentration). While membrane filtration for a stationary system is well understood, the effect of rotation on concentration polarization is not. In this chapter, we devote our discussion to understanding this rather interesting problem. It is perceived that increasing rotation delays the onset of concentration polarization, and the resulting limiting flux (horizontal portion of curve) under gel condition is higher than without rotation, as depicted in Figure 14.2.

### **14.1.3 Membrane Fouling and Cake Formation**

Fine suspended solids can also deposit on the membrane surface, leading to fouling (chemical and physical adsorption) of the membrane surface. In microfiltration of large macromolecules and micron-sized suspended solids, more solids deposit on the membrane, forming a thin cake layer there. Under this scenario, the cake becomes the filtering medium instead of the membrane.

### **14.1.4 Two Scenarios of Rotational Effect on Membrane Filtration**

The effect of rotation on permeate flux is investigated in the rest of the chapter. In what follows, two different arrangements will be studied, one for which the membrane takes the form of a rotating disk and the membrane surface is parallel to the  $G$ -force. It is not the  $G$ -force that affects separation, instead the rotational effect sets up a secondary flow that keeps the membrane clean from solid deposition. A second configuration is that a spintube centrifuge is equipped with a membrane module, wherein the membrane surface is predominantly perpendicular to the  $G$ -force operating under the 'dead-end' filtration mode.

## **14.2 Rotating Disk Membrane with Surface Parallel to the $G$ -Force**

In the first configuration, as shown in Figure 14.3, the membrane is parallel to the direction of the centrifugal acceleration  $G$ . In other words, the membrane is oriented perpendicular to the rotation vector  $\Omega$ . An example of such configuration is that a membrane is mounted on a porous disk support and the entire membrane-support assembly is immersed in

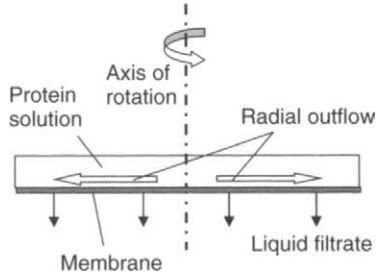


**Figure 14.3** Rotating disk membrane

a pressurized protein solution [3]. Under pressure gradient, liquid and small soluble species are forced through the pores of the rotating membrane, while larger soluble molecules are retained on the membrane surface. The thickness of this build-up, or concentration polarization, controls the mass transfer rate. In accordance to Fick's law on mass diffusion, the mass flow rate  $M$  per unit area  $A$  (i.e. mass flux) is given by

$$\frac{M}{A} = -D \frac{dC}{dy} \quad (14.1a)$$

All the solids referred herein are soluble solids; specifically,  $C$  is the solute (small molecules such as sodium chloride and macromolecules such as protein) concentration. The  $y$  in Equation 14.1a is the transverse coordinate normal to the membrane. Mass transfer takes place from a region of high-solids concentration to a region of low-solids concentration. The proportionality constant is the diffusion coefficient  $D$ , which has a dimension of second power of length over time. In Equation 14.1a, the distance between the two regions can be approximated by the mass boundary layer  $\delta$ , and the differential concentration can be approximated by the difference of wall solid concentration  $C_w$  and the bulk/feed solids concentration  $C_b$ . Thus

$$\frac{M}{A} \approx D \frac{(C_w - C_b)}{\delta} \quad (14.1b)$$

Given that the wall and bulk solids concentrations stay relatively constant, if the layer of solute build-up on the membrane surface can be reduced (i.e. small  $\delta$  in Equation 14.1b) by the hydrodynamics of the membrane module geometry, the mass flux  $M/A$  in Equation 14.1b can be greatly enhanced. The conventional approach is to provide a flow with high shear near the membrane wall to suppress the mass boundary

layer, such as a turbulent flow or with eddy promoters. Here, the rotational flow effect is used to reduce the mass boundary layer.

Due to the high-speed rotation, the momentum boundary layer responsible for momentum transfer between the rotating disk and the bulk fluid stays constant independent of radius. This is related to the two-dimensional Taylor Proudman phenomenon, as discussed in Chapter 2. On the other hand, the mass boundary layer is much thinner than the momentum boundary layer (also known as the Ekman layer). Thus, efficient mass transfer can be realized by controlling a thin momentum boundary layer, which in turn controls the mass boundary layer  $\delta$ . The permeation curve in Figure 14.2 can be increased by increasing rotation speed  $\Omega$  as compared with that of the stationary membrane,  $\Omega = 0$ .

### 14.2.1 Dimensionless Numbers

A few dimensionless numbers are needed for the study of mass transfer using rotating membrane. The Ekman number  $E$  measures the viscous effect versus convective effect due to rotation.

$$E = \frac{(\mu/\rho)}{\Omega d^2} \quad (14.2a)$$

Usually  $E$  is small, which reflects a small viscous effect compared to significantly large convective effect in most of the region of the flow. However, there is one small region in which the viscous effect can be comparable to, or become more dominant than, that of convection – the momentum boundary layer or the Ekman layer, as will be discussed subsequently.

The Reynolds number  $Re$  is exactly the reciprocal of the Ekman number.

$$Re = \frac{1}{E} = \frac{\Omega d^2}{(\mu/\rho)} \quad (14.2b)$$

The Schmidt number  $Sc$  is a ratio of the momentum diffusion versus the mass diffusion.

$$Sc = \frac{(\mu/\rho)}{D} \quad (14.3)$$

It can be shown that the mass boundary layer thickness is related to that of the momentum boundary layer by the 1/3-power of the Schmidt

number. Therefore, the ratio of mass boundary layer to Ekman layer becomes

$$\frac{\delta}{\delta_{\text{Ek}}} \propto O(\text{Sc}^{-1/3}) \quad (14.4)$$

It is best to use an example to illustrate the magnitudes and significance of these dimensionless numbers.

### Example 14.1

$$\Omega = 300 \text{ rev/min}$$

$$d = 10 \text{ cm}$$

$$\nu = \mu/\rho = 0.1 \text{ cm}^2/\text{s}$$

$$\text{Re} = 31,400$$

$$E = 3.2 \times 10^{-5}$$

$$\delta_{\text{Ek}} \sim E^{1/2}d = 0.6 \text{ mm}$$

$$D = 10^{-7} \text{ cm}^2/\text{s}$$

$$\text{Sc} = 10^6$$

$$\delta/\delta_{\text{Ek}} \sim 0.01$$

$$\delta \sim 0.01 \text{ mm}$$

The above calculation demonstrates that when the disk is rotating at 300 rev/min, the Ekman momentum layer  $\delta_{\text{Ek}}$  is about 0.6 mm, which is quite thin. On the other hand, the mass boundary layer  $\delta$  is even thinner than the Ekman layer  $\delta_{\text{Ek}}$  due to the large Schmidt number (ratio of viscosity to diffusivity)  $\sim 10^6$ . From Equation 14.4, the mass boundary layer to that of the Ekman layer is of the order  $\text{Sc}^{-1/3}$ , which is 1%. For the example, the momentum boundary layer, or Ekman layer, is 0.6 mm  $\sim O(1 \text{ mm})$ , while the mass boundary layer is about 0.01 mm, which is 1/100 times smaller!

## 14.2.2 Governing Equations and Solutions

### 14.2.2.1 Model

Despite it being small, the mass boundary layer controls the mass transfer across the membrane. The concentration of dissolved solids (e.g. protein)  $C$  can be obtained from the transport equation:

$$\frac{1}{R} \frac{\partial}{\partial R} (RuC) + \frac{\partial}{\partial y} (\nu C) = \frac{\partial}{\partial y} \left( D \frac{\partial C}{\partial y} \right) \quad (14.5)$$

$R$  is the radial coordinate and  $y$  is the transverse coordinate from the membrane. The boundary conditions are:

$$y = 0; u = 0, v = v_w(r), C = C_g \quad (14.6a,b,c)$$

$$y = \delta(R); C = C_b \quad (14.6d)$$

Note that we consider the boundary condition, Equation 14.6c, as the concentration at the membrane surface reaches the gel concentration or solubility per Michael's model [1]. In addition to the set of boundary conditions, Equations 14.6a–d, there is one more condition that stipulates diffusion and convection of solute. Diffusion of solute away from the membrane balances advection of solute toward the membrane minus permeation of solute through the membrane to the permeate side. Thus

$$v_w C_w \Re = D \left( \frac{\partial C}{\partial y} \right)_w \quad (14.7)$$

Note that reactivity  $\Re$  of membrane is a complement of selectivity by membrane on a given specie, thus

$$\Re = 1 - \frac{C_p}{C_w} \quad (14.8)$$

Note that  $\Re$  depends on molecular weight cut-off (abbreviated hereafter as MWCO) of the membrane, solute size, and membrane skin layer pore openings. There are two extremes for consideration. If  $C_p = 0$ , rejection of protein by the membrane is 100% with  $\Re = 1$  from Equation 14.8, therefore convection of protein towards the membrane is exactly balanced by diffusion of protein away from the membrane. The other extreme is when  $C_p = C_w = C_b$  then  $\Re = 0$  from Equation 14.8, therefore convection of protein toward the membrane is exactly equaled to protein permeation through the membrane. Both concentration at the membrane surface and permeate equals that of the bulk feed. The membrane is leaking with no retention of protein and there is no mass boundary layer or backward diffusion.

### 14.2.2.2 Approximate Analytical Solution

The mass boundary layer equation can be obtained from solving Equation 14.5 subject to the boundary conditions, Equation 14.6a–d and ancillary equations, Equation 14.7 and Equation 14.8. An approximate integral method [4] has been developed to solve the equation. The

velocity profile of the Ekman layer flow field is adopted as input to the integral method. Using the integral method, it can be shown that the mass boundary layer can be approximated by the analytical form

$$\delta(R) = 2^{1/3} \left( \frac{D_g^{1/3} (\mu/\rho)^{1/6}}{\Omega^{1/2}} \right) \left[ 1 - \left( \frac{R_1}{R} \right)^6 \right]^{1/3} \left( \frac{C_b}{C_g} \right)^{1/3} \quad (14.9)$$

Note that the mass boundary layer thickness increases moderately with increasing gel diffusion coefficient  $D_g$  of the macromolecules, decreases with increasing rotation speed or decreasing Ekman/momentum-boundary layer thickness, and only slightly increases with increasing kinematic viscosity  $\mu/\rho$ . From Equation 14.9, it is clear that  $\delta$  is zero at  $R_1$  and  $\delta$  grows rapidly to a constant maximum thickness after  $R > 2R_1$ . This is illustrated in Figure 14.5.

Similarly, the average flux is given by

$$v_{wa} = -1.59 \frac{D_g^{2/3} \Omega^{1/2}}{(\mu/\rho)^{1/6}} [(C_g/C_b)^{1/3} - (C_g/C_b)^{-2/3}] f \quad (14.10a)$$

$f$  is the distribution function defined below; it depends on the starting and ending radii  $R_1$  and  $R_2$ . There are two scenarios for consideration.

1 Membrane extends outward from initial radius  $R_1$ :

$$f \left( \frac{R_2}{R_1} \right) = \frac{2}{[(R_2/R_1)^2 - 1]} \int_1^{R_2/R_1} \frac{\xi^3 d\xi}{(\xi^6 - 1)^{1/3}}, \quad R_1 \neq 0 \quad (14.10b)$$

$\xi$  is an integration variable in Equation 14.10b.

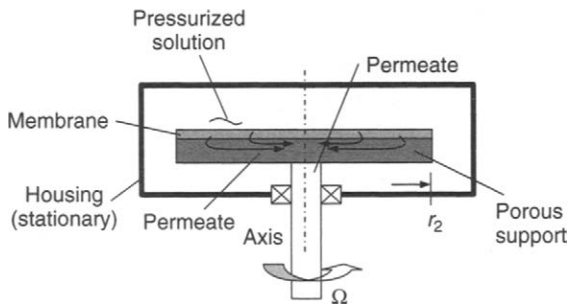


**Figure 14.4** Simple rotating membrane setup (rotating coupling and stationary pipe not shown)

- 2 Membrane extends outwards from the axis, i.e.  $R_1 = 0$ . In this case,  $f$  does not depend on  $R_2$  and is a constant equaled to unity regardless.

$$f = 1, \quad R_1 = 0 \quad (14.10c)$$

Figure 14.4 shows a rotating membrane test unit. A membrane is mounted on a porous stratum through which the permeate flows through and is collected in a tube located at the axis. The liquid is transferred from the rotating portion of the pipe to a stationary pipe through rotating coupling. Experiments have been carried out [3] using similar setup, as shown in Figure 14.4, using solution of bovine serum albumin (BSA). Different disk angular speeds and feed concentrations of BSA have been tested.

Table 14.1 tabulates some of the raw test results [3], and other data in the table are our analysis. The raw data included in Table 14.1 from Reference 1 are bulk (or feed) concentration of BSA solution  $C_b$ , rotation speed  $\Omega$ , average permeate flux  $v_{wa}$ , and diffusivity of the bulk/feed solution  $D_b$ . The Ekman number  $E$ , Reynolds number  $Re$ , and Schmidt number  $Sc$  are calculated based on, respectively, Equations 14.2a, 14.2b, and 14.3. The diffusivity  $D_g$  at gel concentration  $C_g$ , Nusselt number  $Nu$ , and  $v_{wa-pred}$  in Table 14.1 are obtained from prediction of the present model.

### (a) Mass boundary layer

The theoretical mass boundary layer at large radius approaches an asymptotic constant after  $R/R_1 > 1.5$ , where  $R_1$  is the starting radius. From Equation 14.9, the boundary layer starts out at zero at  $R_1$  and quickly reaches an asymptote  $\delta_\infty$ . The layer thickness  $\delta$  is thus normalized with respect to the asymptotic value, and the normalized boundary layer thickness  $\delta' (= \delta/\delta_\infty)$  is shown by the bottom curve in Figure 14.5.

### (b) Membrane flux

The local membrane flux  $v_w$  from prediction, after being normalized by flux at large radius  $v_{w\infty}$ , is plotted in Figure 14.5 as a function of  $R/R_1$ . The normalized flux  $v'_w (= v_w/v_{w\infty})$  approaches infinitely at  $R_1$ . This can be understood given  $M/A = v_w \sim 1/\delta$  from Equation 14.1b, when  $\delta = 0$  at  $R_1$  corresponds to infinite flux there (mathematically a singularity). The flux drops quickly down to an equilibrium steady value corresponding to that of a large radius after  $R/R_1 > 1.5$ . Despite being slightly higher than the local flux, the normalized average flux  $v'_{wa}$  (averaged over radius) exhibits similar trend as the local flux, and it approaches an asymptotic value  $R/R_1 > 2$  after an initial escalation at  $R = R_1$ .

**Table 14.1** Table of test data (Courtesy Professor E.N. Lightfoot [3]) and analyzed results on rotating ultrafiltration of BSA solution

$C_b$ g/100 mL	Speed rev/min	$Re^*$	$E$	$Sc$	$v_{wa}$ expt cm/min	$D_b$ $cm^2/s$	$D_g$ $cm^2/s$	$D_g/D_b$	$Nu$ expt	$v_{wa}$ pred** cm/min
7.9	91	7781	1.29E-04	2.84E+04	0.025	3.52E-07	1.13E-07	0.32	3.38E+03	0.028
7.9	273	23,343	4.28E-05	2.84E+04	0.044	3.52E-07	1.16E-07	0.33	5.95E+03	0.049
7.9	700	59,855	1.67E-05	2.84E+04	0.073	3.52E-07	1.22E-07	0.35	9.87E+03	0.079
5.9	30	2565	3.90E-04	2.14E+04	0.02	4.67E-07	1.52E-07	0.33	2.04E+03	0.019
5.9	91	7781	1.29E-04	2.14E+04	0.034	4.67E-07	1.46E-07	0.31	3.47E+03	0.033
5.9	273	23,343	4.28E-05	2.14E+04	0.057	4.67E-07	1.39E-07	0.30	5.81E+03	0.056
5.9	700	59,855	1.67E-05	2.14E+04	0.1	4.67E-07	1.60E-07	0.34	1.02E+04	0.090
2.2	30	2565	3.90E-04	1.47E+04	0.027	6.80E-07	1.31E-07	0.19	1.89E+03	0.028
2.2	91	7781	1.29E-04	1.47E+04	0.05	6.80E-07	1.44E-07	0.21	3.50E+03	0.048
2.2	273	23,343	4.28E-05	1.47E+04	0.08	6.80E-07	1.28E-07	0.19	5.60E+03	0.084
1.47	30	2565	3.90E-04	1.33E+04	0.036	7.52E-07	1.62E-07	0.22	2.28E+03	0.032
1.47	91	7781	1.29E-04	1.33E+04	0.058	7.52E-07	1.44E-07	0.19	3.67E+03	0.056
1.47	273	23,343	4.28E-05	1.33E+04	0.095	7.52E-07	1.33E-07	0.18	6.02E+03	0.097

\* For  $Re$  calculation  $d = 2.86$  cm,  $\mu/\rho = 0.01$   $cm^2/s$ \*\*  $C_g = 58.5$  g/100 mL and mean  $D_g$ Mean  $D_g = 1.38E-07$   $cm^2/s$

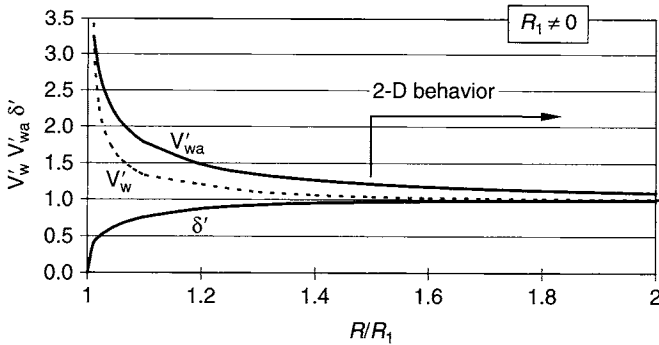


**Figure 14.5** Local flux  $v_w$ , average flux  $v_{wa}$  and mass transfer boundary layer thickness  $\delta$

Figure 14.5 brings out the important message that when  $R > R_1$  rotation dictates the mass transfer behavior it is constant independent of radius. This is due to the Taylor-Proudman phenomenon or two-dimensional phenomenon for rotating flow. Also the flow field can be controlled by the rotational speed of the membrane, which in turn controls the mass transfer rate, given the mass boundary layer is much smaller than that of the momentum boundary layer under the condition that  $Sc \gg 1$ .

### 14.2.3 Gel Concentration

Using the analytical solution, a semi-log plot of the experimental average membrane flux  $v_{wa}$  [3] versus bulk concentration is shown in Figure 14.6. According to the prediction, the behavior should be  $(C/C_b)^{1/3} - (C/C_b)^{-2/3}$ . Using this behavior to match the experimental data,  $v_{wa}$  becomes zero when the bulk concentration reaches 58.5 g/100 cc. This is also known as the gel concentration [2]. The behavior of  $(C/C_b)^{1/3} - (C/C_b)^{-2/3}$  can also be approximated by  $\log(C/C_b)$ . The logarithm behavior is plotted in Figure 14.6 side-by-side with the more exact behavior for reference. As can be seen, the bootstrapped  $C_g$  is close to each other for the two methods.

### 14.2.4 Determining Diffusivity

A most useful result from running rotating UF experiments is to determine protein diffusivity based on the measured permeate flux under gel condition (fully polarized) for different rotating membrane speeds. To facilitate this, let us take  $R_1 = 0$  and therefore  $f = 1$ . Equation 14.10a can be expressed explicitly as

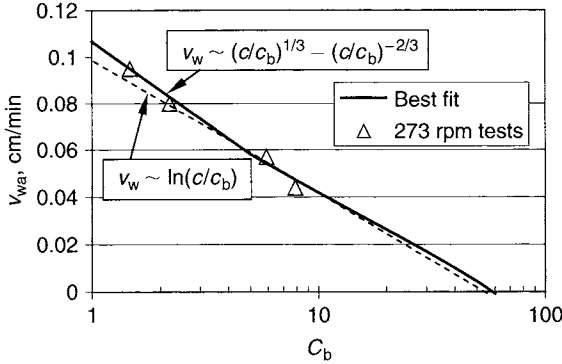


**Figure 14.6**  $C_g$  determined from bootstrapping  $v_{lim} = 0$

$$D_g = \frac{1}{2} \left[ \frac{(\mu/\rho)(v_{wa})^6}{\Omega^3} \right]^{1/4} \frac{1}{\left( \left[ \frac{C_g}{C_b} \right]^{1/3} - \left[ \frac{C_g}{C_b} \right]^{-2/3} \right)^{3/2}} \quad (14.11)$$

In this procedure, the gel concentration of the protein needs to be determined separately, as discussed in the foregoing.

### Example 14.2

$$\mu/\rho = 0.01 \text{ cm}^2/\text{s}$$

$$v_{wa} = 0.034 \text{ cm/min} = 0.000567 \text{ cm/s}$$

$$C_g = 58.5 \text{ g/100 cc}$$

$$C_b = 5.9 \text{ g/100 cc}$$

$$C_g/C_b = 9.915$$

$$\Omega = 91 \text{ rev/min} = 9.529/\text{s}$$

$$\begin{aligned} D_g &= \frac{1}{2} \left[ \frac{(0.01)(0.000567)^6}{9.529^3} \right]^{1/4} \frac{1}{\left( (9.915)^{1/3} - (9.915)^{-2/3} \right)^{3/2}} \\ &= 1.46 \times 10^{-7} \text{ cm}^2/\text{s} \end{aligned}$$

A more comprehensive calculation on other conditions of the gel diffusivity is given by Table 14.1. The calculated gel diffusivity ranges between  $1.13 \times 10^{-7} \text{ cm}^2/\text{s}$  and  $1.62 \times 10^{-7} \text{ cm}^2/\text{s}$ , with the mean value of  $D_g$  being  $1.38 \times 10^{-7} \text{ cm}^2/\text{s}$ . The protein diffusivity  $D$  is plotted in Figure 14.7 as a function of protein concentration under the physical-chemical

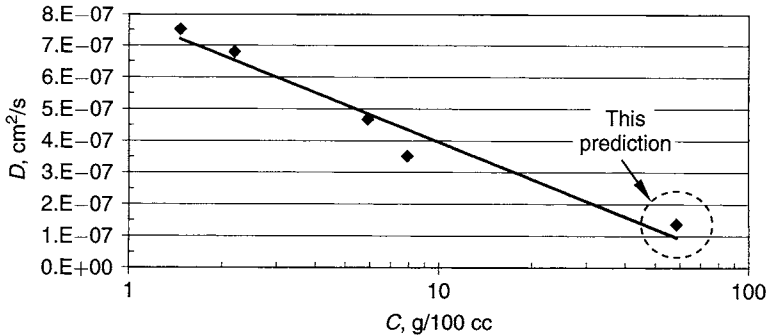


**Figure 14.7** BSA diffusivity at gel concentration with pH = 7, ionic strength = 0.275 M

condition that pH = 7 and ionic strength = 0.275 M. There were four feed concentrations used in the experiments, 1.47, 2.2, 5.9, and 7.9 g/100 cc, with diffusivity of the feed reported from direct measurement [3] as  $7.52 \times 10^{-7} \text{ cm}^2/\text{s}$ ,  $6.8 \times 10^{-7} \text{ cm}^2/\text{s}$ ,  $4.67 \times 10^{-7} \text{ cm}^2/\text{s}$ , and  $3.52 \times 10^{-7} \text{ cm}^2/\text{s}$ , respectively. Additional data is added from the present finding on gel diffusivity of  $1.38 \times 10^{-7} \text{ cm}^2/\text{s}$  under gel concentration of 58.5 g/100 cc. This extrapolated data from the indirect method developed herein on gel diffusivity is very much in alignment with the direct measurement of diffusivity taken under lower feed concentration. A similar method has been used [5] for non-rotating membrane systems.

## 14.2.5 Parametric Effects

### 14.2.5.1 Effect of Reynolds Number

The permeate flux under gel polarization can be predicted from the model described. The average flux expressed in cm/min is plotted in a log-log chart, Figure 14.8, versus Reynolds number  $Re$  defined by Equation 14.2a. According to the theoretical prediction, the flux should increase to the square root of  $Re$ . Indeed, each theoretical curve corresponding to a fixed Schmidt number becomes a straight line with a 0.5 slope in a log-log plot. Smaller  $Sc$  has a higher flux than one with larger  $Sc$  for the same  $Re$ . By definition of Equation 14.3,  $Sc$  is a ratio of kinematic viscosity to the diffusivity. When the kinematic viscosity is the same, lower  $Sc$  infers higher diffusivity, which leads to higher mass transfer.

The experimental data [3] are included in Figure 14.8 for comparison. In general, experiments and prediction compare well with each other. Perhaps it is more direct to chart out the average permeate flux

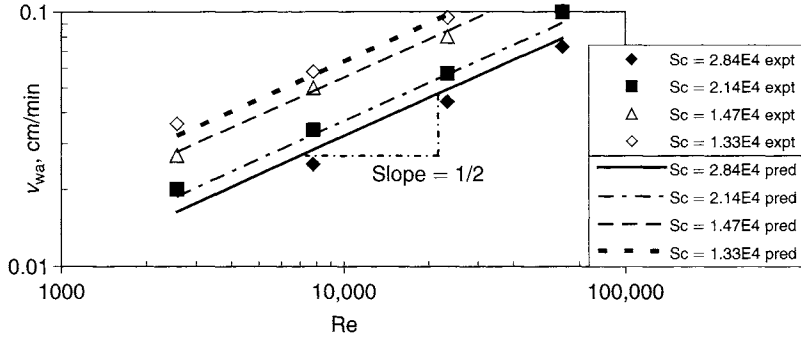


**Figure 14.8** Wall permeate flux versus Reynolds number

versus the rotation speed, which is by far the most convenient parameter to control in the experiment, as given by Figure 14.9. Both theoretical prediction and experimental data are replotted in this form in Figure 14.9 for comparison, and they are indeed in accord with each other. According to the prediction Equation 14.10a, the average permeate flux varies as the square root of the rotation speed, which is clearly delineated in the figure.

#### 14.2.5.2 Schmidt Number Effect

It is appropriate to define a dimensionless Nusselt number  $Nu$ , which measures the permeate flux  $v_{wa}$  to a characteristic diffusive velocity. The latter is related to the ratio of diffusivity and characteristic length, taken as the membrane peripheral diameter  $2R_2$ . Also, using the definition of  $Re$  and  $Sc$  from Equation 14.2b and Equation 14.3, respectively,  $Nu$  can be expressed as

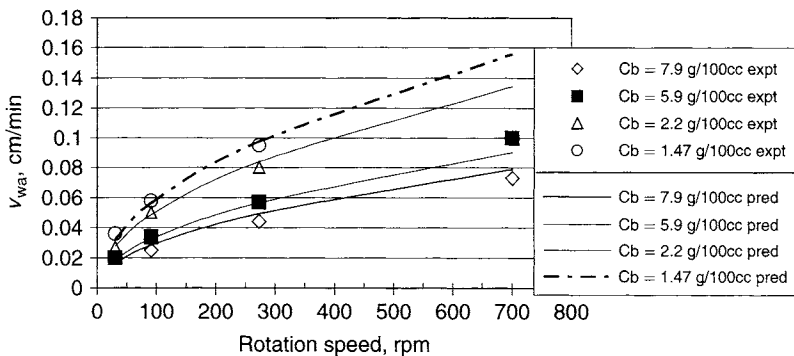


**Figure 14.9** Wall permeate flux versus rotation speed

$$\begin{aligned} \text{Nu} &= \frac{(-v_{wa})(2R_2)}{D_b} \\ &= 1.59 \left( \frac{D_g}{D_b} \right)^{2/3} \text{Sc}^{1/3} \text{Re}^{1/2} \left( \left[ \frac{C_g}{C_b} \right]^{1/3} - \left[ \frac{C_g}{C_b} \right]^{-2/3} \right) f \quad (14.12) \end{aligned}$$

Note that  $v_{wa}$  is negative, hence  $\text{Nu}$  is positive in Equation 14.12. Further, Equation 14.12 can be rearranged so that only  $1.59\text{Sc}^{1/3}$  is on the right side of the equation and the rest of the terms are on the left side of the equation. Such a Cartesian plot with the abscissa  $\text{Sc}^{1/3}$  yields a straight line with a slope of 1.59 passing through the origin. Also,  $f$  is taken to be unity for simplicity as  $R_1 \approx 0$ . Figure 14.10 shows such a plot with test data [3] recast in a similar format for making comparison. Despite some scattering, the straight line prediction passes through the data reasonably well.

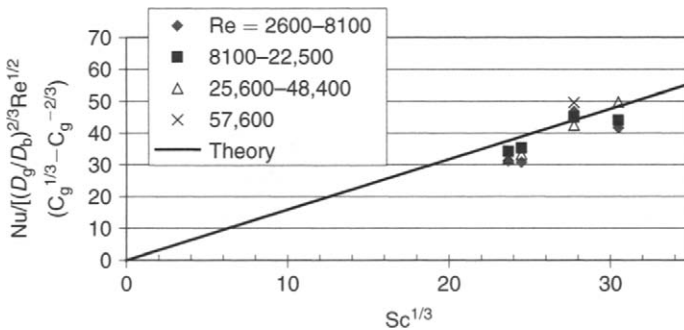


**Figure 14.10** Dimensionless flux versus Schmidt number to the one-third power

#### 14.2.5.3 Effect of Bulk/Feed Concentration

Equation 14.11 can be rearranged so that only the group involving concentration remains on the right side of the equation, and the rest of grouping stays with the  $\text{Nu}$  on the left side of the equation. The complex group plotted against the concentration group is given by the semi-log plot of Figure 14.11. Again,  $f$  is taken to be unity for simplicity (i.e.  $R_1 \approx 0$ ) in the prediction. The rotating membrane test data [3] is recast in the same format for comparison with the prediction. As is evident in the figure, the prediction is in good agreement with the experimental results.

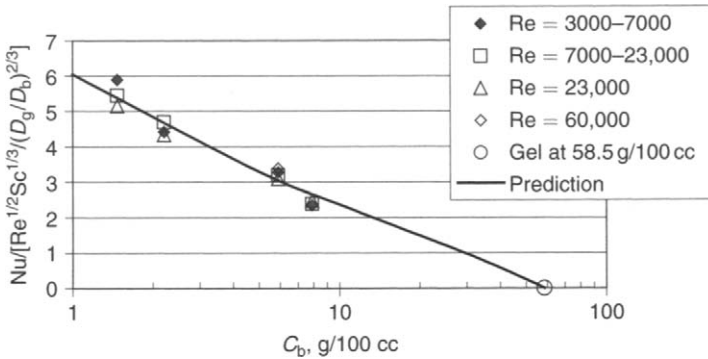


**Figure 14.11** Dimensionless permeate flux versus protein bulk/feed concentration

### 14.3 Rotating Membrane with Membrane Perpendicular to the *G*-Force

In the second part of this chapter, we investigate the transient effect for an innovative small-scale spintube installed with a filter or membrane absorber (chromatography), in which separation, concentration, and purification can be carried out sequentially in single equipment equipped with different modules serving different functions. Only the membrane is considered in the following discussion.

In a special case, the membrane is oriented perpendicular to the centrifugal acceleration  $G$ , and a pressure field is established by  $G$  effecting filtration. This is depicted in Figure 14.12. The pressure differential across the membrane helps to drive liquid and small solute molecules through the semi-permeable membrane, while protein and larger macromolecules are retained behind. The flow can be set up as a batch unit or as dead-end filtration, wherein the domain labeled ‘protein solution’ can be a part of a closed container, or as part of continuous cross-flow with feed coming in from the left of the domain ‘protein solution’

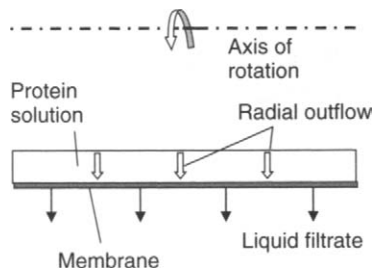


**Figure 14.12** Membrane perpendicular to  $G$ -force

and exiting to the right. This crossflow can suppress concentration polarization or deposition of protein on the membrane surface by carrying the deposited particles away from the membrane surface, reducing polarization.

### 14.3.1 Spintube Equipped with Membrane Module – Centrifugal Filter

In bioseparation, analytical rotating-tube centrifuge [6] is used to separate the suspended phase in the form of a pellet or sediment (see Figure 14.13a). The supernatant is decanted, after which a buffer or wash liquid can be introduced to recondition the sediment or wash the contaminant (e.g. salt) off the sediment. The resultant suspension is further filtered using UF membrane or with MF membrane, depending on the size and nature of the solids. Figures 14.13b and 14.13c show, respectively, schematics of a rotating tube equipped with different geometry membrane or filter medium.

The membrane geometry can take the form of a disk with the membrane parallel to the axis of rotation (Figure 14.12 and Figure 14.13b), or with the membrane perpendicular to the centrifugal acceleration  $G$ . Alternatively, it can be a cylindrical-shaped funnel or a cassette shape with its axis perpendicular to the rotation axis (Figure 14.13c). The funnel or cassette geometry, which fits nicely in a small diameter spintube, provides several advantages: an increase in filtration area with the cylindrical (funnel)/flat (cassette) surfaces, a larger effective radius with higher  $G$ , and reduces concentration build-up on the membrane with the Ekman flow keeping a thin controlled mass boundary layer. The limitation is the integrity of the seal and glue between the support and the membrane funnel/cassette when subject to centrifugal force. This design is suitable only for a small diameter spintube.

Tubes are available in swinging-bucket configuration, as shown in Figure 14.13a–c, or they are angled (such as shown in the left diagram of Figure 3.1) [5]. Fixed-angle tubes usually rotate at slightly higher speed. Maximum centrifugal acceleration is in the approximate 12,000  $g$  range. The centrifugal filters are for one-time or limited uses, to eliminate problems related to sanitation and cross-contamination.

For concentration of protein, the requirement is to use low adsorption membrane, such as hydrophilic regenerated cellulose membrane, so that protein does not bind or be adsorbed to the membrane, resulting in high protein recovery, typically upwards of 90%. Also, for a design after concentration, the sample reservoir can be spun inverted to force trapped liquid (with concentrated protein) in the medium-and-support back to

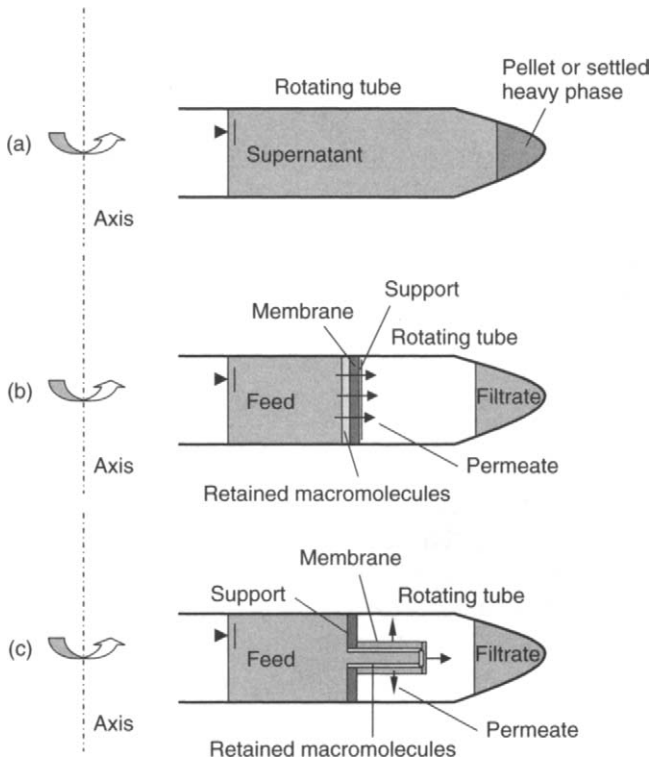


**Figure 14.13** (a) Schematic of spintube (swing bucket type), (b) schematic of spintube equipped with disk-shaped membrane or filter medium, (c) schematic of spintube equipped with cylindrical/cassette-shaped membrane or filter medium

the sample reservoir under reduced centrifugal force. The molecular weight cut-off (MWCO) of the membrane varies from 5000 to 100,000. Typically, the MWCO of the membrane is selected to be two to three times larger than the solute (i.e. protein) molecular weight MW.

With high  $G$ 's in the range of 4000–5000  $g$  for swinging-bucket design and up to 7000  $g$  for smaller tube fixed-angle design, a very high concentration factor of 50 (small tube)–100 or more (large tube) can be achieved. Also, the higher  $G$  reduces the centrifugation time, which translates to higher throughput capacity. On the other hand, the centrifugation time depends on the desired recovery and concentration factor; it varies anywhere between 10 and 30 minutes. Sample feed volumes are available from 2 to 15 mL.

For desalting, a wash liquid can be added to the feed if it is desired to remove salt, or a buffer solution can be added for buffer exchange and reconditioning. This would have been done in a continuous membrane

process by adding the wash liquid or buffer liquid in diafiltration in one step, or repeated steps as necessary to achieve the desired purity.

Larger tubes with 20 mL and 80 mL, which typically fit centrifuge spintubes respectively of 50 mL and 250 mL, are also available for separating larger samples. The  $G$ -force is somewhat lower, as compared to the smaller spintube discussed in the foregoing, in the range of 3500–4000  $g$  depending on the size. However, this can be compensated by increasing centrifugation time. The tubes are made of polypropylene (autoclavable) while the UF membrane is made of regenerated cellulose, which is compatible with a wide range of solvents.

Alternatively, there are also smaller units available commercially with higher  $G$ -force exceeding 10,000  $g$  for finer filtration, such as for DNA and RNA separation and concentration.

Some examples of applications are concentration and desalting of chromatography elutes, clean-up of cell lysate, concentration of monoclonal antibodies, virus concentration from culture supernatants, and clarification of tissue homogenates.

A centrifugal microtube filter has a small volume of 250  $\mu\text{L}$  and a UF membrane. The microtube is typically operated at much higher  $G$ -force, in the neighborhood of 10,000–15,000  $g$ . The hold-up volume is maintained small, say 5  $\mu\text{L}$ , to ensure a high CF (concentration factor) for concentration applications. Also, microporous absorber can be used to retain the macromolecules, like protein and enzyme, while allowing smaller solute, such as DNA, to pass through. One application is to separate the DNA from the enzyme protein for a reaction mixture. After centrifugation, say for a minute or less, the enzyme is adsorbed to the membrane while the DNA and solution freely pass through the membrane. In the event that the DNA concentrate needs to be desalted or buffer exchanged, another UF filter is placed in between the membrane absorber and the microtube so that the original sample diluted with wash liquid and buffer solution are all centrifuged. The result is that the enzyme is adsorbed, the DNA is concentrated by the downstream UF membrane, while the wash liquid containing the removed salt passes through the UF membrane to be collected at the bottom of the microtube or vial (see Figure 14.14a). For further purification, the membrane absorber is removed with additional wash liquid to wash the concentrated DNA trapped on the UF membrane followed by centrifugation to spin off the washed liquid (see Figure 14.14b). Very high purity can be achieved with this batch-wise diafiltration. An important note is that the DNA is not altered in this separation and purification step, which is vital for downstream processing. This can all be accomplished in a few minutes. This purification step of DNA eliminates the traditional heat process to deactivate the enzyme.

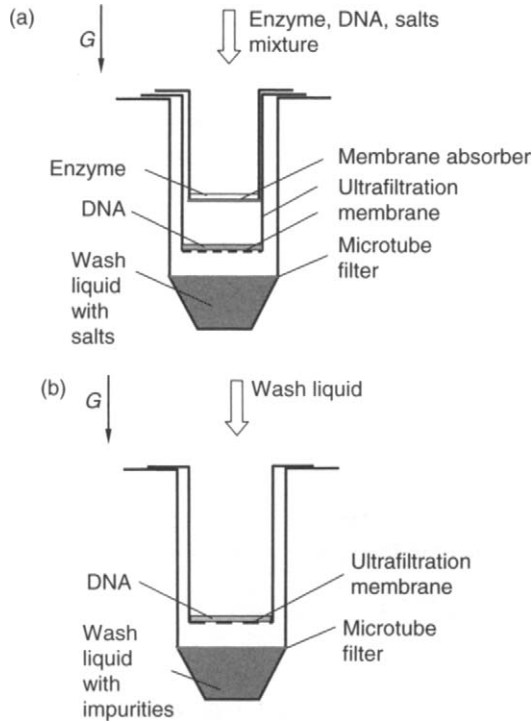


**Figure 14.14** (a) Mixture of enzyme, DNA, salts and other impurities separated by the microfilter equipped with two concentric modules with membrane absorber and ultrafiltration membrane, respectively. (b) The absorber module is removed and the trapped DNA is washed with wash liquid to remove impurities

Microporous membranes are available as a filter media. The objective is to filter out suspended solids and particulates, such as cell debris in a protein solution, without losing the protein (solute). The particulates are trapped in the filter medium acting as a depth filter or on the surface of the medium, forming a deposit/sediment. Microporous membrane is spec out with nominal pore sizes between  $0.1 \mu\text{m}$  and  $5 \mu\text{m}$ , and they are characterized with low-protein binding, such as PVDF membrane, or with a strong solvent resistance property, such as PTFE membrane.

### 14.3.2 Model on Swinging Bucket Equipped with UF Membrane

A simple model is developed for dead-end filtration using an ultrafiltration membrane with the geometry as depicted in Figure 14.13b,c. (In the case of Figure 14.13c, an equivalent membrane radius from the axis of rotation needs to be defined.) Assuming the resistance to filtration

across the membrane is primarily due to the back pressure from osmosis as a result of concentration polarization on the pressure side of the membrane. Further, the concentration is assumed uniform in the bulk solution, which is strictly not valid. One possible source of mixing in the solution is due to secondary flow, which arises as liquid flows radially outwards in a centrifugal field (from permeation through the membrane), causing concurrently a retrograde motion of liquid rotating backwards with respect to rotation. The liquid flows from the side wall to the bulk solution, resulting in circulating eddies and causing mixing.

The permeate flux is given by

$$v_w = \frac{\Delta p - \pi(C)}{r_m} \quad (14.13)$$

$v_w$  is the permeate flux and  $\Delta p$  is the transmembrane pressure.  $\pi$  is the osmotic pressure and depends on the concentration of the wall upstream, typically represented by a polynomial correlation of the form [7]

$$\pi(C) = a_0 + a_1C + a_2C^2 + a_3C^3 + \dots \quad (14.14)$$

The solute concentration  $C$  is assumed uniform across the solution upstream of the membrane.  $r_m$  is the membrane resistance; embodied in it is the permeability of the membrane  $K_m$ , viscosity of the solution  $\mu$ , and the thickness of the membrane  $\ell$ . Note that the viscosity of the liquid is a function of operating temperature. Thus,

$$r_m = \frac{\mu \ell}{K_m} \quad (14.15)$$

Under centrifugal field, the transmembrane pressure  $\Delta p$  is given by

$$\Delta p = \frac{1}{2} \rho \Omega^2 (R_b^2 - R_p^2) \quad (14.16)$$

$R_p$  is the radius of the pool surface and is a function of time.  $R_b$  is the radius of the filter medium which in this case corresponds to the membrane. Initial condition requires

$$R_p = R_o \quad \text{at } t=0 \quad (14.17)$$

Also, by continuity the permeate flux velocity is directly related to the increase in liquid-pool radius,  $dR_p/dt$ ,

$$\frac{dR_p}{dt} = v_w = \frac{\frac{1}{2} \rho \Omega^2 (R_b^2 - R_p^2) - \pi(C)}{r_m} \quad (14.18a)$$

After rearranging

$$\text{Le}_f \equiv \frac{\rho G t}{r_m} = \frac{K_m G t}{(\mu/\rho)\ell} = 2 \int_{R_o/R_b}^{R_p/R_b} \frac{d\zeta}{(1-\zeta^2) - \pi(C)/\left(\frac{1}{2}\rho\Omega^2 R_b^2\right)} \quad (14.18b)$$

$\text{Le}_f$  is a dimensionless parameter measuring the kinetics of filtration and  $\zeta$  is a variable used in integration.  $\text{Le}_f$  is proportional respectively to the membrane permeability  $K_m$ ,  $G$  the centrifugal acceleration measured with respect to the radius of the membrane, and time  $t$ . It is inversely proportional to the kinematic viscosity  $\mu/\rho$  and the membrane thickness  $\ell$ .

$$G = \Omega^2 R_b \quad (14.19)$$

The rejectivity of macromolecule by the membrane is assumed to be 100%, and by mass balance the average concentration  $C(t)$  on the pressure side of the membrane is given by

$$(R_b - R_o)C_o = (R_b - R_p)C$$

or

$$C(t) = \frac{1 - R_o/R_b}{1 - R_p(t)/R_b} C_o \quad (14.20)$$

By stepping in small increments in  $R_p/R_b$  from an initial value  $R_o/R_b$ ,  $C$  can be determined from Equation 14.20, and  $\text{Le}_f$  can be calculated numerically from Equation 14.18b for a given osmotic pressure behavior  $\pi(C)$ . Thus,  $R_p/R_o$  can be determined as a function of  $\text{Le}_f$ , which is directly proportional to time  $t$ . By mass conservation the ratio of the filtrate volume  $V(t)$  to the initial feed volume  $V_o$  is related to the radii as follows:

$$\frac{V(t)}{V_o} = \frac{R_p(t)/R_b - R_o/R_b}{1 - R_o/R_b} \quad (14.21)$$

The concentration factor for the separation is defined as the initial feed volume  $V_o$  to the volume of the concentrate or retentate,  $(V_o - V)$ ,

$$\text{CF} = \frac{V_o}{V_o - V(t)} = \frac{1}{1 - V(t)/V_o} \quad (14.22)$$

The CF can be very large for these devices. Also, it is important to have a small hold-up volume due to the membrane and the membrane support, so that the retentate can be fully recovered. As discussed, in a commercial design the modular sample reservoir, which is integral with the membrane unit, can be removed from the cup holder, capped at the opposite end, and reversely placed in the holder. After being centrifuged at relatively lower speed, a fraction of liquid trapped in the membrane and support is recovered, together with the retentate in the sample reservoir, to achieve an over 90% retentate recovery.

### 14.3.3 Comparing Test Results with Predictions

#### Example 14.3

Bovine serum albumin (BSA) with MW of 67,000 was tested with two different sizes of spintubes equipped with an UF membrane with nominal MWCO of 10,000. The first was a spintube with a sample volume of 20 mL, typically used with a holder for 50-mL spintube without filter element. The second was a large spintube with a sample volume of 80 mL typically used with a holder for 250-mL spintube without filter element.

Several feed concentrations of the BSA have been tested respectively, 0.25 mg/mL, 1.0 mg/mL and 5.0 mg/mL. Figure 14.15a shows the test data for the 20-mL tube, while Figure 14.15b shows test data for the 80-mL tube. Each case was tested with these three different concentrations of BSA protein solutions. For reference, the pure phosphoric buffer saline (PBS) is also shown. The saline flux shows the permeability of the membrane without the macromolecular solution, and gives the highest accumulated filtrate over time. Increasing feed solids (dissolved solids) concentration only increases the viscosity and further hampers filtration. In each case of filtering a given BSA solution of predetermined concentration, the filtrate volume eventually reaches the maximum volume of the sample, less the concentrate or retentate retained in the sample reservoir. Given the retentate is much smaller than the original sample (feed), CF can be very large, on the order of 50 to 100 and higher.

The slope to the curve is the rate of filtration  $v_w$ , and it decreases sharply with time due to an increase in the osmotic pressure in the protein solution in the sample reservoir upstream of the membrane with reduced feed volume and consequently higher solute concentration. In contrast, the driving liquid head (i.e. transmembrane pressure) also decreases as the pool radius  $R_p$  increases (see Equation 14.16). In the vicinity of the maximum filtrate volume, the filtration rate  $v_w$ , which is the slope of the curve, drops almost to zero.

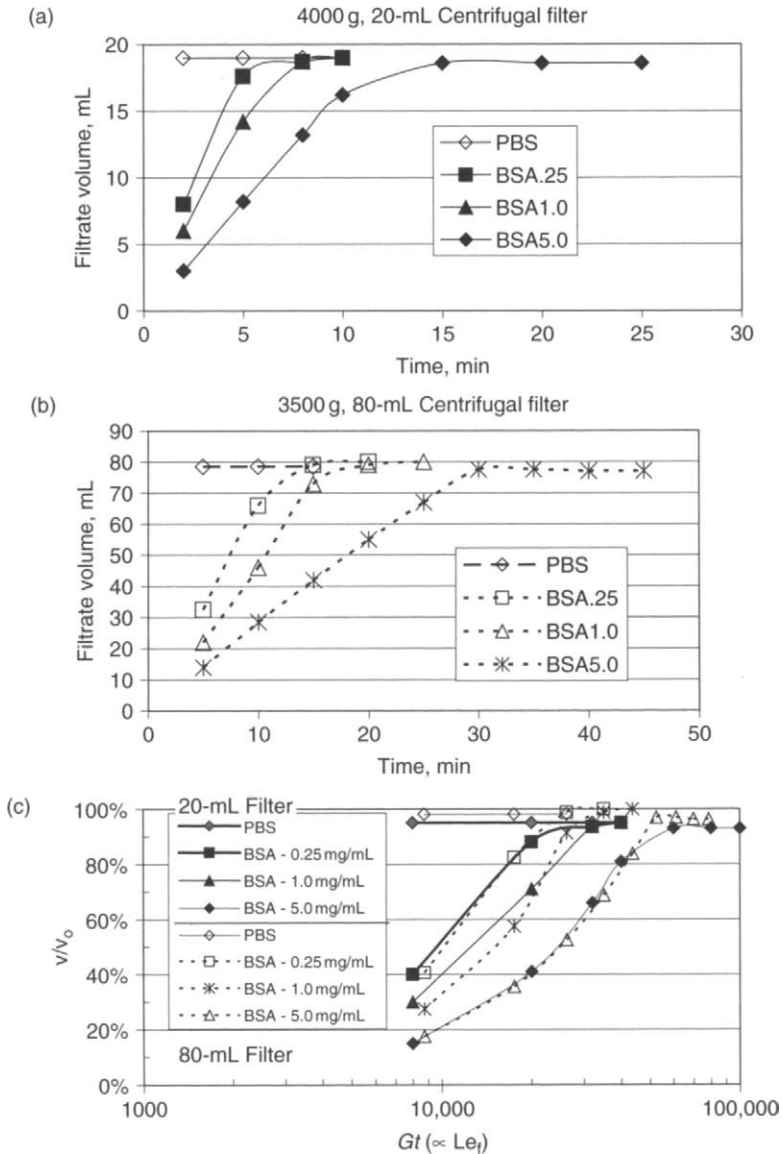


**Figure 14.15** (a) Filtrate versus centrifuged time under  $G = 4000$  g for a spintube with a UF membrane with initial volume of 20 mL of BSA solution with different initial solute concentrations (Reproduced by permission of Millipore Corporation). (b) Filtrate versus centrifuged time under  $G = 3500$  g for a spintube with a UF membrane with initial volume of 80 mL of BSA solution with different initial solute concentrations (Reproduced by permission of Millipore Corporation). (c) Results from two different centrifugal filter test geometries on BSA are normalized with respect to variation in  $G$  and  $t$  based on consideration of  $Le_f$

Figures 14.14a and 14.14b are re-charted in Figure 14.15c, wherein the abscissa is plotted in terms of  $Gt$ , and the ordinate in  $V/V_o$  (filtrate to the maximum filtrate volume) inspired by the scale-up law of Equation 14.18b in that only  $G$  and  $t$  vary in the tests for a given feed concentration. The nominal  $G$  as measured at the large radius of the spintube for the 20-mL tube and the 80-mL tube is, respectively, 4000 g and 3500 g. It is taken that the effective membrane radius  $R_b$  for the 20-mL tube is twice that for the 80-mL tube due to the design difference of the membrane between the two models (one with a cylindrical membrane design at a larger radius in a small polypropylene tube similar to Figure 14.13c, and the other with a disk membrane design at a smaller radius located in a large tube similar to Figure 14.13b).

Assuming further that the viscosity of the filtrate is related to the feed solids concentration by

$$\frac{\mu(C)}{\mu(C^*)} = \left( \frac{C_o}{C^*} \right)^n \quad (14.23)$$

The experimental data in Figure 14.15 is replotted in Figure 14.16a using the above ad hoc correlation in which  $n$  is taken as  $1/3$ . As can be seen in Figure 14.16a, all the curves are collapsed into one common curve which provides a basis of correlation for different  $G$ ,  $t$ , and feed solids concentration. Furthermore, using a normalized osmotic pressure form in Equation 14.16a

$$\frac{\pi}{\frac{1}{2} \rho \Omega^2 R_b^2} = 0.002 + 0.003 C^2 \quad (14.24)$$

and with the following properties

$$\begin{aligned} K_m &= 1.3 \times 10^{-13} \text{ cm}^2 \\ \mu/\rho &= 0.02 \text{ cm}^2/\text{s} \\ \ell &= 0.01 \text{ cm} \end{aligned}$$

$Le_f$  can be calculated and the test results are graphed in  $Le_f$  in the abscissa in Figure 14.16b. The data are compared with the theoretical prediction using the osmotic pressure correlation. As can be seen, the agreement is reasonable. The  $S$ -shaped curves for both prediction and test results are similar. Of interest is that the actual data shows a much steeper  $S$ -shape compared to prediction.

As noted above, for the range of  $V/V_o$ , between 0 and 1,  $Le_f$  varies by over one log cycle, as seen in Figures 14.15c, 14.16a and 14.16b.

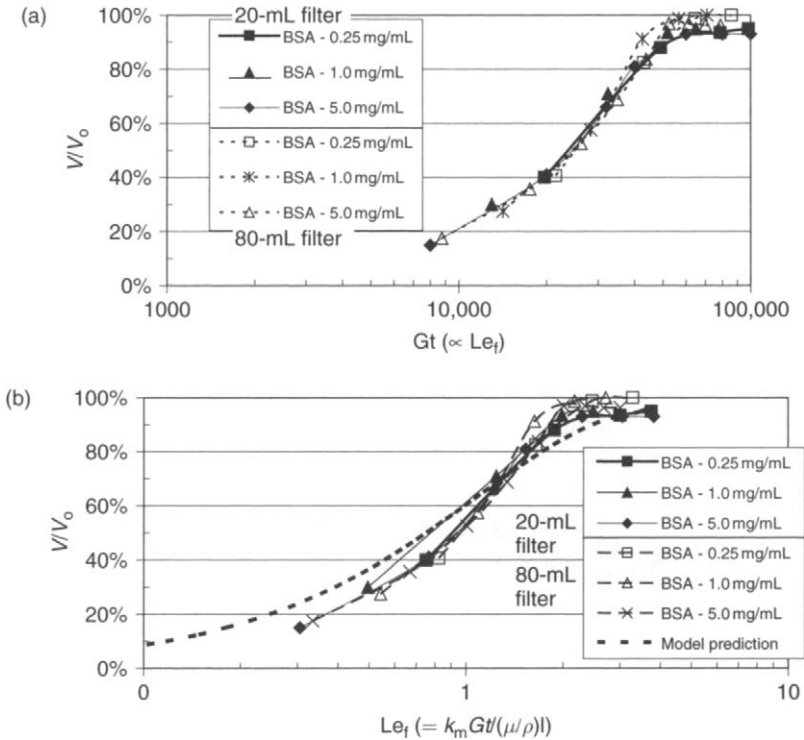


**Figure 14.16** (a) All test results normalized with viscosity,  $G$  and  $t$ . (b) Comparing theoretical prediction using UF model with test data at different  $G$ ,  $t$ , and feed solids

#### Example 14.4

Protein cytochrome  $c$  with concentration  $50 \mu\text{g}/\text{mL}$  has been filtered using both the 20-mL and 80-mL centrifugal filters. The cytochrome  $c$  has MW of 12,400 while the UF membrane used in these filters has NMWCO of 10,000. Very high CF can be achieved in these tests in upwards of 200, with small retentate volume less than 0.3 mL. Also, the recovery of the retentate (minus losses in the hold-up volume from the membrane and support) is quite high in +90%, due to inverting the sample module to recover additional retentate from the membrane and support. The filtrate volumes collected over time, respectively for the 20-mL tube and 80-mL tube, are given in Figure 14.17.

Using the same approach as in Example 14.3, the data are replotted in terms of  $Gt$ , which is proportional to  $Le_f$  in Figure 14.18. Again excellent correlation is found.

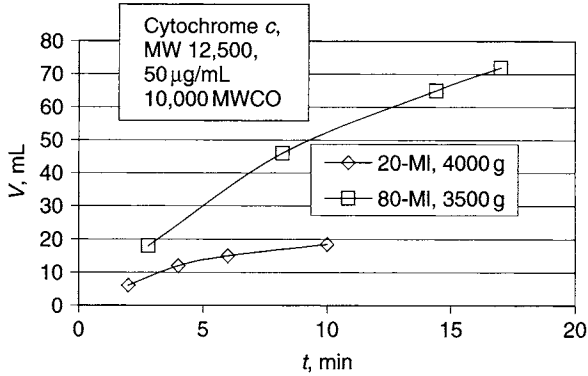


**Figure 14.17** Filtrate volume versus centrifuged time (Reproduced by permission of Millipore Corporation)

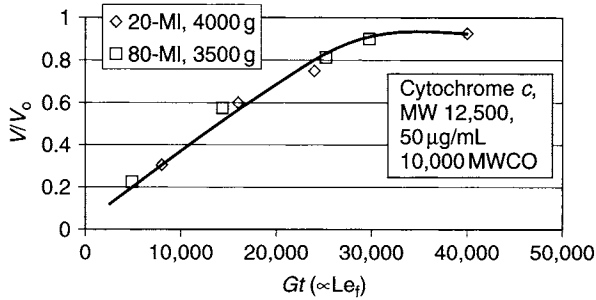


**Figure 14.18** Fraction of filtrate to the maximum volume versus  $Gt$ . Note that  $Gt$  is proportional to  $Le_f$

It is noted that the shape of the curve remains unchanged even if Figure 14.18 was plotted in terms of  $Le_f$ . This is because  $Le_f$  equals to a constant  $[= K_m/(\mu/\rho)\ell]$  multiplied by  $Gt$ . Along the log axis, the multiplicative constant amounts to a translation of the curve without changing the shape of the curve. This is because  $\log(GtK_m/(\mu/\rho)\ell) = \log(Gt) + \log(K_m/(\mu/\rho)\ell)$ .

The spintube equipped with a membrane or appropriate filter medium provides a convenient way of washing and purifying a small sample with good recovery of the concentrate or retentate. The latter is especially the case where the membrane module allows the sample reservoir to be inverted with the  $G$ -force directing the recovered trapped liquid in the medium-and-support and returned to the sample reservoir. Also, a high concentration factor and short spin time can be attained.

## 14.4 Summary

Two scenarios of rotating membrane are discussed in this chapter – one based on steady-state ultrafiltration of macromolecular solution using a rotating disk membrane wherein the  $G$ -field is parallel to the membrane, and the other on transient or time-dependent ultrafiltration using a spintube equipped with a membrane wherein the  $G$ -field is perpendicular to the membrane. The effect of rotation is quite different, as one might have expected in each of the scenarios setting aside the time effect. A third scenario that we have not considered is similar to the first case where the  $G$ -field is parallel to the membrane surface. The secondary flow set up by rotation provides mass boundary layer control, while the membrane transmembrane pressure is provided by the hydrostatic pressure from the  $G$ -field, this is similar to the setup in Figure 14.13c.

UF models under respectively low and high concentration polarization are used to interpret some experimental results on protein solution relating to effects on rotation speed or centrifugal acceleration, centrifugation time (for spintube), filtrate viscosity, and feed solute concentration. Dimensionless parameters for both steady-state rotating disk and unsteady-state centrifugal filter in a spintube are presented. The models facilitate the design of test protocol, interpretation of testing, scale-up to various operating and test conditions, improving the operation of existing filters, as well as optimizing future rotating filter design.

## References

- [1] W.K. Wang (ed.), *Membrane Separations in Biotechnology*, Marcel Dekker, New York, 2001.
- [2] Michaels, A.S., New separation technique for the CPI, *Chem. Engin. Prog.* 64, pp. 31–43, 1968.
- [3] E.N. Lightfoot, private communication.
- [4] J.S. Shen, R.F. Probstein, W.W. F. Leung, Ultrafiltration of macromolecular solutions at high polarization in laminar channel flow, *Desalination*, 24, pp. 1–16, 1978.
- [5] R. Probstein, W.W.F. Leung, Y. Alliance, Determination of diffusivity and gel concentration in macromolecular solutions by ultrafiltration, *J. of Phys. Chem.* 83, pp. 1228–1232, 1979.
- [6] W.W.F. Leung, *Industrial Centrifugation Technology*, McGraw-Hill, New York, 1998.
- [7] W.W.F. Leung and R. Probstein, Low polarization in laminar ultrafiltration of macromolecular solution, *I&EC Fund.*, vol. 18, p. 274, 1979.

## Problems

- (14.1) A rotating disk ultrafiltration membrane of diameter 10 cm is filtering a pressurized protein solution of MW 69,000, viscosity of 10 cP, and density  $1000 \text{ kg/m}^3$ . The diffusion coefficient of the protein solution is  $1 \times 10^{-7} \text{ cm}^2/\text{s}$ . The disk membrane is rotating at 500 rev/min. Calculate the (a) Reynolds number, (b) Ekman number, and (c) Schmidt number.
- (14.2) What is (a) the momentum boundary-layer (or Ekman layer) thickness and (b) the mass boundary-layer thickness for Problem (14.1)?
- (14.3) What would be the (a) momentum and (b) mass boundary-layer thicknesses when the rotating disk slows down to 0.5 rev/min?
- (14.4) The disk membrane of Problem (14.1) is immersed in a protein solution with viscosity 1 cP and liquid density  $1000 \text{ kg/m}^3$ . The membrane disk has an outer diameter of 10 cm. The applied pressure is sufficiently high to trigger gelation of protein on the membrane surface. Further increase in pressure only results in equal increase in flow resistance with no additional increase in permeate flux. Assuming the diffusion coefficient of protein at gelation is determined to be  $1.38(10^{-7}) \text{ cm}^2/\text{s}$ , and the feed concentration and the gel concentration are respectively 4 g/100 mL and 58.5 g/mL, how much permeate liquid will be collected in one minute?
- (14.5) Repeat Problem (14.4) for the case when the rotating membrane slowed down to 0.5 rev/min. Determine again the volume of permeate collected over one minute.
- (14.6) In the transient centrifugal filter in which it is operated below critical flux condition, the osmotic pressure dictates the permeate flux. For the same centrifugal equipment, a lab technician is running a centrifugal filter at 3000 g and for  $t = 20 \text{ s}$ ; the same filtrate amount should be obtained using the same apparatus when the rotor speeds up to 10,000 g and for a shorter time duration. What is this time duration?

# Appendix A: Nomenclature

$A$	area, $m^2$
$a$	coefficient
$a_c$	Coriolis acceleration, $m/s^2$
$b$	coefficient
$c$	insoluble solid concentration, v/v or # cells/mL or coefficient
$C$	solute concentration, g/L
$C_{loss}$	loss coefficient, [-]
CF	concentration factor, [-]
$D$	bowl diameter, m or diffusivity, $m^2/s$
$d$	particle diameter or disk membrane diameter, m
$E$	Ekman number, [-]
$F$	cumulative undersize distribution, %
$f$	frequency distribution or function, [-]
$G$	centrifugal acceleration, $m^2/s$
$g$	Earth gravity ( $9.81 m^2/s$ )
$H$	suspension height, m
$h$	height, depth or thickness, m
$I$	integral, [-]
$K$	cake permeability, $m^2$
KE	kinetic energy, W
$L$	length, m
Le	Leung number in centrifugal separation, [-]
$Le_f$	kinetic parameter for membrane filtration, [-]
$M$	mass flow rate (dry basis), kg/s
$N$	number
Nu	Nusselt number, [-]
$n$	number of disks or exponent
$P$	pitch, m or power, W
$p$	pressure, Pa
$Q$	volumetric flow rate, $m^3/s$
$R$	radius, m
RCF	relative centrifugal force, [-]
Re	Reynolds number, [-]
rpm	revolution per minute
$R'$	effective radius, m

$R_e$	solids recovery in centrate, %
$R_{ex}$	exit of feed accelerator, m
$R_s$	solids recovery in cake/concentrate, %
$r$	gear ratio, [-] or radial coordinate, m
$r_m$	membrane resistance, $\text{kg/m}^2\text{-s}$
$S$	sedimentation coefficient, s
$Sc$	Schmidt number [-]
$SR$	size recovery of a given particle size in centrate, %
$T$	torque, N-m
$t$	time, s
$t_s$	time duration between intermittent discharge from dropping-bottom disk centrifuge, s
$u$	throughflow velocity with transverse variation, m/s
$U$	throughflow velocity, constant across channel, m/s
$V$	volume, $\text{m}^3$
$V_s$	solids hold-up volume in disk centrifuge or sediment volume in spintube, $\text{m}^3$
$v$	velocity, m/s
$v_c$	average Coriolis velocity, m/s
$v_r$	relative velocity, m/s
$v_s$	settling velocity of a concentrate suspension, m/s
$v_{so}$	Stokes' free settling velocity, m/s
$v'_w$	normalized membrane wall flux, [-]
$v'_{wa}$	normalized averaged membrane wall flux, [-]
$v_\theta$	angular velocity, m/s
$W$	solid concentration by weight fraction
$x$	particle size, micron
$Y$	protein yield
$y$	transverse coordinate, m
$Z$	size capture, [-]
$z$	linear spatial coordinate, m

## Subscripts

a	acceleration, average, or atmospheric
b	bowl or bulk region further from membrane
c	concentrate/cake, cut size, or critical trajectory
cake	cake solid
d	dimensionless or concentrate discharge
Ek	Ekman layer
e	centrate

ex	exit of accelerator
f	feed
G	centrifugal acceleration
g	gel
i	index, inner radius, or species
k	index
L	liquid or load
m	membrane
o	reference and outer radius
p	pool, pinion, projected length, or liquid permeate
s	sediment, concentrate, cake, solid, or settling
w	wall
100	100%

## Symbols

$\alpha$	helix angle, radian/degree
$\beta$	beach angle, radian/degree
$\Delta$	change
$\delta$	boundary-layer thickness, m
$\delta'$	normalized boundary layer, [-]
$\eta$	efficiency, [-]
$\mu$	viscosity of liquid, kg/m-s
$\mu'$	effective viscosity, kg/m-s
$\phi$	solid volume fraction, [-]
$\lambda$	hindered settling factor, [-]
$\rho$	density, kg/m <sup>3</sup>
$\Delta\rho$	density difference, kg/m <sup>3</sup>
$\theta$	angle between disk and vertical, deg/rad
$\Delta\Omega$	differential speed, rev/m
$\Omega$	rotational speed, rev/m
$\Delta p$	pressure drop, Pa
$\Re$	membrane rejectivity, [-]
$\pi$	osmotic pressure, Pa
$\ell$	membrane thickness, m



# Appendix B: Answers to Problems in the Chapters

## Chapter 2

- (2.1) 5.1 h
- (2.2) 0.57 h
- (2.3) 21 days
- (2.4) (a) 5.7 h and (b) 0.51 h
- (2.5) 566 h and (b) 51 h
- (2.6) Settling rate varies as particle size to the square power, linearly with  $G$ , and inversely with viscosity.
- (2.7) 25 m/s
- (2.8) 36 m/s and 11 m/s
- (2.9) 531 and 1101
- (2.10) 69%, 48.2%, quadratic power

## Chapter 3

- (3.2) 42.9 mm, 8846 rev/min
- (3.3) 2.94 mL/min
- (3.4) 11.77 mL/min

## Chapter 4

- (4.1) 0.037 s
- (4.2) 0.41 s, 3.67 s, and 40.77 s
- (4.3) 6 s, 1 micron, 3.33 microns, 10 microns
- (4.4) 26 L/min
- (4.5) 194,444 Pa and 192,222 Pa

## Chapter 5

- (5.2) 35 rev/min
- (5.3) 23.3 rev/min

- (5.4) 2400 rev/min (same direction as the rotating bowl)  
 (5.5)  $0.53^\circ$  at cone-cylinder intersection,  $0.80^\circ$  at conical discharge diameter

## Chapter 6

- (6.1) (a) 92.2% (b) 79.2%, (c) 98.4%

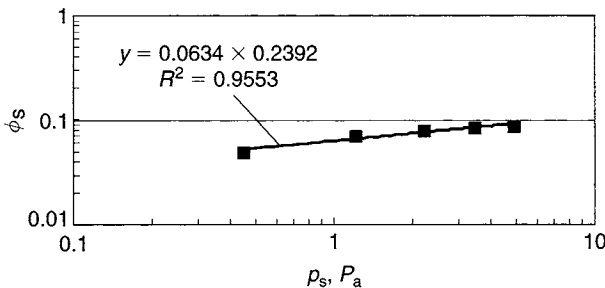
## Chapter 7

- (7.1) 3.8 min, yes  
 (7.2) 6741 rev/min  
 (7.3) See below:  
 (a)

**Table 7A** Example of compaction affecting product yield

Sample	$R$ (cm)	$\phi_s$ [-]	$\Delta p_s$	$p_s$
1	5	0.05	0.45	0.45
2	6	0.07	0.756	1.206
3	7	0.08	1.008	2.214
4	8	0.085	1.224	3.428
5	9	0.088	1.4256	4.8636

- (b) Similar to Figure 7.9.  
 (c) 0.2392



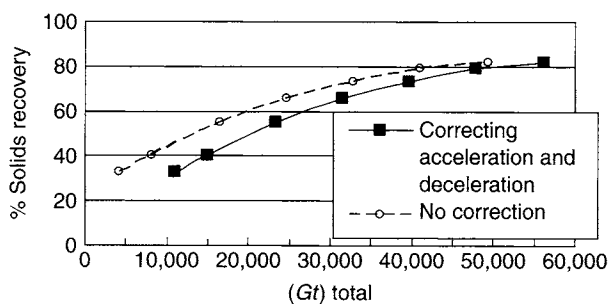
Centrifugal test data shows that solids volume fraction increases as a power law with solids stress/pressure.

## Chapter 8

(8.1)

Table 8A

<i>t, s</i>	<i>Gt at Omega</i>	<i>Gt acc+ dec</i>	<i>G total</i>	<i>Solids recovery (%)</i>
0	0	6847	6847	Nil
5	4108	6847	10955	33
10	8216	6847	15063	40
20	16433	6847	23279	55
30	24649	6847	31496	66
40	32865	6847	39712	73
50	41081	6847	47928	79
60	49298	6847	56145	82



(8.2) 90.5%, 9.5%

(8.3) 2.34 min

## Chapter 9

(9.3) 4.62, 7.82, cut size smaller than the mean yeast size

(9.4) 310 s

(9.5) 120 s

(9.6) 10,000 g

(9.7) 63 L/min

(9.8) 99.2 L/min

(9.9) (a) 4.08 (b) 6.9 microns

(9.10) 9.6 L/min

## Chapter 10

(10.7) -6%

## Chapter 13

(13.2) 2.8

## Chapter 14

(14.1) (a) 52,360 (b)  $1.91(10^{-5})$  (c)  $1(10^6)$

(14.2) (a) 0.44 mm (b) 0.0044 mm

(14.3) (a) 13.8 mm (b) 0.138 mm

(14.4) 28.4 mL

(14.5) 0.9 mL

(14.6) 6 s

# Index

- accelerating 26, 81, 86, 95, 165, 203
- accelerating cone 52
- acceleration 26, 28, 148, 80, 81–84, 147–148
- accelerator 78, 80, 81, 84, 85, 86, 95
- accelerator vanes 48, 79, 84, 86
- acidity 143, 159, 204
- aggregation 29
- alkalinity 143, 159
- angle-head 38, 39, 40
- angle of attack 85
- angular momentum 28
- animal 1, 2, 126
- antibiotics 111
- antibodies 2, 274, 111
  
- back-drive 98, 99, 100
- back-pressure 75, 115, 276
- bacteria 1, 5–6, 10, 12, 78, 88, 111, 119, 240
- baffle 79, 104, 105, 201
- baseline 230
- batch 7, 8, 9, 37, 113
- beach 95, 96, 103, 104
- bench-scale 143–145
- Bernoulli's Equation 75–77
- biopharmaceutical 2, 4, 5, 11–12, 110–112, 165, 195, 252
- bioprocessing 95, 124, 196–197
- bioreactor 5, 11, 15, 65, 112–113, 169, 171, 172, 190, 232
- biosolids 40, 100, 101, 103, 134, 136–137, 144
- biotechnology 1, 4, 141
- blood plasma 125–126
- bottle 171, 173–175
- boundary layer 50, 201, 255, 259–260, 261, 262, 264, 266, 272
- bovine serum albumin 264, 278
  
- bowl 8, 19, 25, 26, 47–48, 50, 51–54, 67, 69, 71, 74, 88, 167, 204, 244
- Boycott effect 58
- buffer 12, 41, 47, 70, 110, 112, 117, 119, 122, 126, 273, 274
  
- cake 7, 10, 54, 56, 95, 96–97, 99, 102, 103–105, 124, 136, 138, 150, 193, 207, 210, 258
- cake baffle 104, 105
- cake formation 258
- cell 31, 126, 159, 174, 180
- cell viability 15, 160, 195
- centrate 14, 50, 53, 113, 122, 130, 141, 156, 158, 159, 160, 190–192, 211, 224, 234–235, 240–242, 248
- centrifugal 6–10, 12–13, 19, 24–26, 44–47, 165
- centrifugal filter 6, 9, 37, 40–42, 126–127, 272, 283
- centrifuge 6–10, 13, 25, 32–33, 37, 59, 95, 165, 198, 201, 229
- centripetal 75–77, 101
- centripetal pump 50, 75, 89, 94, 101, 167
- chamber 8, 62, 71, 167, 181
- characterization 256
- Chinese Hamster Ovary 1, 31, 112, 159
- chromatography 12, 40, 41, 110, 119, 126
- circulatory flow 23, 62
- clarification 14, 33, 64, 65, 71, 100, 110, 112, 113, 115, 116, 117, 123, 141, 195
- classification 5, 9, 14, 29, 31, 33, 47, 109, 123, 141, 212, 215, 241, 242
- Clean-in-Place 50, 55, 70, 88, 166
- climb angle 103

- coagulant 29, 100, 143, 144, 162, 163  
coagulation factor 125–126  
compaction 33, 104, 131, 133,  
134–135, 138, 174, 193  
compatible 97, 143, 159, 244, 274  
concentrate 70–71, 72, 130, 138,  
192–193  
concentration buildup 255, 272  
concentration factor 146, 155, 156,  
273, 274, 277  
concentration polarization 257, 258,  
259, 272, 276, 283  
conductivity 204, 205  
conical screen 10  
construction 87–88  
contaminant 12, 33, 41, 47, 65, 95,  
112, 120, 123, 126, 272  
continuum Phase 219–220  
control 89, 91, 157  
conveyance 100, 103  
conveyor 95, 97–98, 99  
conveyor torque 96, 97  
Coriolis 20–21, 62, 63  
corn 124  
critical flux 257  
crystallization 13, 110, 117, 119, 252  
cumulative size distribution 161, 211,  
230  
cut size 170, 174, 176, 178, 179, 210,  
211, 223  
Cytochrome 281
- Darcy's law 131, 132–133  
debris 6, 10, 31, 33, 47, 112, 118–119,  
120, 123, 141, 174, 224, 240, 275  
decanter 9, 95, 101–102, 105, 122, 123,  
136, 168, 181, 182, 248–250  
deceleration 40, 147–148, 220  
degritting 33  
deliquoring 97, 141  
density 6, 7, 10, 30, 31, 33, 39–40, 44,  
97, 142, 243  
depth 19, 20, 96–97, 138, 201, 244  
depth filter 5, 11, 110, 113–115, 117,  
119, 275  
desalting 41, 273  
dewatering 9, 99, 100, 124, 141, 167,  
168  
diafiltration 10, 11, 12, 274  
diatomaceous earth 10, 115  
differential speed 95, 97–100  
diffusion 23, 43, 262  
diffusion coefficient 21, 259, 263  
diffusivity 266–268, 269  
diluting 33, 64, 144, 145, 196, 218, 220  
discharge frequency 69–70, 133  
discrete 32, 33, 87  
disk centrifuge 59  
dropping bottom 9, 68, 90, 129, 193  
manual 65, 166  
intermittent discharge 9, 67–71,  
143, 166  
nozzle 9, 71–75, 118, 166  
disk stack 61, 66, 71, 84, 88, 89, 91,  
102, 131, 138, 160, 182, 192, 217,  
229, 236, 239, 242, 243, 248  
dispersed phase 220–221  
DNA 1, 41, 115, 274, 275  
drug 1, 5, 12, 251–252  
dry beach 96, 103–104  
drying 4, 10, 96, 110, 193
- efficiency 26, 28, 82, 84, 178, 226,  
230, 236–238  
effluent 50, 75, 114, 138, 204, 211,  
212  
Ekman flow 214–215, 260, 272  
Ekman layer 219, 260, 261, 263  
Ekman number 260  
electrolyte 143  
eluent 46, 47  
Elutriation 44, 46  
emulsion 101, 102  
entrainment 50, 53, 65, 85, 138, 178,  
192, 214–215, 236  
enzyme 119, 122–124, 144, 159,  
242, 274  
*Escherichia coli* 1, 3, 64, 70, 119, 120  
ethanol 124–125  
explosion 89  
expression 13, 29, 31, 112, 130,  
131–133, 134, 138  
extracellular 2, 5, 6, 12, 13, 14, 110,  
111, 112, 116, 122, 144, 159, 242
- feed 50, 65, 78–87, 96, 116, 142–143,  
158, 159, 183–186, 195, 196, 229,  
270–271

- feed accelerator 78, 80, 81, 84, 85–86  
feeding 26, 37, 53, 82, 138, 202, 204  
fermentation 4, 12, 109, 110, 118, 119, 124, 130  
fermenter 11, 15, 89, 118, 121, 122, 124, 169, 170, 171, 172, 190  
Fick's law 259  
filter 5, 7, 10, 15, 40–42, 110, 113, 115, 126–127, 272–275  
filtering 4, 6, 7, 9–10, 258, 278  
filtrate 4, 10, 41, 113, 114, 277, 278, 279, 280, 282  
filtration 4, 6–7, 10–11, 12, 37, 41, 110, 115, 119, 145, 255, 256, 257, 258, 272, 274, 278  
floc 29, 144, 162, 243  
flocculant 29, 100, 122, 143, 144, 159, 162, 244  
flow Visualization 201  
flowsheet 12, 109, 110–112, 115, 118, 119, 121, 122, 123, 124, 255  
flue gas desulfurization 250, 251  
flux 132, 133, 256, 257, 258, 263, 264, 266, 268, 269, 276, 278  
forward-drive 99  
fouling 10, 11, 257, 258  
frequency 69, 81, 82, 97, 98, 133, 143, 161, 193, 221, 239, 240, 249  
friction 60, 98, 209  
  
gear ratio 98, 99  
gel 257, 263, 266, 268  
gel concentration 266, 268  
gel diffusivity 268  
gel resistance 257–258  
gelling 256  
gene 1  
G-force 41, 47, 54, 69, 84, 95, 96, 119, 132, 158, 190, 206, 218, 233, 234, 241, 246, 250, 258, 271, 274  
gravitational acceleration 19, 20, 24, 41, 61, 131  
gravity 6, 29, 40, 103, 125, 157, 177, 233  
  
heavy phase 33, 67  
helix 103  
hermetic 78  
hindered settling 31, 32, 148, 150, 173  
  
hormones 12, 177–118  
host cell 1, 10, 112  
hub 54–55, 56  
hybrid 50, 54  
hydraulic assist 104  
hydrophilic 272  
hydrostatic 19, 20, 131, 132  
  
impurities 12, 33, 41, 109, 255, 275  
inclined plate 59, 60, 62, 177, 178  
inclusion bodies 6, 14, 111, 112, 119–120, 141, 239–242  
inlet 78, 85, 86, 207, 221  
instability 60, 62  
insulin 2, 117, 119  
intermittent discharge 67–68, 166  
intracellular 1, 4, 6, 15, 111, 112, 123–124, 126, 142, 159, 195  
ionic strength 12, 126, 143, 144  
isopycnic 44, 277  
  
kinetic 163  
kinetic energy 72–73, 75, 77, 96, 101  
  
lamella 59–60, 177  
laminar 258  
Le number 170–171, 173, 176, 178, 182, 184, 185, 190, 210, 250, 251  
light phase 33, 67, 102  
limiting flux 257, 258  
liquid 33–34, 64, 75–78, 142  
low shear 78  
lysing 112, 119, 123, 165  
lysosomes 175  
  
macromolecule 43, 256, 257, 263, 274, 277  
mammalian cells 1, 5, 12, 15, 65, 78, 110, 113, 165, 195, 224  
material balance 145–147, 152–154, 212, 235  
mechanical 42, 69, 80, 138, 160, 189–190, 193–194  
membrane 11, 255  
membrane module 40, 258, 272, 282  
membrane resistance 276  
metrics 13, 160, 195, 235  
Michael's model 262  
microbial 111, 165

- microfiltration 10, 11, 41, 255, 258  
microplates 38, 39, 40  
microsomes 44  
microtubule 274  
microtubules 39  
misalignment 194  
mitochondria 44, 174, 175  
mixture 41, 46, 101, 112, 123, 274, 275  
model 48, 55, 206–208, 212–215,  
218–219, 229–230, 261–262,  
275–278  
model validation 224–225  
modeling 201, 217–226  
molecular weight cut off 126, 256, 262,  
273  
momentum 26, 80, 219, 220, 260, 261  
monoclonal antibodies 2, 111, 274  
monodispersed 149–150, 161, 162, 184  
mother liquid 142  
moving layer 206–208, 213  
  
nanofiltration 255  
noise 89, 193  
non-rotating 20, 75, 268  
nozzle decanter 9  
nozzle discharge 71, 72  
nucleic acid 44  
Nusselt number 264, 269  
  
objectives 13, 33, 41, 101, 141, 238,  
248, 255, 275  
oil 67, 101–102  
operating point 190  
optimization 189, 195, 197, 229  
organelle 44, 175  
osmotic pressure 256, 276, 278, 280  
overflow 13, 33, 50, 98, 120, 122, 141,  
206, 209, 211  
oxidation 78, 79, 167  
  
peeler 9, 10  
pellet 37, 126, 172, 174, 272, 273  
percolation 131, 133, 193  
performance 13, 160, 229  
permeability 10, 97, 115, 132, 256,  
276, 277, 278  
permeate 4, 256, 284  
permeate flux 258, 264, 266, 268, 269,  
276  
pilot 141, 224  
  
pinion 98–100  
plough 50, 53, 54, 138  
plunger 50, 54, 134, 138, 166, 167  
pneumatic 89, 90  
polishing 5, 67, 122, 123, 158  
polydispersed 150, 161–162, 184–185  
polyelectrolyte 143  
polymer 29, 42, 143, 144, 159, 163  
pool 96–97, 138, 203–204, 212, 276, 278  
pool emergence 103, 104  
porosity 136  
power 80–81, 99, 136, 169, 180, 196,  
290  
precipitation 13, 110, 117, 118, 125,  
159, 252  
prediction 210–212, 214, 230, 278–282  
pressure 19–20, 86, 135–137, 256–257,  
271, 276, 284  
process 11–12, 32–33, 64–65,  
110–112, 115–119, 120–124, 141,  
159, 190–193, 238–239  
product 121–122, 154–157, 195  
production 15, 100, 112, 119, 121,  
124–125, 152–154, 195, 252  
projection 229  
properties 142, 229, 238, 244, 280  
protein 1–2, 4, 6, 11–12, 14, 110, 112,  
126, 141, 154–157, 159, 195, 272,  
274  
pulley 26  
purification 4, 40–42, 64, 109, 113,  
118, 195–196, 255, 271, 274  
pusher 9, 10  
  
rate 15, 29, 31, 47, 96, 117, 154, 158,  
180, 195, 196, 278  
recombinant 1, 2, 4, 11, 12, 112  
rejectivity 262, 277  
relative centrifugal force 24  
repose angle 68, 69  
repulping 33, 34, 141, 195, 240  
retentate 127, 277–278, 281  
retrograde 20, 21, 276  
reverse osmosis 255  
Reynolds number 260, 268–269  
ribosomes 3, 174–175  
Richardson and Zaki 31, 32  
RNA 41, 115, 142, 274  
rotating membrane 255  
rotation 82, 97, 148, 260

- salt 44, 126, 143, 273, 274, 275  
scale-up 158, 185, 234, 252, 280  
Schmidt number 260, 261, 264, 268,  
269–270  
scraper 51, 53  
screenbowl 9, 10  
secondary flow 21, 23, 26, 63, 258,  
276, 283  
sedimentation 10, 19, 41–42, 43, 100,  
148–151, 212–215  
sedimenting 6, 7–8, 23, 72  
selection 165  
selectivity 255, 256, 262  
separability 143  
separation 6–10, 12–15, 32–33, 44, 65,  
67, 101–102, 119–120, 141,  
195–196, 201, 239–242  
serum 121–122, 264, 278  
settler 59–61, 178  
settling velocity 30, 31, 148–151  
shear 1, 78, 236  
shear sensitive 15, 80, 88  
sheave 26, 97  
shot 70, 139, 160, 190  
simulation 251–252  
siphon 9  
size 33, 169  
size distribution 183–186, 211,  
232–233  
size recovery 211–212  
sizing 165  
slip 25, 26, 78, 99, 116, 122  
smoothener 48, 86–87  
smoothening 87  
solid 142–143  
solid throughput 195  
solid-body 24  
solid-bowl 50, 95–96  
solids 14, 31–32, 133, 64, 65, 70–71,  
129, 142, 158, 159, 160, 161,  
190–192, 195, 196, 210–211, 259  
solids recovery 116–117, 145, 160  
solute 256, 259, 262, 273, 274, 276  
spacing 62, 64, 92, 218  
speed 97–100, 157, 196  
spintube 37–40, 171–175, 250–251,  
272–275  
spin-up 173  
spray drying 110  
steam 88, 101, 121, 124  
steam-in-place 50, 55, 88, 166  
sterile filtration 12, 110, 195  
sterilization 88, 124, 138  
Stokes' law 30, 206, 207, 210, 220  
strategy 251–252  
stress 1, 37, 78, 97, 134–137, 209  
subcritical 177  
submerged hub 54–56  
sucrose 44  
supercritical 177  
supernatant 14, 55, 126, 170, 211,  
272  
surface finish 88  
suspension 41  
Svedberg 42, 43  
swinging bucket 38, 39, 44, 272, 273,  
275  
target cell 46–47  
Taylor Proudman 203, 260, 266  
temperature 12, 21, 30, 40, 85, 89, 142,  
159, 192  
testing 81–84, 134–135, 141  
therapeutic protein 1, 2, 4, 5, 6, 112,  
238, 239  
thickening 33, 64, 96, 104, 120  
three-phase 101–102  
throughput 15, 161, 190, 195  
time 147–148  
tissue 2, 126, 127, 274  
total solid recovery 210, 211, 212,  
213  
trajectory 21, 206, 207, 221  
transmembrane  
flux 257, 264–266  
pressure 257, 276, 278, 283  
Troubleshooting 189  
tubular 47–56, 166, 181–183, 201  
turbidity 158, 160, 163, 190–192  
turbulence 60, 78, 82, 83, 97, 163,  
165  
turbulent 258, 260  
turntable 20–21  
ultracentrifuge 8, 37, 42–44, 165  
ultrafiltration 12, 110, 265, 275  
unbalance 138, 193, 194  
Underflow 112, 113, 130, 137–138,  
159  
unflocculated 242, 243, 244

- vaccine 2, 120, 121, 122
- vane 48, 79, 84, 86, 87
- velocity 148–151, 208–209
- vibration 192, 193, 194
- viscosity 159, 173, 192, 198–199
- volume fraction 136, 140, 152, 154, 155, 290
- vortex 72
  
- washing 5, 10, 33, 65, 88, 109, 112, 119, 122, 252, 282
- waste 29, 72, 100, 101, 112, 118, 123, 141, 146
  
- water 89, 102, 204, 256
- water flux 256, 257
- wave 52, 82, 83
- weir 50, 81, 95, 96, 101, 105, 204, 206, 212
  
- yeast 1, 88, 115–117, 238–239
- yield 14, 154–157, 160, 195
  
- Zeta potential 142, 143
- zonal centrifuge 8, 44, 45